Proceedings of the

Thirty-Fourth DOE Solar Photochemistry Research Conference

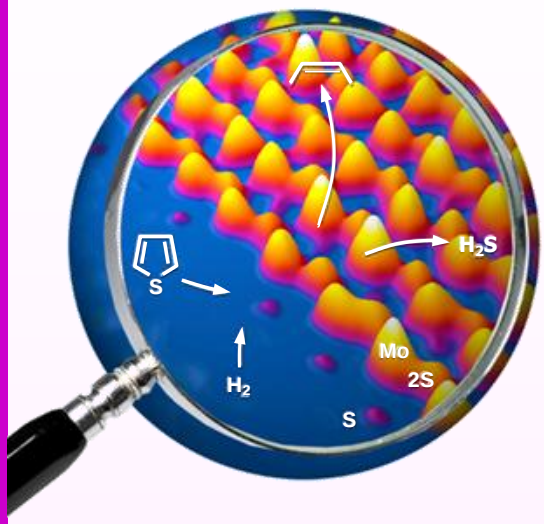

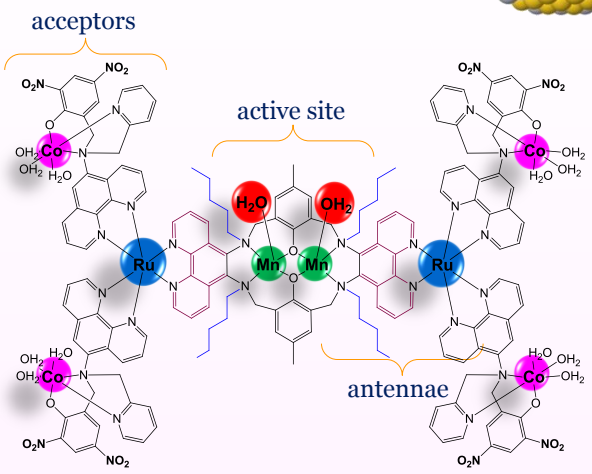

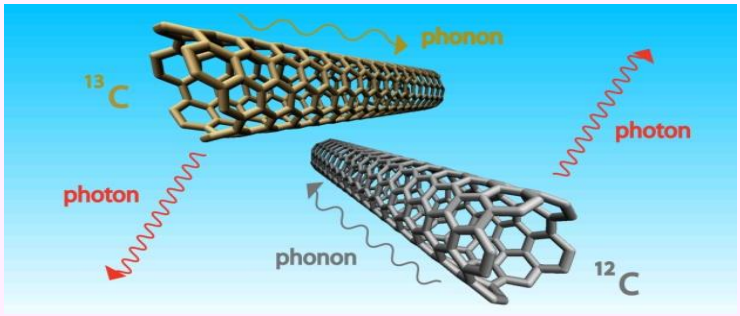

The Westin Annapolis, Annapolis, Maryland, June 3-6, 2012

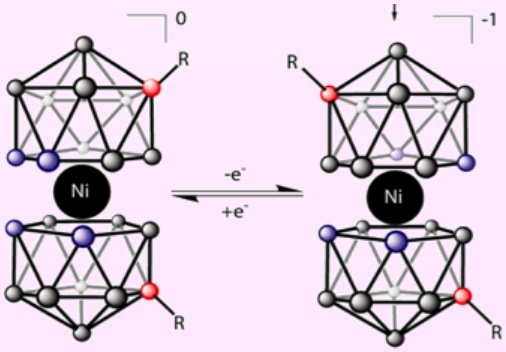

Sponsored by:

Chemical Sciences, Geosciences, and Biosciences Division
U.S. Department of Energy

Cover Graphics

The cover figures are taken from the abstracts of this meeting. The symbol for catalysis (upper right corner) is a 147-atom Au nanoparticle decorated with Pt (Crooks et al., p. 88). In the middle section, from the left, the first figure is a representation of detection of single sulfur atoms at the edge of industry style MoS_2 crystals (Kisielowski et al., p. 187). The second figure shows how ^{13}C-labeled single wall carbon nanotubes modify vibrational energies (Blackburn et al., p. 116). The figure on the right is an idealized heterometallic modular system for water oxidation (Verani et al., p. 53). The bottom figure shows the structure of a new family redox shuttle for dye-sensitized solar cells (Hupp, p. 143).

Program and Abstracts

34th Solar Photochemistry Program Research Meeting

The Westin Annapolis
Annapolis, Maryland
June 3–6, 2012

Chemical Sciences, Geosciences, and Biosciences Division
Office of Basic Energy Sciences
Office of Science
U.S. Department of Energy

This document was produced under contract number DE-AC05-06OR23100 between the U.S. Department of Energy and Oak Ridge Associated Universities.

The research grants and contracts described in this document are supported by the U.S. DOE Office of Science, Office of Basic Energy Sciences, Chemical Sciences, Geosciences and Biosciences Division.

Foreword

The 34th Department of Energy Solar Photochemistry Research Meeting, sponsored by the Chemical Sciences, Geosciences, and Biosciences Division of the Office of Basic Energy Sciences, is being held June 3–6, 2010, at the Westin Annapolis Hotel in Annapolis, Maryland. These proceedings include the meeting agenda, abstracts of the formal presentations and posters of the conference, and an address list for the participants.

This Conference is composed of the grantees who do research in solar photochemical energy conversion with the support of the Chemical Sciences, Geosciences, and Biosciences Division. It will feature presentations on photocatalysis, spectroscopy at nanoparticles, dye sensitized solids, novel molecular structures and charge transfer in organic molecular systems. These Program Meetings provide a unique environment for the initiation of collaborations between researchers as well as exchanges of new concepts and ideas. This synergistic element of research within the program is one of its major strengths and promotes the excellence in research that has sustained this program over the years.

The program is pleased to have Professor Richard Schrock of the Massachusetts Institute of Technology as a special guest lecturer for this conference. He will give a presentation on the history and challenges of the reduction of dinitrogen to ammonia and will illustrate this lecture with a discussion of his own research on this topic. The mechanistic complexity of this reaction will be familiar to many in the Solar Photochemistry Program who have concerned themselves over the past years with the reduction of water and CO_2 to produce fuels. Perhaps it is the case that a means for a photoinduced reduction of dinitrogen to ammonia could be found that would not require the hydrogen gas that is essential for the commercial Haber-Bosch process.

The Solar Photochemistry Research Conference will also have as its guests this year a number of researchers from the Catalysis Program, which is a sibling program in the Chemical Sciences, Geosciences, and Biosciences Division. They will be providing the attendees of this meeting with lectures and posters on their approaches to the study of catalysis at surfaces, which is a research area of recent focus in the Solar Photochemistry Program.

I would like to express my appreciation to Dr. Amy Ryan of the Pacific Northwest National Laboratory, to Diane Marceau of the Division of Chemical Sciences and to Tim Ledford and Connie Lansdon of the Oak Ridge Institute for Science and Education for their assistance with the preparation of this volume and the coordination of the logistics of this meeting. I must also thank all of the researchers whose dedication to scientific inquiry and enduring interest in research on solar energy transduction have enabled these advances in solar photoconversion and made this meeting possible.

Mark T. Spitler
Chemical Sciences, Geosciences,
and Biosciences Division
Office of Basic Energy Sciences

Solar Photochemistry Research Conference Overview

Time	Sunday, June 3	Monday, June 4	Tuesday, June 5	Wednesday, June 6	Time
7:00 AM					7:00 AM
7:15 AM			BREAKFAST		7:15 AM
7:30 AM		BREAKFAST	7:00 - 8:00	BREAKFAST	7:30 AM
7:45 AM		7:30 - 8:15		7:30 - 8:15	7:45 AM
8:00 AM			GUEST SPEAKER		8:00 AM
8:15 AM		Opening Remarks		Introduction	8:15 AM
8:30 AM					8:30 AM
8:45 AM		*Session II*	*Session V*	*Session VIII*	8:45 AM
9:00 AM					9:00 AM
9:15 AM				Surface Structure	9:15 AM
9:30 AM		Sensitized	Complex Catalysis	and Analysis	9:30 AM
9:45 AM		Semiconductors I			9:45 AM
10:00 AM		BREAK	BREAK	BREAK	10:00 AM
10:15 AM		10:00 - 10:30	10:00 - 10:30	10:00 - 10:30	10:15 AM
10:30 AM					10:30 AM
10:45 AM		*Session III*	*Session VI*	*Session IX*	10:45 AM
11:00 AM					11:00 AM
11:15 AM		Sensitized	Photochemical	Catalysis at Surfaces	11:15 AM
11:30 AM		Semiconductors II	Water Splitting	I	11:30 AM
11:45 AM					11:45 AM
12:00 PM					12:00 PM
12:15 PM		LUNCH			12:15 PM
12:30 PM		12:00 - 1:00		LUNCH	12:30 PM
12:45 PM			LUNCH	12:00 - 1:30	12:45 PM
1:00 PM			12:30 - 1:30		1:00 PM
1:15 PM					1:15 PM
1:30 PM					1:30 PM
1:45 PM		Free time		*Session X*	1:45 PM
2:00 PM		1:00 - 5:00			2:00 PM
2:15 PM			Free time	Catalysis at Surfaces	2:15 PM
2:30 PM			1:30 - 4:15	II	2:30 PM
2:45 PM					2:45 PM
3:00 PM				BREAK	3:00 PM
3:15 PM				3:00 - 3:30	3:15 PM
3:30 PM					3:30 PM
3:45 PM	Registration				3:45 PM
4:00 PM	3:00 - 6:00			*Session XI*	4:00 PM
4:15 PM					4:15 PM
4:30 PM				Catalysis at Surfaces	4:30 PM
4:45 PM				III	4:45 PM
5:00 PM			*Session VII*		5:00 PM
5:15 PM		*Session IV*			5:15 PM
5:30 PM	No-Host Reception	Systems for	Electron Transfer		5:30 PM
5:45 PM	5:30 - 6:30	Photoconversion			5:45 PM
6:00 PM	*at the bar*			DINNER BREAK	6:00 PM
6:15 PM		Free time	SOCIAL HOUR	(on your own)	6:15 PM
6:30 PM			6:15 - 7:00	5:30 - 7:30	6:30 PM
6:45 PM		DINNER			6:45 PM
7:00 PM	DINNER	6:30 - 7:30			7:00 PM
7:15 PM	6:30 - 7:45		DINNER		7:15 PM
7:30 PM			7:00 - 8:00		7:30 PM
7:45 PM	Welcome				7:45 PM
8:00 PM		POSTERS		POSTERS	8:00 PM
8:15 PM	*Session I*	odd numbers (1-59)	POSTERS	Catalysis at Surfaces	8:15 PM
8:30 PM	Photocatalysis		even numbers (2-60)	(C1 - C18)	8:30 PM
8:45 PM					8:45 PM
9:00 PM				7:30 - 9:30	9:00 PM
9:15 PM	Reception Continues	7:30 - 10:00	8:00 - 9:45		9:15 PM
9:30 PM	9:00 - 10:00				9:30 PM
9:45 PM	*at the bar*		Program Manager's	Closing Remarks	9:45 PM
10:00 PM			Comments	& Announcements	10:00 PM

Table of Contents

TABLE OF CONTENTS

POSTER ABSTRACTS (BY POSTER NUMBER)

Program

34th DOE SOLAR PHOTOCHEMISTRY
RESEARCH MEETING

June 3–6, 2011

Westin Hotel
Annapolis, Maryland

PROGRAM

Sunday, June 3

3:00 – 6:00 p.m. Registration

5:30 – 6:30 p.m. Reception

6:30 – 7:45 p.m. Dinner

7:45 p.m. Welcome

SESSION I - Photocatalysis
Mark T. Spitler, Chair

8:00 p.m. Nanostructured Photocatalytic Water Splitting Systems
Thomas E. Mallouk, The Pennsylvania State University

8:30 p.m. Effect of Composition and Structure on the Performance of Photocatalytic Materials
Allen J. Bard, The University of Texas at Austin

Monday Morning, June 4

7:30 a.m. Continental Breakfast

8:15 a.m. Opening Remarks
Richard Greene and **Mark Spitler**, U. S. Department of Energy

SESSION II
Opening Session; Sensitized Semiconductors I
C. Michael Elliott, Chair

8:45 a.m. Molecular Design of Zinc Oxide Nanoparticle-Dye Dyads and Triads
W. L. Gladfelter, D. A. Blank, and **K. R. Mann**, The University of Minnesota

9:30 a.m. Tuning the Ultrafast Excited-State Dynamics of First-Row Transition-Metal–Based Chromophores
James K. McCusker, Michigan State University

10:00 a.m. Coffee Break

SESSION III
Sensitized Semiconductors II
Matt Beard, Chair

10:30 a.m. Surface Chemistry for Photoelectrochemical Charge Transfer at Metal Oxide Interfaces
Robert J. Hamers, The University of Wisconsin-Madison

11:00 a.m. Quantum Dot Sensitization of Single Crystal Semiconductors
Bruce A. Parkinson, The University of Wyoming

11:30 a.m. Single-Particle Current Blinking in Semiconductor Quantum Dots
Jao van de Lagemaat, National Renewable Energy Laboratory

Monday Afternoon, June 4

12:00 p.m. Lunch

Monday Evening, June 4

SESSION IV
Systems for Photoconversion
Brian Gregg, Chair

5:00 p.m. Photovoltaic and Photochemical Properties of Conjugated Ionomer Junctions
Mark C. Lonergan, The University of Oregon

5:30 p.m. Nanoscaled Components for Improved Efficiency in a Multipanel Photocatalytic Water-Splitting System
Marye Ann Fox, The University of California at San Diego

6:30 p.m. Dinner

7:30 p.m. **Posters: Odd numbers, Posters 1 - 59**

Tuesday Morning, June 5

7:00 a.m. Continental Breakfast

SESSION V
Complex Catalysis
Mark T. Spitler, Chair

8:00 a.m. ***GUEST SPEAKER***
How to Reduce Dinitrogen Catalytically to Ammonia with Protons and Electrons
Richard R. Schrock, Massachusetts Institute of Technology

9:00 a.m. Solar Fuels from Carbon Dioxide and Water: Catalytic Photoelectrochemical Generation of Alcohols
Andrew Bocarsly, Princeton University

9:30 a.m. Highly Reducing Modular Assemblies for Photochemical CO_2 Reduction
Michael D. Hopkins, The University of Chicago

10:00 a.m. Coffee Break

SESSION VI
Photochemical Water Splitting
Oleg Poluektov, Chair

10:30 a.m. Connecting Structure to Solar Fuels Function in Natural and Artificial Photosynthesis
David M. Tiede, Argonne National Laboratory

11:00 a.m. A Concerted Synthetic, Spectroscopic and Computational Approach towards Water Splitting by Heterometallic Complexes in Solution and on Surfaces
C. N. Verani, J. F. Endicott, and **H. Bernhard Schlegel,** Wayne State University

11:45 a.m. Multicomponent Bio-Nano Integrated Systems for Light-Driven Hydrogen Generation
Kara L. Bren, Richard Eisenberg, and **Todd D. Krauss**,
University of Rochester

Tuesday Afternoon, June 5

12:30 p.m. Lunch

Tuesday Evening, June 5

SESSION VII
Electron Transfer
Mary Beth Williams, Chair

4:30 p.m. Physical Chemistry of Reaction Dynamics in Ionic Liquids
Edward W. Castner, Jr., Mark Maroncelli, and **James F. Wishart**
Rutgers University, Penn State University, Brookhaven National Laboratory

5:15 p.m. Charge Transfer States of Organic Molecular Conjugates
Tunna Baruah, The University of Texas at El Paso

5:45 p.m. Donor/Acceptor Coupling Models for Electron and Excitation Energy Transfer and Related Issues for ET Kinetics at Electrodes
Marshall D. Newton, Brookhaven National Laboratory

6:15 p.m. Social Hour

7:00 p.m. Dinner

8:00 p.m. **Posters: Even numbers, Posters 2 - 60**

9:45 p.m. Program Manager's Comments
Mark T. Spitler

Wednesday Morning, June 6

7:30 a.m. Continental Breakfast

8:15 a.m. **Catalysis at Surfaces**: Introduction

Session VIII
Surface Structure and Analysis
Kyoung-Shin Choi, Chair

8:30 a.m. Studies of Surface Adsorbate Electronic Structure and Femtochemistry at the Fundamental Length and Time Scales
Hrvoje Petek, The University of Pittsburgh

9:00 a.m. Catalysis Characterization by In Situ Resonance Raman Spectroscopy
Peter C. Stair, Northwestern University

9:30 a.m. Atomic Resolution Imaging and Quantification of the Chemical Functionality of Surfaces
Udo D. Schwarz, Yale University

10:00 a.m. Coffee Break

Session IX
Catalysis at Surfaces I
Gary W. Brudvig, Chair

10:30 a.m. New Carbon-Free Nano-Dyads and Triads for Solar-Energy–Driven Catalytic Water Splitting
D. G. Musaev, T. Lian, and **C. L. Hill**, Emory University

11:15 a.m. Correlation of Theory and Function in Well-Defined Bimetallic Electrocatalysts
Richard M. Crooks, The University of Texas at Austin

Wednesday Afternoon, June 6

12:00 p.m. Lunch

Session X
Catalysis at Surfaces II
Michael A. Henderson, Chair

1:30 p.m. In Situ X-ray Studies of Photo- and Electrocatalysis
Anders Nilsson, SLAC National Accelerator Laboratory

2:00 p.m. Inorganic Core-Shell Assemblies for Separating H_2O Oxidation Catalysis from Light Absorber and CO_2 Reduction Chemistry
Heinz Frei, Lawrence Berkeley National Laboratory

2:30 p.m. Nanoscale Surface Chemistry and Electrochemistry on Faceted Substrates
Robert A. Bartynski, Rutgers, The State University of New Jersey

3:00 p.m. Coffee Break

Session XI
Catalysis at Surfaces III
Joseph T. Hupp, Chair

3:30 p.m. Formation and Characterization of Semiconductor Nanorod/Oxide Nanoparticle Hybrid Materials: Toward Vectoral Electron Transport in Hybrid Materials
Neal Armstrong, Jeffrey Pyun, and **S. Scott Saavedra**, The University of Arizona

4:15 p.m. Nanostructured Photoelectrodes
John A. Turner, National Renewable Energy Laboratory

4:45 p.m. Oxomanganese Catalysts for Solar Fuel Production
Victor S. Batista and **Charles A. Schmuttenmaer**, Yale University

Wednesday Evening, June 6

5:30 p.m. Dinner on your own

7:30 p.m. **Posters: Catalysis at Surfaces, C1–C18**

9:30 p.m. Closing Remarks and Announcements

Session X
Catalysis at Surfaces II
Michael A. Henderson, Chair

1:30 p.m. In Situ X-ray Studies of Photo- and Electrocatalysis
Anders Nilsson, SLAC National Accelerator Laboratory

2:00 p.m. Inorganic Core-Shell Assemblies for Separating H_2O Oxidation Catalysis from Light Absorber and CO_2 Reduction Chemistry
Heinz Frei, Lawrence Berkeley National Laboratory

2:30 p.m. Nanoscale Surface Chemistry and Electrochemistry on Faceted Substrates
Robert A. Bartynski, Rutgers, The State University of New Jersey

3:00 p.m. Coffee Break

Session XI
Catalysis at Surfaces III
Joseph T. Hupp, Chair

3:30 p.m. Formation and Characterization of Semiconductor Nanorod/Oxide Nanoparticle Hybrid Materials: Toward Vectoral Electron Transport in Hybrid Materials
Neal Armstrong, Jeffrey Pyun, and **S. Scott Saavedra**, The University of Arizona

4:15 p.m. Nanostructured Photoelectrodes
John A. Turner, National Renewable Energy Laboratory

4:45 p.m. Oxomanganese Catalysts for Solar Fuel Production
Victor S. Batista and **Charles A. Schmuttenmaer**, Yale University

Wednesday Evening, June 6

5:30 p.m. Dinner on your own

7:30 p.m. **Posters: Catalysis at Surfaces, C1–C18**

9:30 p.m. Closing Remarks and Announcements

Session I

Photocatalysis

Nanostructured Photocatalytic Water Splitting Systems

Yixin Zhao, Emil A. Hernandez-Pagan, Nella M. Vargas-Barbosa, John R. Swierk, Seunghyun Anna Lee, W. Justin Youngblood, Nicholas McCool, Landy Blasdel, and Thomas E. Mallouk
Department of Chemistry, The Pennsylvania State University, University Park PA 16802

Jackson D. Megiatto, Jr., Ana L. Moore, Thomas A. Moore, and Devens Gust
Department of Chemistry and Biochemistry, Arizona State University, Tempe AZ 85281

The goal of our DOE-supported work is to explore the assembly and electron/proton transfer kinetics of water-splitting photoelectrochemical cells that employ molecular light absorbers. In the simplest such system, a high surface area TiO_2 electrode is coupled to a ruthenium polypyridyl or porphyrin sensitizer, which is itself linked to a colloidal $IrO_x{\cdot}nH_2O$ water oxidation catalyst. The quantum yield for photoassisted water splitting is low (< 5%) because of rapid back electron transfer and electrode polarization. We are now studying more complex electron transfer assemblies that incorporate an electron transfer mediator between the sensitizer and water oxidation catalyst. To extend this concept to a more efficient molecular Z-scheme, we are also assembling and studying molecular photocathodes for light-driven water reduction. The photocathodes are donor-acceptor assemblies grown layer-by-layer on high surface area transparent conductor substrates and coupled to hydrogen evolution catalysts. Electrochemical and transient spectroscopic techniques are used to study the kinetics of the individual components and donor-acceptor diads, as well more complex systems assembled from them.

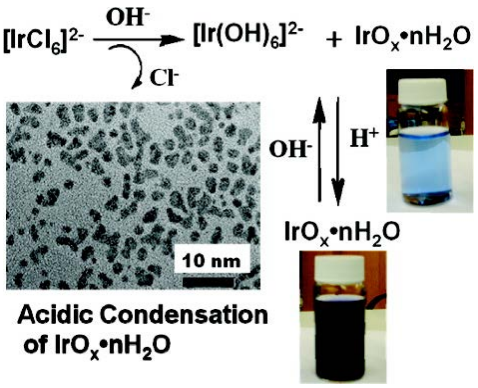

Synthetic scheme for ligand-free IrO_2 nanoparticles.

For the photoanode of the water splitting dye sensitized solar cell (DSSC), we developed an improved synthesis for ligand-free and ligand-protected iridium oxide nanoparticles. Cold acid condensation of $[Ir(OH)_6]^{2-}$ ions yields 1-2 nm diameter particles that are stable over a wide range of pH. These particles are highly active electrocatalysts for water oxidation and bind strongly to molecules terminated with malonate groups. When the nanoparticles are incorporated into porous TiO_2 electrodes containing phosphonated $[Ru(bpy)_3]^{2+}$ sensitizers, stable photocurrents are obtained and the current efficiency for oxygen evolution is near unity.

The initial photocurrent density corresponds to an internal quantum yield of 10-15%. The photocurrent decays over tens of seconds by ~90%, but can be restored if the cell is disconnected briefly. We observe much higher photocurrent and less electrode polarization when I^- is added as an electron donor. This suggests that the injection yield is high, but that slow electron transfer from IrO_2 to the oxidized dye results in a low initial quantum yield. The slow polarization process may be caused by protons generated in the water oxidation reaction, since the driving force for water oxidation is pH-dependent. Flash photolysis experiments with TiO_2 and core-shell ZrO_2/TiO_2 and Nb_2O_5/TiO_2 electrodes showed slower recombination ($e_{(TiO2)} \rightarrow$oxidized dye), and the core-shell structure resulted in a twofold increase in the photocurrent. We are now making core-shell electrodes that contain oxide cores (SnO_2, In_2O_3) with more positive

conduction band edge potentials in order to probe the effect of the driving force on the recombination rate. We are also experimenting with one-electron mediators (analogous to the tyrosine-histidine complex in Photosystem II) that accelerate the regeneration of the oxidized dye molecule. The incorporation of a high potential mediator in the system, anchored to $IrO_x \cdot nH_2O$ nanoparticles by a malonate group, results in faster bleaching recovery of the Ru(II) dye and a threefold increase in the steady-state quantum yield for water splitting.

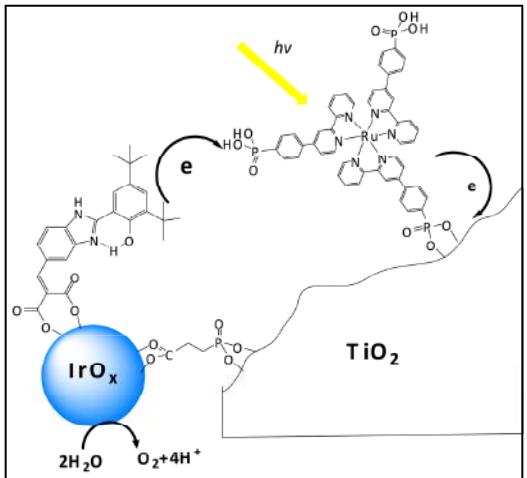

Incorporating a redox mediator into the anode of a water-splitting DSSC.

We are also studying current rectification and light-induced electron transfer in photocathode structures that contain metalloporphyrin sensitizers and viologen electron acceptors separated by unilamellar sheets of oxide semiconductors such as $HTiNbO_5$. In these photocathode assemblies, the porphyrin triplet excited state is quenched by electron transfer to the semiconductor sheet, and subsequent electron transfer to the viologen results in a long-lived charge-separated state. The electron transfer dynamics of these assemblies are being studied by a transient ATR method developed in collaboration with the Saavedra group at the University of Arizona. We have developed a template electrodeposition method for growing high surface area transparent conductor nanowire arrays onto which these layer-by-layer assemblies can be grown. One of the fundamental challenges in this part of the project is to quantify and understand parameters such as the open circuit photovoltage and short circuit photocurrent – quantities that are routinely applied to semiconductor p-n junctions – in the context of rate equations for outer sphere electron transfer in molecular systems.

The recent development of inexpensive catalysts for the oxygen evolution reaction raises the question of whether they can be used in fuel-producing photoelectrochemical cells (PECs). Because these catalysts operate in aqueous buffer solutions at neutral to slightly basic pH, it is important to consider whether electrolytic cells can have low series loss under these conditions. Water-splitting or fuel-forming PECs will likely require porous separators or electrolyte membranes to isolate the cathode products from oxygen produced at the anode. For this reason we have analyzed the potential losses in electrolytic systems of buffers and commercially available anion- and cation-exchange membranes. Potential losses associated with solution resistance, membrane resistance, and pH gradient formation were measured at current densities expected for efficient PECs. The membrane pH gradient is the most problematic source of loss in these systems, but monoprotic buffers can minimize the pH gradient by diffusion of the neutral acidic or basic form of the buffer across the membrane. These results suggest that water-splitting PECs can be viable with properly chosen membrane/buffer combinations.

DOE Sponsored Solar Photochemistry Publications 2009-2012

1. R. Ma, Y. Wang, and T. E. Mallouk, “Patterned Nanowires of Se and Corresponding Metal Chalcogenides from Patterned Amorphous Se Nanoparticles,” *Small*, 5, 356-360 (2009).

2. W. J. Youngblood, S.-H. A. Lee, Y. Kobayashi, E. A. Hernandez-Pagan, P. G. Hoertz, T. A. Moore, A. L. Moore, D. Gust, and T. E. Mallouk “Photoassisted Overall Water Splitting in a Visible Light-Absorbing Dye Sensitized Photoelectrochemical Cell,” *J. Am. Chem. Soc.* 131, 926-927 (2009).

3. K. Maeda, M. Eguchi, S.-H. A. Lee, W. J. Youngblood, H. Hata, and T. E. Mallouk, “Photocatalytic Hydrogen Evolution from Hexaniobate Nanoscrolls and Calcium Niobate Nanosheets Sensitized by Ruthenium(II) Bipyridyl Complexes,” *J. Phys. Chem. C*, 113, 7962-7969 (2009).

4. K. Maeda and T. E. Mallouk, "Comparison of two- and three-layer restacked Dion-Jacobson niobate nanosheets as catalysts for photochemical hydrogen evolution," *J. Mater. Chem.*, 19, 4813-4818 (2009).

5. K. Maeda, M. Eguchi, W. J. Youngblood, and T. E. Mallouk, "Calcium Niobate Nanosheets Prepared by the Polymerized Complex Method as Catalytic Materials for Photochemical Hydrogen Evolution," *Chem. Mater.*, 21, 3611-3617 (2009).

6. W. J. Youngblood, S.-H. A. Lee, K. Maeda, and T. E. Mallouk, "Visible light water splitting using dye-sensitized oxide semiconductors," *Acc. Chem. Res.*, 42, 1966-1972 (2009).

7. N. I. Kovtyukhova and T. E. Mallouk, "Electrochemically-Assisted Deposition as a New Route to Transparent Conductive Indium Tin Oxide Films," *Chem. Mater.* 22, 4939-4949 (2010).

8. T. E. Mallouk, "The emerging technology of solar fuels," *J. Phys. Chem. Lett.* 1, 2110-2111 (2010).

9. N. I. Kovtyukhova and T. E. Mallouk, "Conductive indium-tin oxide nanowire and nanotube arrays made by electrochemically assisted deposition in template membranes: switching between wire and tube growth modes by surface chemical modification of the template," *Nanoscale* 3, 1541-1552 (2011).

10. Y. Zhao, E. A. Hernandez-Pagan, N. M. Vargas, J. L. Dysart, and T. E. Mallouk, "A High Yield Synthesis of Ligand-Free Iridium Oxide Nanoparticles with High Electrocatalytic Activity," *J. Phys. Chem. Lett.*, 2, 402-406 (2011).

11. E. A. Hernandez-Pagan, W. Wang, and T. E. Mallouk, "Template Electrodeposition of Single-Phase p- and n-Type Copper Indium Diselenide ($CuInSe_2$) Nanowire Arrays," *ACS Nano* 5, 3237-3241 (2011).

12. B. D. Sherman, S. Pillai, G. Kodis, J. Bergkamp, T. E. Mallouk, D. Gust, T. A. Moore, and A. L. Moore, "A porphyrin-stabilized water oxidation catalyst," *Can. J. Chem.* 89, 152-157 (2011).

13. Y. Zhao, N. M. Vargas-Barbosa, E. A. Hernandez-Pagan, and T. E. Mallouk, "Anodic Deposition of Colloidal Iridium Oxide Thin Films from Hexahydroxyiridate(IV) Solutions," *Small*, 7, 2087-2093 (2011).

14. S.-H. A. Lee, Y. Zhao, E. A. Hernandez-Pagan, L. Blasdel, W. J. Youngblood, and T. E. Mallouk, "Electron transfer kinetics in water splitting dye-sensitized solar cells based on core-shell oxide electrodes," *Faraday Discussions*, 155, 165-176 (2011).

15. Y. Zhao, J. R. Swierk, J. D. Megiatto, Jr., B. Sherman, W. J. Youngblood, D. D. Qin, D. M. Lentz, A. L. Moore, T. A. Moore, D. Gust, and T. E. Mallouk, "Improving the efficiency of water splitting in dye-sensitized solar cells by using a biomimetic electron transfer mediator," *PNAS*, in press.

16. E. A. Hernandez-Pagan, N. M. Vargas-Barbosa, T.-H. Wang, Y. Zhao, E. S. Smotkin, and T. E. Mallouk, "Resistance and polarization losses in aqueous buffer-membrane electrolytes for water-splitting photoelectrochemical cells," *Energy Environ. Sci.*, in press.

Effect of Composition and Structure on the Performance of Photocatalytic Materials

C. Buddie Mullins and Allen J. Bard
Departments of Chemical Engineering and Chemistry and Biochemistry
Center for Electrochemistry, University of Texas at Austin
Austin, Texas 78712-0231

A key issue in the design of photoelectrochemical (PEC) systems is the discovery of a photocatalyst, generally a semiconductor material that has the required efficiency and stability, which are functions of the chemical composition and morphology. In selecting a semiconductor photocatalyst, the band gap energy, E_g and the location of the conduction and valence bands, E_c and E_v, are the main variables most frequently considered and numerous studies of the effect of addition of other elements (usually called "doping") on E_g have appeared. However, other variables, such as carrier mobility and carrier recombination rates in the bulk and at the surface, can be functions of the nature and amount of dopant and strongly affect the PEC behavior.

Scanning electrochemical microscopy (SECM), which involves studying electrochemical reactions at a closely spaced ultramicroelectrode (UME) tip and a substrate, can be used to screen photocatalysts. In this application the SECM tip is replaced by a modified optical fiber. A robotic piezoelectric dispenser is used, followed by appropriate treatments, to prepare arrays composed of ~300 μm size photocatalyst spots with different compositions onto a fluorine-doped tin oxide (FTO) substrate. The scanning tip is a fiber optic, with or without a conducting detecting ring electrode, connected to a xenon lamp, which is rapidly scanned over the array. In this arrangement the photocatalytic performance of each spot can be evaluated by measuring the substrate photocurrent. The technique allows scans at different substrate potentials, so that the photocurrent-potential behavior can be recorded. Moreover products of the photoreaction can be measured at the tip ring electrode surrounding the fiber optic.

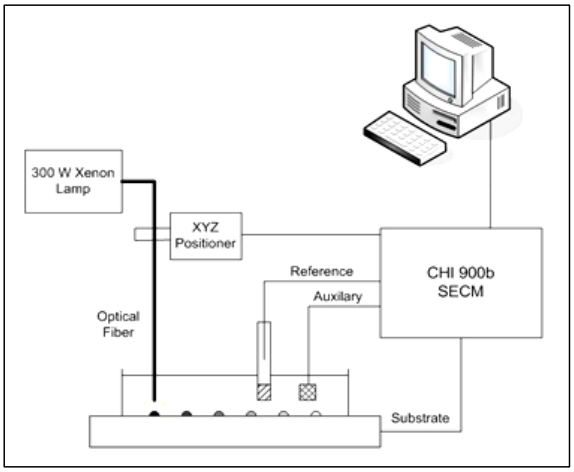

Porous, nanostructured $BiVO_4$ films were doped with Mo and W and synthesis parameters such as the Bi:V:Mo:W atomic ratio and the porosity were adjusted to optimize the films for photoelectrochemical (PEC) water oxidation. Films synthesized with a Bi:V:Mo:W atomic ratio of 46:46:6:2 (6% Mo, 2% W) demonstrate the best PEC performance with photocurrent densities 10 times higher than for pure $BiVO_4$. The evaporated films consist of a directional, nanocolumnar layer beneath an irregular surface structure. Backside illumination utilizes light scattering off the irregular surface structure resulting in 30-45% higher photocurrent densities than for frontside illumination. To improve the kinetics for water oxidation Pt is photo-deposited onto the surface of the 6% Mo, 2% W $BiVO_4$ films as an electrocatalyst. These films achieve quantum efficiencies of 37% at 1.1 V vs. RHE and 50% at 1.6 V vs. RHE for 450 nm light.

Thin films of α-Fe_2O_3 doped with either Ti or Sn were prepared by co-evaporating iron and titanium/tin in a reactive oxygen ambient, and their physical, chemical, and photoelectrochemical properties were studied. It was found that manipulating the deposition angle had a profound effect on the photoelectrochemical water oxidation performance of 4% Ti-doped α-Fe_2O_3 films, and a maximum in photocurrent at 1.4 V *vs*. RHE was achieved for films grown at 75° incidence. It was also found that the nanocolumnar morphology and superior porosity attained using glancing angles improved the relative conversion of visible-light ($\lambda > 420$ nm) photons compared to dense films deposited at normal incidence. Sn-doped films were also prepared for comparison using the same deposition conditions, and although they were substantially better than undoped films, their performance was below that of Ti-doped films. The Ti-doped films deposited using optimum conditions resulted in incident photon-to-current efficiencies (IPCE) reaching 31% at 360 nm and 1.4 V *vs.* RHE. By comparison, Sn-doped films reached only 21% under the same conditions. The increased photo-conversion efficiency brought about through Ti^{4+} or Sn^{4+} incorporation appears to be due to both the improvement of electron transport within the bulk of the film and the suppression of recombination at the film-electrolyte interface due to the stronger electric field near the surface.

Nanostructured Ta_3N_5 photoanodes were synthesized *via* a novel two-step process; first nanocolumnar Ta_2O_5 films were deposited by evaporation of tantalum metal in a vacuum chamber at either normal or glancing angles to the growth surface in a low pressure oxygen ambient followed by heating in an ammonia gas flow to convert Ta_2O_5 into orthorhombic Ta_3N_5 (band gap of ~ 2.1 eV). In 1M KOH solution, under Xenon lamp irradiation (white-light intensity of ~ 73 mW/cm^2), a 100 nm-thick nanoporous Ta_3N_5 electrode deposited at 70^o incidence achieved an anodic photocurrent of ~ 1.4 mA/cm^2 at +0.5 V *versus* Ag/AgCl with ~ 80% of the photocurrent contributed from the visible region ($\lambda \geq 420$ nm). By comparison, a dense film deposited at 0^o incidence achieved ~ 0.4 mA/cm^2 clearly illustrating the importance of nanostructuring for improving the performance of Ta_3N_5 photoanodes. However, X-ray photoelectron spectroscopy (XPS) measurements confirmed evidence of the Ta_3N_5 film's self-oxidation under illumination. The stability and photocatalytic activity of the nanostructured Ta_3N_5 films were improved by application of a cobalt co-catalyst layer.

Our future research efforts will focus on the discovery and characterization of new nanostructured semiconductor photo-materials and electrocatalysts with overall objectives of designing, developing, fabricating, testing and understanding their performance and stability in systems for solar photoelectrochemical (PEC) production of H_2. In particular we will continue our search for new material compositions, including the effects of dopants, and synthesize films of candidate photo-materials by electrodeposition, chemical spray pyrolysis, reactive ballistic deposition, and hydrothermal synthesis for physical and photoelectrochemical characterization. We will also study the performance of amorphous silicon triple junction photovoltaic cells with electrocatalyst/protective coatings applied by means of atomic layer deposition.

Acknowledgments: Nathan T. Hahn, Sean P. Berglund, Hoang Dang, Son Hoang, Hyun S. Park, Kyoung Eun Kweon, Heechang Ye, Eunsu Paek, Gyeong S. Hwang.

DOE Sponsored Solar Photochemistry Publications 2009-2012

1. Yanqing Cong, Shijun Wang, Hoang X. Dang, Fu-Ren F. Fan, C. Buddie Mullins, Allen J. Bard "Synthesis of Ta_3N_5 Nanotube Arrays Modified with Electrocatalysts for Photoelectrochemical Water Oxidation" *J. Phys. Chem. C* submitted.

2. Allen J. Bard, "Inner-Sphere Heterogeneous Electrode Reactions. Electrocatalysis and Photocatalysis: The Challenge," *J. Am. Chem. Soc.* 132, 7559 (2010).

3. Heechang Ye, Joowook Lee, Jum Suk Jang, and Allen J. Bard, "Rapid Screening of $BiVO_4$-Based Photocatalysts by Scanning Electrochemical Microscopy (SECM) and Studies of Their Photoelectrochemical Properties," *J. Phys. Chem. C* 114, 13322 (2010).

4. Guanjie Liu and Allen J. Bard, "Rapid Preparation and Photoelectrochemical Screening of $CuInSe_2$ and $CuInMSe_2$ Arrays by Scanning Electrochemical Microscopy," *J. Phys. Chem. C* 114, 17509 (2010).

5. Guanjie Liu, Chongyang Liu, and Allen J. Bard, "Rapid Synthesis and Screening of $Zn_xCd_{1-x}S_ySe_{1-y}$ Photocatalysts by Scanning Electrochemical Microscopy," *J. Phys. Chem. C* 114, 20997 (2010).

6. Heechang Ye, Hyun S. Park, Vahid A. Akhavan, Brian W. Goodfellow, Matthew G. Panthani, Brian A. Korgel, and Allen J. Bard, "Photoelectrochemical Characterization of $CuInSe_2$ and $Cu(In_{1-x}Ga_x)Se_2$ Thin Films for Solar Cells," *J. Phys. Chem. C* 115, 234 (2011).

7. Hyun S. Park, Kyoung Eun Kweon, Heechang Ye, Eunsu Paek, Gyeong S. Hwang, and Allen J. Bard, "Factors in the Metal Doping of $BiVO_4$ for Improved Photoelectrocatalytic Activity as Studied by Scanning Electrochemical Microscopy and First-Principles Density-Functional Calculation," *J. Phys. Chem. C* 115, 17870 (2011).

8. Son Hoang, Sean P. Berglund, Nathan T. Hahn, Allen J. Bard, and C. Buddie Mullins, "Enhancing visible light photo-oxidation of water with TiO_2 nanowire arrays via co-treatment with H_2 and NH_3: Synergistic effects between Ti^{3+} and N," *J. Am. Chem. Soc.* 134, 3659-3662 (2012).

9. Sean P. Berglund, Alex J. E. Rettie, Son Hoang, and C. Buddie Mullins, "Incorporation of Mo and W into nanostructured $BiVO_4$ films for efficient photoelectrochemical water oxidation performance," accepted by *Phys. Chem. Chem. Phys.*

10. Nathan T. Hahn, Vincent C. Holmberg, Brian A. Korgel, and C. Buddie Mullins, "Electrochemical synthesis and characterization of p-$CuBi_2O_4$ thin film photocathodes," *J. Phys. Chem. C*. **116**, 6459-6466 (2012).

11. Son Hoang, Siwei Guo, Nathan T. Hahn, Allen J. Bard, and C. Buddie Mullins, "Visible-light Driven Photoelectrochemical Water Oxidation on Nitrogen-doped TiO_2 Nanowires," *Nano Lett.* 12, 26-32 (2011).

12. Nathan T. Hahn and C. Buddie Mullins, "Photoelectrochemical Performance of Nanostructured Ti- and Sn-doped α-Fe_2O_3 Photoanodes," *Chem. Mater.* 22, 6474-6482 (2010).

13. Nathan T. Hahn, Son Hoang, Jeffrey L. Self, and C. Buddie Mullins, "Spray pyrolysis deposition and photoelectrochemical properties of n-type BiOI nano-platelet thin films," *ACS Nano* submitted.

Session II

Sensitized Semiconductors I

Molecular Design of Zinc Oxide Nanoparticle-Dye Dyads and Triads

Wayne L. Gladfelter, David A. Blank and Kent R. Mann
Department of Chemistry
University of Minnesota
Minneapolis MN 55455

We are studying the fundamental energy and charge transfer dynamics that govern light absorption and charge separation in zinc oxide-based dye-sensitized solar cells (DSSCs). The overarching goal of this research is to study the relationship between structure, energetics, and dynamics in a set of synthetically controlled donor-acceptor dyads and triads. Through the use of well-defined, dispersible sensitizer/ZnO nanocrystal (NC) ensembles, we minimize the problems associated with film heterogeneity. Monodispersed ZnO NCs in the quantum-confined regime (< 6 nm in diameter), prepared by new as well as by published methods, are used as a dispersible platform to which a variety of new sensitizers are attached for study using ultrafast spectroscopic techniques. This presentation summarizes our studies of two sensitizer/ZnO NC dyads and a set of molecular dyads based on iridium.

The first system studied in detail involved the terthiophenecarboxylic acid, **1-CO_2H**, attached to monodispersed ZnO having diameters from 2.7 to 3.2 nm. The excited state of the dye (E^0* = -1.61 V vs NHE) is quenched upon binding to ZnO nanocrystals. Adsorption isotherms are reported for **1-CO_2H** in ethanol and fit with a Langmuir model yielding a NC size-independent K_{ads} of 2.3 ± 1.0 x 10^5 M^{-1}. The maximum number of attached dyes per nanocrystal depends on the diameter and is consistent with each dye occupying 0.5 ± 0.1 nm^2 at maximum coverage. Time-resolved fluorescence and time- and frequency-resolved pump probe spectroscopy confirm and characterize electron injection from the dye to the semiconductor nanocrystals in room temperature ethanol dispersions at a series of dye:ZnO NC concentration ratios. The spectrum of the dye cation was determined by spectroelectrochemistry. The singlet excited state of the dye (190 ps lifetime in ethanol) is quenched almost exclusively by electron transfer to the ZnO NC, and the electron transfer dynamics exhibit a single time scale of ~3.5 ps at all concentration ratios. In the measured transient responses at different dye:ZnO NC ratios, gain in the amplitude of the electron injection component is anti-correlated with loss of amplitude from unperturbed excited state dye molecules.

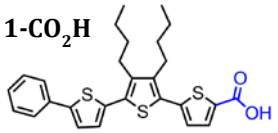

Possibly because the excited state energy of **1-CO_2H** is too far above the conduction band edge, no dependence of the charge injection rate on NC diameter was observed. Use of a substituted zinc tetraphenylporphyrin lowered the excited state energy, which allowed direct measurements of the influence of the available density of acceptor states on the rate of near barrierless electron transfer between the dye sensitizer and the ZnO NCs. The available density of states was tuned by controlling the relative position of the ZnO band edge using quantum confinement as shown in the figure below. The resulting change in the rate was consistent with a simple model of the state density as a function of energy above the ZnO band edge. The relative electron transfer rates were best fit to the Marcus equation in which the reorganization energy (λ) was 0.3 eV (see the right side of the following figure).

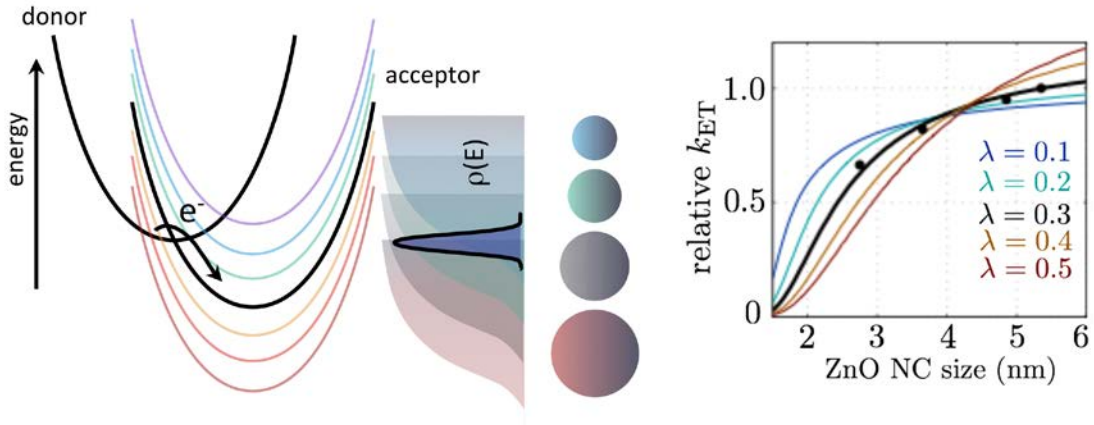

In an effort to increase charge separation we are exploring the impact of adding secondary electron donors to a series of cationic iridium(III) biscyclometalates $[Ir(ppy)_2(bpy)]PF_6$, where ppy and bpy represent phenylpyridine and bipyridine, respectively. Hybrid metal-organic complexes **11** and **12** bear terthiophene pendants ligated through the ppy cap (see structure below). Strong overlap of the intense $\pi \rightarrow \pi^*$ absorptions of the terthiophene pendants with Ir(III) charge transfer bands is evident in complexes of **11** and **12**, precluding the possibility for selective excitation of either chromophore. Photoexcitation (λ_{ex} = 400 nm) affords strong luminescence from the free terthiophene ppy ligand and the complex without terthiophene pendants, with φ_{em} = 0.11. In stark contrast the terthiophene functionalized complexes display near total quenching of luminescence. Computations of the ground and excited state electronic structure using DFT and TD-DFT indicate that both the $-NO_2$ and terthiophene substituents play an important role in excited state deactivation of complexes. A substantial electronic contribution of the $-NO_2$ substituent results in stabilization of the diimine based MO and offers an efficient non-radiative decay pathway for the excited state. Spin-orbit coupling effects of the Ir(III) ion lead to efficient population of the low lying, non-luminescent, triplet states centered on the terthiophene pendants.

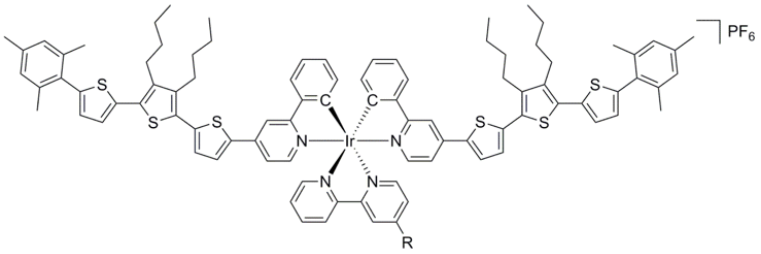

11 R = H $[Ir(3T\text{-}ppy)_2(bpy)]PF_6$

12 R = NO_2 $[Ir(3T\text{-}ppy)(4\text{-}NO_2\text{-}bpy)]PF_6$

Future studies will focus on attaching the molecular dyads to the ZnO NCs, probing the dependence of electron injection rates on the functional group that binds the chromaphore to the surface, and incorporating IR detection into our ultrafast measurements to observe the electron in the ZnO conduction band.

DOE Sponsored Solar Photochemistry Publications 2009-2012

1. Schwartz, K. R.; Chitta, R.; Bohnsack, J. N.; Ceckanowicz, D. J.; Miró, Cramer, C. J.; Mann, K. R. “Effect of Axially Projected Oligothiophene Pendants and Nitro-Functionalize Diimine Ligands on the Lowest Excited State in Cationic Ir(III) bis-Cyclometalates” *Inorg. Chem*. **2012**, *51*, ASAP.

2. Huss, A. S.; Rossini, J. E.; Ceckanowicz, D. J.; Bohnsack, J. N.; Mann, K. R.; Gladfelter, W. L.; Blank, D. A. "Photo-initiated Electron Transfer Dynamics of a Terthiophene Carboxylate on Monodispersed Zinc Oxide Nanocrystals", *J. Phys. Chem. C*, **2011**, *115*, 2-10.

3. Rossini, J. E.; Huss, A. S.; Bohnsack, J. N.; Blank, D. A.; Mann, K. R.; Gladfelter, W. L. "Binding and Static Quenching Behavior of a Terthiophene Carboxylate on Monodispersed Zinc Oxide Nanocrystals", *J. Phys. Chem. C*, **2011**, *115*, 11-17.

4. Schwartz, K. R.; Mann, K. R. “Optical Response of a Cyclometalated Iridium(III) Hydrazino Complex to Carbon Dioxide: Generation of a Strongly Luminescent Iridium(III) Carbazate”, *Inorg. Chem*., **2011**, *50*, 12477-12485.

5. Huss, A. S.; Bierbaum, A, Chitta, R.; Ceckanowicz, D. J.; Mann, K. R.; Gladfelter, W. L.; Blank, D. A. "Tuning Electron Transfer Rates via Systematic Shifts in the Acceptor State Density Using Size Selected ZnO Colloids", *J. Am. Chem. Soc*., **2010**, *132*, 13963-13965.

6. Luo, B.; Kucera, B. E.; Gladfelter, W. L. "Synthesis and Structures of Zinc Alkoxo, Aryloxo and Hydroxo Complexes with an Amido-Diammine Ligand", *Polyhedron*, **2010**, *29*, 2795-2801.

7. Luo, B.; Rossini, J. E.; Gladfelter, W. L. "Zinc Oxide Nanocrystals Stabilized by Alkylammonium Alkylcarbamates" *Langmuir*, **2009**, *25*, 13133-13141.

8. Adam S. Huss, Ted Pappenfus, Jon Bohnsack, Michael Burand, Kent R. Mann, David A. Blank, “The Influence of Internal Charge Transfer on Nonradiative Decay in Substituted Terthiophenes.” *J. Phys. Chem., A*, **2009**, *113*, 10202-10210.

Tuning the Ultrafast Excited-state Dynamics of First-row Transition Metal-based Chromophores

Allison M. Brown, Lindsey L. Jamula, and James K. McCusker
Department of Chemistry
Michigan State University
East Lansing, Michigan 48824-1322

The goal of our research program continues to be the development of chromophores based on earth-abundant first-row transition metal ions for use in dye-sensitized, nanoparticle-based solar cells (DSSCs). A key scientific issue impeding the incorporation of such compounds into solar energy conversion strategies is the profound difference that exists in the intrinsic photophysics of first-row transition metal complexes – particularly those occurring on picosecond and sub-picosecond time scales – relative to their second- and third-row congeners. Our work is therefore focused on developing a fundamental understanding of the nature and origin(s) of these differences through a confluence of synthetic chemistry, a range of steady-state and time-resolved spectroscopies, as well as theory, and to use that knowledge toward the realization of first row-based chromophores that are viable options as sensitizers for DSSCs. This presentation will describe two related trajectories of our research over the past two years, both of which concern complexes of Fe(II).

Identifying the Reaction Coordinate for Ultrafast Excited-state Dynamics. We have been exploring the notion of whether torsional coordinates could be playing a role in the ultrafast CT-to-LF relaxation dynamics exhibited by low-spin Fe(II) chromophores; the idea traces back to work by Purcell in which twisting motions of the primary coordination sphere differentially stabilizes triplet ligand-field excited states (e.g., $^3T_1$), thereby facilitating racemization by increasing $^1A_1/^5T_2$ mixing. Although there is no evidence to suggest (or refute) the notion that the reaction coordinate driving $^5T_2 \rightarrow {}^1A_1$ relaxation will mirror that for charge transfer-state deactivation, we viewed this as a reasonable and synthetically accessible starting point. Our approach was to take a series of related Fe(II) terpyridyl complexes wherein the ligands would be modified with a variety of bulky substitutents with the intention of interfering with motion along twisting coordinates of the compound. As shown in Figure 1, the ultrafast dynamics of this system actually reveal an *acceleration* of the charge transfer-to-ligand-field conversion in response to increased steric bulk; although this not the result we were anticipating, the data shows that we have succeeded in modulating the rate constant for charge transfer-state conversion to the ligand-field manifold. We have therefore studied the photophysics of these compounds in greater detail in order to understand the origin of this result with the goal of reverse-engineering the system to increase the lifetime of the charge-transfer state. Results from variable-temperature time-resolved spectroscopic measurements will be described that point to an increase in the reorganization energy with added steric bulk as

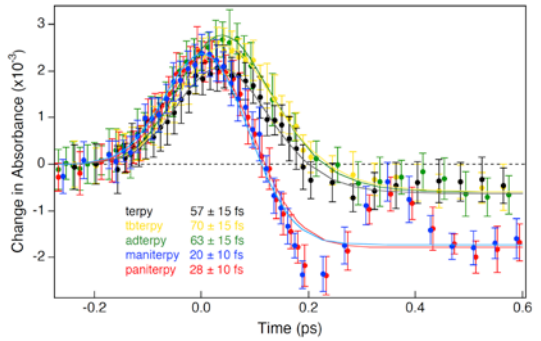

Figure 1. Femtosecond time-resolved absorption data of all five members of the "terpy" series in order of increasing steric bulk. Data were acquired at probe wavelengths appropriate for sampling the terpyridyl radical anion following MLCT excitation in CH_3CN solution.

giving rise to the acceleration in charge transfer-to-ligand field state conversion; this in turn suggests a new synthetic strategy for redesigning the molecular architecture that we believe holds considerable promise for achieving our goal of extending MLCT-state lifetimes so as to make interfacial electron transfer of suitably modified chromo-phores kinetically competitive.

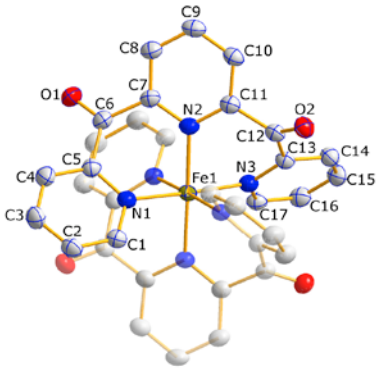

Figure 2. Single-crystal x-ray structure of the cation of $[Fe(dcpp)_2](PF_6)_2$, where dcpp is 2,6-(dicarboxy-pyridyl)pyridine.

Excited-state Inversion: A New Class of Fe(II) Chromophores. The most exciting development over the past two years has been associated with the synthesis and characterization of $[Fe(dcpp)_2]^{2+}$ (where dcpp is di-(carboxylpyridyl)pyridine, Figure 2). Although we often approximate six-coordinate metal polypyridyl complexes such as $[Fe(bpy)_3]^{2+}$ and $[Fe(terpy)_2]^{2+}$ as possessing O_h symmetry, their actual symmetries are much lower (D_3 and C_2 for $[Fe(bpy)_3]^{2+}$ and $[Fe(terpy)_2]^{2+}$, respectively). We therefore sought to develop a compound of much higher symmetry as a means of decreasing the density of states and thereby slow down rates of non-radiative decay. There are a number of unusual features concerning the physical and photophysical properties of $[Fe(dcpp)_2]^{2+}$; in the interest of brevity, we will simply list the most significant ones here: (1) electrochemical measurements reveal a ~600 mV positive shift in the Fe(II)/Fe(III) couple relative to $[Fe(bpy)_3]^{2+}$ and $[Fe(terpy)_2]^{2+}$; (2) the reduction potential of dcpp is ~700 mV positive of both bpy and terpy; (3) the electronic absorption spectrum of $[Fe(dcpp)_2]^{2+}$ in fluid solution (Figure 3) is red-shifted relative to those of both $[Fe(bpy)_3]^{2+}$ and $[Fe(terpy)_2]^{2+}$, exhibiting an absorption maximum near 620 nm that is responsible for the unusual blue color of the compound as both a solid and in solution; (4) the long-lived excited-state lifetime (i.e., the time constant for ground-state recovery) of 280 ± 40 ps for $[Fe(dcpp)_2]^{2+}$ is nearly 4-fold shorter than that of $[Fe(bpy)_3]^{2+}$ under the same conditions. We believe these data point to our having synthesized the first Fe(II) polypyridyl compound possessing a $^3T_1$ term as its lowest-energy excited state (Figure 4). Additional data supporting this assertion will be presented, along with plans to modify this system in such a way as to invert the relative energies of the ligand-field and charge-transfer excited states to produce an Fe(II) complex with photophysical properties analogous to $[Ru(bpy)_3]^{2+}$.

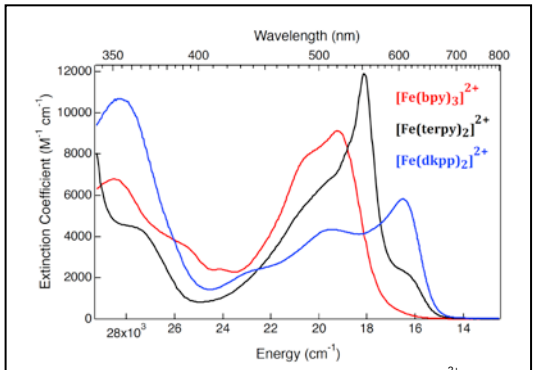

Figure 3. Electronic absorption spectra of $[Fe(bpy)_3]^{2+}$ (red), $[Fe(terpy)_2]^{2+}$ (black), and $[Fe(dcpp)_2]^{2+}$ (blue) in CH_3CN solution.

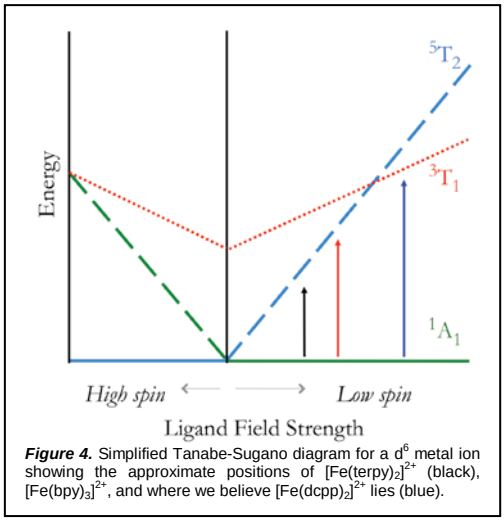

Figure 4. Simplified Tanabe-Sugano diagram for a d^6 metal ion showing the approximate positions of $[Fe(terpy)_2]^{2+}$ (black), $[Fe(bpy)_3]^{2+}$, and where we believe $[Fe(dcpp)_2]^{2+}$ lies (blue).

DOE Sponsored Solar Photochemistry Publications 2009-2012

1. "Probing Reaction Dynamics of Transition-Metal Complexes in Solution via Time-Resolved Soft X-Ray Spectroscopy", Nils Huse, Tae Kyu Kim, Munira Khalil, Lindsey Jamula, James K. McCusker, and Robert W. Schoenlein, in *Ultrafast Phenomena XVI*, Springer Series in Chemical Physics, P. Corkum, S. de Silvestri, and K. Nelson, eds., Springer-Verlag, Berlin, 2009, pp. 125-127.
2. "Photo-induced Spin-State Conversion in Solvated Transition Metal Complexes Probed by Time-resolved Soft X-Ray Spectroscopy", Nils Huse, Tae Kyu Kim, Lindsey Jamula, James K. McCusker, Frank M. F. de Groot, and Robert W. Schoenlein, *J. Am. Chem. Soc.* **2010**, *132*, 6809-6816.
3. "Synthesis and Spectroscopic Characterization of CN-Substituted Bipyridyl Complexes of Ru(II)", Catherine E. McCusker and James K. McCusker, *Inorg. Chem.* **2011**, *50*, 1656-1669.
4. "Femtosecond Soft X-Ray Spectroscopy of Solvated Transition Metal Complexes: Deciphering the Interplay of Electron and Structural Dynamics", Nils Huse, Hana Cho, Kiryong Hong, Tae Kyu Kim, Lindsey Jamula, Frank M. F. de Groot, James K. McCusker, and Robert W. Schoenlein, *J. Phys. Chem. Lett.* **2011**, *2*, 880-884.
5. "Stabilization of a Triplet Ligand-field Excited State in an Octahedral Fe(II) Complex", Lindsey L. Jamula, Allison M. Brown, Dong Guo, and James K. McCusker, *J. Am. Chem. Soc.*, **2012**, under revision.
6. "Transient X-Ray Absorption Spectroscopy of Fe(II) Polypyridyl Complexes", Hana Cho, Matthew L. Strader, Kiryong Hong, Lindsey Jamula, James K. McCusker, Tae Kyu Kim, Robert W. Schoenlein, and Nils Huse, *Faraday Discussions*, submitted for publication.
7. "Determination of the Reorganization Energy for Spin-State Conversion in Six-Coordinate Fe(II) Complexes", Allison M. Brown, Lindsey L. Jamula, J. Andrew Kouzelos, and James K. McCusker, *Chem. Sci.*, submitted for publication.
8. "Vibrational Relaxation Dynamics in Transition Metal-based Charge-Transfer Excited States: A Combined Ultrafast Electronic and Infrared Absorption Study", Catherine E. McCusker, Allison M. Brown, Ana Maria Blanco-Rodriguez, Michael Towrie, Ian P. Clark, Antonin Vlcek, Jr. and James K. McCusker, manuscript in preparation for submission to *J. Am. Chem. Soc.*
9. "Spectroelectrochemical Identification of Charge-Transfer Excited States in Metal Polypyridyl Complexes", Allison M. Brown, Catherine E. McCusker, and James K. McCusker, manuscript in preparation for submission to the *J. Phys. Chem. A.*
10. "Experimental Methodologies for Probing Ultrafast Electron Injection in Dye-Sensitized Solar Cells", Allison M. Brown and James K. McCusker, manuscript in preparation as an invited Perspective for *J. Phys. Chem. Lett.*

Session III

Sensitized Semiconductors II

Surface Chemistry for Photoelectrochemical Charge Transfer at Metal Oxide Interfaces

Robert J. Hamers
Department of Chemistry
University of Wisconsin-Madison
Madison WI 53706

We are developing new interfacial chemistries that will facilitate charge transfer at molecule-semiconductor interfaces and semiconductor-semiconductor heterojunctions. A key element is to explore "click" chemistry as a modular approach to forming interfaces for solar applications. We explored Fe_2O_3, WO_3, TiO_2, SnO_2, and ZnO as model systems spanning oxidation states from 2+ (ZnO) to +6 (WO_3) and electronic structures ranging from sp-band (ZnO and SnO_2) to d-band (TiO_2, WO_3), but have recently focused on SnO_2 and ZnO because of their particularly promising surface chemistry, high electron mobility, and ability to be grown in both nanoparticle and nanorod form, thereby facilitating working on several different nanostructured geometries.

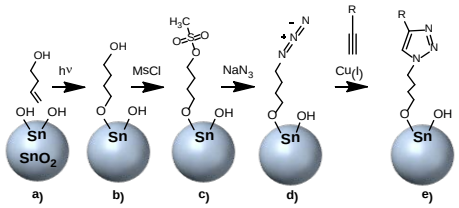

Fig. 1. "Click" chemistry for molecule-surface junctions.

We demonstrated that the Cu(I)-catalyzed Azide-Alkyne Cycloaddition (CuAAC) "click" reaction (Fig. 1) forms a facile, modular route to charge-transferring structures. Photochemical grafting of an OH-terminated alkene to oxide surfaces via UV-initiated grafting yields the best route to azide-terminated surfaces. Using this approach we investigated the photoelectrochemical response of the alkyne-modified $Ru(tpy)_2^{2+}$ complex (Fig. 2) as a model system for a photoelectrochemical charge transfer of molecule-oxide interfaces. XPS, FTIR, transient surface photovoltage (SPV) measurements, and cyclic voltammetry measurements were used to characterize the structure, stability, and electronic properties of the surface adducts; we also compared these with similar adducts on thin-film diamond to help identify the factors controlling long-term stability on oxide surfaces. Our results showed that the "click" chemistry yields adducts with very good charge transfer properties and good stability. The linker length has only a small effect on charge injection, demonstrating that charge transfer occurs largely by "through-space" rather than through-bond tunneling.

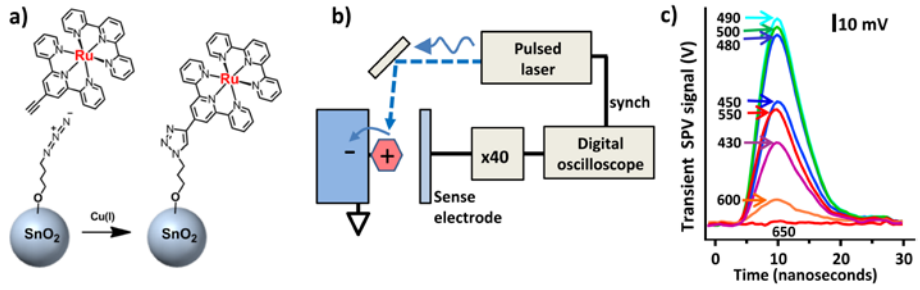

Fig. 2. a) "Click" step to form $Ru(tpy)_2^{2+}$ complex; b) schematic of time-resolved surface photovoltage measurement, and c) Initial charge injection for $Ru(tpy)_2^{2+}/SnO_2$ at different wavelengths.

We extended these ideas to achieve the chemical assembly of oxide-oxide heterojunctions, using the WO_3-TiO_2 , SnO_2-TiO_2 systems, and SnO_2-Fe_2O_3 systems. To make alkyne-modified nanoparticles we synthesized a new citric acid derivative (Fig.3). Together with the azidation

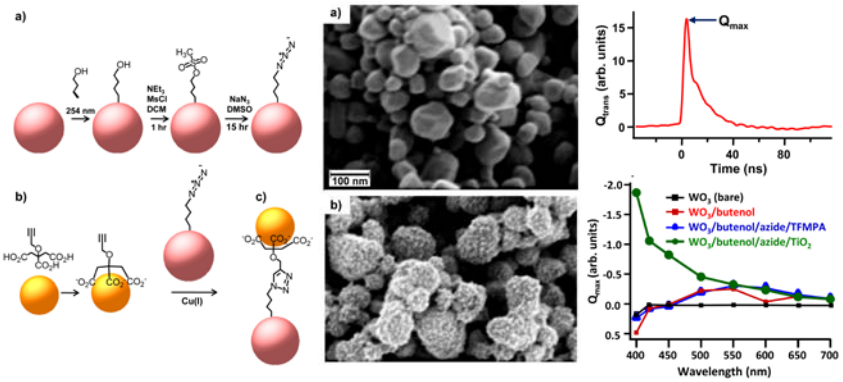

Fig. 3 Chemically assembled WO_3-TiO_2 nanoparticle-nanoparticle heterojunctions and resulting charge transfer properties measured via time-resolved SPV

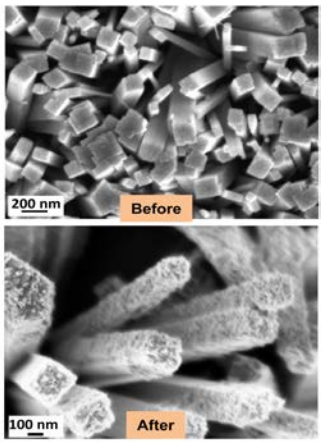

Fig. 4. "Click" assembly of TiO_2 nanoparticles onto SnO_2

process above, this enabled us to fabricate different varieties of particle-nanoparticle and nanoparticle-nanorod adducts. SEM images of TiO_2-WO_3 adducts (Fig. 3) show a conformal coating of 6 nm-diameter TiO_2 nanoparticles over the entire WO_3 surface. Time-resolved surface photovoltage measurements showed excellent charge transfer, and photooxidation of methylene blue demonstrated that the addition of the TiO_2 nanoparticles to the WiO_3 film increased the photocatalytic activity. A similar approach was used to click TiO_2 nanoparticles onto SnO_2 nanorods grown by hydrothermal methods (Fig. 4); TiO_2/SnO_2 and Fe_2O_3/SnO_2 nanoparticle/nanorod adducts were formed and characterized by time-resolved SPV measurements, both showing good charge-transfer properties.

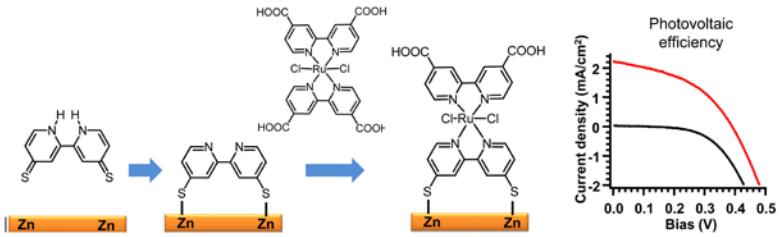

Fig. 5. Interaction of ZnO surface with dithione tautomer of dithio ligand and subsequent "on-surface" assembly of heteroleptic Ru light-harvesting complex. Right: Photovoltaic response measurements in light(red, AM1.5 conditions) and dark (black).

We have also been developing alternative methods for grafting light-harvesting molecules to oxides. Using AFM + XPS we found that 2,2'-dithio-4,4'-bipyridine grafts well to ZnO nanorods, forming high-density, robust layers. We formed thio-containing heteroleptic complexes in solution followed by surface grafting, and compared with a two-step process binding the dithio-bpy ligand to nanorods first and then doing "on-surface" assembly of the remainder of the complex with different bpy derivatives; both approaches were successful. Using complete cells with the I^-/I_3^- redox couple, photovoltaic efficiencies of 1.5% have been achieved thus far.

Future plans are to leverage the expertise developed thus far and using it to form Ru- and Cu-based coordination complexes, focusing primarily on enhancing charge transfer properties of (bpy)- and (tpy)-based light-harvesting molecules linked to high-mobility oxides (HMOs) such as SnO_2 and ZnO. Specific questions include (1) identifying whether additional conformation flexibility enhances packing and charge-transfer efficiency, (2) optimizing the "two-step" approach to form light-harvesting complexes on HMOs and comparing with "click" assembly, (3) identifying how ultra-thin "nano-layer" coatings of d-band oxides such as ZrO_2 or TiO_2 on ZnO and SnO_2 nanorods influence the molecular binding and charge-transfer properties.

DOE Sponsored Solar Photochemistry Publications 2009-2012

Published or accepted manuscripts

1. Rose E. Ruther, Matthew L. Rigsby, James B. Gerken, Stephanie R. Hogendoorn, Elizabeth C. Landis, Shannon S. Stahl, and Robert J. Hamers, "Highly stable redox-active molecular layers by covalent grafting to conductive diamond, *J. Am. Chem. Soc*. **2011**, *133*, 5692-5694 .

2. James B. Gerken, Elizabeth Landis, Robert J. Hamers, Shannon S. Stahl, "Fluoride-modulated cobalt catalysts for electrochemical oxidation of water under non-alkaline conditions" *ChemSusChem* **2010**, *3*, 1176-1179.

3. Michelle C. Benson, Rose E. Ruther, James B. Gerken, Matthew L. Rigsby, Lee M. Bishop, Yizheng Tan, Shannon S. Stahl, and Robert J. Hamers, Modular "Click" Chemistry for Electrochemically and Photoelectrochemically Active Molecular Interfaces to Tin Oxide Surfaces , *ACS Applied Materials and Interfaces*, **2011**, *3*, 3110-3119

4. Lee M. Bishop, Joseph C. Yeager, Xin Chen, Jamie N. Wheeler, Marco D. Torelli, Michelle C. Benson, Steven D. Burke, Joel A. Pedersen, and Robert J. Hamers, "A citric acid-derived ligand for modular functionalization of metal oxide surfaces via "click" chemistry", *Langmuir, **2012**, 28, 1322-1329.*

5. Allison C. Cardiel, Michelle Benson, Lee Bishop, Kacie M. Louis, Joseph C. Yeager, Yizheng Tan, and Robert J. Hamers, "Chemically Directed Assembly of Photoactive Metal Oxide Nanoparticle Heterojunctions via the Copper-Catalyzed Azide–Alkyne Cycloaddition "Click" Reaction", *ACS Nano* **2012**, *6*, 310-318. (Highlighted in C&E News "News of the Week").

6. Ruben Gonzalez-Moreno, Peter L. Cook, Ioannis Zegkinoglou, Xiaosong Liu, Phillip S. Johnson Wanli Yang ,Rose E. Ruther, Robert J. Hamers, Ramon Tena-Zaera, Franz J. Himpsel, J. Enrique Ortega, Celia Rogera, "Attachment of Protoporphyrin Dyes to Nanostructured ZnO Surfaces: Characterization by Near Edge X-ray Absorption Fine Structure Spectroscopy", *Journal of Physical Chemistry C*, **2011**, *115*, 18195-1820.

7. Sohil Shah, Michelle C. Benson, Lee M. Bishop, Alex M. Huhn, Rose E. Ruther, Joseph C. Yeager, and Robert J. Hamers, " Chemically assembled heterojunctions of SnO_2 nanorods with TiO_2 nanoparticles via "click" chemistry" *Journal of Materials Chemistry*, **accepted**.

Submitted manuscripts currently under review

8. Jixin Chen, Rose E. Ruther, Yizheng Tan, Lee M. Bishop, Robert J. Hamers, "Molecular Adsorption on ZnO(10-10) Single Crystal Surfaces: Morphology and Charge Transfer", *Langmuir*, **submitted**.

In preparation:

9. Jixin Chen, Rose E. Ruther, Yizheng Tan, Robert J. Hamers "Bipyridine Dithione as an Efficient Linker to Graft Heteroleptic Ruthenium Dyes to ZnO Nanowire Surfaces", *Journal of the American Chemical Society*, submission planned 4/2012.

10. Robert J. Hamers, Michelle Benson, Rose Ruther, Rebecca Putans, Jixin Chen: "Click" chemistry for Modular Assembly of 'Smart' Surfaces, *Chemical Communications* (invited paper), submission planned 4/2012.

11. Michelle Benson, Jixin Chen, Rose Ruther, and Robert J. Hamers, "Electrochemical and Photoelectrochemical Properties of Ruthenium Coordination Complexes Grafted to SnO_2 nanorods and fluorinated tin oxide (FTO) surfaces by "click" Chemistry", submission planned 5/2012.

Invited papers currently in preparation (all will feature DOE-supported work with planned submission before end of current grant period)

12. Invited Feature paper, Journal of Physical Chemistry (target date June, 2012)

13. Invited Feature article, Energy and Environmental Science (target date July, 2012)

Quantum Dot Sensitization of Single Crystal Semiconductors

Justin B. Sambur[1], Dae Jin Choi[1], Shannon Riha[2], Thomas Novet[3] and B. A. Parkinson[1]

[1]Department of Chemistry and School of Energy Resources
University of Wyoming
Laramie WY 82071

[2]Department of Chemistry
Colorado State University
Ft. Collins CO 80523

[3]Voxtel Inc.
Beaverton OR 97006

The last few years our studies of single crystal oxide sensitization have concentrated on covalently bound quantum dot (QD) sensitizers. QDs have been investigated as sensitizers because of their potential for enhanced stability compared to conventional dyes, as well as high light absorption cross sections that can be tuned to cover a large fraction of the solar spectrum simply by varying the particle size. Despite such beneficial attributes, quantum dot sensitized solar cells (QDSSCs) have not achieved efficiencies or stabilities competitive with conventional dye sensitized solar cells. One reason for this is that the surface chemistry for the chemical attachment of the QDs to the TiO_2 surface was not well understood or controlled. In several of our recent studies we used single crystals of both the anatase and rutile forms of TiO_2 as simple model systems to evaluate the influence of different QD attachment procedures on the electronic coupling of CdSe QDs and CdSe/ZnS core/shell QDs to the TiO_2 surface by measuring the photocurrent yields due to electron transfer from photoexcited QDs into TiO_2. We utilized a surface chemistry strategy whereby short-chain, bifunctional passivating ligands such as 3-mercaptopropionic acid (MPA) stabilize the QDs in water while chemically binding the nanocrystals to the TiO_2 surface via thiolate and carboxylic acid moieties, respectively. Atomic force microscopy (AFM) confirmed that our surface chemistry strategy reproducibly resulted in a single layer of QDs covalently bound to the atomically flat single crystal substrates with no three dimensional QD clusters.

Once we had established that we could reproducibly bind and characterize CdSe QDs to TiO_2 crystal surfaces, we turned our attention to another possible benefit of QD sensitization where multiple carriers could be generated from a single photon of energy greater than twice the energy gap of the QD. The multiple exciton generation (MEG) process had been well established in colloidal QD systems but there were no demonstrations of actually collecting the current due to MEG (MEC – multiple electron collection) in a photovoltaic system. The energy band alignment needed for MEG collection could be obtained from switching to PbS QDs that have a low bulk band gap value of 0.37-0.41 eV at 300 K. PbS QDs are readily synthesized with band gap energies ranging from 0.5 to 2.0 eV, making it possible to measure sensitized photocurrents associated with MEG using photons sufficiently low in energy to preclude direct excitation of the TiO_2 band gap (3.0 eV for rutile and 3.2 eV for anatase).

The kinetically controlled pathways and the rates for photogenerated electrons and holes for a QD sensitization process are depicted in Fig. 1. Where it is apparent that electron injection and regeneration can compete with the biexciton lifetime.

Fig. 1. Band energy diagram indicating the relevant energy levels and kinetic processes that describe PbS QD electron and hole transfer (ET and HT) into the TiO_2 conduction band and the sulfide/polysulfide electrolyte, respectively. (A) Energy level alignment of the TiO_2 conduction band with variously sized PbS QDs and the S/S^{2-} redox couple at pH 13. The inset shows the band gap energies of TiO_2 and the QDs. (B) Representation of a QD adsorbed on a TiO_2 single crystal and the approximate time scales for efficient ET and HT compared to the biexciton lifetime (τ_{xx}) as well as other possible recombination pathways. $1S_e$ and $1S_h$ refer to the first excited electron and hole state, respectively. Red and brown arrows indicate the favorable processes and possible recombination pathways, respectively.

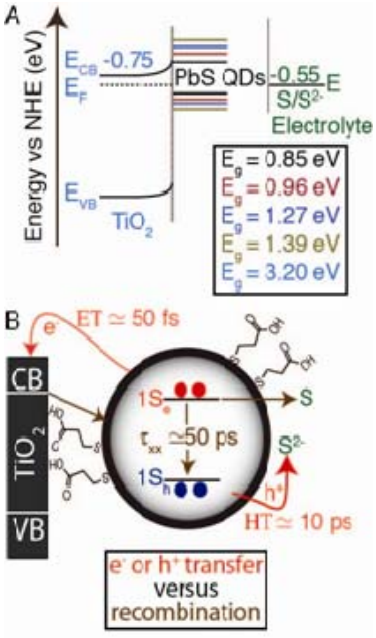

Figure 2 shows the absorbed photon photocurrent efficiencies (APCE) obtained for a monolayer of PbS QDs on an anatase (001) crystal surface. It shows that for PbS QDs with an energy gap of about 1 eV there is a transition from quantum yields less than one to values that are greater than one at about 2.7 times the band gap of the PbS QDs demonstrating the MEG can be harvested effectively at the semiconductor QD interface. Recent work has involved designing QD semiconductor systems where APCE values approaching 3 can be achieved.

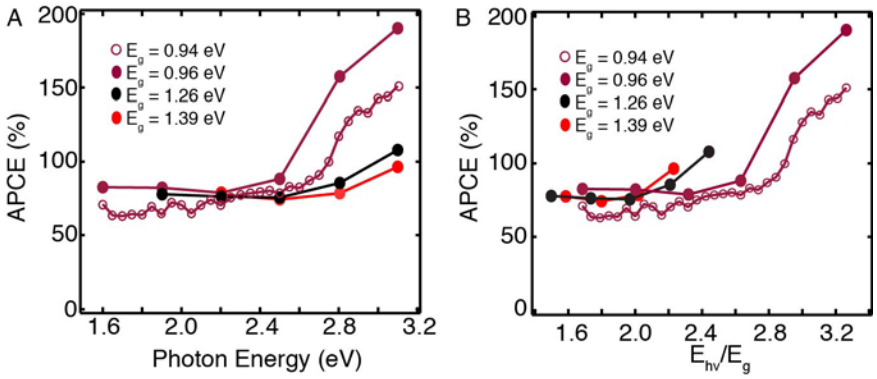

Fig. 2. Absorbed photon to current efficiency (APCE) values as a function of the illumination energy. (A) APCE vs. the absolute incident photon energy. (B) APCE vs. the incident photon energy divided by the QD band gap energy (indicating the multiples of the band gap). Adjustments to increase the APCE due to solution absorption and reflection from the cell window and TiO_2 crystal were not performed.

DOE Sponsored Solar Photochemistry Publications 2009-2012

1. Justin B. Sambur, Christopher M. Averill, Colin Bradley, Jennifer Schuttlefield, Seoung Ho Lee, John R. Reynolds, Kirk S. Schanze and B. A. Parkinson, "Interfacial Morphology and Photoelectrochemistry of Conjugated Polyelectrolytes Adsorbed on Single Crystal TiO_2", Langmuir, 27, 11906-11916, (2011)
2. Douglas Shepherd, Justin B. Sambur, Yong-Qi Liang, B. A. Parkinson, Alan Van Orden, "In-Situ Studies of Photoluminescence Quenching in Single Crystal Quantum Dot Sensitized Solar Cells", J. Phys. Chem., submitted
3. Justin B. Sambur, Thomas Novet and B. A. Parkinson, "Multiple Exciton Collection in a Sensitized Photovoltaic System", Science, 330, 63-66, (2010)
4. Justin B. Sambur and B. A. Parkinson, "CdSe/ZnS Core/Shell Quantum Dot Sensitization of Low Index TiO_2 Single Crystal Surfaces", J. Am. Chem. Soc., 132 (7), 2130–2131, (2010)
5. Justin B. Sambur, Shannon C. Riha, Dae Jin Choi and B. A. Parkinson, " The Influence of Surface Chemistry on the Binding and Electronic Coupling of CdSe Quantum Dots to Single Crystal TiO_2 Surfaces", Langmuir, 26(7), 4839–4847, (2010)
6. Mark T. Spitler and B. A. Parkinson, "Dye Sensitization of Single Crystal Semiconductor Electrodes", Accounts of Chemical Research, 42, 2017-2029, (2009)

Single-Particle Current Blinking in Semiconductor Quantum Dots

Klara Maturova and Jao van de Lagemaat
Chemical and Materials Sciences Center
National Renewable Energy Laboratory
Golden, Colorado 80401

Blinking of the fluorescence of single molecules and single semiconductor quantum dots (QDs) has been observed by many authors before.[1-4] For semiconductor quantum dots, the most common explanation is trapping at the quantum dot surface[2] but the explanation for this phenomenon remains controversial though the fluorescence blinking of single quantum dots has been widely studied, the correlated phenomenon of single particle conduction has not been widely studied. If luminescence blinking is caused by trapped charges, one expects that the tunneling current also blinks due to Coulomb blockade effects. There are many observations of single quantum dot tunneling spectroscopy in scanning tunneling microscopy setups where energy level positions, charging energies, correlation energies, electron-phonon coupling and more have been determined.[5,6] It was also observed that it is possible to obtain structures where the tunneling into a dot is dependent on the presence of another charge trapped on the dot.[7] Similar effects on the current through a particle should be observed in single particle tunneling but have not yet been demonstrated.

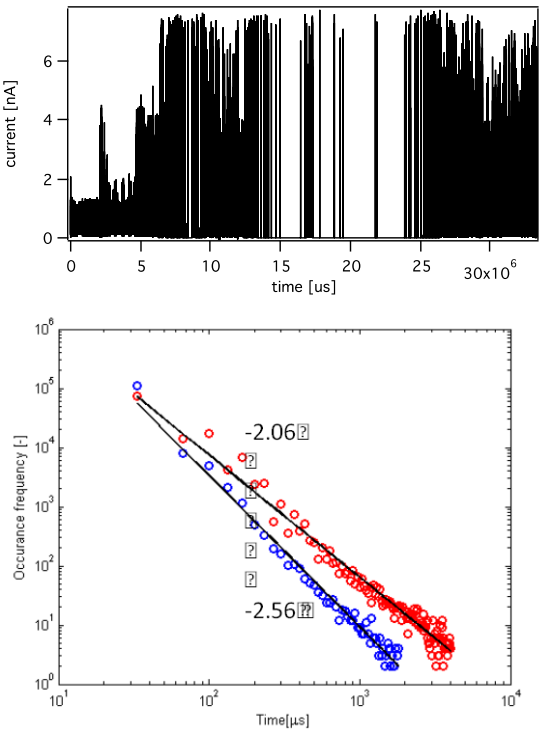

Figure 1. Top: Current through a single CdSe QD. 'on' and 'off' behavior is observed as as well as multiple current levels. Bottom: Current blinking statistics of a single PbS QD for the "bright" (red) and dark (blue) states.

We have recently extended our AFM/STM setup to allow for time-resolved injection of current using a tapping mode scheme. The tip is oscillated above the surface and on the downward "tap", when the tip is in contact with the surface, current is injected. This scheme allows for microsecond resolution of the current depending on the oscillation frequency of the tip while at the same time decoupling the current from the microscope's height feedback mechanism. We are currently applying this new technique to semiconductor QDs and quantum rods (Qrods) such as CdSe, PbS, and PbSe connected to atomically flat gold substrates using dithiol linkers. In these experiments, when the tip injects into gold, only a single pulse of current is observed. However, when the tip is addressing a QD, we observe multiple current pulses that are clearly distinct during a single tapping event, as well as complete current suppression throughout the tap. Our hypothesis is that these current oscillations are caused by a dynamic charging effect owing to electrons becoming trapped, turning on and off the conduction channel to the substrate. We also observe multiple

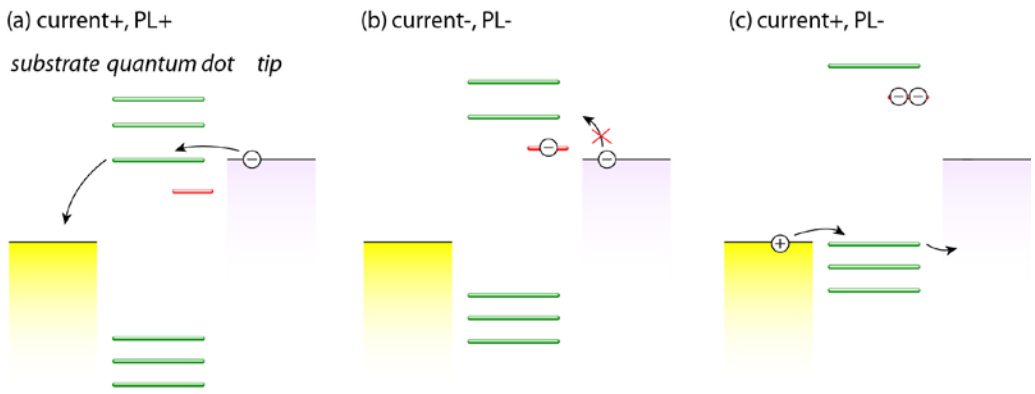

Figure 2. Scheme for correlation between luminescence and current blinking for a single quantum dot. In (a) there is no trapped charge on the surface and both current and PL are active. In (b) there is a single charge on the dot, turning off the current by Coulomb blockade and simultaneously turning off the PL. In (c) two charges reside on the dot, enabling a new current channel through the valence levels of the dot, while still showing no PL. In all cases, the tip/substrate voltage difference is constant and the dot's energy levels shift because of the charging of the dot's capacitance by the trapped charge.

charge states of the dots as distinctly different current plateaus in the current blinking behavior (Fig. 1 top panel). These different levels are likely due to different valence levels on the dot becoming resonant. The proposed mechanism (Fig. 2) for the current blinking is similar to that for luminescence blinking where an electron is trapped at the surface of the QD and extinguishes the PL. The presence of this trapped electron also shifts energy levels bringing the QD out of resonance for current flow. This assertion is supported by the observation of power-law behavior of the on and off times of current (Fig. 1, bottom panel). Such power law behavior is observed in our experiment for CdSe, PbS, and PbSe Qrods and QDs. Figure 2 illustrates the mechanism that is hypothesized for the current blinking observed in the current experiment. This mechanism predicts that there is a correlation between current blinking and luminescence blinking. In the ground state of the dot (no trapped charge), the dot is active both in current and photoluminescence (PL). With a single charge on the dot, it becomes inactive in both current and PL. However, with multiple charges trapped on the dot's surface, it is expected that the dot becomes active again in current spectroscopy but remains "dark" in the PL. A better understanding of the blinking of the current is relevant for the understanding of charge transport in larger systems such as QD arrays. Fluctuating conduction through individual particles because of Coulomb blockade effects should have an effect on conduction in assemblies.[8] Also, the power-law behavior of the on and off statistics of conduction through the dots can be expected to result in an approximately power law behavior of charge mobilities in arrays similar to that observed when exponential band tails are present such as those observed in TiO_2 and other nanoparticle systems.[9,10]

Future experiments will involve correlating the current blinking with PL as well as with photocurrent in single quantum dots and rods as well as small clusters of dots to study the influence of the current blinking on longer scale conduction. We also plan to more closely study the influence of surface plasmon fields and surface plasmon/exciton hybridization on the blinking dynamics.[11]

References

(1) Peterson, J.; Krauss, T. *Nanolett.* **2006**, *6*, 510–514.

(2) Galland, C.; Ghosh, Y.; Steinbrück, A.; Sykora, M.; Hollingsworth, J. A.; Klimov, V. I.; Htoon, H. *Nature* **2011**, *479*, 203–207.

(3) Crouch, C. H.; Mohr, R.; Emmons, T.; Wang, S.; Drndić, M. *J Phys Chem C* **2009**, *113*, 12059–12066.

(4) Neuhauser, R.; Shimizu, K.; Woo, W.; Empedocles, S.; Bawendi, M. G. *Phys. Rev. Lett.* **2000**, *85*, 3301–3304.

(5) Sun, Z.; Swart, I.; Delerue, C.; Vanmaekelbergh, D.; Liljeroth, P. *Phys. Rev. Lett.* **2009**, *102*, 196401.

(6) Overgaag, K.; Vanmaekelbergh, D.; Liljeroth, P.; Mahieu, G.; Grandidier, B.; Delerue, C.; Allan, G. *J Chem Phys* **2009**, *131*, 224510.

(7) Swart, I.; Sun, Z.; Vanmaekelbergh, D.; Liljeroth, P. *Nanolett.* **2010**, 100414140231023.

(8) Romero, H.; Drndić, M. *Phys. Rev. Lett.* **2005**, *95*, 156801.

(9) van de lagemaat, J.; Kopidakis, N.; Neale, N. R.; Frank, A. J. *Phys. Rev. B* **2005**, *71*, 035304.

(10) Gao, J. B.; Johnson, J. C. *ACS Nano* **2012**, accepted.

(11) Romero, M. J.; van de lagemaat, J. *Phys. Rev. B* **2009**, *80*, 115432.

DOE Sponsored Solar Photochemistry Publications 2009-2012

1. Morfa A.J., R. T. H., Johnson J.C., van de Lagemaat J. (2009). "Plasmons in solar energy conversion." SPIE Newsroom. Doi:10.1117/2.1200906.1651
2. Romero, M. J., A. J. Morfa, T. H. Reilly, III, J. van de Lagemaat and M. Al-Jassim (2009). "*Nanoscale Imaging of Exciton Transport in Organic Photovoltaic Semiconductors by Tip-Enhanced Tunneling Luminescence*." Nano Lett. **9**(11): 3904-3908. Doi:10.1021/nl902105f
3. Romero, M. J. and J. van de Lagemaat (2009). "*Luminescence of quantum dots by coupling with nonradiative surface plasmon modes in a scanning tunneling microscope*." Phys. Rev. B **80**(11): 115432. Doi:10.1103/PhysRevB.80.115432
4. Johnson, J. C., T. H. Reilly, III, A. C. Kanarr and J. van de Lagemaat (2009). "*The Ultrafast Photophysics of Pentacene Coupled to Surface Plasmon Active Nanohole Films*." Journal of Physical Chemistry C **113**(16): 6871-6877. Doi:10.1021/jp901419s
5. Morfa, A. J., A. M. Nardes, S. E. Shaheen, N. Kopidakis and J. van de lagemaat (2011). "*Time-of-Flight Studies of Electron-Collection Kinetics in Polymer:Fullerene Bulk-Heterojunction Solar Cells*." Adv. Funct. Mat. **21**(13): 2580-2586. Doi:10.1002/adfm.201100432
6. Yu, E. T. and J. van de Lagemaat (2011). "*Photon management for photovoltaics*." MRS Bull. **36**(6): 424-432. Doi:10.1557/mrs.2011.109
7. Liang, Z., A. M. Nardes, J. van de Lagemaat and B. A. Gregg (2012). "*Activation Energy Spectra: Insights into Transport Limitations of Organic Semiconductors and Photovoltaic Cells*." Advanced Functional Materials **22**(5): 1087-1091. Doi:10.1002/adfm.201102813
8. Senyuk, B., J. S. Evans, P. J. Ackerman, T. Lee, P. Manna, L. Vigderman, E. R. Zubarev, J. van de Lagemaat and I. I. Smalyukh (2012). "*Shape-Dependent Oriented Trapping and Scaffolding of Plasmonic Nanoparticles by Topological Defects for Self-Assembly of Colloidal Dimers in Liquid Crystals*." Nano Lett. **12**(2): 955-963. Doi:10.1021/nl204030t

Session IV

Systems for Photoconversion

Photovoltaic and Photochemical Properties of Conjugated Ionomer Junctions

Thomas J. Mills, Stephen G. Robinson, Ethan M. Walker, Chris Weber, and Mark C. Lonergan
Department of Chemistry
University of Oregon
Eugene OR 97403

We are studying several aspects of the photochemistry of conjugated polymers with ionic functional groups (conjugated ionomers or polyelectrolytes). We have described how the asymmetry in ion content at a junction between a conjugated anionomer and cationomer can give rise to a photovoltaic effect, that ionic functional groups can be used to control the redox chemistry of conjugated polymers in a way that enables the synthesis of p-n homojunctions with control over dopant density, and that ionic functional groups have a substantial affect on the photochemical oxidation of conjugated polymers due to a dramatic stabilization of the oxygen-conjugated polymer charge-transfer complex.

Typical organic photovoltaics rely on an asymmetry in frontier orbital positions to separate excitons. We have explored other possible asymmetries for that same purpose. In one area, we have studied the asymmetry created by an interface between anionically and cationically functionalized versions of the same conjugated polymer, as shown inset in Figure 1. In principle, the exchange of ions at the interface can give rise to a charge depletion region and built-in electric field, just as in a conventional p-n junction. Indeed a photovoltaic effect is observed as shown in Figure 1. Using transient absorption spectroscopy, we demonstrated that the photovoltaic effect results from the photochemical doping of the anionomer layer to form a p-type region and the cationomer layer to form an n-type region; light pumps ions to create a transient p-n junction. This photochemical doping creates the electronic quasi-Fermi level splitting required for a photovoltaic effect. We have further explored this photochemical doping using a quasi-free electron, numerical model as part of an effort to understand charge injection in conjugated ionomers, both photoinduced and from electrified interfaces.

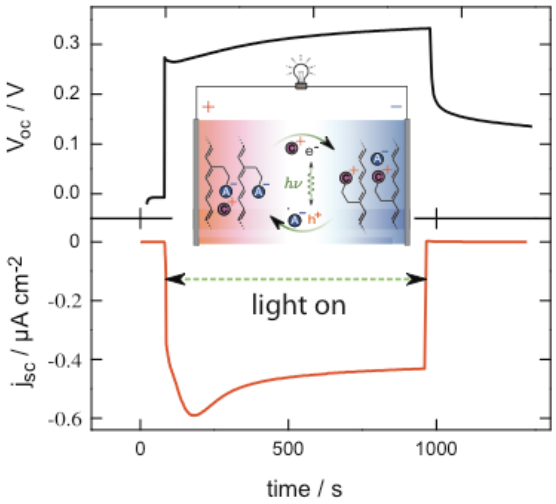

Figure 1. Photochemical doping and photovoltaic effect at a polyacetylene anionomer/cationomer junction.

The p-n junction created by ion motion and the photochemical doping of the polyacetylene anionomer/cationomer junction is only transient. Once the light is removed the junction returns to its initially undoped state. In principle, a stable p-n junction can be formed if the ions are removed to create internally compensated states, where the charges injected into the polymer backbone are balanced by covalently bound ionic functional groups. We have developed

polyelectrolyte mediated electrochemistry (PMEC) as a route to p-n homojunctions. It is important to note that here, and above, the terms n- and p- mean truly doped states, rather than labels of donor and acceptor as is common usage in organic photovoltaics. To date, all methods of forming doped p-n junctions have been two-electrode approaches where the doping levels of the n- and p-type region cannot be independently controlled. Using a three-electrode PMEC technique, we have fabricated p-n junctions with independent control over n- and p-doping. Using this technique, we have systematically studied the affect of doping level on the electrical and photovoltaic properties of conjugated polymer p-n junctions. For instance, Figure 2 shows a series of current density-voltage curves for junctions where the dopant density of the n-type layer is varied by a factor of 20. Both the asymmetry and equilibrium exchange current are strongly affected by the doping level. The incident photon to electron conversion efficiency for the is low, but it systematically varies with dopant density.

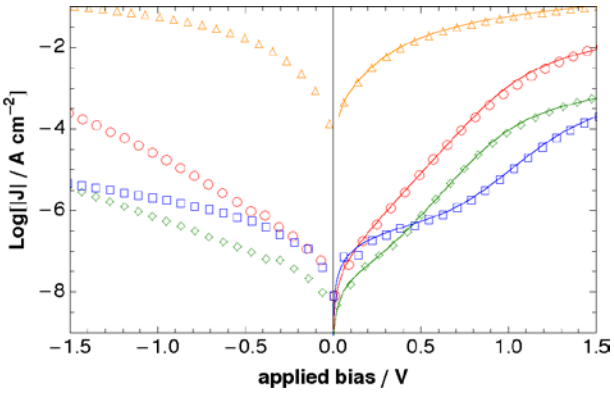

Figure 2. Current density-voltage curves for polyacetylene p-n junctions as a function of the doping level of the n-type region.

In our exploration of the photochemistry of conjugated ionomer junctions, we have discovered that their reactivity with oxygen to form charge-transfer complexes is very different than with their non-ionic counterparts. Conjugated polymers are well known to undergo photochemical autoxidation. We have demonstrated that anionic functional groups and their associated cations dramatically alter the stability of the oxygen-conjugated polymer charge transfer complex. For instance, Figure 3 shows the results of a photochemical oxidation study performed on a thin film of a sulfonate functionalized polyacetylene with regions containing different counterions. The polymer is a Na^+ salt except for the O-shaped region where it is a tetramethylamonium (TMA^+) salt. The left image was taken immediately after solid-state ion exchange. The change in color is due to the rapid formation of the polymer-oxygen charge transfer complex, as is clearly evident in the NIR spectrum of the polymer. Despite this initial reaction with oxygen, the overall photobleaching of the Na^+ salt is much slower than the TMA^+ salt. The image on the right shows the same film after 15 days under photooxidative conditions. As can be seen, the TMA region is completely bleached, whereas the Na^+ region remains highly colored. The sulfonate functional groups and Na^+ counter-ion are believed to participate in the charge-transfer complex resulting in its substantial stabilization. The stability depends on the charge density of the cation, and the same effect is observed in polythiophene-based polyelectrolytes.

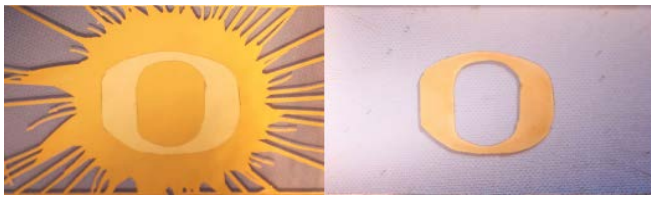

Figure 3. Sulfonate functionalized polyacetylene ionomer with tetramethylammonium (O-shaped region) and Na^+ counter ion immediately after ion exchange (left) and after 15 days under photo-oxidative conditions (right).

DOE Sponsored Solar Photochemistry Publications 2009-2012

1. S.G. Robinson, D.H. Johnston, Christopher D. Weber, Mark C. Lonergan, "Polyelectrolyte-Mediated Electrochemical Fabrication of a Polyacetylene p-n Junction," *Chem. of Mater*. **22**, 241 (2010).

2. D.P. Stay, S.G. Robinson, M.C. Lonergan in *Iontronics*, "Development and Application of Ion-functionalized Conjugated Polymers," edited by J. Leger, M. Berggren, and S. Carter (CRC Press, Taylor and Francis Group, Boca Raton, Fl, 2011).F. Lin, E.M. Walker, M.C. Lonergan, "Photochemical Doping of an Adaptive Mix-Conducting p-n Junction," *J. Phys. Chem. Lett.* **1**, 720 (2010).

3. B.D. Rose, D.T. Chase, C.D. Weber, L.N. Zakharov, M.C. Lonergan, M.M. Haley, "Synthesis, Crystal Structures, and Photophysical Properties of Electron-Accepting Diethynylindenofluorenediones," *Org. Lett.* **13**, 2106 (2011).

4. C.D. Weber, S.G. Robinson, and M.C. Lonergan, "Ionic Functionality and the Polyacetylene–Oxygen Charge-Transfer Complex," *Macromolecules* **44**, 4600 (2011).

5. D.T. Chase, A.G. Fix, B.D. Rose, C.D. Weber, S. Nobusue, C. E. Stockwell, L. N. Zakharov, M. C. Lonergan, M. M. Haley, "Electron-Accepting 6,12-Diethynylindeno[1,2-b]fluorenes: Synthesis, Crystal Structures, and Photophysical Properties" *Angew. Chem.* **50**, 11103 (2011) .

6. T.J. Mills, and M.C. Lonergan, "Charge injection and transport in low-mobility mixed ionic/electronic conducting systems: Regimes of behavior and limiting cases" *Phys. Rev. B* *85, 035203 (2012)

7. Christopher D. Weber, Stephen G. Robinson, David P. Stay, Chris L. Vonnegut, and Mark C. Lonergan, "Ionic Stabilization of the Polythiophene-Oxygen Charge-Transfer Complex" ACS *Macro Letters*, Web: DOI: 10.1021/mz300046x (2012).

8. Stephen G. Robinson and Mark C. Lonergan, "Ionically Functionalized Polyacetylenes" in *Conjugated Polyelectrolytes: Fundamentals and Applications in Emerging Technologies*, B. Liu and G. Bazan, eds., *in press* (2012).

9. Chase, Daniel; Fix, Aaron; Kang, Seok Ju; Rose, Bradley; Weber, Christopher; Zhong, Yu; Zakharov, Lev; Lonergan, Mark; Nuckolls, Colin; Haley, Michael "6,12-Diarylindeno[1,2-b]fluorenes: Syntheses, Photophysics and Ambipolar OFETs," *J. Amer. Chem. Soc.*, submitted (2012).

Nanoscaled Components for Improved Efficiency in a Multiplanel Photocatalytic Water-Splitting System

Marye Anne Fox, James K Whitesell and Xuebin Shao
Department of Chemistry and Biochemistry
University of California, San Diego
La Jolla, CA 92093-0358

We have constructed a practical photolytic system for quantum efficient production of hydrogen. Our approach is based on the assembly of a multi-component integrated system for direct photocatalytic splitting of water for the efficient production of hydrogen. We propose to produce hydrogen as an energy source that is cost competitive with fossil fuels and without the concomitant production of greenhouse gases.

The concept is quite straightforward. In order to achieve the over potential required for direct water splitting, the device is composed of multiple dye-sensitized cells directly linked in series, as illustrated in the figure below. The advantage of this concept is that each cell need contribute only a fraction of the overall potential required for water splitting, thus permitting device engineering to maximized efficiently without regard to electric potential. Progress and barriers to practical application will be described.

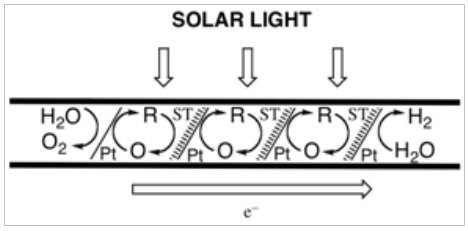

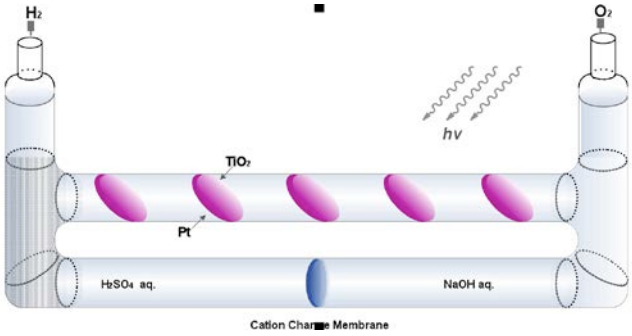

ST = Sensitizer Dispersed on metal oxide or polymer support
Pt = Platinum
R = Reduced Species
O = Oxidized Species

TiO_2 photocatalytic materials are especially attractive for their non-toxic, clean and low-cost properties as well as their thermal stability. Usually, TiO_2 can be prepared by wet process (e.g. sol-gel), anodization or sputtering method. As shown in some papers, the thin TiO_2 films synthesized by a wet process have shown high photocatalytic reactivity, but their mechanical durability is less stable. In our previous efforts in this field, TiO_2 films were prepared by the

high-voltage anodization technique. Formation of H_2 and O_2 gas was observed using our multipanel photocatalytic water-splitting device under Xe lamp.

We have prepared a new series of ruthenium based dye sensitizers T1, T2, & T2) that exhibit broad absorption in the region of the solar spectrum. The preparation of these materials is straight forward and proceeds in good overall yield. The syntheses are readily amendable for the preparation of derivatives in order to fine tune absorption characteristics.

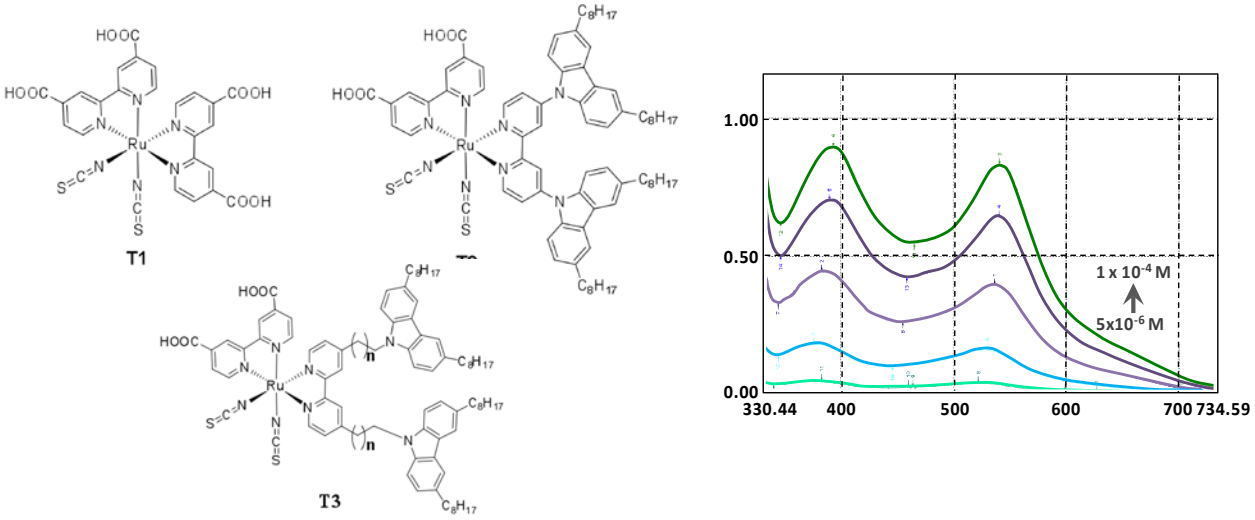

1) Krishnan, M.; White, J.R.; Fox, M.A.; Bard, A.J. J. Am. Chem. Soc. 1983, 105,7002. Smotkin, E. Bard, A.J.; Campion, A.; Fox, M.A.; Mallouk, T.; Webber, S.E.; White, J.M. J. Phys. Chem. 1986, 90, 4604. Smotkin, E. Bard, A.J.; Campion, A.; Fox, M.A.; Mallouk, T.; Webber, S.E.; White, J.M. J. Phys. Chem. 1987, 91, 6. Dabestani, R.; Bard, A.J.; Campion, A.; Fox, M.A.; Mallouk, T.; Webber, S.E.; White, J.M. J. Phys. Chem. 1988, 92, 1872.

The consequences of stable and continuing investment in basic research

In response to recent agency inquiries on the value of uninterrupted sponsored research, we have undertaken an analysis of the productivity of the DOE Solar Photochemistry program as a source for evolutionary and revolutionary progress. This program, having been funded continuously by the DOE Office of Science for over three decades, is likely to provide special insight into how fundamental science is enhanced or impeded by shifts in programmatic direction. A description of the analysis and a call for assistance in identifying patents and other IP deriving from this long term investment will be presented.

DOE Sponsored Solar Photochemistry Publications 2009-2012

"The Effect of Dye Density on the Efficiency of Photosensitization of TiO2 Films: Light-Harvesting by Phenothiazine-labeled Dendritic Ruthenium Complexes," Marye Anne Fox, James K. Whitesell, Linyong Zhu, and Douglas Magde, *Molecules* **2009**, *14*, 3851-3867.

"Optical and Electrochemical Properties of Shell-Core Dendrimers: Ruthenium Coordination Complexes Capped with a Range of Sized Phenothiazine-substituted Bipyridines," Linyong Zhu, Douglas Magde, James K. Whitesell, and Marye Anne Fox, *Inorg. Chem.* **2009**, *48*, 1811-1818.

Session V

Complex Catalysis

How to Reduce Dinitrogen Catalytically to Ammonia with Protons and Electrons

Richard R. Schrock
Department of Chemistry
Massachusetts Institute of Technology
Cambridge MA 02139

Isolation of the first dinitrogen complex, $[Ru(NH_3)_5(N_2)]^{2+}$,[1] sparked decades of research aimed toward the reduction of dinitrogen to ammonia catalytically under mild conditions in solution with protons and electrons, or toward the combination of dinitrogen with other elements in a selective manner under mild conditions. Catalytic reduction of dinitrogen to ammonia in solution with protons and electrons proved to be extraordinarily challenging since (*inter alia*) protons typically are reduced to dihydrogen readily whereas dinitrogen is relatively resistant to reduction. The principles of reduction of dinitrogen to ammonia at a single Mo(0) or W(0) center were established in studies that began in the late 60's, primarily by the groups directed by Chatt and Hidai, but no catalytic reduction of dinitrogen to ammonia in the presence of protons and electrons was ever achieved.

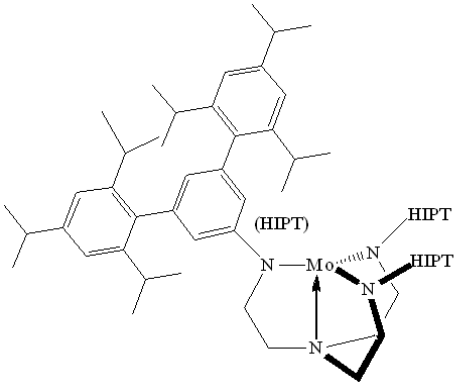

Figure 1. The Mo(III) core of $[HIPTN_3N]Mo$ complexes.

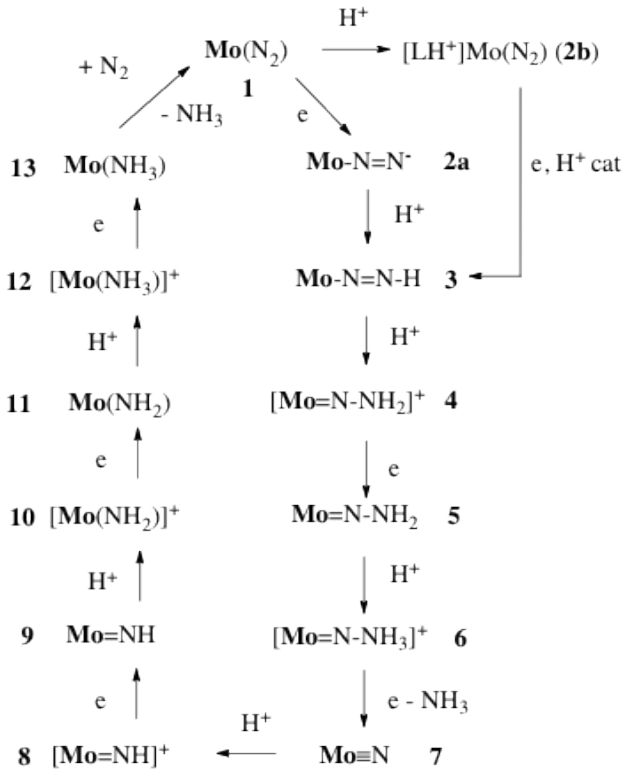

Figure 2. The proposed mechanism of N_2 reduction

In 2003 we reported the first catalytic reduction of dinitrogen with protons and electrons.[2] The process employs a molybdenum complex that contains a hexaisopropylterphenyl-substituted triamidoamine ligand ($[HIPTN_3N]Mo$, Figure 1). Dinitrogen is bound end-on in the trigonal coordination pocket and is reduced through a stepwise addition of protons and electrons. The original proton source was [2,6-lutidinium]BAr'_4 (Ar' = 3,5-$(CF_3)_2C_6H_3$) and the electron source was decamethylchromocene. Dinitrogen is reduced in heptane to yield 7-8 equivalents of NH_3 with the remaining electrons being used to make dihydrogen. Eight of the proposed intermediates (Figure 2) have been

isolated and characterized crystallographically. Extensive calculations of the mechanism of reduction in the [HIPTN$_3$N]Mo system support the proposed mechanism.[3]

All variations of the [HIPTN$_3$N]Mo catalyst system so far have led to lower yields of ammonia, and in some cases, no catalytic turnover. It has been proposed that decomposition of **Mo**N=NH (**Mo** = [HIPTN$_3$N]Mo) is a significant limitation to catalytic turnover, and that catalytic turnover ceases when the supporting ligand is lost from the metal.

A second example of the catalytic reduction of dinitrogen with a Mo complex has been reported.[4] The starting compound is [Mo(L)(N$_2$)$_2$]$_2$(μ-N$_2$)]$_2$ (where L is a "PNP pincer" ligand), protons are added in the form of 2,6-lutidinium triflate, and electrons are added in the form of cobaltocene; the solvent is toluene. Approximately 11-12 equivalents of NH_3 were formed per molybdenum atom, which is an efficiency ~50% higher than that employing [HIPTN$_3$N]Mo catalysts. Loss of ligand from the metal is proposed to be a limiting factor in the [PNP]Mo system also. No mechanistic details for this system have been elucidated. It seems plausible that the metal in the Nishibayashi system is oxidized by protons to give hydrogen and that dinitrogen is reduced at a single metal center in a manner analogous to that found with the [HIPTN$_3$N]Mo catalysts, although there is no proof for this proposal.

A recent paper explores cyclic voltammetry studies provide strong evidence for some variation of proton coupled electron transfer in several of the proposed steps in the catalytic reduction of dinitrogen by [HIPTN$_3$N]Mo complexes. The basic finding is that all relevant isolable proposed intermediate complexes are reduced near the acid reduction potential in the presence of acid. Hydrogen bonding followed by electron transfer (PCET) is likely to be more facile than separate proton transfer followed by electron transfer. Unproductive proton-coupled-electron-transfer reactions result in catalyst decomposition through loss of the triamidoamine ligand and consequent loss of catalytic activity.

After approximately ten years of research in catalytic reduction of dinitrogen to ammonia, only two catalytic reductions of dinitrogen are known. Both employ Mo catalysts, an acid that is readily reduced, and an organometallic reducing agent. Both are limited by loss of ligand from the metal. Both produce hydrogen as a byproduct (~1 equiv or more).

Much has been proposed about iron in the context of reduction of dinitrogen to ammonia with protons and electrons at 22 °C by nitrogenases, perhaps in view of the use of an iron catalyst in the Haber-Bosch process. But many metals are more efficient than iron in reducing dinitrogen to ammonia in the HB process, uranium and osmium being two, and pure iron is in fact relatively inefficient. There is no evidence that suggests that iron is the most efficient metal for reducing dinitrogen by protons and electrons under mild conditions.

References

1. Allen, A. D.; Senoff, C. V. *Chem. Commun.* **1965**, 621.
2. (a) Yandulov; D. V.; Schrock, R. R. *Science* **2003**, *301*, 76
   (b) Schrock, R. R. *Acc. Chem. Res.* **2005**, *38*, 955.
3. Schenk, S.; Le Guennic, B.; Kirchner, B.; Reiher, M. *Inorg. Chem.* **2008**, *47*, 3634.
4. Arashiba, K.; Miyake, Y.; Nishibayashi, Y. *Nature Chem.* **2011**, *3*, 120.
5. Munisamy, T.; Schrock, R. R. *Dalton Trans.* **2012**, *41*, 130.

Solar Fuels from Carbon Dioxide and Water:
Catalytic Photoelectrochemical Generation of Alcohols

Andrew Bocarsly, Kate Keets and Amanda Morris
Chemistry Department
Princeton University
Princeton, New Jersey 08544

The visible light driven photoelectrochemical production of energy rich liquids from carbon dioxide is appealing both in terms of climate change issues and new sustainable energy resources. To this end, we have proposed the electrosynthesis of alcohols from CO_2 as an energy conversion and storage approach, which recycles carbon that would otherwise end up as an atmospheric greenhouse gas. The thermodynamically uphill nature of this reaction coupled with the large activation energy associated with this multielectron, multiproton reduction makes conversion of CO_2 problematic. Alternate energy schemes for this conversion only become possible if the typically observed system activation overpotentials ($\geq$1V) can be significantly reduced. Thus, key to a successful process is the development of a stable catalytic system.

We have discovered that a wide variety of aromatic amines are effective catalyst for the efficient conversion of CO_2 to oxygenated organic products, including formic acid and methanol as well as higher order alcohols containing multiple carbons. The pyridinium catalyzed electrochemical reduction of CO_2 to methanol at an illuminated p-GaP photocathodes is the prototypical reaction, where we find that faradaic efficiencies are >95%, when run at several hundred millivolts of underpotential. The observed reduction involves a mediated charge transfer process, which is initiated by the one electron reduction of pyridinium leading to the formation of formic acid through the reduction of a carbamate intermediate (Scheme I).

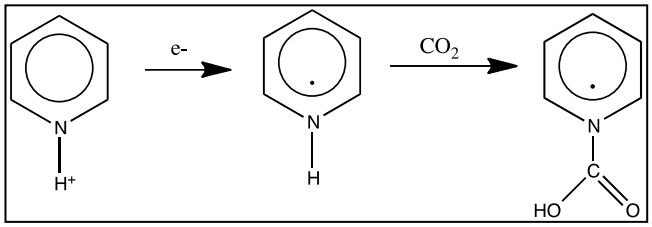

Scheme I: Initial pyridal reduction to form a radical carbamate.

Strong support for this first step is given by the observation that N-methylpyridinium is not a catalyst for the transformations of interest, but methylation of any of the ring carbons produces a catalytic species. It is interesting to note that there are strong solvent dependences to this reaction, with the reduction of either pyridinium or N-methylpyridinium occurring at ~-1.3V vs. SCE in acetonitrile, while the reduction of either of these species occurs at ~-0.6V vs. SCE in aqueous electrolyte (at pH~5.2), supporting the concept that the initial reduction is into the π^* LUMO of the pyridinium species. Once reduced, we propose that the radical species reacts via a concerted proton transfer/nucleophilic attack on the carbon of CO_2 to produce the carbamate radical shown in scheme I.

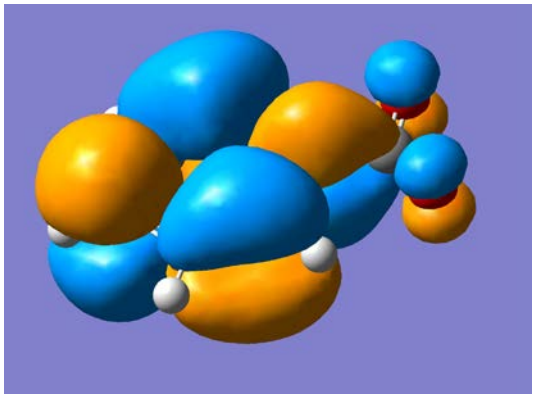

Figure 1: Singly occupied molecular orbital of the key intermediate carbamate as calculated using Gaussian 03 DFT. the delocalization of this electron accepting orbital over both the aromatic ring system and the CO_2 moiety nicely provides a mechanism for the further reduction of this species to generate formic acid.

Theoretical MO calculations (DFT) of the radical carbamate indicate that the SOMO of this intermediate species is delocalized over the whole compound as shown in Figure 1. Thus, further electroreduction of this species directly places a second electron into the π-system of the CO_2 moiety forming formic acid.

Reaction with two more equivalents of reduced pyridyl radical generates formaldehyde with close to 100% faradaic efficiency. A final two equivalents of reduced pyridyl radical produces methanol at this interface. The initial formation of formic acid is found to be rate limiting with an activation barrier of ~70kJ/mole when carried out at a platinum electrode interface.

We find that the CO_2 reduction chemistry is extremely surface sensitive. For example, both the product yield and the distribution of products can be dramatically affected by varying the type of electrode material used or the preparation of the electrode surface. For example, substitution of $GaInP_2$ for p-GaP as the photocathode allows one to generate carbon-carbon bonded products when certain catalysts such as 4,4'-bipyridinium are employed. Specifically, in this case, isopropanol becomes an important component of the produce distribution. As a second, example, we find little in the way of interesting products when a basal plane mounted p-MoS_2 photocathode is utilized in combination with a pyridinium catalyst. However, ethanol becomes a major product when the edge planes of p-MoS_2 are exposed to a pyridinium containing aqueous electrolyte. Thus, not only the composition of the electrode, but the specific atomic geometry of the electrode surface is critical to catalytic reduction of carbon dioxide.

DOE Sponsored Solar Photochemistry Publications 2009-2012

1. Keets, K., et al. *Catalytic conversion of carbon dioxide to methanol and higher order alcohols at a photoelectrochemical interface*. in Solar Hydrogen and Nanotechnology V. 2010. San Diego, CA: SPIE.
2. Morris, A.J., R.T. McGibbon, and A.B. Bocarsly, *Electrocatalytic Carbon Dioxide Activation: The Rate-Determining Step of Pyridinium-Catalyzed CO_2 Reduction.* Chemsuschem, 2011. **4**(2): p. 191-196.
3. Cole, E.B., P. Lakkaraju, and A. Bocarsly, *Substituent Effects in the Pyridinium Catalyzed Reduction of CO_2 to Methanol: Further Mechanistic Insights.* J. Electrochemical Soc., 2012. Submitted.

Highly Reducing Modular Assemblies for Photochemical CO_2 Reduction

Michael D. Hopkins
Department of Chemistry
The University of Chicago
Chicago, Illinois 60637

Objectives. The goal of this project is to develop artificial-photosynthetic assemblies capable of producing solar fuels from CO_2, with a particular emphasis on systems that perform these transformations using renewable reducing equivalents in place of conventional sacrificial donors. We have focused on assemblies derived from metal–alkylidyne (MCR) building blocks of form $M(\equiv CR)L_4X$, rather than standard inorganic photosensitizers, because this class of luminophores combines the highly reducing excited states and proton-coupled electron-transfer (PCET) chemistry necessary to achieve these aims. Current research is directed along three lines: (1) to develop catalytic MCR PCET chemistry for the extraction of reducing equivalents; (2) to understand the excited-state energy- and electron-transfer processes of synthetically modular antenna–MCR dyads, both at a fundamental level and in order to exert the control over excited-state kinetics necessary to drive catalytic CO_2 reduction; and (3) to integrate the photochemical CO_2 and PCET MCR chemistry into functional assemblies.

Highly reducing zinc–porphyrin/tungsten–alkylidyne dyads and triads. We have designed and studied two types of modular ZnPor–MCR dyads in which the porphyrin acts as antenna and primary acceptor. These possess highly reducing $[ZnPor^{-}]–[W]^{+}$ charge-separated states ($E_{1/2}(ZnPor^{0/-})$ = –1.85 V vs Fc) suitable for photosensitizing CO_2 reduction catalysts and deriving reducing equivalents from hydrogen (at $[W]^{+}$). Covalently linked dyads of type ***n*R** (Fig. 1; **1H**, **1Me**, **2Me**, **3Me**) provide systematic distance and orbital-overlap control over the lifetime of charge separation. Near-infrared transient-absorption spectroscopy (λ = 800–1400 nm) has demonstrated that these lifetimes vary across the ranges τ_{CS} = 4–600 ps and τ_{CR} = 0.5–23 ns in polar solvents ($\beta \cong 0.3$). In datively assembled **4**, which is designed to allow dissociation following charge separation to facilitate the relatively slow CO_2/PCET chemistry, electron transfer is substantially slower than in the **1R** analogues. Attachment of CO_2 reduction catalysts of form $Re(bpy)(CO)_3L$ to the ***n*R** dyads via dative ligation at Zn produces triads that, upon excitation, yield catalyst sensitization even from the shortest-lived dyad charge-separated states (i.e., **1H**). Studies of the photochemical reactions of the triads with CO_2 are underway. In nonpolar solvents, we previously reported that **1H** and **1Me** exhibit extremely large (10^3-fold) luminescence lifetime reservoir effects. New time-resolved studies indicate that the energy-transfer equilibrium is also preceded by charge separation, yielding a "ping-pong" electron/energy-transfer sequence ZnP $S_1 \rightarrow CS \rightarrow$ZnP $T_1 \rightarrow$MCR $T_1 \rightarrow S_0$. We believe this accounts for the "heavy atom" quenching of porphyrin fluorescence invoked in a number of other studies of metal-appended porphyrins.

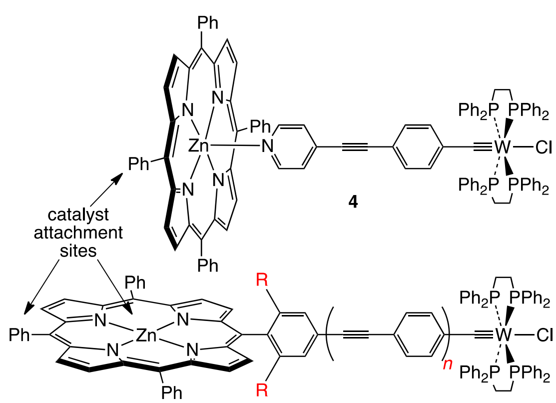

***n*R**: R = H, *n* = 1; R = Me, *n* = 1,2,3

Fig. 1. ZnPor–MCR dyads ***n*R** and **4**.

Electronic-spectroscopic studies and DFT calculations on **1H** and **1Me** demonstrate that their different electron- and energy-transfer properties arise from an interesting breakdown in **1H** of the electronic modularity typical of ZnTPP-derived assemblies. The larger formal π overlap between ZnPor and MCR units of **1H** enabled by the non-orthogonal phenylene connector is found to be of consequence only because the $W(dppe)_2Cl$ unit produces an accidental near degeneracy between the ZnPor and MCR π systems; such mixing is absent in organic analogues. Indeed, the MCR character in the Gouterman a_{2u} orbital can be varied over a range of ~0–25% via substitution of the axial chloride ligand in **1H** (X = F, CN). The ability to fine-tune these dyads across the localized/delocalized continuum via remote substituents opens interesting possibilities for studying the dependence of electron transfer rates on bridge-state energetics under conditions of nearly constant distance and driving force.

Proton/electron/H-atom transfer chemistry of MCR complexes. Previously, we showed that d^2 tungsten–alkylidyne compounds exhibit reversible electron- and proton-transfer reactions to form, respectively, d^1 and hydrido d^0 congeners (Fig. 2). We recently discovered that d^1 $[W(CPh)(dppe)_2Cl]^+$ reacts with H_2 at room temperature to form 7-coordinate d^0 $[W(CPh)(H)(dppe)_2Cl]^+$, which has been structurally characterized. The completion of the cycle of reactions in Fig. 2 is an important milestone toward achieving the goal of replacing conventional sacrificial donors in photochemical CO_2 reduction reactions with renewable reducing equivalents; for example, it enables a photochemical energy-storing reaction such as reverse water-gas shift. While the direct reaction with H_2 is slow, acceleration by several orders of magnitude can be achieved using $CpCr(CO)_3H$ as a catalytic H-atom-transfer shuttle.

To better understand the energetic barriers involved in these processes, we conducted X-ray crystallographic studies of the structures of d^2/d^1 MCR redox congeners and X-ray transient absorption spectroscopic studies (in collaboration with Dr. Lin Chen at Argonne) of the excited-state structures, complemented with (TD)DFT calculations. These studies indicate that the inner-sphere reorganization energy associated with ground-state and excited-state electron transfer is small for this class of compounds. For the hydrido compounds, the mechanism of proton and H-atom transfer is still under investigation; DFT calculations indicate that 6-coordinate alkylidene complexes are energetically accessible (or, for some ancillary substituents, the ground state).

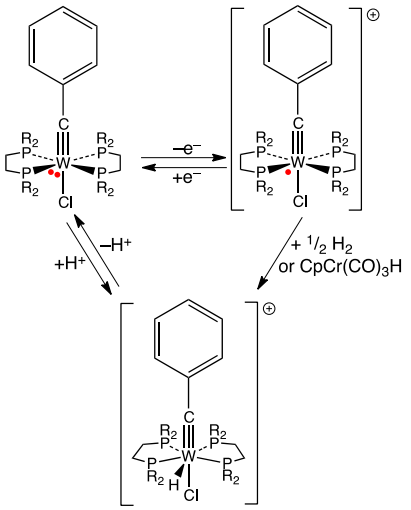

Figure 2. MCR proton/electron/H-atom transfer reactivity

Future directions. We have begun work along three new lines aimed at testing the generality and expanding the scope of the approaches described above. First, we are studying assemblies in which the MCR unit is replaced with non-luminescent but higher-efficacy centers for extracting reducing equivalents. These include Dubois' $Ni(P\text{-}N\text{-}P)_2$ (P-N-P = diphosphinoamine) catalysts and $CpM(CO)_{3-n}(PR_3)_n$ (M = Cr, Mo, W) complexes. Second, we are preparing nanoparticle/catalyst (NP = CdS, CdSe) and NP/MCR dyads, to explore opportunities for storing multiple reducing equivalents needed for multielectron transformations of CO_2. Third, we have begun study of new mechanistic schemes for photosensitization of catalysts that form C–C bonds between CO_2 and unsaturated organic molecules.

DOE Sponsored Solar Photochemistry Publications 2009-2012

1. Cohen, B. W.; Lovaasen, B. M.; Simpson, C. K.; Cummings, S. D.; Dallinger, R. F.; Hopkins, M. D. "1000-Fold Enhancement of Luminescence Lifetimes via Energy-Transfer Equilibration with the T_1 State of Zn(TPP)." *Inorg. Chem.* **2010**, *49*, 5777.
2. Lovaasen, B. M.; Lockard, J. V.; Cohen, B. W.; Yang, S.; Zhang, X.; Simpson, C. K.; Chen, L. X.; Hopkins, M. D. "Ground State and Excited State Structures of Tungsten–Benzylidyne Complexes." *Inorg. Chem.* **2012**, *ASAP*. (Cover article.)
3. Moravec, D. B.; Lovaasen, B. M.; Hopkins, M. D. "Near-Infrared Transient-Absorption Spectroscopy of Zinc Tetraphenylporphyrin and Related Compounds." *Phys. Chem. Chem. Phys.*, submitted.
4. Haines, D. E.; O'Hanlon, D. C.; Manna, J.; Jones, M. K.; Shaner, S. E.; Sun, J.; Hopkins, M. D. "Oxidation Potential Tuning of Tungsten–Alkylidyne Complexes over a 2 V Range, and its Correlation with Redox Orbital Energy." *Inorg. Chem.*, submitted.
5. Morales Verdejo, C. A.; Cohen, B. W.; Hopkins, M. D. "Dihydrogen Cleavage by Paramagnetic Tungsten–Alkylidyne Complexes." Manuscript in preparation.
6. Lovaasen, B. M.; Cohen, B. W.; Dallinger, R. F.; Cummings, S. D.; Hopkins, M. D. "Luminescence Lifetime Reservoir Effects in Zinc–Porphyrin/Tungsten–Alkylidyne Dyads. The interplay of Electron-Transfer and Energy-Transfer Pathways." Manuscript in preparation (invited).

Session VI

Photochemical Water Splitting

Connecting Structure to Solar Fuels Function in Natural and Artificial Photosynthesis

David M. Tiede[1], Pingwu Du[1], Oleksandr Kokhan[1], Karen L. Mulfort[1], Oleg G. Poluektov[1], Lisa M. Utschig[1], Lin X. Chen[1], Gary Wiederrecht[2], Karena W. Chapman[3], Peter J. Chupas[3], and Libai Huang[4]

[1]Chemical Sciences and Engineering Division, [2]Center for Nanoscale Materials and [3]X-ray Science Division, Argonne National Laboratory, Argonne IL 60439, [4]Radiation Laboratory, University of Notre Dame, Notre Dame IN 46556

This program investigates fundamental mechanisms for coupling photons to fuels in hierarchical, photosynthetic assemblies, and develops strategies for the design of sustainable photosynthetic systems for solar energy conversion. Characteristic features of natural photosynthetic architectures are the modular architectures and module-specific, protein host-cofactor guest chemistries. These design features allow the individual light-harvesting, charge separation, water-splitting and fuels catalysis tasks of solar energy conversion to be optimized within individual functional modules, which can then be integrated for overall solar energy conversion function. This program demonstrated a significant milestone by achieving efficient, self-assembled, non-covalent coupling of hydrogen-evolving catalysts to photosynthetic electron transfer in photosystem I.[3,6] On-going work is investigating fundamental mechanisms for solar-driven charge-separation and coupled fuels catalysis in natural and artificial photosynthesis. Research in two areas is discussed below.

Resolution of photosynthetic cofactor-specific excited-state photochemistry. A conserved feature of photosynthesis is the pseudosymmetric hexameric cofactor core that converts optically generated excited states to charge separated states in photosynthetic reaction centers (RCs), although mechanisms and pathways for primary charge separation vary in different RC types. We have achieved a high resolution mapping of cofactor-specific photochemistry in RCs by polarization selective ultrafast spectroscopy in single crystals at cryogenic temperature. The fixed orientation of cofactors within crystals was found to allow selective excitation of single transitions within the cofactor manifold, and allowed site-specific photochemical functions to be resolved. Remarkably, transient spectra associated with the initial excited states were found to involve a delocalized set of cofactors that differed depending upon which of the symmetry-related monomeric bacteriochlorophylls, $BChl_A$, $BChl_B$, or the special pair bacteriochlorophyll dimer, P, was chosen for excitation. Proceeding from these initial excited states, characteristic photochemical functions were resolved. Specifically, our measurements provide direct evidence for an alternative charge separation pathway initiated by excitation of $BChl_A$ that does not involve P*. Conversely, the initial excited state produced by excitation of

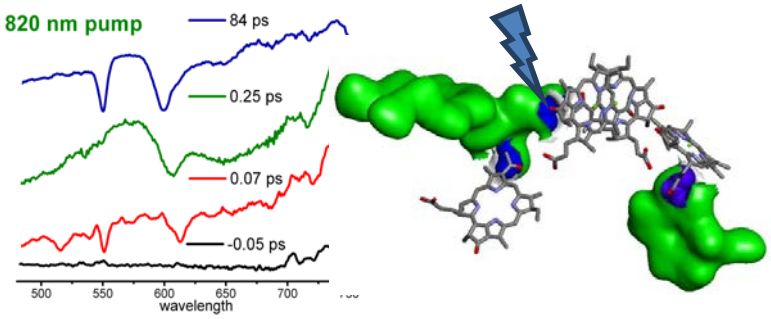

Figure 1. Polarized transient spectra in RC crystals using 120 fs pulse excitaton of the $BChl_B$ cofactor.

$BChl_B$ was found to decay by energy transfer to P. A clear sequential kinetic resolution of $BChl_A$ and the A-side bacteriopheophytin, BPh_A, in the electron transfer proceeding from P* was achieved. The newly resolved cofactor-specific RC photochemistry provides a model for comparative analysis of photochemistry in RCs from oxygenic photosynthesis.

In-situ structural characterization of photosensitizers and catalysts in artificial photosynthesis. Bio-mimetic approaches to solar energy conversion offers opportunities for atomic-scale resolution of mechanisms for solar fuels catalysis that are relevant to both natural and artificial photosynthesis. We have begun an investigation of *in-situ* structure analyses for a variety of metal coordination complex photosensitizers and catalysts that function in solar-driven photocatalysis using high energy X-ray scattering (HEXS) and pair distribution function analysis (PDF).

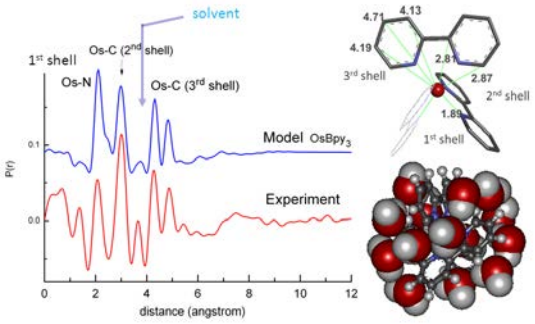

Figure 2. HEXS-PDF analysis of $Os(II)(bpy)_3$ complexes in solution.

HEXS-PDF analysis for a series of metal-*tris*-bipyridyl photosensitizer complexes in solution was found to be capable of resolving the full inner and outer sphere metal-ligand atom pair correlations and solvation layer structure, Figure 2, with a precision that is sufficient to allow coordination dynamics coupled to solar fuels catalysis to be investigated. For example, HEXS-PDF analysis of the electrodeposited cobalt-oxide water splitting catalyst found the film to be composed of disordered, molecular-dimensioned domains of edge-sharing CoO_6 octahedra in an edge-sharing lattice sheet structure, and possibly containing a Co_4O_4 cubane "defect", Figure 3. The analysis identifies the domains to be constrained to 13-14 cobalt atoms that have distorted coordination geometries for terminal oxygen atoms. Phosphate is detected as a disordered counter ion in the film. This distorted Co-O edge structure suggests a possible role in the catalytic reaction mechanism. On-going work is examining both electro- and photo-chemical approaches for investigating mechanisms of solar-driven water-splitting catalysis.

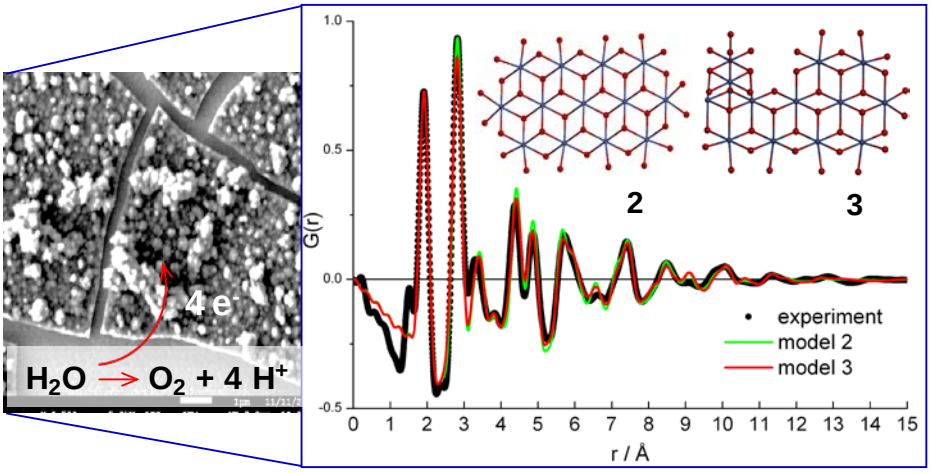

Figure 3. HEXS-PDF analysis of the Co-oxide water-splitting catalyst and comparison to model structures.

DOE Sponsored Solar Photochemistry Publications 2009-2012

1. Resolution of Cofactor-Specific Excited States and Charge Separation Pathways in Photosynthetic Reaction Centers by Single Crystal Spectroscopy, Libai Huang, Nina Ponomarenko, Gary P. Wiederrecht, and David M. Tiede (2012) Proc. Nat. Acad. Sci. USA *109(13)*, 4851-4856.

2. The Hydrogen Catalyst Cobaloxime – a Multifrequency EPR and DFT Study of Cobaloxime's Electronic Structure, Niklas, J., Mulfort, K. L., Rakhimov, R. R, Mardis, K. L., Tiede, D. M., and Poluektov, O. G. (2012) *J. Phys. Chem. B*, **116**, 2943-2957.

3. Nature-Driven Photochemistry for Catalytic Solar Hydrogen Production: A Photosystem I–Transition Metal Catalyst Hybrid, Lisa M. Utschig, Sunshine C. Silver, Karen L. Mulfort, and David M. Tiede (2011) J. Am. Chem. Soc. *133:*16334-16337. Highlighted in *Chemical & Engineering News,* **2011**, *89*(40), 35.

4. Metal Nanoparticle Plasmon-Enhanced Light-Harvesting in a Photosystem I Thin Film, I. Kim, S. L. Bender, J. Hranisavljevic, L. M. Utschig, L. Huang, G. P. Wiederrecht, and D.M. Tiede (2011) Nano Letts. *11 (8)*: 3091–3098.

5. Comparing Photosynthetic and Photovoltaic Efficiencies and Recognizing the Potential for Improvement, R. E. Blankenship*, D. M. Tiede*, J. Barber, G. W. Brudvig, G. Fleming, M. Ghirardi, M. R. Gunner, W. Junge, D. M. Kramer, A. Melis, T. A. Moore, C. C. Moser, D. G. Nocera, A. J. Nozik, D. R. Ort, W. W. Parson, R. C. Prince, R. T. Sayre (2011) Science *332*: 805-809.

6. Photocatalytic Hydrogen Production from Noncovalent Biohybrid Photosystem I/Pt Nanoparticle Complexes, L.M. Utschig, N.M. Dimitrijevic, O.G. Poluektov, S.D. Chemerisov, K.L. Mulfort, and D.M. Tiede (2011) J. Phys. Chem. Letts. *2:* 236-241. Highlighted in *Chemical & Engineering News,* **2011**, *89*(5), 44-45.

7. Light-induced Alteration of Low Temperature Interprotein Electron Transfer between Photosystem I and Flavodoxin, L.M. Utschig, D.M. Tiede, and Poluektov, O.G. (2010) Biochemistry *49 (45),* 9682–9684.

8. Supramolecular cobaloxime assemblies for H_2 photocatalysis: An initial solution state structure-function analysis, K.L. Mulfort and D.M. Tiede, (2010) J. Phys. Chem. B. *114,* 14572–14581.

9. Transient Structure Determination During Solar Energy Conversion, L.X. Chen, D.M. Tiede, K. Attenkofer, G. Jennings, X. Zhang, (2010) Synchrotron Radiation News *23:* 22-24.

10. Solution structure of the cap-independent translational enhancer and ribosome-binding element in the 3 ' UTR of turnip crinkle virus, X.B. Zuo, J.B. Wang, P. Yu, D. Eyler, H. Xu, M.R. Starich, D.M. Tiede, A.E. Simon, W. Kasprzak, C.D. Schwieters, B.A. Shapiro, Y.X. Wang, (2010) Proc. Natl. Acad. Sci. U.S.A. *107*:1385-1390.

11. A Method for Helical RNA Global Structure Determination in Solution Using Small-Angle X-Ray Scattering and NMR Measurements, J.B. Wang, X.B. Zuo, P. Yu, H. Xu, M. R. Starich, D. M. Tiede, B.A. Shapiro, C. D. Schwieters, and Y.-X. Wang, (2009) J. Mol. Biol. *393*:717-734.

12. X-ray Scattering Combined with Coordinate-Based Analyses for Applications in Natural and Artificial Photosynthesis, D. M. Tiede, K.L. Mardis, and X. Zuo, invited review, (2009), Photosyn. Research, *102*: 267-279.

13. Hydrophobic Dimerization and Thermal Dissociation of Perylenediimide-Linked DNA Hairpins, M. Hariharan, Y. Zheng, H. Long, T. A. Zeidan, G. C. Schatz, J. Vura-Weis, M. R. Wasielewski, X. Zuo, D. M. Tiede, and F. D. Lewis, (2009) J. Amer. Chem. Soc. *131(16)*: 5920-5929.

14. Solution-State Conformational Ensemble of a Hexameric Porphyrin Array Characterized Using Molecular Dynamics and X-ray Scattering, K. L. Mardis, H. M. Sutton, X. Zuo, J.S. Lindsey, and D. M. Tiede, (2009), J. Phys. Chem. A **113**: 2516-2523.

15. *In Situ* Measurement of the Preyssler Polyoxometalate Morphology upon Electrochemical Reduction, M. R. Antonio, M.-H. Chiang, S. Seifert, D. M. Tiede, and P. Thiyagarajan, (2009), J. Electroanal. Chem. **626**:103-110.

A Concerted Synthetic, Spectroscopic and Computational Approach towards Water Splitting by Heterometallic Complexes in Solution and on Surfaces

Cláudio N. Verani, John F. Endicott, H. Bernhard Schlegel
Department of Chemistry
Wayne State University, Detroit, Michigan 48202

The basic premise of our collaboration is to investigate the development of heterometallic complexes in solution and on surfaces aiming to interrogate the requirements for integrating antennae, active center and acceptors into a single modular molecule. The modular antenna functions as a sensitizer absorbing solar radiation and generating an excited state that can transfer an electron to the acceptor module and a hole to the active site module. The modular active site acts as a donor implying that the metal center present will reach a high-valent oxidation state capable of water oxidation. Aiming to use Earth-abundant metals, we focused our efforts on Cobalt acceptors and Manganese active sites attached to Ru-antennae, Figure 1.

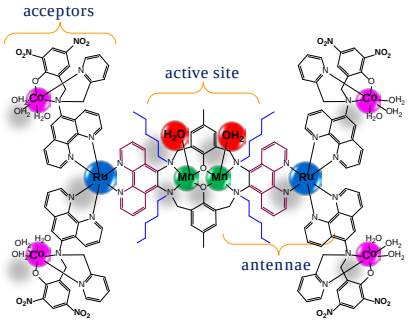

Figure 1. Idealized modular system for water oxidation

Progress in the synthesis and characterization of manganese active sites modules includes two monometallic high-spin complexes, the hexacoordinate [$Mn^{III}L^{1}MeOH$] and the pentacoordinate [$Mn^{III}L^{2}$] with asymmetric [N_2O_3] ligands, Figure 2. Electrochemical and spectroelectrochemical behavior, and DFT calculations suggest that oxidation of the ligand should be favored over stabilization of Mn(IV), believed to play a key role in water splitting. Interestingly, the metal-based oxidation in the hexacoordinated species was predicted to be a mere 3 kcal/mol higher in energy and experimental EPR measurements support the presence of Mn(IV). TD-DFT also proved to be diagnostic: a band at 440 nm, usually attributed to an MLCT is in fact a phenolate $\pi \rightarrow$ imine π^* transition. This prediction was confirmed spectroelectro-chemically and the band disappeared upon ligand oxidation. Based on these results, the opportunities and limitations of the use of phenolate-based ligands as catalysts can be assessed, reactive intermediates will be evaluated, and the necessary ligand modifications will be addressed. Using similar ligand design, two new ligands with hydrophilic and hydrophobic moieties were developed to yield redox-responsive Mn(III) complexes for Langmuir-Blodgett film formation. These ligands form the complexes, [$Mn^{III}L^{3}$], and [$Mn^{III}L^{4}$] and their amphiphilic behavior was probed using isothermal compression and Brewster angle microscopy, indicating homogeneous film formation at the air/water. The molecular integrity of the films on solid interfaces was analyzed by infrared reflection/absorption spectroscopy and UV-visible spectroscopy and show well-packed assemblies that retain the same vibrational and electronic properties observed for the individual molecules. Progress on cobalt species will also be reported.

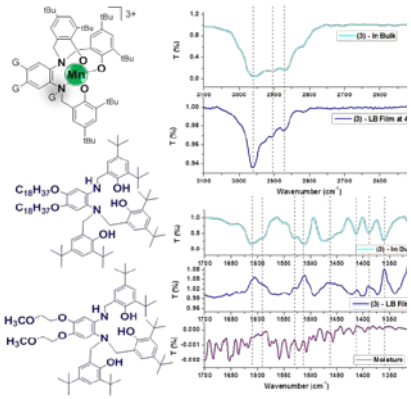

Figure 2. Manganese-N_2O_3 complexes and IRRAS spectra of their LB films.

The efficiencies of excited state electron transfer ultimately depend on: (1) their potential to act as an oxidant or reductant; (2) the differences in molecular structures of the ground and excited state (leading to ET reorganizational energy); and (3) an electronic matrix element, H_{TA}. None of these parameters is readily available for MLCT excited states. We have examined the patterns of the variations in the first two of these properties of the lowest energy ^{3}MLCT excited states (T_0) among a series of Ru(II)-polypyridyl complexes based largely on a combination of 77 K emission spectra and computational modeling. The molecular distortions of the Ru-bpy complexes are generally in a large number (> 12) of nuclear coordinates and they fall mostly in the low frequency (*lf*; metal-ligand) and medium frequency (mf; polypyridyl) ranges of vibrational modes. At 77 K the vibronic components arising from *lf* modes are broad and overlap with the emission band origin making it difficult to determine the excited state energy ($E^{0'0}$) while the vibronic components arising from *mf* modes often give rise to some structured emission sideband contributions. The *mf* vibronic sidebands tend to dominate the emission spectrum at high energies and decrease systematically as $E^{0'0}$ decreases; this pattern is reproduced in the computational modeling (**Figure 3**). The modeling suggests that the origins of the variations in *mf* sidebands are: (1) configurational mixing between T_0 and $^3\pi\pi^*$ bpy-excited state; (2) electronic delocalization in the ground state arising from mixing with MLCT excited states. So far we have modeled the distortions in a few $[Ru(L)_4bpy]^{2+}$ complexes and in these the $E^{0'0}$ component accounts for less than 1/3 of the amplitude of the highest energy emission component and is about 250 cm^{-1} higher in energy. Assuming that the effective oxidation potential of T_0 can be estimated from emission maximum then for an extended series of Ru-bpy complexes $^*E_{1/2}(ox)$ decreases with excited state energy, and: $^*E_{1/2}(ox) \approx (-8.2\pm0.6)10^{-3} \times \lambda_{max(MLCT)} + 4.1\pm0.4$ V ($r^2 = 0.91$); $\lambda_{max(MLCT)}$ is the dominant absorption maximum. The electron transfer reorganizational energies appear to be smaller for Ru-tpy chromophores than for Ru-bpy chromophores.

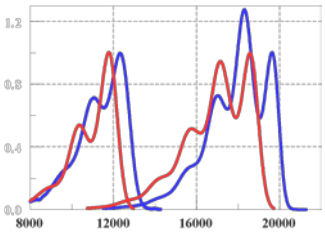

Figure 3. Comparison of the observed (blue) and calculated (red) emission spectra of $[[Ru(NH_3)_4bpy]^{2+}$ (left) and $[Ru(CH_3CN)_4bpy]^{2+}$ (right).

To evaluate systematically the effect of excited state energy on the vibronic sidebands (Figure 4), we varied the nuclear charge of Ru in $[Ru(NH_3)_4(bpy)]^{2+}$. The results mimicked variations in L experimentally with Z_{Ru}=43.5 showing little structure like L=acac, and Z_{Ru}=44.5 showing significant bpy distortion like L=MeCN. Bond length changes for bpy C–N and C–C in these species suggest, naively, that bpy is reduced by more than one electron from S_0 to T_0. The orbital interaction scheme in Figure 10 shows which frontier orbitals interact to give the SOMOs in T_0 and suggests a different interpretation; if Z_{Ru} increases enough the dπ orbitals mix with the occupied bpy π orbitals (Z_{Ru}=44.5). This leads to a donor orbital for T_0 (left SOMO) that has significant bpy character. Alternatively, this can be framed as configurational mixing between the MLCT and bpy $3\pi\pi^*$ states and helps explain the much larger *mf* distortions associated with high energy triplet states.

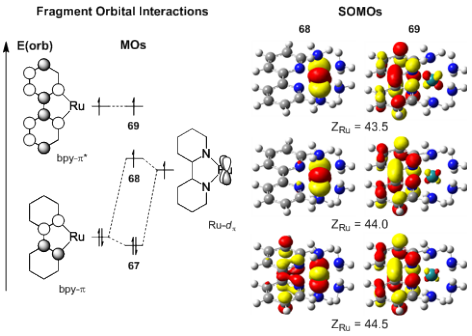

Figure 4 . Orbital interaction (left) for the ^{3}MLCT state using bpy^- and $Ru^{III}(NH_3)_4$. Isosurface plots (0.05 au) of the SOMOs **68** and **69** (right) are for three different Ru nuclear charges (Z_{Ru}; and ^{3}MLCT energies).

DOE Sponsored Solar Photochemistry Publications 2009-2012

1. Ondongo & Endicott "Contrasts between the Vibronic Contributions in the tris-(2,2′-bipyridyl)Osmium(II) Emission Spectrum and the Implications of Resonance-Raman Parameters" *Inorganic Chemistry* **2009**, *48*, 2818-2829

2. Allard, Odongo, Lee, Chen, Endicott, Schlegel: "Effects of Electronic Mixing in Ruthenium(II) Complexes with Two Equivalent Acceptor Ligands. Spectroscopic, Electrochemical, and Computational Studies" *Inorganic Chemistry* **2010**, *49*, 6840–6852.

3. Lesh, Allard, Shanmugam, Hryhorczuk, Endicott, Schlegel, Verani "Investigation of the Electronic, Photosubstitution, Redox, and Surface Properties of New Ruthenium(II)-Containing Amphiphiles" *Inorganic Chemistry* **2011**, 50, 969-977 (listed among the top-read articles in January).

4. Odongo, Allard, Schlegel, Endicott "Observations on the Low-Energy Limits for Metal-to-Ligand Charge-Transfer Excited-State Energies of Ruthenium(II) Polypyridyl Complexes" *Inorganic Chemistry*, **2010**, *49*, 9095–9097.

5. Lin, Tsai, Huang, Endicott, Chen, Chen: "Nearest- and Next-Nearest-Neighbor Ru(II)/Ru(III) Electronic Coupling in Cyanide-Bridged Ruthenium Square Complexes," *Inorganic Chemistry* **2011**, 50, 8274–8280.

6. Tsai, Allard, Lord, Luo, Chen, Schlegel, Endicott "Characterization of Low Energy Charge Transfer Transitions in (terpyridine)(bipyridine)Ruthenium(II) Complexes and their Cyanide-Bridged Bi- and Tri-Metallic Analogues" *Inorganic Chemistry*, **2011**, *50*, 11965–11977.

7. Lesh, Lord, Heeg, Schlegel, Verani "Unexpected Formation of a Cobalt(III) Phenoxazinylate Electron Reservoir" *European Journal of Inorganic Chemistry* **2012**, 463–466 (invited contribution).

8. Allard, Sonk, Heeg, McGarvey, Schlegel, Verani "Bioinspired Five-Coordinate Iron(III) Complexes for Stabilization of Phenoxyl Radicals" *Angewandte Chemie Int. Ed.* **2012**, *51*, 3178-3182.

9. Shakya, Lord, Xavier, Heeg, Schlegel, Verani "Comparative Behavior of Pentacoordinate and Hexacoordinate Manganese(III) Complexes with Phenol-rich [N2O3] Ligands" *Inorganic Chemistry*, **2012,** *provisionally accepted.*

10. Allard, Heeg, Schlegel, Verani "On the Sequential Rich Redox Chemistry of a Series of Cobalt(III) Complexes with Pentadentate Electroactive Complexes" *Eur. J. Inorg. Chem.* **2012**, *provisionally accepted pending minor changes* (invited contribution to the cluster issue "Modern coordination chemistry and its impact for meeting global challenges").

11. Lord, Allard, Thomas, Odongo, Schlegel, Chen, Endicott "The Distortions of Triplet Metal-to-Ligand-Charge-Transfer Excited States of Mono-Bipyridine-Ruthenium (II) Complexes Based on 77 K Emission Spectra and Computational Modeling," *Inorganic Chemistry*, *submitted*.

The following manuscripts are currently in the final stages of preparation:

12. Wickramasinghe, Verani **"**Asymmetric manganese complexes with redox and amphiphilic properties" *To be submitted.*

13. Lesh, Lord, Allard, Heeg, Schlegel, Endicott, C. N. Verani*: "Complexes as electron reservoirs for catalysis: Experimental and DFT evaluation of the electronic and redox properties of iron(III) and gallium(III) species with aminocatecholate ligands" *To be submitted.*

14. Basu, Xavier, Heeg, Verani "Determination of rate constants for Co(III) reduction in electron acceptors based on halogenated-[N_2O_3] systems" *Manuscript in preparation (revision of second draft, temporary title).*

15. Lord, Tsai, Chen, Schlegel, Endicott "Emission Spectral Probes of the Lowest Energy Metal-to-Ligand Excited States of (Terpyridine)(Bipyridine)Ruthenium(II) Complexes and their Cyanide-Bridged Multimetallic Analogs" *Manuscript in preparation*.

16. Odongo, Allard, Lord, Schlegel, Endicott, "On the Nature of the Lowest Energy Metal-to-Ligand Excited states in Simple Bipyridyl-Ruthenium Complexes: Evaluation of Excited State Redox Properties," *Manuscript in preparation*.

17. Chen & Endicott, "Electronic Coupling between Metals in Cyanide-Bridged Ground State and Excited State Mixed Valence Complexes," *Coord. Chem. Reviews, Manuscript in preparation* (invited review).

18. Tsai, Tian, Endicott, Chen "Luminescence of the Metal-to-Ligand Charge-Transfer Excited States in Monometallic and Pyrazine-Bridged, Bimetallic Ruthenium(II)-Ammine Complexes," *Manuscript in preparation*.

19. Wanniarachchi, Heeg, Verani "Enhanced water-splitting activity in ruthenium polypyridyl species containing electron-withdrawing substituents" *Manuscript in preparation (first draft near completion).*

Multicomponent Bio-Nano Integrated Systems for Light-Driven Hydrogen Generation

Kara L. Bren, Richard Eisenberg, Patrick L. Holland, Todd D. Krauss
Department of Chemistry
University of Rochester
Rochester NY 14627-0216

Conversion of solar energy into chemically stored energy via artificial photosynthesis (AP) represents a promising approach to providing renewable energy needed for global development. In general, systems for AP are designed to split water photochemically into its constituent elements, with water oxidation to O_2 and aqueous proton reduction to H_2. This project focuses on integrated, multi-component systems consisting of visible light absorbers, catalysts, and electron transfer media for generating H_2 from aqueous solutions using visible light. We have pursued a *modular design* that enables rapid progress through parallel development of modules. The modular components are: (1) engineered zinc-substituted heme proteins (cytochromes) and heme-peptide conjugates that use visible light to create well-separated electron/hole pairs, (2) vertically aligned carbon nanotube (NT) membranes that rapidly transfer electrons to a proton-reducing catalyst, and (3) coordination complexes that incorporate earth-abundant metals to produce H_2 from the photogenerated electrons.

With respect to **catalyst design and study**, efforts have concentrated on homogeneous systems containing known photosensitizers (PS), sacrificial electron donors and complexes of 3d transition metal ions as catalysts. Homogeneous systems are used because it is possible to understand the photochemical and catalytic mechanisms in detail. We investigated nickel thiolate complexes because they mimic the [Fe-Ni]-hydrogenase active site, and dimeric metal complexes based on nickel thiolate hydrides have been shown to be catalytically active for proton reduction. We discovered that photocatalytic H_2 generation from nickel phosphine complex **1** is long-lived (> 2700 turnovers (TON)), but the activity of the system is low. We subsequently hypothesized that nickel(II) complexes containing pyridine-2-thiolate ligands might be even more active. We found that the complex $[Ni(pyS)_3]^-$ (pyS = pyridine-2-thiolate - **2**), shows high activity for the photocatalytic production of H_2 with fluorescein as the PS and triethylamine as the sacrificial electron donor. This system had achieved the highest activity for a homogeneous noble-metal-free system for light-driven H_2 production to date, with over 5500 TON. The *photochemical mechanism* involves electron transfer from the singlet excited state of fluorescein to the catalyst, which avoids the formation of the long-lived triplet state of the excited PS and resultant unstable radical anions. We envision this as a useful strategy in the future to avoid PS decomposition that has plagued solution photocatalytic H_2 generation work.

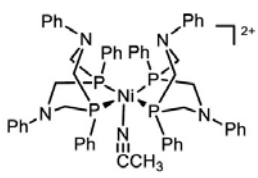

1

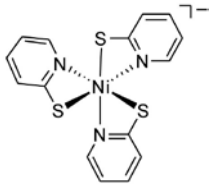

2

We were also studying complexes with redox-active ligands as potential H_2 generation catalysts. We discovered that $(Bu_4N)[Co(bdt)_2]$ is an active electrocatalyst and photocatalyst for proton reduction in aqueous/organic media with high activity (>2700 TON with respect to catalyst and an initial turnover frequency of >800/h). In the last year we have expended these initial results to a family of cobalt dithiolene complexes with much greater photocatalytic activity (>9000 TON).

With respect to **electrically conductive NT membranes**, we have optimized the synthesis of dense forests of vertically aligned carbon nanotubes (VANTs) by chemical vapor deposition (Figure 1). VANTs were synthesized over 150 microns long and a polymer was used to fill in the gaps between the VANTs to form a solid membrane material. Preliminary measurements show that after exposing the VANTs on the membrane surface, the NT membranes conduct electrical current very well and follow Ohm's law. This result was somewhat expected as the MWNTs in the membrane are known to be metallic. Also, preliminary studies have shown that protons can be transported through the membrane to an aqueous solution.

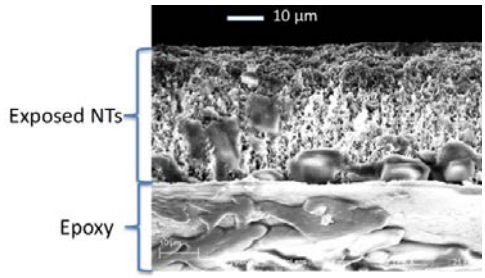

Figure 1. Cross sectional SEM image of vertically aligned multi-walled NTs encased in epoxy showing exposed NTs.

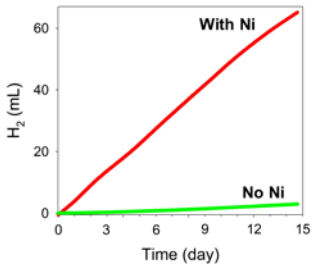

Figure 2. Hydrogen production from systems containing CdSe-DHLA, $Ni(NO_3)_2$ and ascorbic acid in H_2O at pH 4.5 upon irradiation with 520 nm light.

We have also discovered that CdSe colloidal semiconductor quantum dots (QDs) in combination with Ni^{2+}-ions reduce protons to form H_2 photochemically with the addition of a sacrificial donor (ascorbic acid). We found that the efficiency of the process depended on the size of the QD. Significantly, under the optimal conditions, H_2 was produced over the course of two weeks with over 0.3 million TON (Figure 2)! Strong evidence suggests that Ni is coordinating to the capping ligands for the QDs (dihydrolipoic acid, DHLA) and it is that complex which may be involved in the catalysis.

With regards to **bio-inspired light harvesting**, we have developed novel biosynthetic methods for preparing metalloporphyrin-peptide conjugates. The *E. coli* cytochrome *c* maturation apparatus in the cell periplasm was used to add a heme to a peptide fused to the N-terminus of a self-cleaving protease. Upon activating the protease, the heme peptide is cleaved. Purification is by a histidine affinity chromatography method developed earlier by our group. We also prepared heme peptide tags matured using the cytochrome *c* heme lyase (CCHL) enzyme from yeast, where CCHL catalyzes heme attachment in the cytoplasm. The advantage of this method is it does not require excretion to periplasm, a process not possible for all proteins. The availability of these two methods will facilitate the construction of artificial cytochromes and cytochrome fusions with other proteins to yield biomolecules with novel properties and functions. Also, we have performed metal substitutions on heme peptides prepared using these methods, replacing the native iron with zinc and with cobalt. The zinc derivatives are being employed as agents for charge transfer to nanotubes, and the cobalt derivatives will be tested in coming months for proton reduction activity using electrocatalysis and photocatalysis.

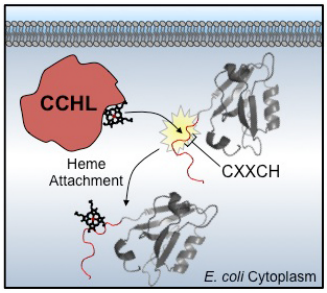

Figure 3 Cartoon showing CCHL attaching heme to a fusion peptide composed of the N-terminal residues (red)) of cyt *c* fused to a PDZ3 domain protein (gray, PDB: 1BFE).

DOE Sponsored Solar Photochemistry Publications 2009-2012

1. Theresa M. McCormick, Zhiji Han, David J. Weinberg, Patrick L. Holland, Richard Eisenberg, "The Impact of Ligand Exchange in Hydrogen Production from Cobaloxime-Containing Photocatalytic Systems," *Inorg. Chem.* **2011**, *50*, 10660-10666.
2. Matthew P. McLaughlin, Theresa M. McCormick, Richard Eisenberg, Patrick L. Holland, "A Stable Molecular Nickel Catalyst for the Homogeneous Photogeneration of Hydrogen in Aqueous Solution," *Chem. Commun.* **2011**, *47*, 7989-7981.
3. William R. McNamara, Zhiji Han, Paul J. Alperin, William W. Brennessel, Patrick L. Holland, Richard Eisenberg, "Cobalt-Dithiolene Complex for the Photocatalytic and Electrocatalytic Reduction of Protons," *J. Am. Chem. Soc.* **2011**, *133*, 15368-15371.
4. Zhiji Han, William R. McNamara, Min-Sik Eum, Patrick L. Holland, Richard Eisenberg, "A Nickel Thiolate Catalyst for the Long-Lived Photocatalytic Production of Hydrogen in a Noble-Metal-Free System," *Angew. Chem. Int. Ed.* **2012**, *51*, 1667–1670.
5. McNamara, W. R.; Han, Z.; Yin, M.; Brennessel, W. W.; Holland, P. L.; Eisenberg, R. "Highly Active Cobalt-Dithiolene Complexes for Photocatalytic and Electrocatalytic Proton Reduction in Aqueous Solutions," submitted for publication.
6. Erin C. Kleingardner, Wesley B. Asher, and Kara L. Bren, "Efficient and Flexible Preparation of Biosynthetic Heme *c* Peptides," submitted for publication.
7. Wesley B. Asher and Kara L. Bren, "Cytochrome *c* Heme Lyase can Mature a Fusion Peptide Composed of the Amino-terminal Residues of Horse Cytochrome *c*," submitted for publication.

Session VII

Electron Transfer

Physical Chemistry of Reaction Dynamics in Ionic Liquids

David A. Blank,[1] Edward W. Castner, Jr.,[2] Claudio J. Margulis,[3]
Mark Maroncelli,[4] and James F. Wishart[5]

[1]Dept. of Chemistry, University of Minnesota, Minneapolis, MN 55455

[2]Dept. of Chemistry and Chemical Biology, Rutgers University, Piscataway, NJ 08854

[3]Dept. of Chemistry, University of Iowa, Iowa City, IA 52242

[4]Dept. of Chemistry, Penn State University, University Park, PA 16802

[5]Chemistry Dept., Brookhaven National Laboratory, Upton, NY 11973

Ionic liquids (ILs) are becoming ubiquitous in energy-related applications, particularly in those requiring the light-induced separation of charge, charge transport, and thermal electron-transfer reactions.[1-3] The objective of our collaboration is to understand the chemical and physical principles that determine reactivity in these important liquids. We report our recent progress on understanding ionic liquids in several areas: bulk liquid structure;[4-5,8-11] bimolecular electron-transfer reaction rates;[1,3,16] excess electrons in ILs;[7,15] solvation, diffusion and transport in ILs,[6,13-14] and several novel electron-donating and electron-accepting ILs.[16,17]

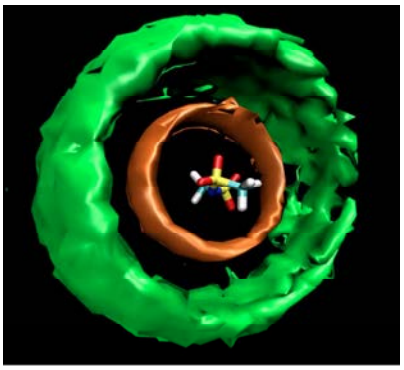

Fig. 1. Isodensity surfaces of $P_{14,666}^{+}$ cations (orange) and anions (green) surrounding a NTf_2^- anion.[11]

The structure of ionic liquids is dominated by the alternant charge ordering of the cations and anions, as is found in all molten salts. With increasing lengths of alkyl substituents on the cations, a signature of intermediate range ordering is observed in either the x-ray or neutron structure functions. These features are quantitatively reproduced by molecular simulations, which are then analyzed in terms of inter- vs. intra-molecular correlations, as well as ion-ion self versus distinct correlations. Simulations also provide visual insights, as illustrated by the concentric shells of isodensity surfaces shown in Fig. 1.[4-5,8-11]

Wishart and coworkers are studying charge-type effects on electron transfer reactions in ionic liquids using a set of virtually isostructural biaryl electron carriers (biphenyl, N-phenylpyridinium cation and methylviologen dication, selected so that their reduced forms have charges of -1, 0, and +1, respectively) with a series of substituted benzoquinones.[17] Bimolecular rate constants for quinone reduction by the neutral phenylpyridinyl radical at low driving forces are similar to those of the biphenyl radical anion at much higher driving forces, indicating faster diffusion of the neutral radical that will be quantified by further analysis. This work has also demonstrated that solvated electrons diffusion rates in ILs are more like those of molecular anions than quantum particles.

The Blank group has complemented Wishart's radiolysis work on excess electrons in ionic liquids with the first reliable femtosecond time-resolved spectra of electrons in the liquid $[Pr_{14}][Tf_2N]$. Because of the prevalence of secondary photoproducts, a special closed flow system was designed and implemented. The first ultrafast spectra of photochemically generated excess electrons in ILs are shown in Fig. 2.[15] The Margulis group has recently completed a theoretical study of a similar ionic liquid sharing the same Tf_2N anion.[7]

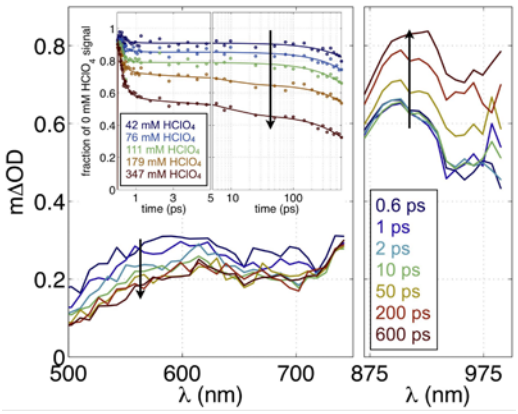

Fig. 2: Transient absorption spectrum of $[Pr_{41}][NTf_2]$ in the presence of quencher and the proposed composition of the spectrum.

Bimolecular electron-transfer reactions have been reported to occur much faster than the diffusion limit in ionic liquids.[1] To investigate this phenomenon, fluorescence quenching data were collected for one particular donor-acceptor pair in a variety of ionic liquids and in conventional solvents. Detailed modeling of these data (Fig. 3) showed that the "anomalously" high rates previously reported were due to the application of kinetic analyses that are inappropriate for the high-viscosity conditions prevalent in ionic liquids.[12] High viscosities amplify the importance of the "transient" portion of a bimolecular reaction, and neglect of this fact can lead to erroneous conclusions. Another contributing factor is that diffusion of neutral reactants in ionic liquids can be considerably faster than Stokes-Einstein predictions, an effect corroborated by direct measurements of self-diffusion coefficients by pulsed field gradient NMR methods.[18]

The large differences in observed vs. predicted self-diffusion coefficients inspired a theoretical study aimed at understanding the nature of charge transport in electrolyte solutions versus ionic liquids. This work addressed the effects of the cross-terms that contribute to the observed conductivity relative to the self-terms that determine the self-diffusion observed via NMR methods.[6]

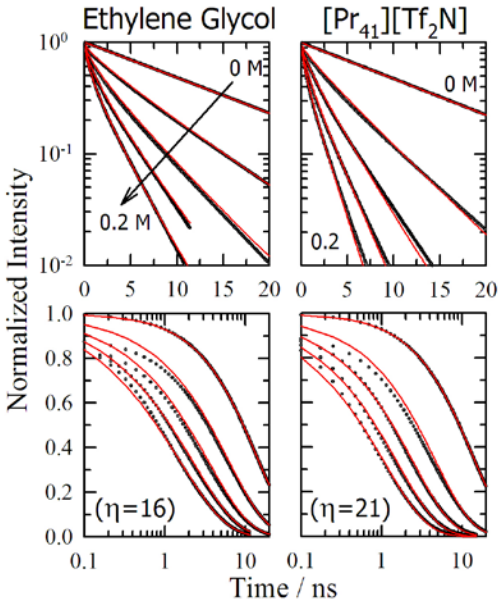

Fig. 3: Fits (red curves) of electron transfer quenching data (points) on the system dicyanoanthracene + dimethylaniline (DMA) in ethylene glycol and a pyrrolidinium ionic liquid of comparable viscosity (cP). Five different DMA concentrations are shown.

Electron-donating ionic liquids (ED-ILs) based on derivatives of N,N-dimethylaniline have been synthesized and shown to have very similar redox properties to the parent compound.[16] By comparing the rates of bimolecular electron transfer of the ED-IL with a homologous neutral donor, we demonstrated that anionic donors have slower rates than neutral ones. Since the rates are diffusion-limited, this unusual result is explained by the faster self-diffusion of the neutral relative to the anionic donor species. The reactivity of the ED-ILs will be compared with electron-accepting ionic liquids created using derivatives of methyl viologen.[18] Work on both the electron donor and acceptor liquids will be complemented by *photonic* ionic liquids, where the photo-excited donor or acceptor chromophore is either the cation or anion of the IL. Such materials will permit detailed studies of high optical concentrations needed for light-harvesting aggregates and thin-film technologies.

DOE Sponsored Publications 2009-2012

1. E. W. Castner, Jr., C. J. Margulis, M. Maroncelli, and J. F. Wishart, Ionic Liquids: Structure and Photochemical Reactivity, *Ann. Rev. Phys. Chem.* **62,** 85-105 (2011).
2. E. W. Castner, Jr. and J. F. Wishart, Spotlight on ionic liquids, *J. Chem. Phys.* **132,** 120901 (2010).
3. J. F. Wishart, Importance of Ionic Liquid Solvation Dynamics to Their Applications in Advanced Devices and Systems, *J. Phys. Chem. Lett.* **1,** 1629-1630 (2010).
4. H. V. R. Annapureddy, H. K. Kashyap, P. M. De Biase, and C. J. Margulis, What is the Origin of the Prepeak in the X-ray Scattering of Imidazolium-Based Room-Temperature Ionic Liquids?, *J. Phys. Chem. B* **114,** 16838-16846 (2010).
5. H. V. R. Annapureddy, H. K. Kashyap, P. M. De Biase, and C. J. Margulis, What is the Origin of the Prepeak in the X-ray Scattering of Imidazolium-Based Room-Temperature Ionic Liquids? [Erratum], *J. Phys. Chem. B* **115,** 9507-9508 (2011).
6. H. K. Kashyap, H. V. R. Annapureddy, F. O. Raineri, and C. J. Margulis, How Is Charge Transport Different in Ionic Liquids and Electrolyte Solutions?, *J. Phys. Chem. B* **115,** 13212-13221 (2011).
7. C. J. Margulis, H. V. R. Annapureddy, P. M. De Biase, D. Coker, J. Kohanoff, and P. M. G. Del, Dry Excess Electrons in Room-Temperature Ionic Liquids, *J. Am. Chem. Soc.* **133,** 20186-20193 (2011).
8. C. S. Santos, H. V. R. Annapureddy, N. S. Murthy, H. K. Kashyap, E. W. Castner, Jr., and C. J. Margulis, Temperature-dependent structure of methyltributylammonium bis(trifluoromethylsulfonyl)amide: X ray scattering and simulations, *J. Chem. Phys.* **134,** 064501 (2011).
9. C. S. Santos, N. S. Murthy, G. A. Baker, and E. W. Castner, Jr., Communication: X-ray scattering from ionic liquids with pyrrolidinium cations, *J. Chem. Phys.* **134,** 121101 (2011).
10. H. K. Kashyap, J. J. Hettige, H. V. R. Annapureddy, and C. J. Margulis, SAXS Anti-Peaks Reveal the Length-Scales of Dual Positive/Negative and Polar/Apolar Ordering in Room-Temperature Ionic Liquids, *Chem. Commun.***,** in press (2012).
11. H. K. Kashyap, C. S. Santos, H. V. R. Annapureddy, N. S. Murthy, C. J. Margulis, and E. W. Castner, Jr., Temperature-dependent structure of ionic liquids: X-ray scattering and simulations, *Faraday Discuss.* **154,** 133-143 (2012).
12. M. Liang, A. Kaintz, G. A. Baker, and M. Maroncelli, Bimolecular Electron Transfer in Ionic Liquids: Are Reaction Rates Anomalously High?, *J. Phys. Chem. B* **116,** 1370-1384 (2012).
13. D. Roy and M. Maroncelli, Simulations of Solvation and Solvation Dynamics in an Idealized Ionic Liquid Model, *J. Phys. Chem. B***,** *in press* (2012).
14. X.-X. Zhang, M. Liang, N. P. Ernsting, and M. Maroncelli, The Complete Solvation Response of Coumarin 153 in Ionic Liquids, *J. Phys. Chem. B***,** submitted (2012).
15. F. M. Domenech, B. FitzPatrick, A. Healy, and D. A. Blank, Anion photo-detachment and

electron reactivity in 1-methyl-1-butyl-pyrrolidinium bis(trifluoromethylsulfonyl)amide, *J. Chem. Phys.*, submitted (2012).

16. C. S. Santos, M. Manpadi, A. J. Baranowski, L. J. Williams, and E. W. Castner, Jr., Bimolecular electron transfer reactions faster than the diffusion limit using ionic liquid donors, *J. Am. Chem. Soc*., submitted (2012).
17. M. Gohdo, D. J. Szalda, H. K. Kashyap, C. J. Margulis, and J. F. Wishart, Structures of redox-active arylpyridinium and methylviologen bis(trifluoromethylsulfonyl)amide salts: contributions from hydrogen bonding and electrostatic interactions, manuscript in preparation (2012).
18. A. Kaintz, G. A. Baker, A. Benesi, and M. Maroncelli, Solute Diffusion in a Series of Pyrrolidinium Ionic Liquids, in preparation (2012).

Charge Transfer States of Organic Molecular Conjugates

Tunna Baruah, Rajendra Zope, Marco Olguin, Subhendu Paul, and Luis Basurto
Department of Physics
University of Texas at El Paso
El Paso TX 79968

The charge-transfer (CT) energies of organic molecular conjugates typically used for photovoltaics determine the open-circuit voltage. Theoretical calculations of CT energies of systems of practical interest (100-200 atoms) pose a challenge. A practical method to obtain CT energies for systems containing 100-400 atoms is developed and refined within the density functional theory. It is a variant of delta-SCF method but maintains the orthogonality between the ground and the excited state and prevents variational collapse of the excited state. The method is implemented in the NRLMOL code. Benchmark of the method on a set of smaller molecular (mostly TCNE-hydrocarbons) conjugates used in literature for similar purpose showed mean absolute deviation from experimental (or very accurate calculations) results for the HOMO to LUMO CT energies to be 0.09 eV (Table I). An estimated average solvent shift of 0.3 eV was applied to calculated CT energies to facilitate comparison with experimental values in solution (labeled with (*S*) in table).

Table 1: Comparison of calculated charge tranfer energies with expt.

DA complexes	Singlet (eV)	Including solvent shift (eV)	Expt. (eV)
TCNE-naphtalene*	2.72		2.6
TCNE-xylene*	3.05		3.15
TCNE-benzene*	3.63		3.59
TCNE-toluene*	3.42		3.36
TCNE-9-10-dimethanth(*S*)	1.64	1.34	1.44
TCNE-9-cmo-anth(*S*)	2.19	1.89	1.84
TCNE-9f-10ch-anth(S)	2.33	2.03	1.96
TCNE-9-methanth(S)	1.84	1.54	1.55
TCNE-9-chloro-anth(S)	2.06	1.76	1.74
TCNE-9-form-anth(S)	2.3	2.0	1.9
TCNE-anthracene(S)	1.95	1.65	1.73
C_2H_4-C_2F_4	12.2		12.5

Using the above method, we have studied the charge transfer states of the various organic donor-acceptor systems used in laboratory such as porphyrin-fullerene, porphyrin-pentacene, P3MT-IC60MA etc. The combination of porphyrins and fullerenes is one of the most extensively studied organic donor-acceptor pairs. Various factors which contribute to the electron-transfer efficiency and the lifetime of the charge-separated state are the donor-acceptor distance and relative orientation, electronic coupling, linker, and the nature of the bonding interaction between the fullerene and porphyrin systems. We have considered four different non-covalently bonded porphyrin-fullerene (P-F) dyads with Zn and base tetra-phenyl-porphyrin (ZnTPP/TPP) combined with C_{60} or C_{70} fullerenes. The study shows that the lowest CT energy increases by about 0.3 eV when the C_{60} replaced by C_{70} but replacing TPP by ZnTPP has marginal effect on the lowest CT energy. Similar studies are carried out on pentacene-C_{60} and mono-adduct of C_{60} conjugated with P3MT. In each case we determined several lowest CT

energies and examined the orientation dependence on CT energies and exciton binding energies. In most systems the orientation effects on charge transfer energies are strong.

Molecular wire-like light harvesting systems often are floppy and therefore structure determination becomes a major issue in such molecules. We have studied the vibrational modes and isomers of a carotenoid-porphyrin-C_{60} triad molecule in gas-phase which was found to exhibit a very large dipole moment upon photo-induced charge transfer. We optimized structures of 18 isomers out of which 6 were obtained by following eigenvectors of low/unstable frequency modes. In gas-phase and at low temperature we find that the structure of the triad is linear. We have also studied the charge transfer energies of several isomers of the triad. For each isomer, several lowest transitions were calculated to determine the lowest CT state. For one isomer solvation effects were estimated.

Most of the systems that are of practical interest are often quite large for ab-initio calculations. Our workhorse code is the NRLMOL code which was originally written in Fortran77. We are restructuring the NRLMOL code to make it applicable to large systems. Major issue is memory requirement when system size exceeds 200 atoms and when large basis sets are employed. By eliminating 2D large arrays using their packed version and through restructuring we reduced memory requirement by about 40%. We have applied the leaner version of the code to a large molecule which we refer to as hexad antenna molecule (~500 atoms, ~13000 basis functions). It contains a hexaphenyl-benzene core that organizes a set of antenna chromophores which are ZnTPP, bisphenyl anthracene and boron dipyrromethane (Fig. 1). Several HOMO orbitals and the LUMO orbital of the molecule are shown in the Figure 1. The various chromophores absorb energy at different frequencies yielding antenna-like behavior for capturing photons. The charge transfer occurs from the chromophores to the fullerene. The results on CT energies, exciton binding energies and their dependence on orientation will be presented.

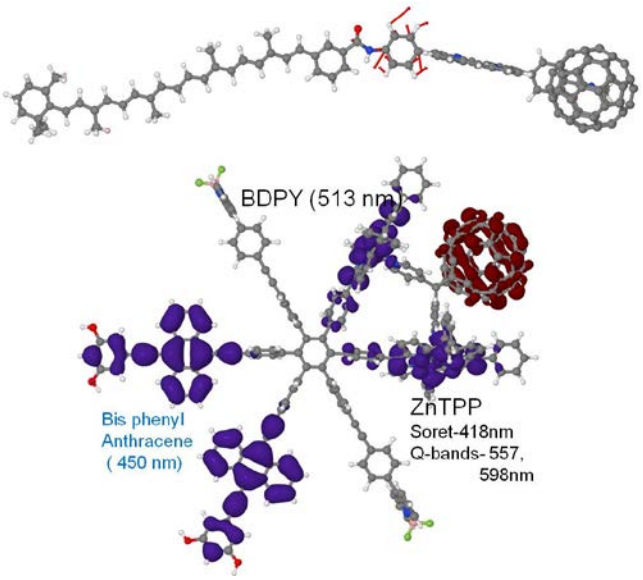

Figure 1: A Carotenoid-porphyrin –C60 triad normal mode with large IR peak; Hexad antenna with six chromophores attached to a hexaphenyl benzene core. HOMOs = Blue, LUMO=Red

DOE Sponsored Solar Photochemistry Publications 2009-2012

1. Charge transfer excitations in co-facial fullerene-porphyrin complexes, R. R. Zope, M. Olguin, T. Baruah, Journal of Chemical Physics (under review).
2. Charge transfer excited state energies by perturbative delta self consistent field method, T. Baruah, M. Olguin, and R. R. Zope, Journal of Chemical Physics (under review).

Donor/Acceptor Coupling Models for Electron and Excitation Energy Transfer and Related Issues for ET Kinetics at Electrodes

Marshall D. Newton
Chemistry Department
Brookhaven National Laboratory
Upton NY 11973

Electronic coupling between local donor (D) and acceptor (A) sites (typically represented as the matrix element H_{DA}), either 'direct' or mediated by 'spacers' is a crucial factor controlling electronic transport in molecular systems, including '1-particle' electron (ET) and '2-particle' excitation energy (EET) transfer. While such coupling for ET, both intra- and intermolecular, has been investigated for decades using theoretical and computational techniques, similar attention has been paid recently to coupling for EET, dealing with many of the same electronic structure and dynamical issues already familiar for ET.

In the case of ET, there is broad interest in processes occurring in both homogeneous solution and interfacial assemblies, such as SAM film-modified electrodes in contact with electrolyte, where the acceptor species may be covalently linked to the film or free in the electrolyte phase. The mechanistic analysis of ET kinetics at electrodes, including D/A coupling and activation parameters and their role in controlling overpotential, is especially important for the design and enhancement of solar conversion schemes.

Here we address some of these issues, providing analysis based on calculated results for several illustrative molecular systems. For both ET and EET coupling, the methodology involves selecting a suitable basic electronic structure model (employing many electron configurations constructed from an orbital basis), followed by the formulation and evaluation of diabatic states and their properties, using a physical criterion broadly applicable to intra- as well as intermolecular systems, where in the former case, the identification of local D and A moieties is nontrivial.The question as to the 'best' diabatic state formulation in turn raises the question as to the optimal size of the reduced electronic state space, a tradeoff between the desire for compactness of the model, but without sacrificing important electronic detail, and the need for compatibility with the dynamical or kinetic model for the overall process. While the diabatic states for modeling ET and EET are designed to yield spatially localized D and A states, the usual constraint of orthogonality, chosen for convenience, entails unavoidably some electronic delocalization, and the possibility of resultant artifactual behavior must be considered.

For bridge (B)-mediated coupling (DBA), we (with Cave *et al*) have assessed the utility of the popular 2-state (2-st) electronic model for H_{DA}, with two important findings: **(1)** for three different Ru^{II}-pz-Ru^{III} complexes (pz ≡ pyrazine), the 2-st model efficiently captures (via superexchange (se)) the important electronic tails essential for overall D/A coupling. This coupling was found to be too large to permit incorporation into a nonadiabatic (Fermi Golden Rule) transition state theory (TST) dynamical model (*ie*, perturbative (PT) treatment of the time dependent quantum mechanics). However, for 2 of the cases (with pyridine and CO axial ligands, but not the Creutz-Taube complex), the coupling could be accurately (within ~10%) accounted for by a 2-st se model (*ie*, PT treatment of the time-dependent electronic structure);
(2) when orthogonal diabatic states are employed, the non-nearest-neighbor (NNN) couplings

inferred from n-state models (n>2), are found to be quite different from those obtained by pairwise (*ie*, 2-st, in the absence of se) estimates of H_{DA} for the same NNN pairs of states.

To eleucidate H_{DA} for EET and the factors contributing to the overall coupling, we (Vura-Weis *et al*) have focussed on the asymptotic distance (R) dependence for two *in vacuo* systems, the $(HeH^{+})_2$ dimer and the perylenemonoimide-perylenediimide (PMI-PDI) dimer. The calculated results were decomposed into Coulomb (J), exchange (K), and an additional '1-electron' term (O). In both cases the salient feature for the conventional 2-state model (based on the two lowest singlet excited dimer adiabatic states (electronic eigenstates)) is that in the asymptotic region (D/A separations > 10 Å), all three terms displayed algebraic falloff ($1/R^3$), whereas exponential falloff for K and O was expected. The issue was resolved by observing that the exponential behavior of K and O was restored for larger state spaces, revealing that the 2-state results are influenced by small tails (an A component in the D state and *vice versa*). These tails do not noticeably affect the total coupling values, in spite of their marked effect on the individual components.

Among our preliminary results and conclusions regarding ET kinetics at electrodes, we note the following (with Sutin, Brunschwig, Feldberg, and Smalley): **(1)** The dense band of electrode states (energies $\{\varepsilon\}$) leads to a sum or integral over the manifold of Marcus nonadiabatic rate constants, $k(\varepsilon)$. Since the discrete sum is generally replaced by an integral, the electrode density of electronic states, ρ_e, is an essential factor in the rate constant. Furthermore, ρ_e and $(H_{\varepsilon A})^2$ are coupled in the sense that they must be normalized in a mutually consistent manner, yielding an invariant product. When one attempts to extend the kinetic framework towards an adiabatic limit (either within the TST framework or involving solvent dynamics), the fate of the invariant factor in any generalized prefactor (*eg*, Landau Zener (LZ)) is an issue requiring further theoretical attention. Among current models in the literature, some separate the two components of the factor, while others maintain its integrity (*eg*, in the exponential argument of the LZ probablility); **(2)** it is well known that for transition metal electrodes, rate constants for nonadiabatic kinetics involve an additive superposition of contributions from s/p and d bands. This has been investigated in detail for Pt, but we emphasize that it appears to be significant for Au as well, indicating that the relevant ρ_e is the s/p copmponent (~ 0.1 states/eV atom, based on calculations), in contrast to the total rhos (~ 0.3 states/eV atoms); **(3)** we have reexpressed the integral over metal states as an effective (or 'quasi') 2-st model, in which the Marcus rate constant **i)** employs the state whose energy (ε_m) maximizes the integrand and **ii)** is modified by a factor characterizing the 'width' of the integrand centered about ε_m. This formulation is general for any driving force, reproducing the results based on the full integral to reasonable accuracy (~20%) and thus supplements the earlier model of Hsu and Marcus for zero driving force.

DOE Sponsored Solar Photochemistry Publications 2009-2012

1. Reduced Electronic Spaces for Modelling Donor/Acceptor Interactions; Robert J. Cave, Stephen T. Edwards, and J. Andrew Kouzelos, and Marshall D. Newton, *J. Phys. Chem.* B **114,** 14631 (2010).
2. Characterizing the Locality of Diabatic States for Electronic Excitation Transfer By Decomposing the Diabatic Coupling, J. Vura-Weis, M.l Newton, M. Wasielewski and J. Subotnik, *J. Phys. Chem.* B **114,** 20449 (2010).
3. Multi-State Treatments of the Electronic Coupling in Donor-Bridge-Acceptor Systems: Insights and Caveats from a Simple Model, Robert J. Cave and Marshall Newton, PCCP (submitted).

Session VIII

Surface Structure and Analysis

Studies of Surface Adsorbate Electronic Structure and Femtochemistry at the Fundamental Length and Time Scales

Hrvoje Petek
Department of Physics and Astronomy and Chemistry
University of Pittsburgh
Pittsburgh PA 15260

Our research focuses on the electronic structure and dynamics of solids, surfaces, and molecule covered surfaces. We are interested in the surface electronic excitation and the subsequent dynamics leading to charge transfer or photochemistry. The correct description of surface electronic structure, photoexcitation, interfacial charge transfer, energy and momentum relaxation of carriers, and femtochemistry are essential for the intellectual framework for applications of photoinduced phenomena at interfaces, such as solar energy conversion. In this abstract we introduce examples of our femtosecond time-resolved multi-photon photoemission (TR-MPP) and low-temperature STM studies of electronic surfaces and interfaces.

Transient exciton formation in metals. When light interacts with a solid it creates a coherent polarization field, i.e., an exciton-polariton, which has both particle and field properties. An exciton can lose coherence through scattering or be emitted as a coherent field. Excitons have never been found in metals because Coulomb interaction is fully screened by charge density fluctuations. The screening response takes time, but is thought to occur on the sub-femtosecond time scale in typical metals. An exception may be silver, which has a sharp bulk plasmon resonance at ~3.8 eV. Sudden introduction of a charge in Ag creates surface plasmon oscillation with ~1 fs period, which dephases on a few femtosecond time scale. When the screening response occurs on a time scale comparable to the laser pulse duration, it may be possible to observe a correlated electron-hole pair state, hence a transient exciton, in an MPP measurement.

We have investigated MPP spectra from the occupied Shockley surface (SS) state, via two or three photon resonance with the unoccupied image potential (IP) state on Cu(111) and Ag(111) surfaces. IP states of metals are not features of the static electronic structure of metals. Rather, they form as a consequence of the many-body screening of an external charge. In other words, they are the asymptotic states in an MPP process where the screening has become saturated.

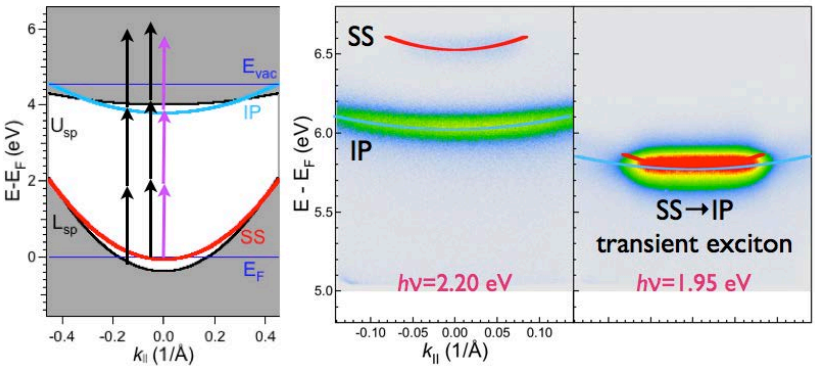

Fig. 1. *The projected band structure of Ag(111) surface showing the resonant (purple) and nonresonant (black) excitation pathways for the SS and IP states, and 3PP spectra (final state energy vs. parallel momentum) under nonresonant (2.20 eV) and resonant (1.95 eV) conditions.*

Figure 1 shows the band structure of Ag(111) and 3PP spectra for resonant and nonresonant excitation conditions. For the non-resonant condition, the energy-momentum image of photoemitted electrons shows

dispersive SS and IP states. At the resonant condition, however, the dispersive surface bands collapse into a nondispersive feature. Such non-dispersive spectra are expected for photoemission from excitonic states, because in a correlated *e-h* pair, the electron can take on any momentum spanned by the occupied part of the hole band, as long as the exciton momentum is conserved. Similar experiments on Cu(111) surface do not show the nondispersive feature, consistent with faster screening suppressing the *e-h* correlation.

2D superatom states. In the spatial domain, we have investigated the formation of a molecular quantum-well with single-molecule resolution. Several years ago 2PP spectroscopy provided the evidence that a monolayer of flat lying C_6F_6 molecules on Cu(111) surface forms a molecular quantum well with an effective mass of $2m_e$ for its LUMO state of σ* character. How flat lying π-conjugated molecules can hybridize into a delocalized band has remained a mystery.

We have performed low temperature STM measurements on C_6F_6 on Cu and Au surfaces from single molecule to multilayer coverages. By dz/dV spectroscopy we could measure the σ* state energy as a function of the number of nearest neighbors, and found that the energy is stabilized consistent with an intermolecular hopping integral β=0.026 eV. This behavior could be reproduced nearly quantitatively by a DFT calculation of the electronic structure of unsupported C_6F_6 from a single molecule to a monolayer film. The calculations show that the band formation is an intrinsic property of C_6F_6 molecules, which raises the question of the origin of the intermolecular interaction that enables the dispersive band formation.

We have therefore investigated the electronic properties of the σ* state. As required for the strong intermolecular interaction, the σ* state has a diffuse wave function with a long tail extending past the F atom periphery (Fig. 2). This behavior is reminiscent of the superatom molecular orbitals (SAMOs) of hollow molecules, which we discovered in C_{60} and related materials. SAMOs of hollow molecules are bound to the hollow core rather than the ions of the hollow cage. Examining the probability density of the σ* state, we find that it is distributed in nonnuclear regions with the maximum density within the hollow benzene ring. This leads us to the conclusion that the σ* state is in fact a 2D superatom state, and suggests a new paradigm for designing molecular semiconducting materials with nearly-free electron band transport.

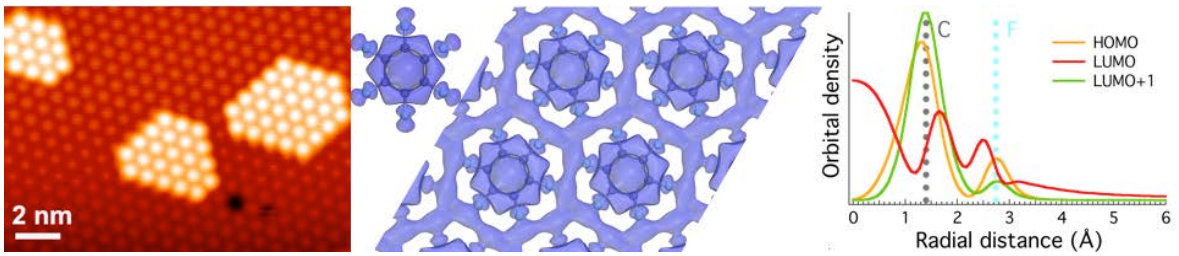

Figure 2. *STM image of C_6F_6 monolayer and second monolayer islands on Cu(111) surface. The calculated probability density of the σ* state for a single molecule and σ* band for a monolayer quantum well. The density projecting beyond F atoms forms the delocalized state. The radial wave function cross sections for the π HOMO, σ* LUMO, and π* LUMO+1 orbitals. The SAMO characteristics of σ* are responsible for the nonnuclear density in the molecular center and beyond the F atom periphery.*

DOE Sponsored Solar Photochemistry Publications 2009-2012

1. Achilli, S., Trioni, M.I., Chulkov, E.V., Echenique, P.M., Sametoglu, V., Pontius, N., Winkelmann, A., Kubo, A., Zhao, J., & Petek, H., "Spectral properties of Cs and Ba on Cu(111) at very low coverage: Two-photon photoemission spectroscopy and electronic structure theory." *Phys. Rev. B* **80**, 245419 (2009).
2. Huang, T., Zhao, J., Feng, M., Petek, H., Yang, S., & Dunsch, L., "Superatom orbitals of $Sc_3N@C_{80}$ and their intermolecular hybridization on Cu(110)-(2x1)-O surface." *Phys. Rev. B* **81**, 085434 (2010).
3. Hu, S., Zhao, J., Jin, Y., Yang, J., Petek, H., & Hou, J.G., "Nearly Free Electron Superatom States of Carbon and Boron Nitride Nanotubes." *Nano Lett.* **10**, 4830 (2010).
4. Feng, M., Zhao, J., Huang, T., Zhu, X., & Petek, H., "The Electronic Properties of Superatom States of Hollow Molecules." *Acc. Chem. Res.* **44**, 360 (2011).
5. Wang, L.-M., Sametoglu, V., Winkelmann, A., Zhao, J., & Petek, H., "Two-Photon Photoemission Study of the Coverage-Dependent Electronic Structure of Chemisorbed Alkali Atoms on a Ag(111) Surface." *J. Phys. Chem. A* **115**, 9479 (2011).
6. Feng, M., Cabrera-Sanfelix, P., Lin, C., Arnau, A., Sánchez-Portal, D., Zhao, J., Echenique, P.M., & Petek, H., "Orthogonal Interactions of CO Molecules on a One-Dimensional Substrate." *ACS Nano* **5**, 8877 (2011).
7. Huang, T., Zhao, J., Feng, M., Popov, A.A., Yang, S., Dunsch, L., & Petek, H., "A Molecular Switch Based on Current-Driven Rotation of an Encapsulated Cluster within a Fullerene Cage." *Nano Lett.* **11**, 5327 (2011).
8. Feng, M., Lin, C., Zhao, J., & Petek, H., "Orthogonal Intermolecular Interactions of CO Molecules on a One-Dimensional Substrate." *Annu. Rev. Phys. Chem.* **63**, 201 (2012).
9. Lin, C., Feng, M., Zhao, J., Cabrera-Sanfelix, P., Arnau, A., Sánchez-Portal, D., & Petek, H., "Theory of orthogonal interactions of CO molecules on a one-dimensional substrate." *Phys. Rev. B* 85, 125426 (2012).
10. Petek, H., Feng, M., & Zhao, J., The Electronic Structure of Metal–Molecule Interfaces in *Current-driven phenomena in nanoelectronics*, edited by T. Seideman (World Scientific 2010).
11. Winkelmann, A., Chiang, C.-T., Tusche, C., Ünal, A.A., Kubo, A., Wang, L., & Petek, H., Ultrafast multiphoton photoemission microscopy of solid surfaces in the real and reciprocal space in *Dynamics of interfacial electron and excitation transfer in solar energy conversion: theory and experiment*, edited by P. Piotrowiak (Royal Society of Chemistry, London, 2012).
12. Bovensiepen, U., Petek, H., & Wolf, M. eds., Dynamics at Solid State Surfaces and Interfaces, Vol. 1: Current Developments, 1 ed. (Wiley-VCH Verlag Gmbh & Co., Weinheim, 2010).
13. Bovensiepen, U., Petek, H., & Wolf, M. eds., Dynamics at Solid State Surfaces and Interfaces, Vol. 2: Fundementals, 1 ed. (Wiley-VCH Verlag Gmbh & Co., Weinheim, 2012).

Catalysis Characterization by In-Situ Resonance Raman Spectroscopy

Hack-Sung Kim and Peter C. Stair
Department of Chemistry
Northwestern University
Evanston, IL 60208
and
Chemical Sciences and Engineering Division
Argonne National Laboratory
Argonne, IL 60439

Raman spectroscopy (RS) is one of the most powerful methods for the characterization of heterogeneous catalytic processes because it can provide information about both the catalyst and the molecular species involved in the reaction in a single measurement.[1, 2] Like other spectroscopic techniques, RS also has some drawbacks, which limit its usefulness. In the field of heterogeneous catalysis, the drawbacks include (1) strong background emission due to fluorescence which makes Raman bands weak or completely undetectable, (2) the intrinsic low sensitivity of RS particularly at low loadings of active material, and (3) the possibility of sample degradation induced by the excitation laser (especially in the UV).[1] In common with other scattering measurements quantitative analysis via Raman intensities is made difficult by uncertainty and variation in the sampling volume.[3] This presentation will highlight work from our laboratory on the application of ultraviolet resonance Raman spectroscopy to catalysis with a particular focus on overcoming problems 1-3 along with methods that address the issue of quantitative analysis.

The so-called "fluorescence background" has been a major hindrance to the application of Raman spectroscopy in heterogeneous catalysis. Fluorescence backgrounds appear primarily in the visible and sometimes near IR (NIR) region and are associated with the CW visible excitation used in conventional Raman spectroscopy. It can largely be avoided using ultraviolet laser excitation. In UV Raman the features of interest are in the ultraviolet region at wavelengths near the excitation laser and at much higher energy than fluorescence. As an example, the acquisition of Raman spectra from γ-Al_2O_3, one of the most widely used catalyst supports, has long been unsuccessful. With 244 nm excitation, a clear Raman band has been observed at 855 cm^{-1} for γ-Al_2O_3.[4] This methodology

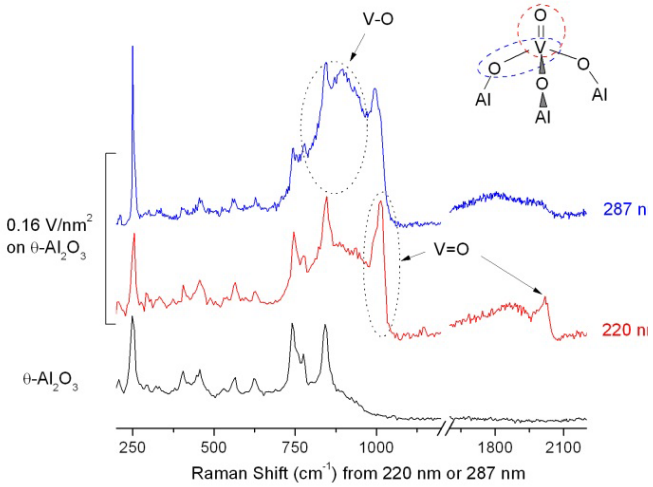

Fig. 1 UV resonance Raman spectra excited at 220 nm and 287 nm for alumina supported vanadium oxide monomers. The symmetric V=O stretching mode is selectively enhanced with 220 nm excitation, while the symmetric and asymmetric V-O stretching modes are selectively enhanced with 287 nm excitation.

methodology is also particularly useful for avoiding strong fluorescence from catalysts containing hydrocarbon fragments.

The main application for resonance Raman spectroscopy (RRS) is the identification and monitoring of molecular and surface species in catalysis. For example, monomeric and polymeric vanadium oxide supported on alumina can be distinguished via RRS.[4] The quantification of different surface vanadia species and their hydrogen reduction can be studied using diffuse reflectance measurements to account for self-absorption.[5] The spectroscopic details can also provide additional information on the atomic and electronic structures of surface catalytic species. For example, with monomeric $O=V-(OAl)_3$ surface species in alumina supported vanadium oxide, V=O and V-O stretching modes are selectively enhanced in RR spectra excited at 220 nm and 287 nm, respectively (See Fig. 1).[6] V=O overtones are quite intense with 220 nm excitation where V=O fundamental band is most strongly enhanced. In contrast, V-O overtones are very weak with 287 nm excitation where the V-O fundamental is most strongly enhanced. The difference in overtone intensity is indicative of a significant increase in the V=O bond length and a negligible increase of V-O bond length in the corresponding excited electronic states.,

In situ or operando Raman measurements require a cell that can be used under the desired conditions. Various cell designs applied to heterogeneous catalysis have been described in reviews. The laser beam focused onto the top surface of a solid sample may cause thermal- or photo-degradation. The sensitivity to degradation depends on the (1) thermal and optical properties of catalyst (thermal conductivity, specific heat, absorption coefficient at the laser excitation wavelength, etc), (2) excitation laser power density at the sample, (3) residence time of the sample in the laser beam, and (4) the thermal- or photo-stability of the sample. These problems are avoided with the fluidized bed (FB) cell.[7] The FB-method is suitable for measurements of catalytic kinetics, flow-through reactions, and shortening the laser beam residence time. A comparison between the FB, fixed bed, and spinning pellet methods shows that the FB method is the best for suppressing laser-induced degradation of adsorbates on solid catalysts and should be the method of choice for *in situ* and operando Raman experiments.

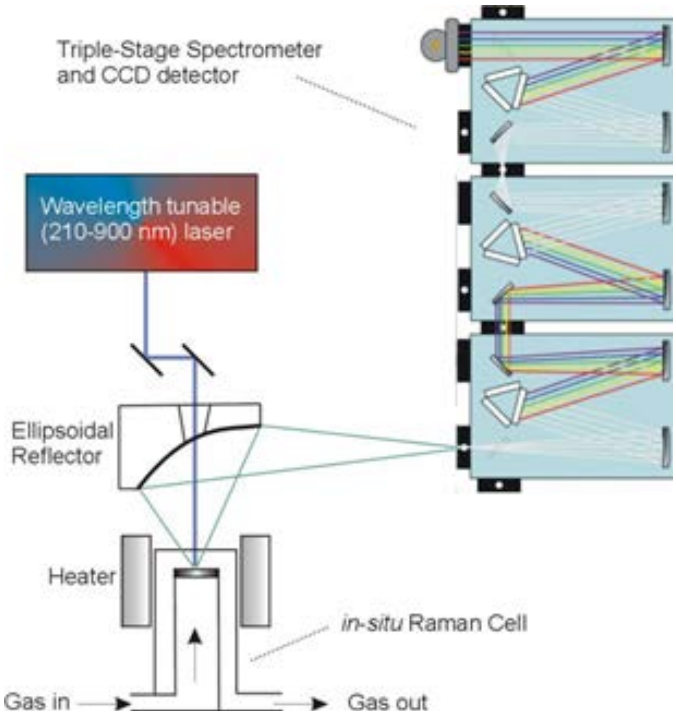

Fig. 2 UV resonance Raman system at Argonne National Laboratory. It consists of wavelength-tunable excitation lasers emitting from deep UV to near IR, a fluidized bed reactor (*in situ*, operando Raman cell), an ellipsoidal reflector for light collection, and a triple-grating spectrometer.

Selected Publications Supported by BES Chemical Sciences, Catalysis Science

1. Kim, H., K.M. Kosuda, R.P. Van Duyne, and P.C. Stair, Resonance Raman and surface- and tip-enhanced Raman spectroscopy methods to study solid catalysts and heterogeneous catalytic reactions. *Chemical Society Reviews*, 2010. **39**(12): p. 4820-4844.
2. Stair, P.C., The Application of UV Raman Spectroscopy for the Characterization of Catalysts and Catalytic Reactions. *Advances in Catalysis*, 2007. **51**: p. 75-98.
3. Wu, Z., C. Zhang, and P.C. Stair, Influence of Absorption on Quantitative Analysis in Raman Spectroscopy. *Catalysis Today*, 2006. **113**: p. 40-47.
4. Wu, Z., H.-S. Kim, P.C. Stair, S. Rugumini, and S.D. Jackson, On the Structure of Vanadium Oxide Supported on Aluminas: UV and Visible Raman Spectroscopy, UV-Visible Diffuse Reflectance Spectroscopy, and Temperature-Programmed Reduction Studies. *Journal of Physical Chemistry*, 2005. **109**: p. 2793-2800.
5. Wu, Z., P.C. Stair, S. Rugmini, and S.D. Jackson, Raman Spectroscopic Study of V/θ-Al_2O_3 Catalysts: Quantification of Surface Vanadia Species and Their Structure Reduced by Hydrogen. *Journal of Physical Chemistry C*, 2007. **111**(44): p. 16460-16469.
6. Kim, H.-S. and P.C. Stair, Resonance Raman Spectroscopic Study of Alumina-Supported Vanadium Oxide Catalysts with 220 and 287 nm Excitation. *J. Phys. Chem. A*, 2009. **113**(16): p. 4346-4355.
7. Chua, Y.T. and P.C. Stair, A Novel Fluidized Bed Technique for Measuring UV Raman Spectra of Catalysts and Adsorbates. *J. Catal.*, 2000. **196**(1): p. 66-72.

Atomic Resolution Imaging and Quantification of the Chemical Functionality of Surfaces

Mehmet Z. Baykara[1], Harry Mönig[1,2], Todd C. Schwendemann[1,3], Özhan Ünverdi[1], Milica Todorovic[4], Ruben Perez[4], Eric I. Altman[2], and Udo D. Schwarz[1,2]

[1] Department of Mechanical Engineering and Materials Science
[2] Department of Chemical and Environmental Engineering
Yale University, New Haven CT 06520 USA

[3] Physics Department
Southern Connecticut State University, New Haven CT 06515 USA

[4] Departamento de Física Teórica de la Materia Condensada
Universidad Autónoma de Madrid, 28049 Madrid, Spain

Scope

The work carried out under current support comprises an atomic-scale study of the local chemical interactions that govern the catalytic properties of model catalysts of interest to DoE. This goal is achieved through three-dimensional atomic force microscopy (3D-AFM), a new measurement mode that allows the mapping of the complete surface force and energy fields with picometer resolution in space (*x*, *y*, and *z*) and piconewton/millielectron volts in force/energy. In combination with the simultaneous recording of tunneling current (3D-AFM/STM), chemically well-defined tips, and comparison to simulations, it enables precise quantification and assignment of local chemical interactions to exact positions within the lattice.

Recent Results

The left part of Figure 1 illustrates the principle of 3D-AFM/STM: A metal tip scans the three-dimensional space above the oxygen-reconstructed copper (100) surface while the tip-sample force and the tunneling current flowing between tip and sample are recorded as a function of *x*, *y*, and *z* (the green/red inset represents the corresponding 3D map of interaction forces on that surface). This Cu_3O_2 surface phase [a $(2\sqrt{2}\times\sqrt{2})R45°$ missing row reconstruction] was chosen as model system because it combines catalytically interesting properties (Cu-based materials are active catalysts for a number of important reactions including methanol synthesis, the water gas shift reaction, and reduction of nitrogen oxides) with favorable structural properties featuring defects and a distinct structure of the Cu and O sublattices that is ideally suited to demonstrate the potential of 3D-AFM/STM. Data sets recorded in ultrahigh vacuum and at low temperatures using a home-built tuning fork-based microscope enable site-specific quantification of force interactions and tunneling currents, with drastically different types of contrast in simultaneously recorded data channels that depend critically on tip chemistry. To further validate the experimental results, DFT total-energy calculations and Non-equilibrium Green's Function (NEGF) methods for electronic transport have been used to determine the force interaction and the tunneling current for a large set of tip models. The analysis of our experimental results allows for the identification of atomic species and defects on the sample surface through the comparison of simultaneously recorded force and current data, as well as the study of defect-induced stress fields and their influence on local chemical reactivity and topographical deformation.

We have then moved to investigate rutile TiO_2, the most widely employed photocatalyst. Also on this material, chemical sensitive imaging is demonstrated (middle and right pictures in Figure 1).

While the force channel highlights the oxygen rows (defect appears dark), the simultaneously collected tunneling current features the titanium rows (defect between lines, appears bright). Again, based on modification of the tip chemistry, interactions of interest can be singled out for a quantitative, in-depth analysis.

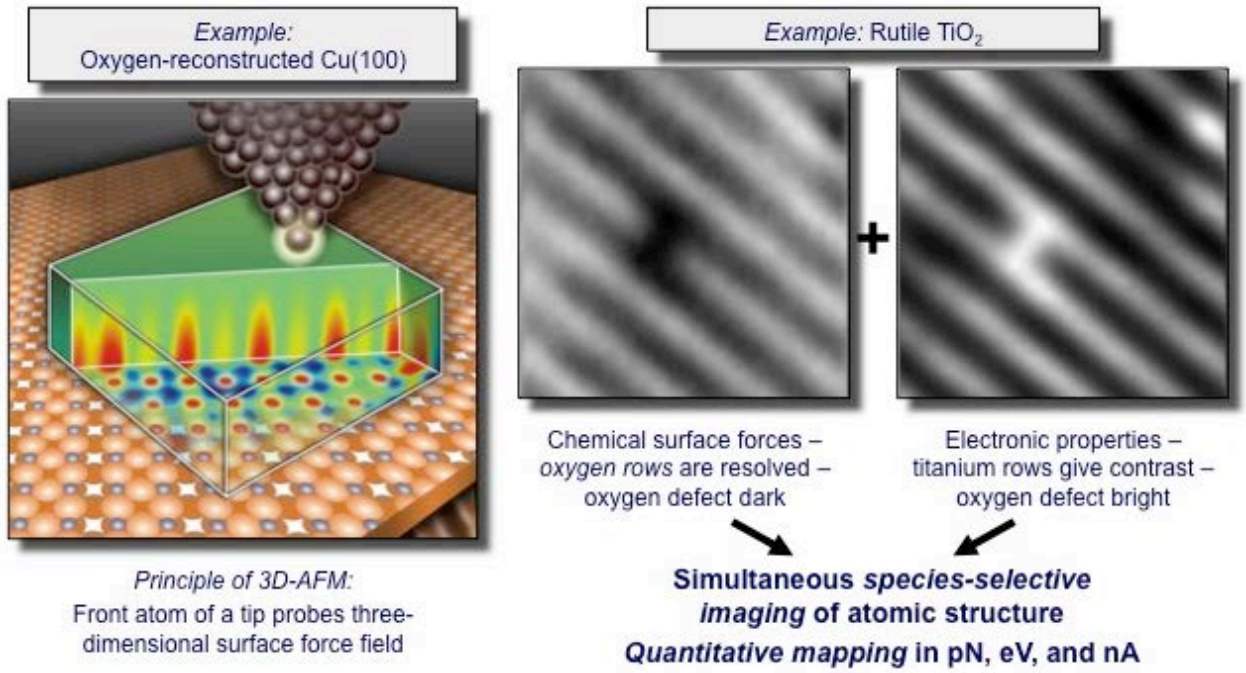

Fig. 1. Figure illustrating 3D-AFM/STM with chemical specificity. *Left:* Strong attractive force interactions between a metallic tip scanning the 3D space over an oxygen-induced surface reconstruction on copper (100) reveal the positions of the O atoms (grey in the model, red/yellow in the data), but not the ones of the Cu atoms (orange in the model). *Middle and right:* Demonstration of chemical selectivity on a rutile TiO_2 surface: The force channel (middle) and the tunneling current channel (right) provide complementary chemical information (O vs. Ti imaging). Images represent maps at constant height with the brightness representing quantitative forces/currents in pN/nA.

Future Plans

A long-term goal of the proposed work is to map out chemical reactivity of surfaces on the atomic scale by functionalizing the tip with different molecules that are sensitive to different chemical properties. For calibration purposes, it is beneficial to also deposit molecules that have a known chemical termination on surfaces. Towards this goal, we are currently depositing molecules such as 2,2-dimethyl butyric acid on TiO_2 that will subsequently be mapped in 3D mode. In addition, we started working on layers of silica grown on Pd(100) due to the importance of materials constructed from SiO_4 tetrahedra in catalysis. Although the film is not crystalline, atomic-scale details can be readily discerned in the images. The surface includes pockets of hexagonally packed pores with a typical spacing of 5.8 Å, as well as smaller pores, and larger irregularly shaped pores that appear darker or deeper. By collecting 3D-AFM data sets of this amorphous silica surface with bare Pt-Ir tips, the variation in the size and shape of the pores and the rings surrounding them will allow us to directly determine how bond angles in the silica framework influence local chemical interactions.

Session IX

Catalysis at Surfaces I

New Carbon-Free Nano-Dyads and Triads for Solar-Energy-Driven Catalytic Water Splitting

J. Fielden, X. Xiang, A. L. Kaledin, Z. Huang, W. Rodríguez-Córdoba, N. Zhang, Z. Luo, Y. Geletii, D. G. Musaev, T. Lian and C. L. Hill

Department of Chemistry
Emory University
Atlanta GA 30322

Charge Transfer Dynamics in Semiconductor–Chromophore–Polyoxometalate Interfaces: Towards Water-Oxidizing Photoelectrodes. Triadic photoelectrodes have been assembled from semiconducting metal oxides (TiO_2 and SnO_2), Ru-polypyridyl photosensitizers (P2 and C2P2, see Figure at right) and the water oxidation catalyst $[\{Ru_4O_4(OH)_2(H_2O)_4\}(\gamma\text{-}SiW_{10}O_{36})_2]^{10-}$ (Ru_4POM). Electron transfer processes in these triads and their parent metal oxide–sensitizer dyads have been studied by visible and mid-IR transient absorption spectroscopy (TAS), and preliminary investigations made of the photoelectrochemical (PEC) performance of the systems. Upon excitation at 515 nm, TiO_2–P2 shows femtosecond and picosecond timescale electron injection processes from the sensitizer to the TiO_2 conduction band (monitored at 5000 nm), respectively corresponding to injection from the unrelaxed ^{1}MLCT and relaxed ^{3}MLCT excited states. For the TiO_2–P2–Ru_4POM triad, the slower injection is suppressed: possibly due to competing electron transfer from the ^{3}MLCT excited states of P2 to Ru_4POM. On SnO_2, however, electron injection is independent of the presence of Ru_4POM, as the lower conduction band edge increases the driving force for electron transfer to the metal oxide. Visible TAS of both TiO_2 and SnO_2 based systems indicates substantially faster (*ca*. 1 ns) decay of the P2 ground state bleach (GSB) in the presence of Ru_4POM, suggesting electron transfer from the catalyst to the oxidized dye. Furthermore, in the SnO_2–P2–Ru_4POM system a long-lived positive absorption band is observed after the GSB decay is completed, which by spectroelectrochemistry is tentatively assigned to oxidized Ru_4POM. Triads based on the crown–ether derivatized sensitizer C2P2 have similar overall behavior to the P2-based systems, but show improved electron injection when the crown ether is metallated with Li^+/Na^+. PEC measurements indicate substantial (up to 100%) photocurrent enhancements in the presence of Ru_4POM, with metallated C2P2 based electrodes showing higher photocurrents and greater stability than those based on P2.

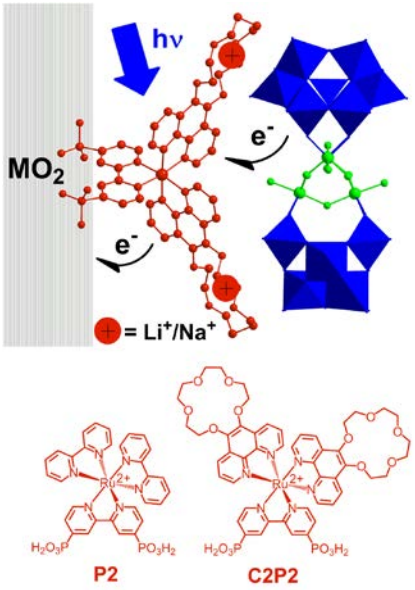

Molecular Metal-to-Metal (MMCT) and Metal-to-Polyoxometalate (MPCT) Chromophores. One of the specific technical objectives of our integrated experimental-computational grant is to prepare and characterize tunable and POM-based molecular metal-to-metal charge transfer (MMCT) chromophores for use as the light-harvesting component of our all-inorganic photo-driven water oxidation triads to overcome the well-known hydrolytic instability of organic dyes. Progress here has been made on two complementary fronts. First, we

recently reported that $[P_4W_{35}O_{124}\{Re(CO)_3\}_2]^{16-}$ (**1**, X-ray structure below), a complex comprising the $[Re(CO)_3]^+$ unit supported on a POM, the defect Wells-Dawson-type $[\alpha_2\text{-}P_2W_{17}O_{61}]^{10-}$, exhibits an intense Re-to-POM CT transition (the UV-vis spectrum of **1** shows an intense broad absorption (up to 700 nm) covering the entire UV and visible regions with high absorptivity (ε_{400nm} ~ 6,200 and 4,500 $M^{-1}\cdot cm^{-1}$ in water and CH_2Cl_2, respectively). Importantly, **1** is free of the oxidatively and hydrolytically unstable polypyridyl ligands. Computational studies indicate that the origin of high visible absorptivity of **1** is attributed to a Re-to-POM ligand CT transition.

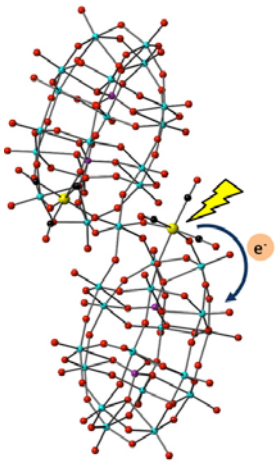

Second, we are incorporating redox active transition metal(s) into a POM framework as an initial foray into tunable intra-POM MMCT chromophores. Initially, we are focusing on the cobalt-centered Keggin anions, $[Co^{II}_2(H_2O)W_{11}O_{39}]^{8-}$ (**2**), $[Co^{III}Co^{II}(H_2O)W_{11}O_{39}]^{7-}$ (**3**), $[Co^{II}W_{12}O_{40}]^{6-}$ (**4**) and $[Co^{III}W_{12}O_{40}]^{5-}$ (**5**). Extensive studies show that **2** and **3** have strong absorptions that tail into the visible, giving extinction coefficients of around 1000 $M^{-1}cm^{-1}$ at 400 nm. Photo-excitation of **2** at 400 nm produces a ground-state bleach at 620 nm, and an intense absorption band at 475 nm. Decay kinetics indicate an excited state lifetime of ca. 100 ps, and the excited state absorption spectrum shows similar features to its one-electron-oxidized ($Co^{III}Co^{II}$) counterpart **3** suggesting photo-induced injection of the electron into the polytungstate ligand resulting in a $Co^{II}Co^{III}$ inter-valence-charge transfer chromophoric unit. This conclusion has also been confirmed by DFT calculations. Both DFT and EPR indicate that the central Co atom is oxidized in **3**.

Charge Separation Dynamics in Covalently Linked Sensitizer-POM Dyads. The development of efficient and robust electrode-sensitizer-catalyst triads remains one of the major challenges in the field of solar fuel generation. Our team is investigating multiple approaches for constructing triadic/dyadic photoelectrode systems. First, dyads of Ir- and Ru- polypyridyl complexes covalently bonded to a polyoxometalate (POM) through connectors of varying length and electronic structure, including alkynyl phenyl groups and others, have been synthesized and characterized. This work is in collaboration with Anna Proust's group at the University of Paris 6, France. Using transient absorption (TA) spectroscopy and computation, we have demonstrated that upon excitation of the MLCT transition in the Ir complex, the electron is transferred to the POM. This assignment is confirmed by spectroelectrochemistry and DFT calculations. The TA spectra of the charge separated state consist of reduced POM and oxidized Ir complexes. The charge separation and recombination rates depend sensitively on the structure of the POM and the chemical linkage between the sensitizer and the POM. The charge separation rate is faster with the –Si-O- linkage between these two units compared to that of the structural analogue with a Sn-O linkage between these units. The ET rate to the Keggin POM is much faster than that to the Wells-Dawson POM. Second, we have directly attached WOCs to narrow band gap oxide semiconductor electrodes (such as Fe_2O_3) and are in the process of studying the dynamic, photoelectrochemical, and stability properties of these systems.

DOE Sponsored Solar Photochemistry Publications 2009-2012

1. Geletii, Y. V.; Huang, Z.; Hou, Y.; Musaev, D. G.; Lian, T.; Hill, C. L. "Homogeneous Light-Driven Water Oxidation Catalyzed by a Tetraruthenium Complex with All Inorganic Ligands" *J. Am. Chem. Soc.* **2009**, *131*, 7522-7523.
2. Cao, R.; Ma, H.; Geletii, Y. V.; Hardcastle, K. I.; Hill, C. L. "Structurally Characterized Iridium(III)-Containing Polytungstate and Catalytic Water Oxidation Activity" *Inorg. Chem*. **2009**, *48*, 5596-5598.
3. Besson, C.; Musaev, D. G.; Lahootun, V.; Cao, R.; Chamoreau, L.-M.; Villaneau, R.; Villan, F.; Thouvenot, R.; Geletii, Y. V.; Hill, C. L.; Proust, A. "Vicinal di-nitridoruthenium substituted polyoxometalates, γ-$[XW_{10}O_{38}\{RuN\}_2]^{6-}$ (X=Si or Ge)" *Chem., Eur. J.* **2009**, 15(39), 10233-10243.
4. Kaledin, A. L.; Huang, Z.; Geletii, Y. V.; Lian, T.; Hill, C. L.; Musaev, D. G. "Insights into photoinduced electron transfer between $[Ru(bpy)_3]^{2+}$ and $S_2O_8^{2-}$ in water: computational and experimental studies, *J. Phys. Chem. A*. **2010**, *114*, 73-80.
5. Fang, X.; Speldrich, M.; Schilder, H.; Cao, R.; O'Halloran, K.; Hill, C. L.; Kögerler, P. "Switching slow relaxation in a $Mn^{III}_3Mn^{IV}$ cluster: an example of grafting single-molecule magnets onto polyoxometalates" *Chem. Commun*. **2010**, *46*, 2760-2762.
6. Besson, C.; Huang, Z.; Geletii, Y. V.; Lense, S.; Hardcastle, K. I.; Musaev, D. G.; Lian, D. G.; Lian, T.; Proust, A.; Hill, C. L. "$Cs_9[(\gamma\text{-}PW_{10}O_{36})_2Ru_4O_5(OH)(H_2O)_4]$, a new all-inorganic, soluble catalyst for the efficient visible-light-driven oxidation of water" *Chem. Commun*. **2010**, *46*, 2784-2786.
7. Kaledin, A. L.; Huang, Z.; Yin, Q.; Dunphy, E. L.; Constable, E. C.; Geletii, Y. V.; Lian, T.; Hill, C. L.; Musaev, D. G. "Insights into Photoinduced Electron Transfer Between [Ru(mptpy)2]4+ (mptpy = 4′(4-methylpyridinio)-2,2′:6′,2″-terpyridine) and $[S_2O_8]^{2-}$: Computational and Experimental Studies" *J. Phys. Chem. A*. **2010**, *114*, 6284–6297.
8. Song, J.; Luo, Z.; Zhu, H.; Huang, Z.; Lian, T.; Kaledin, A. L.; Musaev, D. G.; Lense, S.; Hardcastle, K. I.; Hill, C. L. "Synthesis, structure, and characterization of two polyoxometalate-photosensitizer hybrid materials" *Inorg. Chim. Acta*, **2010**, *363*, 4381 (Special Issue dedicated to Achim Müller).
9. Boulesbaa, A.; Huang, Z.; Wu, D.; Lian, T. "Competition between Energy and Electron Transfer from CdSe QDs to Adsorbed Rhodamine B", *J. Phys. Chem. C*, **2010**, *114*, 962-969.
10. Huang, Z.; Luo, Z.; Geletii, Y. V.; Vickers, J. W.; Yin, Q.; Wu, D.; Hou, Y.; Ding, Y.; Musaev, D. G.; Hill, C. L.; Lian, T. "Efficient Light-Driven Carbon-Free Cobalt-Based Molecular Catalyst for Water Oxidation" *J. Am. Chem. Soc*. **2011**, *133*, 2068–2071.
11. Zhu, G.; Lv, H.; Vickers, J. W.; Geletii, Y. V.; Luo, Z.; Song, J.; Huang, Z.; Musaev, D. G.; Hill, C. L. "Structural and mechanistic studies of tunable, stable, fast multi-cobalt water oxidation catalysts", *Proceedings of SPIE*, **2011**, 8109 (Solar Hydrogen and Nanotechnology VI), 81090A-81090A-6.
12. Huang, Z.; Geletii, Y. V.; Musaev, D. G.; Hill, C. L.; Lian T. "Spectroscopic Studies of Light-driven Water Oxidation Catalyzed by Polyoxometalates", *Industrial & Engineering Chemical Research*, **2012**, in press.
13. Hill, C. L; Lv, Hongjin, Song, J.; Zhao, C.; Geletii, Y. V.; Zhu, G.; Musaev, D. G.; Vickers, J. W.; Zhang, N.; Luo, Z. "Multi-electron-transfer catalysts for solar fuel production", *Preprints of Symposia, American Chemical Society, Division of Fuel Chemistry*, **2012**, *57*, 33.

14. Huang, Z.; Geletii, Y. V.; Wu, D.; Anfuso, C. L.; Musaev, D. G.; Hill, C. L.; Lian, T. "Interfacial charge transfer dynamics in TiO_2-Sensitizer-Ru_4POM photocatalytic systems for water oxidation", *SPIE proceedings*, **2011**, 8109 (Solar Hydrogen and Nanotechnology VI), 810903-810903-10.
15. Anfuso, C. L.; Snoeberger, R. C., III; Ricks, A. M.; Liu, W.; Xiao, D.; Batista, V. S.; Lian, T. Covalent Attachment of a Rhenium Bipyridyl CO_2 Reduction Catalyst to Rutile TiO_2. *J. Am. Chem. Soc.* **2011**, *133*, 6922-6925.
16. Zhu, H.; Song, N.; Lv, H.; Hill, C. L.; Lian, T. "A colloidal quasi-type II nanorod based system for efficient light-driven redox mediator reduction and H_2 generation", *Angew. Chem. Intl. Ed.*, submitted.
17. Wu, K.; Zhu, H.; Liu, Z.; Rodríguez-Córdoba, W.; Lian, T. "Ultrafast Charge Separation and Long-lived Charge Separated State in Photocatalytic CdS-Pt Nanorod Heterostructures", *J. Am. Chem. Soc*. submitted.

Publications that cite DOE solar (Hill, PI) and DOE catalysis (Musaev, PI) grants

18. Kuznetsov, A. E.; Geletii, Y. V.; Hill, C. L.; Morokuma, K.; Musaev, D. G. "Dioxygen and Water Activation Processes on Multi-Ru-Substituted Polyoxometalates: Comparison with the "Blue-Dimer" Water Oxidation Catalyst" *J. Am. Chem. Soc.* **2009**, *131*, 6844-6854.
19. Geletii, Y. V.; Besson, C.; Hou, Y.; Yin, Q.; Musaev, D. G.; Quiñonero, D.; Cao, R.; Hardcastle, K. I.; Proust, A.; Kögerler, P.; Hill, C. L. "Molecular, Stable and Fast Water Oxidation Catalysts for Solar Fuel Production" *ACS Preprints; Fuel Division* **2010**, *55,* 359.

Correlation of Theory and Function in Well-Defined Bimetallic Electrocatalysts

Richard M. Crooks, Graeme Henkelman, Anatoly Frenkel, Hyun You Kim,
Daniel Sheppard, Emily Carino, Nathan Froemming, V. Sue Myers, Wenjie Tang,
David Yancey, Liang Zhang, Sam Chill, and Chun-Yuang Lu

Department of Chemistry and Biochemistry
The University of Texas at Austin
Austin TX 78712-0165

Goal. The objective of this research project is to correlate the structure of nanoparticles that are comprised of ~100 atoms to their catalytic function. The project is based on a growing body of evidence suggesting that catalytic properties can be tailored through controlled synthesis of nanoparticles. What is missing from many of these studies, and what we are contributing, is a model catalyst that is sufficiently small and well-characterized that its function can be directly predicted by theory. Specifically, our work seeks to develop a fundamental and detailed understanding of the relationship between the structure of nanoscopic oxygen-reduction catalysts and their function. We have assembled a team with expertise in theory, synthesis, and advanced characterization methods to address the primary objective of this project. We anticipate the outcomes of the study to be: (1) a better theoretical understanding of how nanoparticle structure affects catalytic properties; (2) the development of advanced, *in-situ* and *ex-situ*, atomic-scale characterization methods that are appropriate for particles containing about 100 atoms; and (3) improved synthetic methods that produce unique nanoparticle structures that can be used to test theoretical predictions.

DOE Interest. Our proposed research directly addresses two of the DOE Grand Challenges for Basic Energy Sciences. Specifically, we endeavor to use synthesis and theory to develop first-principles rules for predicting the structure of new forms of matter that have programmable catalytic functions. The rules and principles discovered during this project will likely be useful for designing other (noncatalytic) materials as well. Within this broader context, our proposal specifically addresses the Hydrogen Fuel Initiative and Catalysis for Energy components of the DOE BES Use-Inspired Discovery Science research thrusts.

Recent Progress. *Pt@Cu DENs:* The synthesis of Pt@Cu DENs by UPD of Cu onto 3 different-sized Pt cores was described. The voltammograms indicate that Cu UPD is a two-step deposition and stripping process which is believed to correspond to Cu deposition on the (100) and (111) facets of cubooctahedral Pt DENs. The core@shell configuration was confirmed by in-situ EXAFS. The Cu UPD process was modeled on Pt DENs consisting of 147 atoms. The results of DFT indicate that Cu shell decorates just the facets, not the edges and corners that adjoin the facets and the first part of the Cu shell selectively deposits on the (100) facet. The findings from recent electrochemical and EXAFS studies of Pt@Cu DENs with just partial shell coverage are in good agreement with the DFT models.

Au@Pb and Au@Pt DENs: Au nanoparticles consisting of 147 atoms have been synthesized within PAMAM dendrimer templates. The surface structure of these particles has been determined using Pb UPD and suggests that Au DENs have (100) and (111) facets. UPD Pb is also used as a sacrificial monolayer for galvanic exchange for Pt. The amount of Pt surface decoration on the Au DENs can be controlled by the extent of Pb UPD. Certain surface features

of the Au nanoparticles are decorated with Pt by only forming UPD Pb on particular facets of the particles. Au_{147}@Pt particles were then tested for their activity toward the oxygen reduction reaction (ORR). The structures of Au@Pb and Au@Pt particles have been modeled using DFT as well as the binding energies of oxygen to the surface of Au@Pt particles having varying amounts of surface Pt. While Au@Pb structures are structurally stable, the Au@Pt structure undergoes a surface reorganization, shown below, such that the Pt atoms all align in a (111) orientation. These calculations indicate very good agreement to the experimental system.

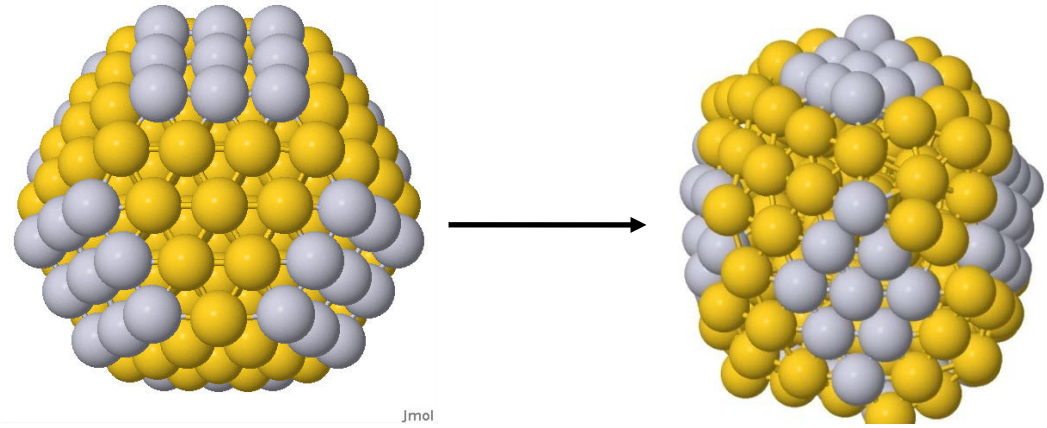

Future Plans. *Site-specific catalysis*: We plan to use Au@Pt and Pt@Cu DENs to examine site-specific catalysis of CO oxidation, water-gas shift, and the ORR by blocking particular catalyst sites with UPD metals.

Au@Bi DENs: Au surfaces having Bi UPD layers have shown activity for the ORR. We have observed similar trends on Au@Bi DENs. We plan to determine the structure of the Bi UPD layer on Au DENs. Preliminary results indicate that Bi forms an alloy with Au_{147} DENs upon Bi UPD.

DOE Sponsored Publications 2012

This project is supported by the DOE Catalysis Program. Recent publications include:

1. E. V. Carino; H. Y. Kim; G. Henkelman; R. M. Crooks "Site-Selective Cu Deposition on Pt Dendrimer-Encapsulated Nanoparticles: Correlation of Theory and Experiment" *J. Am. Chem. Soc.* **2012**, *134*, 4153-4162 (DOI: 10.1021/ja209115e).

2. D. F. Yancey; L. Zhang; R. M. Crooks; G. Henkelman "Au@Pt Dendrimer Encapsulated Nanoparticles as Model Electrocatalysts for Comparison of Experiment and Theory" *Chem. Sci.* **2012**, *3*, 1033-1040 (DOI: 10.1039/C2SC00971D).

3. V. S. Myers; A. I. Frenkel; R. M. Crooks "In-situ Structural Characterization of Platinum Dendrimer-Encapsulated Oxygen Reduction Electrocatalysts" *Langmuir* **2012**, *28*, 1596-1603 (DOI: 10.1021/la203756z).

Session X

Catalysis at Surfaces II

In-situ X-ray Studies of Photo-and Electrocatalysis

Anders Nilsson, Daniel Friebel, Sarp Kaya, Hernan Sanchez, Hirohito Ogasawara
SLAC National Accelerator Laboratory
Menlo Park CA 94025

In order to develop new catalysts for solar energy conversion to useful fuels we need to obtain a fundamental understanding of the molecular processes occurring at the solid-electrolyte interface. We have undertaken to develop in-situ spectroscopic methods to probe the interface during real electrocatalytic conditions in order to derive intermediates on the surface and the chemical state of the operating catalyst. I will present how various spectroscopic techniques can be used to address the hydrogen evolution reaction (HER), oxygen evolution reaction (OER) and the corresponding oxygen reduction reaction (ORR) using a combination of hard and soft x-ray spectroscopies and ambient pressure x-ray photoelectron spectroscopy.

In collaboration with Alex Bell's group in Berkeley resonant inelastic x-ray scattering (RIXS) and high energy resolution fluorescence detection x-ray absorption spectroscopy (HERFD XAS) were used *in situ* to determine the chemical identity of an OER catalyst prepared by electrodepositing Co oxide layers on a Au(111) substrate. Knowledge of electronic structure in the working catalyst is essential for establishing structure-activity correlations that can be used for catalyst design. Figure 1 shows that the as-deposited Co oxide is most similar to a CoOOH. Under OER conditions, cation intercalation from the electrolyte leads to replacement of H^+ with Na^+. Theoretical calculations are in progress indicating that this replacement might be critical for the high activity of the CoOOH system.

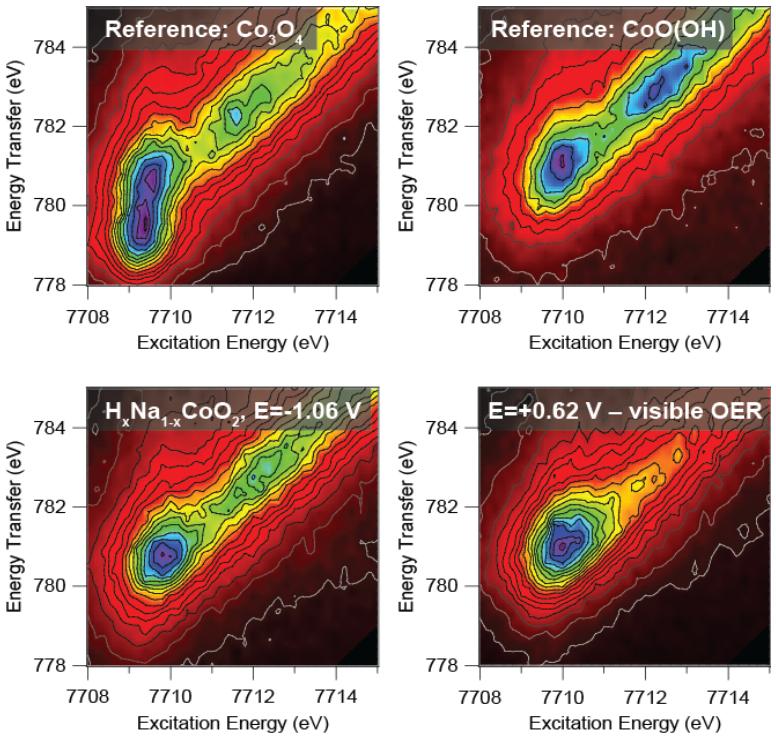

Figure 1. RIXS planes of Co oxide reference compounds (top) and the Co oxohydroxide OER catalyst electrodeposited on Au(111) (bottom). The intensity maxima (purple) are due to Co 1s → 3d transitions and can be interpreted in terms of the unoccupied Co 3d band in the presence of a core-hole. In the reference data for Co_3O_4, the off-diagonal maximum at the lowest energy transfer can be seen as characteristic signature of Co(II), which is clearly absent in the in situ RIXS measured on the Co/Au(111) sample. At low potentials, the chemical nature of the catalyst can be identified as most similar to CoO(OH) but with some substitution of H with Na from the electrolyte causing a reduction of the relative intensity at 7712 eV excitation energy. This substitution appears to further proceed when the potential is increased, indicating a composition much closer to $NaCoO_2$ under OER working conditions.

Many surface science techniques have been most successful to obtain a lot of detailed information regarding structure and bonding on surfaces. One draw back is that most of methods operate in a vacuum environment. We have designed and constructed an electrochemical that can work in an ambient pressure XPS (APXPS) system. The cell, shown in Figure 2, utilizes the principals of a fuel cell. A Nafion membrane separates the electrolyte chamber from the gas phase. The working electrode, illustrated here as MoS_2, is deposited on the gas-phase side of the membrane, and Pt deposited on the electrolyte side of the film serves as the counterlectrode. I will show examples of the application to probe with XPS MoS2 catalyst for HER in collaboration with Tom Jaramillo's group at Stanford and Pt catalyst for ORR under real electrocatalytic conditions.

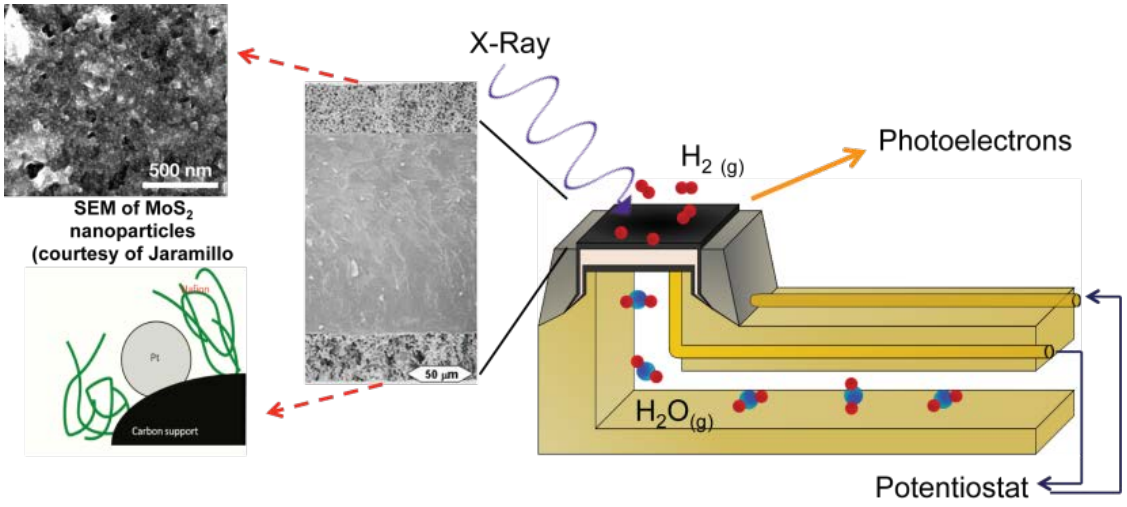

Figure 2. Schematic of an electrochemical cell that operates in an ambient pressure XPS system.

Inorganic Core-Shell Assemblies for Separating H_2O Oxidation Catalysis from Light Absorber and CO_2 Reduction Chemistry

Heinz Frei
Physical Biosciences Division
Lawrence Berkeley National Laboratory
Berkeley CA 94720

The long term goal of our research is the direct conversion of carbon dioxide and water with visible light to a liquid fuel in a nanoscale assembly. Focusing on robust inorganic molecular light absorbers and metal oxide nanocatalysts, geometries are explored that afford the coupling of the components across a proton transmitting nanoscale silica layer under separation of the water oxidation catalysis from all other photosynthetic processes. Using recently developed heterobinuclear charge-transfer units anchored on silica as visible light chromophores, Co_3O_4 nanoparticles as multi-electron catalysts for water oxidation, and core-shell geometry for separating the O_2 evolution catalysis from light absorber and reduction chemistry, we are developing an assembly for closing the photosynthetic cycle. Recent materials synthesis effort has focused on the coupling of light absorber with the water oxidation catalyst across a nanometer thin silica layer under tight control of electron transport through embedded molecular wires, the development of Co_3O_4-SiO_2 core-shell nanotubes, and the discovery of a new binuclear chromophore for visible light CO_2 reduction. Structural and functional characterization of components and assemblies by transient optical and time-resolved infrared spectroscopy, EXAFS analysis, XRD measurements and high resolution TEM imaging plays a key role in this effort.

Coupling water oxidation catalyst with visible light sensitizer through molecular wires embedded in Co_3O_4-SiO_2 core-shell nanospheres and nanotubes: Starting with spherical Co_3O_4 catalyst particles (4 nm, turnover frequency of 0.03 s^{-1} per surface Co atom for O_2 evolution at pH 7), rectifying molecular wires of the type oligo(para phenylene vinylene) with 3 aryl units (abbrev. PV3) were covalently attached on the Co oxide surface by tripodal hydroxy methylene anchors. Negatively charged SO_3^- groups on the opposite end of the PV3 wire enforced radial (vertical) arrangement of the molecules. Casting of a dense phase silica shell around the PV3 molecules (2 nm deep) resulted in uniform Co_3O_4-SiO_2 core-shell particles as shown in the transmission electron microscope (TEM) images of Figure 1. FT-Raman (Fig. 1), FT-IR and optical spectra confirmed that the anchored wire molecules remained intact upon casting of the silica shell.

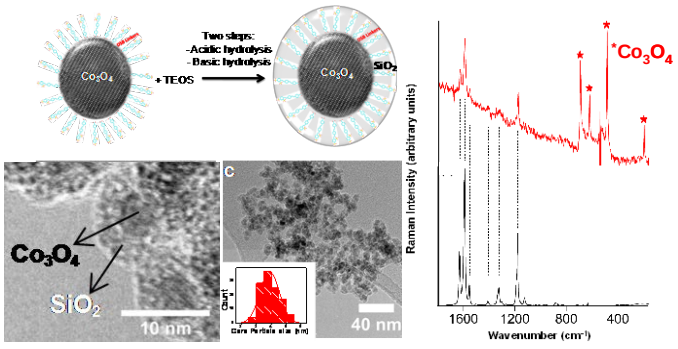

Figure 1: Co_3O_4-SiO_2 core-shell nanoparticles with PV3 molecular wires providing tight control of hole transport across separating silica barrier. HR-TEM images show uniformity of silica shells. FT-Raman spectrum confirms integrity of PV3 wire molecules and Co_3O_4 structure upon silica casting.

Evidence for hole injection from a visible light chromophore into wires embedded in the silica shell was obtained by transient optical absorption spectroscopy. Using $[Ru(bpy(CO_2Me)_2)_3]^{2+}$ coupled with $Co(NH_3)_5Cl_3$ electron acceptor as a convenient visible light sensitization system, diffusion controlled hole injection from the oxidized sensitizer ($[Ru(bpy(CO_2Me)_2)_3]^{3+}$) into PV3 molecules was detected by the recovery of the Ru^{2+} bleach at 470 nm. While concurrent formation of $PV3^+$ radical cation was observed by the characteristic transient absorption band at 600 nm for wire molecules anchored on insulating SiO_2 nanoparticles, no 600 nm signal was detected on the time scale of nanoseconds or longer for wires anchored on Co_3O_4. This result is consistent with hole transfer to the HOMO of Co_3O_4 on the sub-nanosecond time scale, a process that cannot take place for wires anchored on silica. The result was further confirmed by millisecond rapid-scan FT-IR monitoring of light-on/ light-off experiments of visible light hole injection: For solutions of Co_3O_4-SiO_2 core-shell particles with embedded wires, the characteristic IR spectrum of the oxidized Ru^{3+} sensitizer was immediately converted to the Ru^{2+} spectrum upon termination of the light pulse, indicating efficient charge transport to Co_3O_4 catalyst across molecular wires embedded in the nanoscale silica shell.

While spherical core-shell particles are suitable for the characterization of charge transport by transient spectroscopy, Co_3O_4-SiO_2/PV3 core-shell nanotube geometry is required for demonstrating catalytic water oxidation driven by charge transport across the silica/wire shell. We have prepared crystalline Co_3O_4 nanotubes with a large range of sizes by a new surfactant-free solvothermal method that exhibit similarly high catalytic activity as Co_3O_4 nanospheres. Atomic resolution imaging at the National Center for Electron Microscopy's TEAM0.5 microscope is currently being explored for structural characterization of the embedded organic wire molecules in Co_3O_4-SiO_2 nanotubes by low voltage – low electron dose methods.

Visible light-induced CO_2 reduction at $ZrOCo^{II}$ charge transfer unit anchored on silica surface: We have discovered a new heterobinuclear metal-to-metal charge-transfer unit anchored on a silica surface (SBA-15) for visible light-induced reduction of CO_2 to gas phase CO and formate (Figure 2). This photocatalytic unit is of particular interest because transient Co^{III} formed by $Zr^{IV}OCo^{II}$ → $Zr^{III}OCo^{III}$ visible light excitation may have sufficient potential for driving a water oxidation catalyst. The oxo-bridged structure of the unit was established by curve fitting analysis of Zr and Co K-edge EXAFS measurements, and by the observation of a blue shift of the visible Co^{II} $^4A_2(F)$ → $^4T_1(P)$ spin-orbit components due to electronic perturbation of the bridging oxygen by the Zr center. CO and HCO_2^- product were confirmed by $^{13}CO_2$ and $C^{18}O_2$ photolysis experiments. In contrast to the $ZrOCu^I$ unit for CO_2 splitting reported previously, which did not require the presence of a sacrificial electron donor for driving the half reaction, an amine donor is needed in the case of the $ZrOCo^{II}$ unit.

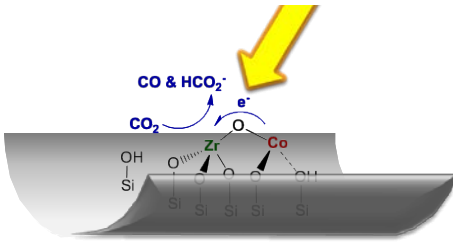

Figure 2: $Zr^{IV}OCo^{II}$ MMCT unit for visible light CO_2 reduction

Future effort will focus on the anchoring of binuclear charge-transfer chromophores such as the $ZrOCo^{II}$ unit on the outer silica surface of Co_3O_4-SiO_2 core-shell nanotubes for driving water oxidation catalysis under separation of products. In parallel, ongoing studies of electron transfer processes of excited MMCT units by transient optical spectroscopy in transparent mesoporous silica films, and time-resolved FT-IR studies of elementary H_2O oxidation steps at Co_3O_4

catalyst nanoparticles are pursued in order to gain a detailed mechanistic understanding of elementary charge transport and catalytic processes of the photosynthetic assembly.

DOE Sponsored Solar Photochemistry Publications 2009-2012

1. W. W. Weare and H. Frei. Artificial Photosynthesis, In: *Yearbook of Science and Technology;* Weil, J., Ed.; McGraw Hill: New York (2009); pp.28-31.

2. X. Wu, W. W. Weare, and H. Frei. Binuclear TiOMn Charge-Transfer Chromophore in Mesoporous Silica. *Dalton Trans.*, 10114-10121 (2009) (Hot Article).

3. H. Frei. Polynuclear Photocatalysts in Nanoporous Silica for Artificial Photosynthesis. *Chimia* **63**, 721-730 (2009).

4. F. Jiao and H. Frei. Nanostructured Cobalt Oxide Clusters in Mesoporous Silica as Efficient Oxygen-Evolving Catalysts. *Angew. Chem. Int. Ed.* **48**, 1841-1844 (2009).

5. T. Cuk, W. W. Weare, and H. Frei. Unusually Long Lifetime of Excited Charge-Transfer State of Binuclear $TiOMn^{II}$ Unit Anchored on Silica Nanopore Surface. *J. Phys. Chem. C* **114**, 9167-9172 (2010).

6. F. Jiao and H. Frei. Nanostructured Manganese Oxide Clusters Supported on Mesoporous Silica as Efficient Oxygen-Evolving Catalysts. *Chem. Commun.* **46**, 2920-2922 (2010).

7. F. Jiao and H. Frei. Nanostructured Cobalt and Manganese Oxide Clusters as Efficient Water Oxidation Catalysts. *Energy Environ. Sci.* **3**, 1018-1027 (2010).

8. F. Jiao and H. Frei. Nanostructured Cobalt Oxide and Manganese Oxide Clusters Supported on Mesoporous Silica as Efficient Water Oxidation Catalysts. *U.S. Patent Appl. Ser. No. 61/298,876,* Jan 27, 2010.

9. N. Sivasankar, W. W. Weare, and H. Frei. Direct Observation of Hydroperoxide Surface Intermediate upon Visible Light-Driven Water Oxidation at Ir Oxide Nanocluster Catalyst by Rapid-Scan FT-IR Spectroscopy. *J. Am. Chem. Soc.* **133**, 12976-12979 (2011)

10. H. S. Soo, W. W. Weare, J. Yano, and H. Frei. EXAFS Spectroscopic Analysis of Heterobinuclear TiOMn Charge-Transfer Chromophore in Mesoporous Silica. *J. Phys. Chem. C* **115**, 24893-24905 (2011).

11. H. S. Soo, A. Agiral, A. Bachmeier, and H. Frei. Visible Light-Induced Hole Injection into Rectifying Molecular Wires Anchored on Co_3O_4 and SiO_2 Nanoparticles. *J. Am. Chem. Soc.*, submitted.

12. Agiral, H. S. Soo, and H. Frei. Coupling Co_3O_4 Water Oxidation Catalyst with Visible Light Sensitizer by Molecular Wires Embedded in Co Oxide-Silica Core-Shell Nanoparticles. *J. Am. Chem. Soc.*, submitted.

13. M. L. Macnaughtan and H. Frei. Binuclear $ZrOCo^{II}$ Charge-Transfer Chromophore Anchored on Silica Nanopores for Visible Light-Induced CO_2 reduction to CO and Formate. To be submitted.

Nanoscale Surface Chemistry and Electrochemistry on Faceted Substrates

Robert A. Bartynski, Wenhua Chen, Quantong Shen, and Grant Junno
Department of Physics & Astronomy and Laboratory for Surface Modification
Rutgers, The State University of New Jersey
Piscataway NJ 08854

Goal

The goal of this work is to explore new aspects of nanoscale phenomena in surface chemistry and electrochemistry with the aim to characterize the relationships between nanoscale surface features (facets and clusters) and catalytic reactivity/selectivity. A long-term goal is to improve reactivity and selectivity by controlling the shape and size distribution of nanoscale surface features. Our emphasis is on atomically rough and morphologically unstable surfaces that undergo nanoscale faceting when covered by adsorbate (gas or metal) and annealed to elevated temperatures. There are three parts of the project: faceting of model catalytic surfaces, growth of metallic nanoparticles on the faceted surfaces, and reactivity/selectivity of the nanoscale facets in catalytic reactions.

DOE Interest

Recent work has demonstrated that reactivity and selectivity in catalysis can be tuned by controlling the nanoparticle size and shape. However, highly dispersed supported catalysts used in industry usually have a wide distribution of sizes and shapes of nanoparticles. Great progress has been recently made in controlling shape and size of nanoparticles. To elucidate the reaction mechanism, which is in turn beneficial to the design and development of new catalysts, macroscale model catalysts (planar single crystals) and nanoscale model catalysts are usually used to catalyze the reactions. These structures can exhibit new phenomena in heterogeneous catalysis, as well as in electrochemical reactions.

Recent Progress

Faceting of Re and electrochemistry of Pt/Re: C-induced faceting of Re(11-21) has been discovered. Upon annealing in C_2H_2, initially planar Re(11-21) becomes nano-faceted and covered by three-sided nanopyramids. This nano-faceted surface is then utilized as a nanotemplate to synthesize a Pt monolayer electrocatalyst. We have found that the monolayer of Pt on the C/Re nanotemplate exhibits higher activity for the hydrogen evolution reaction compared to pure Pt.

Faceting of Ir and surface chemistry on facted Ir(210): Clean planar Ir(210) and clean faceted Ir(210) with tailored sizes of three-sided nanopyramids have been prepared to investigate reactions of NO+ CO and NO+C_2H_2. Evidence is found for structure sensitivity in both reactions on faceted Ir(210) versus planar Ir(210). In addition, NO+CO reactions exhibits size effects on faceted Ir(210) for average facet size ranging from 5 to 14nm. Moreover, when planar Ir(210) is pre-covered by 1ML CO and then exposed to NO, "explosive" evolution of N_2 and CO_2 has been observed.

Faceting of Ru and application of faceted O/Ru surfaces: O-induced nano-faceting of Ru(11-20) and Ru(11-21) has been found. By depositing gold onto the faceted O/Ru(11-20) surface held at room temperature, gold nanoparticles with regular spacings are fabricated. Gold nanoparticles are found to nucleate preferentially within valleys of the faceted surface.

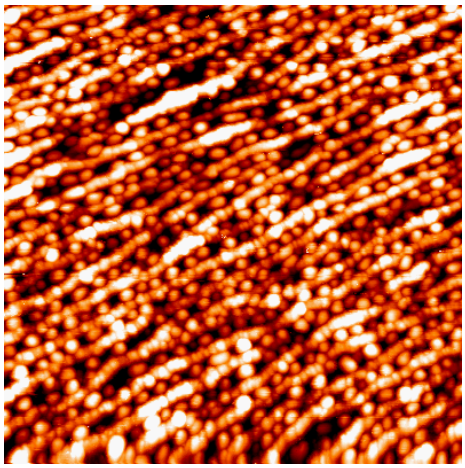

Fig. 1: STM image (100nm × 100nm) showing Au nanoclusters on a faceted O/Ru$(11\bar{2}0)$ surface.

Future Plans:

Identifying new faceted surfaces as model nanocatalysts: To search for and to characterize (with atomic resolution) nanoscale faceting of adsorbate (gas or metal)-covered metallic (fcc Cu, hcp Re and Ru) and bimetallic (FeAl) surfaces; to identify factors that cause faceting of surfaces with different crystal structures; to develop procedures to generate clean faceted surfaces.

Use faceted surfaces as templates for nanoparticle growth: To search for growth of metallic nanoparticles on oxygen-covered faceted surfaces (Ir, Re, Ru, and FeAl) with a narrow size distribution and regular spacing at specific sites.

Explore surface and electrochemistry of faceted surfaces: To correlate surface morphology with catalytic reactivity and selectivity in surface reactions over clean and metal-covered faceted surfaces; to search for special kinetic phenomena associated with nanometer-scale size effects.

In this presentation, I will also discuss recent work on energy level alignment of chromophores at metal oxide and metal surfaces, and their relevance for interfacial charge separation and charge transfer. Using a combination of ultrahigh vacuum surface sensitive spectroscopic techniques, including direct and inverse photoemission, energy loss spectroscopy, near edge x-ray absorption and scanning tunneling microscopy, I will also explore the relationship between chromophore binding geometry at the surface and the opening of new channels for exciton diffusion.

DOE Sponsored Publications 2009-2011

1. P. Kaghazchi, T. Jacob, H. Wang, W. Chen and T.E. Madey, "First principles studies on adsorbate-induced faceting of Re(11-21)", *Phys. Rev. B (Brief Reports)*, **79** (2009) 132107-4.
2. W. Chen, A.L. Stottlemyer, J.G. Chen, P. Kaghazchi, T. Jacob, T.E. Madey and R.A. Bartynski, "Adsorption and decomposition of NO on O-covered planar and faceted Ir(210)", *Surf. Sci.*, **603** (2009) 3136-3144.
3. Govind, W. Chen, H. Wang and T.E. Madey, "Growth of oxygen induced nanoscale-pyramidal facets on Rh(210) surface", *Phys. Rev. B*, **81** (2010) 085415-9
4. Q. Shen, W. Chen, H. Wang, Govind, T.E. Madey and R.A. Bartynski, "Nano-faceting of the Ru(11-20) surface", *Surf. Sci.*, **604** (2010) L12-15.
5. W. Chen, Q. Shen, R.A. Bartynski, P. Kaghazchi and T. Jacob, "Reduction of NO by CO on unsupported Ir: Bridging the materials gap", *ChemPhysChem*, 11 (2010) 2515-2520. (***featured on the front cover of Issue 12/2010 and highlighted in the news section of ChemPhysChem***)
6. B.V. Yakshinskiy, Q. Shen, R.A. Bartynski, "Interaction of benzene and toluene vapors with Ru(0001) surface: Relevance to MLM contamination", Proc. SPIE, 7969 (2011) 796922-10.
7. Q. Shen, W. Chen, R.A. Bartynski, "Growth of gold nanoparticles on faceted O/Ru(11-20) nanotemplate", Surf. Sci., **605** (2011) 1454-1458.
8. X.-F. Yang, B.E. Koel, H. Wang, W.H. Chen, and R.A. Bartynski, "Nanofaceted C/Re(11-21): Fabrication, Structure, and Template for Synthesizing Nanostructured Model Pt Electrocatalyst for Hydrogen Evolution Reaction," ACS Nano **6** (2012) 1404-09.

Session XI

Catalysis at Surfaces III

Formation and Characterization of Semiconductor Nanorod/Oxide Nanoparticle Hybrid Materials: Toward Vectoral Electron Transport in Hybrid Materials

Neal R. Armstrong, Jeffrey Pyun, S. Scott Saavedra
Department of Chemistry/Biochemistry
University of Arizona
Tucson, Arizona 85721

Overview: The development and characterization of new semiconductor nanorod (NR) materials, coupled asymmetrically to both metallic and metal oxide nanoparticle (NPs) catalytic sites, is at the heart of multiple efforts to harvest solar energy in the form of solar fuels, and conceptually overlaps efforts to use semiconductor nanocrystals (NCs) and NRs as active layers in emerging photovoltaic platforms. These nanomaterials must be designed to be compositionally and energetically asymmetric, ensuring vectoral electron transfer in photoelectrochemical fuel-forming processes. Our recent research efforts have been focused the vertical integration of approaches to new catalytic nanometers, the characterization of their energetics, including: (i) the demonstration of photoelectrochemical processes with CdSe NCs tethered to the surface of a conducting polymer; (ii) the formation of new NCs and NRs decorated with both metallic and metal oxide catalytic sites; (iii) the characterization of valence band energies (E_{VB}) of monolayer-tethered bare NCs, NRs and metal/oxide decorated NRs, by photoemission spectroscopies; (iv) spectroelectrochemical estimation of conduction band energies (E_{CB}) and rates of charge injection into surface-tethered NCs on unique electroactive waveguide platforms.

Photoelectrochemical processes with CdSe NCs tethered to a conducting polymers:

Variable diameter CdSe semiconductor nanocrystals, with ProDOT-terminated capping ligands were electrochemically captured at the outer surface of $P(Et)_2$ProDOT, PProDOT, and PEDOT electrodeposited host polymer films, providing for nearly close-packed monolayers of the NCs at the host polymer/solution interface. These polymer-confined CdSe NCs were used as sensitizers in the photoelectrochemical reduction of a sacrificial electron acceptor (methyl viologen (MV^{++})), demonstrating high internal quantum efficiencies (IQE). Cathodic photocurrents were limited by the rate of hole-capture by the host polymer from photoexcited NCs, governed by: a) the onset potential for reductive de-doping of the host polymer film; b) the concentration ratio of neutral to oxidized forms of the host polymer ([P(n)]/[P(ox)]); and c) the NC diameter, which controls its valence band energy, E_{VB}, consistent with control of photoinduced electron transfer by Marcus-like excess free energy relationships. These relationships control rates of ET in emerging photocatalytic systems, and guide our design of integrated photocatalytica semiconductor nanorods (NR) and NR arrays, with and without metal and metal oxide nanoparticle modification.

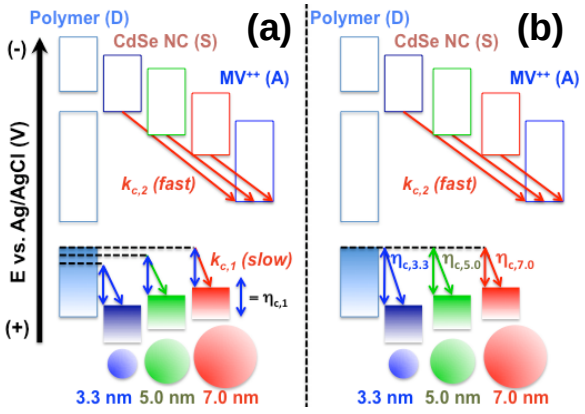

New CdS@CdSe NRs decorated with both metallic and metal oxide catalytic sites:

Our efforts have also focused on the preparation of complex heterostructured semiconductor nanorods with precise nanoscopic and energetic control of Pt and p-type cobalt oxide inclusions (nanoparticles, NP) as photocatalysts. We have synthesized a novel class of CdSe@CdS nanorods, where a CdSe nanocrystal is the seed, with nanoinclusions of metallic Pt, Co and Co_xO_y controllably deposited onto nanorod termini. There is still a need, however, to develop robust and facile synthetic methods to enable the controllable and asymmetric placement of co-catalysts for oxygen evolution reactions (OER) and hydrogen evolution reactions (HER), onto a single semiconductor nanorod. Our presentation will discuss our recent efforts to prepare CdSe@CdSe nanorods with a single metallic NP tip, or two metallic NP tips on nanorod termini, exhibiting, "matchstick," or "dumbbell" morphologies.

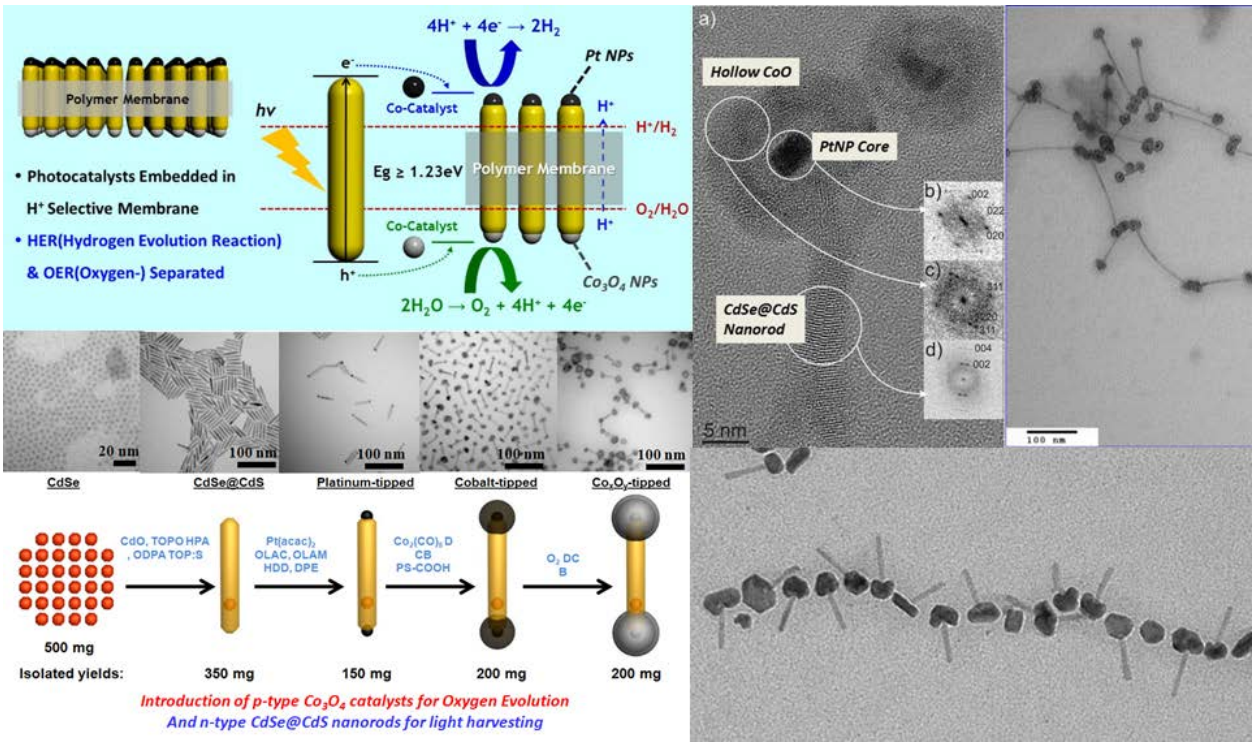

Energetics of monolayer-tethered bare NCs, NRs and metal/oxide decorated NRs using photoemission spectroscopies:

Band edge energies (E_{VB}, E_{CB}) dictate the excess free energies in photocatalytic processes involving both semiconductor NCs and NRs, and we have advanced two complementary approaches to the estimation of these energies. The first of these approaches uses UV-photoemission spectroscopies to determine both the ionization potential (IP) of the NC or NR, and shifts in local effective work function of NC films as a function of the dipolar nature of the NC and of the capping ligands themselves. Bare CdSe NCs on Au substrates show significant shifts in local vacuum energy due to the dipolar nature of these NCs. Various thiol-capping ligands produced additional shifts in local vacuum level by as much as 0.3 eV, and for the most dipolar of these ligands, an increase in the effective IP (E_{VB}) of CdSe NCs. More recent studies

have focused on the addition of low and high dielectric constant films to the surface of the CdSe NC to estimate the importance of dielectric constant of the surrounding medium on the apparent E_{VB} of the NC. We have also extended this characterization protocol to copper-zinc-tin-sulfide (CZTS) NCs, a promising PV active layer and sensitizer for photoelectrochemical cells, where vacuum level shifts, coupled with difference between near-surface and bulk composition strongly affect our estimates for E_{VB} for these materials. Even more recently these studies have been extended to CdS@CdSe NRs and Pt-decorated, cobalt-oxide-decorated CdS@CdSe NRs, to determine the extent to which metal or oxide decoration of the NR influences the average E_{VB} for these promising photocatalysts. Once E_{VB} energies are estimated, we use the direct optical gap energy for the NC or NR material to estimate E_{CB}, as a function of capping ligand, NC-NC interactions, and addition of metal or metal oxide inclusions.

Spectroelectrochemical characterization of energies and rates of charge injection into surface-tethered CdSe NCs on electroactive waveguide platforms:

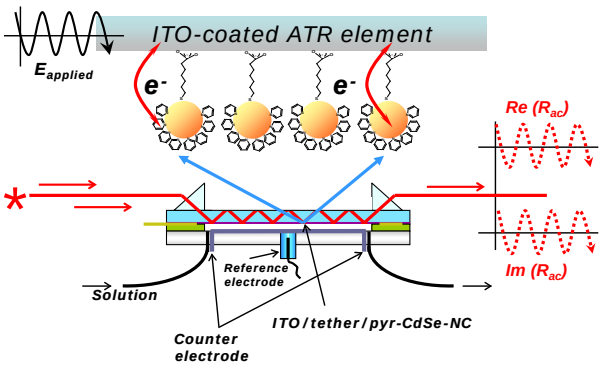

Estimates of E_{CB} and rates of electron injection into CdSe NCs have been obtained from waveguide-based spectroelectrochemical experiments. Reversible electron injection into pyridine-capped CdSe NCs, tethered to indium-tin oxide (ITO) substrates has been characterized using attenuated total reflectance (ATR) spectro-electrochemistry on electroactive (ITO-coated) planar waveguides. High sensitivity IOWs provide for characterization of redox processes in submonolayer films of NCs. Optically determined onset potentials for bleaching/recovery of the exciton absorption band (reversible electron injection), provide estimates for E_{CB} which are displaced from those predicted by our vacuum photoemission experiments by ca. 0.8 eV. Potential-modulated attenuated total reflectance (PM-ATR), in which the in-phase and out-of-phase reflectance response is measured as a function of modulation frequency, provides estimates for rates of electron injection, with apparent rate coefficients nearly independent of tether chain length. Recent experiments with higher coverages of CdSe NCs, where "chain-like"aggregates form on the ITO surface, suggest that NC-NC interactions shift the apparent E_{CB} energy farther from vacuum (i.e. reduction is easier, electron affinity is higher), which is likely to be a critical observation for electrocatalytic applications of these materials.

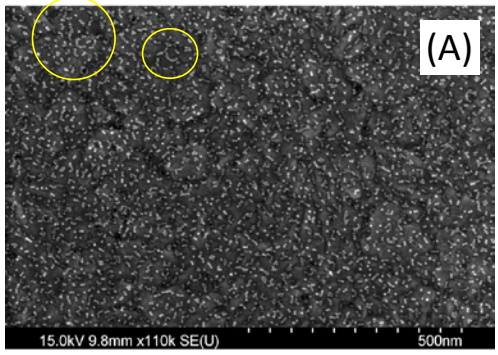

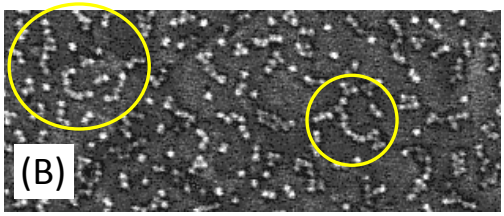

DOE Sponsored Solar Photochemistry Publications 2009-2012

1. "Efficient CdSe Nanocrystal Diffraction Gratings Prepared by Microcontact Molding," R. Clayton Shallcross, Gulraj S. Chawla, F. Saneeha Marikkar, Stephanie Tolbert, Jeffrey Pyun, Neal R. Armstrong, ACS Nano, 3, 3629-3637 (**2009**).
2. "Ferrocene Functional Polymer Brushes on Indium Tin Oxide via Surface-Initiated Atom Transfer Radical Polymerization," Kim, Bo Yun, Ratcliff, Erin L., Armstrong, Neal R., Kowalewski, Tomasz, Pyun, Jeffrey, Langmuir, 26, 2083-2092 (**2009**).
3. "Colloidal Polymerization of Polymer Coated Ferromagnetic Nanoparticles into Cobalt Oxide Nanowires," Pei Yuin Keng, Bo Yun Kim, Inbo Shim, Rabindra Sahoo, P. Alex Veneman, Neal R. Armstrong, Heemin Yoo, Jeanne E. Pemberton, Mathew M. Bull, Jared J. Griebel, Erin L. Ratcliff, Kenneth G. Nebesny, Jeffrey Pyun, ACS Nano, 3, 3143-3157 (**2009**).
4. "Potential-modulated attenuated total reflectance (PMATR) characterization of charge injection processes in monolayer-tethered CdSe nanocrystals, Zeynep Ozkan Araci, Clayton R. Shallcross, Neal R. Armstrong and S. Scott Saavedra, JPC Letters, 1, 1900–1905, (**2010**).
5. "Photoemission spectroscopy of tethered CdSe nanocrystals: Shifts in ionization potential and local vacuum level as a function of nanocrystal capping ligand," Andrea Munro, Brian Zacher, Amy Graham, Neal R. Armstrong, ACS Applied Materials and Interfaces, 2, 863-869, (**2010**).
6. "Synthesis and Colloidal Polymerization of Ferromagnetic Au- Co Nanoparticles into Au-Co_3O_4 Nanowires, Bo Yun Kim, In-Bo Shim, Zeynap Ozkan, S. Scott Saavedra, Oliver L.A. Monti, Neal R Armstrong, Rabindra Sahoo, Divesh N. Srivastava, and Jeffrey Pyun, J. Amer. Chem. Soc., 132, 3234-35, (**2010**).
7. "Photoelectrochemical Processes in Polymer-Tethered CdSe Nanocrystals, R. Clayton Shallcross, Gemma D. D'Ambruoso, Jeffrey Pyun, Neal R. Armstrong, J. Amer. Chem. Soc., 132, 2622-2632, (**2010**).
8. "Colloidal Polymerization of Polymer-Coated Ferromagnetic Cobalt Nanoparticles into Pt-Co_3O_4 Nanowires," Pei Yuin Keng, Mathew M. Bull, In-Bo Shim, Kenneth G. Nebesny, Neal R Armstrong, and Jeffrey Pyun, Chemistry of Materials, 23, 1120–1129 (**2011**)
9. "Directing the deposition of metallic cobalt onto Pt-tipped CdSe@CdS nanorods: Synthetic and Mechanistic Insights ," Hill, L.J.; Bull, M.M.; Sung, Y.; Simmonds, A.G.; Dirlam, P.T.; Richey, N.E.; DeRosa, S.E.; Guin, D.; Shim, I.-B.; Costanzo, P.J.; Pinna, N.; Willinger, M.-G.; Vogel, W.; Char, K.; Pyun, J. in preparation for *ACS Nano* **2012.**
10. "Synthesis and Colloidal Polymerization of Dipolar Heterostructured Nanorods of CdSe@CdS with core-shell tips of Pt@Co and Pt@CoxOy," Hill, L.J.; Sung, Y.-H.; Bull, M.M.; Pinna, N.; Vogel, W.; Shim, I-.B.; Char, K.; Pyun, J. in preparation for *J. Am. Chem. Soc.* **2012**.

Nanostructured Photoelectrodes

J. Oh, F. Toor, T. G. Deutsch, J. W. Pankow, W. Nemeth, H-C Yuan, H. Branz, A. J. Nozik, D. R. Ruddy, S. E. Habas, N. R. Neale, S-H Wei and J. A. Turner

National Renewable Energy Laboratory
Golden CO 80401

The application of well-understood single-crystal semiconductors like silicon allows us to separate out and study the important new PEC science introduced by nanostructuring and the interactions of catalysts with the nanostructures. In the current phase of this work, we developed and studied a nanoporous Si photocathode for hydrogen evolution. The nanoporous Si was fabricated using a novel nano-catalytic etching chemistry and consists of pores with average diameter of ~20 nm and with randomly distributed depths up to 500 nm producing a ~10x larger surface area ("black silicon"). We demonstrated that this nanoporous Si improves three important characteristics in the PEC sub-system: (1) the nanoporous photocathode the rate of the hydrogen-evolution reaction (HER) at a given light intensity by suppressing photon reflection from the electrolyte/photocathode interface; (2) by providing increased surface reaction sites on the photocathode the nanoporosity shifts the photocurrent onset anodically and (3) the nanostructured surface promotes H_2 bubble evolution at the surface without the use of surfactant in an electrolyte. However, we also showed that the increased surface area leads to greater surface recombination rates of photo-carriers excited very near the nanostructured surface (blue/violet wavelengths), thereby decreasing the possible efficiency. Additionally, Au or Ag nanoparticles left behind from the etching process may act as efficient charge recombination centers at the Si/electrolyte interface. Figure 1 shows the impact on the onset of photocurrent from a p/n Si junction in the black silicon.

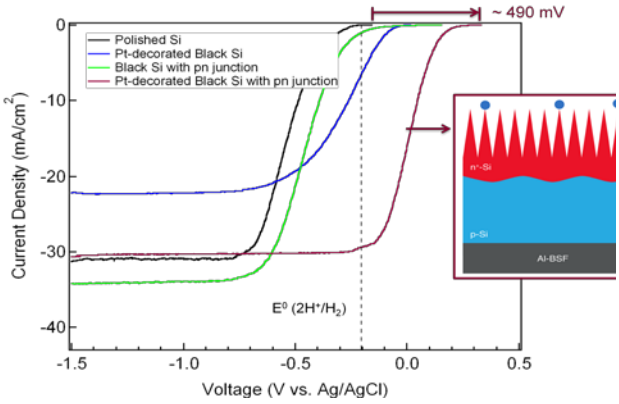

Figure 1. I-V plots under AM 1.5 showing the improvement in onset potential from a silicon p/n junction.

We have observed changes to the Si photocathode itself caused by continuous hydrogen evolution under illumination and cathodic bias. The use history improves subsequent hydrogen reduction rates and reduces the rate of dark oxidative degradation of the photocathode under anodic bias. The prolonged hydrogen production enhances the charge transfer rate at the Si-electrolyte interface and lowers the required overpotential by an as-yet unknown mechanism. In carrying out the photoelectrochemisty in D_2O we have been able to observe intercalation of D into the Si with secondary ion mass spectrometry (SIMS). We are now extending these experiments to determine the transport and intercalation kinetics of D (or H) in Si, in order to relate the electrochemical and PEC rates to the hydrogenation state of the semiconductor.

In the next phase of this research, we will address a key question critical to the understanding of photoelectrochemisty in nanostructured silicon photocathodes: What is the interplay between surface defects, catalysts, and high surface area (nanostructured surfaces) in PEC H_2 production and photo-corrosion reactions?

Hydrogenated amorphous silicon (a-Si:H) represents a low-cost thin-film alternative to x-Si for water splitting photocathodes. However we have observed that corrosion of the planar electrodes involves reduction of the underlying SnO_2 contact layer by electrolyte that penetrates through pinholes in the a-Si:H. We have demonstrated a novel micropixelation strategy for the stabilization of *p-i* hydrogenated amorphous silicon (a-Si:H) photocathodes. In this approach we photolithographically isolate square pixels (100μm × 100μm) of a-Si:H by etching narrow channels in the a-Si:H and filling the channels with protective a-SiN_x, as shown in figure 2. Under illumination and bias, we observed improved durability of the micropixelated photocathodes compared to planar electrodes. Extended dark potentiostatic testing also exhibits the slowing and isolation of corrosion by the micropixelated electrode. Implementation of this micropixelation strategy is a key toward creating a water-splitting based on micron-scale Si p-n junction pixels. Micropixelation could also improve stability other in photoelectrochemical solar fuel production systems.

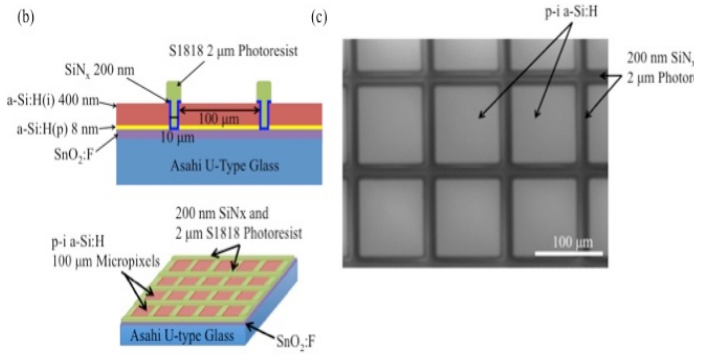

Figure 2. Micropixelated *p-i* a-Si:H photocathodes.

The literature on Group IV QDs primarily deals with Si and despite many efforts, the doping behavior in Si QDs is still not well understood. Theoretical work for perfectly hydrogen

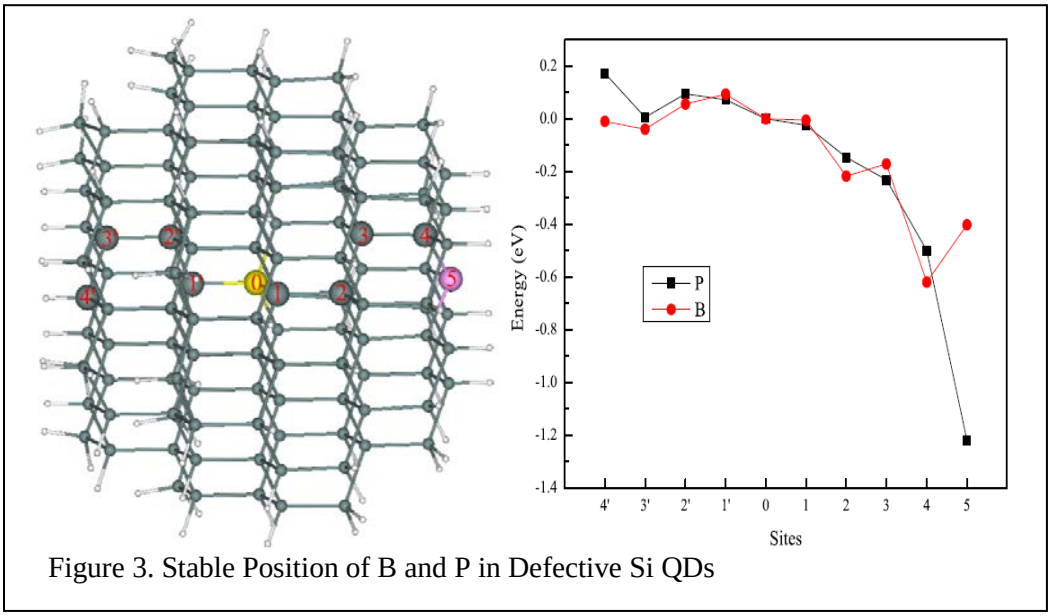

Figure 3. Stable Position of B and P in Defective Si QDs

passivated QD shows that boron as an acceptor prefers to stay near the surface and phosphorous as a donor stays close to the center. However, experimental studies seemed to suggest an opposite trend. Using first-principle methods we showed that the discrepancy could be explained by imperfect surface passivation; in QDs with hydrogen-deficient or oxygen-rich surfaces, phosphorous prefers the surface sites while boron stays inside, consistent with experimental observations (Figure 3). These results illustrate the crucial role of surface chemistry in determining the energetics of doped nanocrystals.

DOE Sponsored Solar Photochemistry Publications 2009-2012

1. J. Oh, T. G. Deutsch, H.-C. Yuan and H. M. Branz. “Nanoporous black silicon photocathode for H2 production by photoelectrochemical water splitting.” Energy Environ. Sci., 2011, **4**, 1690-1694.
2. J. Ma, S.-H. Wei, N. R. Neale, A. J. Nozik, “Effect of surface passivation on dopant distribution in Si quantum dots. The case of B and P doping”, Appl. Phys. Lett. 98, 173103 (2011)
3. Fatima Toor, Todd G. Deutsch, Joel W. Pankow, William Nemeth, Arthur J. Nozik and Howard M. Branz, "Novel Micropixelation Strategy to Stabilize Semiconductor Photoelectrodes for Solar Water Splitting Systems" J. Phys. Chem, Submitted
4. D. R. Ruddy, S. E. Habas, N. R. Neale, “Doping main-group elements into germanium nanocrystals using the mixed-valence reduction method”, J. Mater. Chem., Submitted.

Oxomanganese Catalysts for Solar Fuel Production

Victor S. Batista, Charles A. Schmuttenmaer, Robert H. Crabtree and Gary W. Brudvig
Department of Chemistry, Yale University
New Haven CT 06520-8107

The design principles for efficient heterogeneous photocatalysis remain unclear and are the focus of this project. High-valent oxomanganese (oxo-Mn) complexes have been studied in great detail to understand how Nature makes O_2 from water in photosynthesis. Sensitized TiO_2 nanoparticles (NPs) are robust materials for efficient light harvesting by photoexcitation of surface complexes and interfacial electron transfer (IET). The goal of this project is to integrate these two systems to construct solar-driven photocatalytic cells, based on our own water-oxidation catalysts, and to investigate how to achieve the efficiency breakthroughs necessary to make photocatalytic water oxidation an economically viable solar fuel resource. Four research groups in the Chemistry Department at Yale University are working together to synthesize TiO_2 NPs and anchor-linker-ligand conjugates, develop new methods for surface attachment of catalysts using oxidation-resistant anchors and linkers that are stable in water, develop and apply computational methods to analyze IET and characterize catalytic water-oxidation complexes, and use spectroscopic methods to characterize the photochemistry. See also posters by Crabtree and Brudvig.

Molecular rectifiers. We have characterized the electronic rectification properties of molecular linkers that covalently bind transition metal catalysts to TiO_2 surfaces. We focused on Mn complexes with phenyl-terpyridine ligands attached to 3-phenylacetylacetonate anchors via amide bonds. We found that a suitable choice of the amide linkage yields directionality of interfacial electron transfer, essential to suppress recombination (Figure 1). Our findings are supported by calculations of current-voltage (I-V) characteristics at metallic atomic junctions, based on first-principles methods that combine non-equilibrium Green's function techniques with density functional theory. Our computational results are consistent with EPR measurements, confirming an asymmetry of electron transfer rates for linkers with significant rectification. The

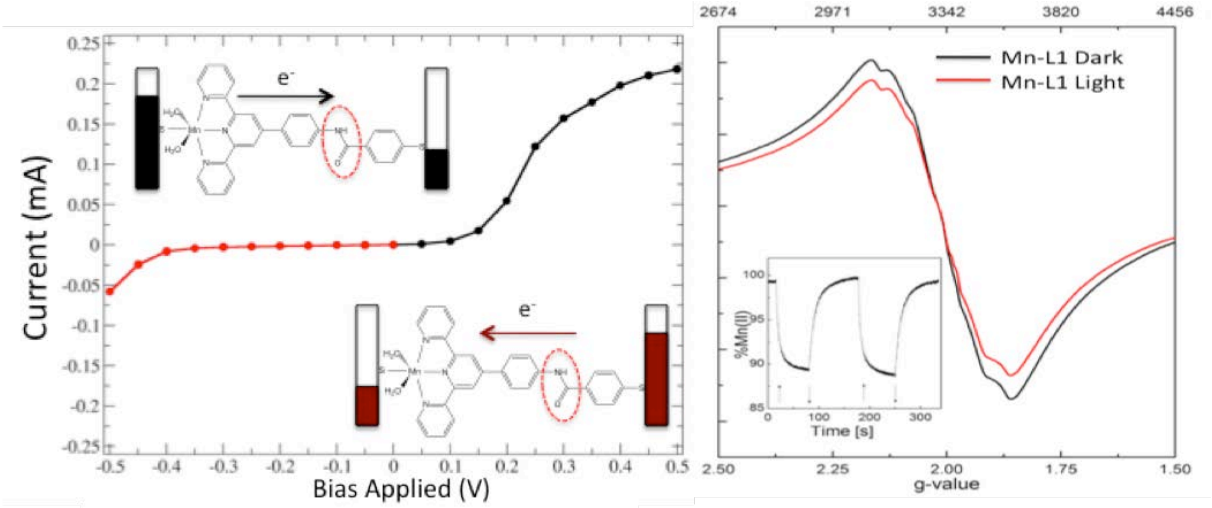

Figure 1. Left: Calculated I-V characteristic curves for Mn-L1. Current under negative (red) and positive (black) bias voltages are represented in the -500−500 mV range. Right: EPR spectra of TiO_2 nanoparticles functionalized with Mn-L1-acac before (black) and after (red) illumination

reported studies are particularly relevant for the development of photovoltaic, or photocatalytic, devices based on functionalized metal oxide thin-films where the overall performance is affected by recombination processes competing with interfacial electron injection.

High-potential photoanodes. We describe the charge injection time scale and efficiency for a selection of high-potential photoanodes (HPPAs) for photo-electrochemical cells.[20,31] The anodes consist of bis- and tris-pentafluorophenyl free-base and metallo-porphyrin sensitizers anchored to TiO_2 and SnO_2 nanoparticles (Figure 2a). Photoelectrochemical measurements demonstrate that the photosensitizers extend the absorption of the bare anode well into the visible region (Figure 2b). THz spectroscopic studies demonstrate the sensitizers used in these HPPAs are capable of injecting electrons into the conduction band of the metal-oxide materials in those cases where the energies of the donor (excited state dye) and acceptor (metal oxide conduction band minimum) components are appropriate. Importantly, the potentials photogenerated at the anode surface are high enough to permit the oxidation of high-potential electron sources.

Alternative Binding Mode. We have also investigated complexing the pentafluorphenyl Zn-porphyrin sensitizers to an isonicotinic acid anchor or variants thereof rather than binding them directly to the metal oxide surface (Figure 2c). We compare their binding stability in water, as well as their photoexcited interfacial electron transfer efficiency when using carboxylic acid, hydroxamate, acetylacetonate and phosphonate as anchors.

Transport and Conductivity. Finally, we report fluctuation-induced tunneling conduction (FITC) in nanoporous films of sintered TiO_2 and SnO_2 nanoparticles.[22,26] Measured dark DC conductivities span over four orders of magnitude, exhibit a gradual transition from thermally activated behavior to temperature-independent tunneling with decreasing temperature, and are in quantitative agreement with a model describing interparticle FITC (Figure 2d). Extracted tunnel junction parameters are consistent with a fully atomistic model of TiO_2 contact junctions and characterization of the films by diffraction and microscopy measurements. We are in the process of extending these measurements and calculations to other metal oxide nanoparticles such as ZnO and Fe_2O_3, and extending the DC measurements to AC frequencies from 0.1 Hz to 100 kHz.

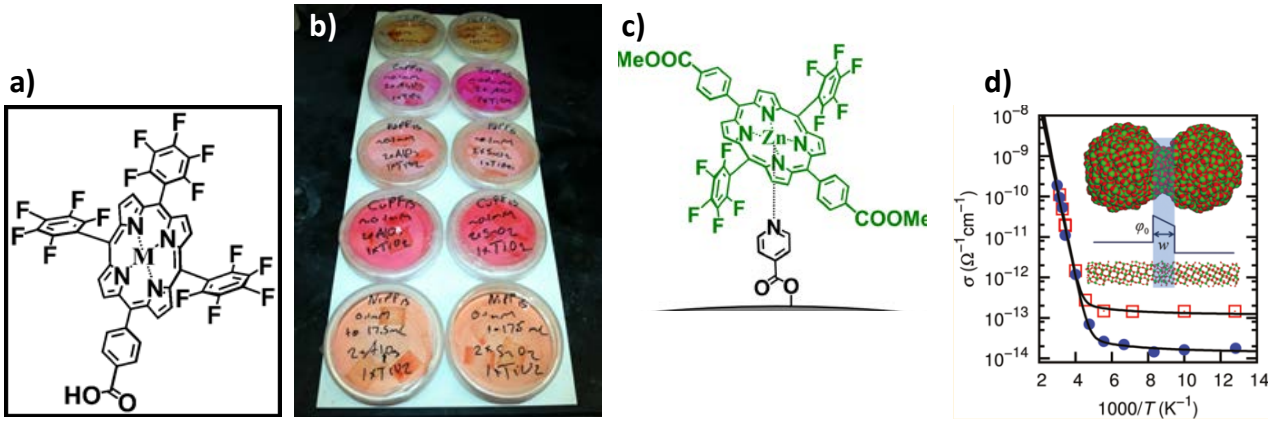

Figure 2. Part (a) shows the structure of the tris-pentafluorophenyl metallo-porphyrins studied. Part (b) displays their dichloromethane solutions where M = Ni^{2+}, Cu^{2+}, Pd^{2+}, Zn^{2+}, and H_2 in going from the bottom to the top. Part (c) shows a high-potential Zn porphyrin complexed to isonicotinic acid that is anchored to a metal oxide surface. Part (d) displays an Arrhenius plot of the dark DC conductivities of TiO_2 nanoparticle films with two different particle sizes. The solid lines are obtained by using our fluctuation-induced tunneling conduction (FITC) model.

Plans. In the future, we aim to continue with the development of photocatalytic systems. We plan to use self-assembly methods to attach photosensitizers and water-oxidation catalysts to TiO_2, or other metal oxide semiconductor, as in Figure 2c. In parallel with these measurements, IET will be investigated by time-resolved THz spectroscopy and modeled by computational methods. We also aim to investigate fuel-forming reactions at a (photo)cathode and to implement first-generation photoelectrochemical cells that would connect the photochemical oxidation of water to a fuel-forming reaction.

DOE Sponsored Solar Photochemistry Publications 2009-2012

1. "Deposition of an Oxomanganese Water Oxidation Catalyst on TiO_2 Nanoparticles: Computational Modeling, Assembly and Characterization", Gonghu Li, Eduardo M. Sproviero, Robert C. Snoeberger III, Nobuhito Iguchi, James D. Blakemore, Robert H. Crabtree, Gary W. Brudvig and Victor S. Batista (2009) *Energy & Environ. Sci.* **2**, 230–238.
2. "Coherent Control of Quantum Dynamics with Sequences of Unitary Phase-Kick Pulses", Luis G.C. Rego, Lea F. Santos and Victor S. Batista (2009) *Ann. Rev. Phys. Chem.* **60**, 293–320, 2009.
3. "Hydroxamate Anchors for Functionalization of Semiconductor Surfaces", William R. McNamara, Robert C. Snoeberger III, Gonghu Li, Christiaan Richter, Laura J. Allen, Rebecca L. Milot, Charles A. Schmuttenmaer, Robert H. Crabtree, Gary W. Brudvig and Victor S. Batista (2009) *Energy & Environ. Sci.* **2**, 1173–1175.
4. "Synergistic Effect between Anatase and Rutile TiO_2 Nanoparticles in Dye-senstized Solar Cells", Gonghu Li, Christiaan Richter, Rebecca L. Milot, Charles Schmuttenmaer, Robert H. Crabtree, Gary W. Brudvig and Victor S. Batista (2009) *J. Chem. Soc., Dalton Trans.***45**, 10078–10085.
5. "Interfacial Electron Transfer in TiO_2 Surfaces Sensitized with Ru(II)-polypyridine Complexes", Elena Jakubikova, Robert C. Snoeberger III, Victor S. Batista and Enrique R. Batista (2009) *J. Phys. Chem. A* **113**, 12532–12540.
6. "The Influence of Surface Hydration on the Interfacial Electron Transfer Dynamics from Rhodamine B into SnO_2", Robert C. Snoeberger III, Tianquan Lian, and Victor S. Batista. (2009) *Proc. SPIE 7396*, 739604.
7. "The Mod-QM/MM Methodology for Structural Refinement of Photosystem II and Other Biological Macromolecules", Sproviero, E. M.; Newcomer, M. B.; Gascon, J. A.; Batista, E. R.; Brudvig, G. W.; Batista, V. S. (2009) *Photosynth. Res.* **102**, 455-470.
8. "Visible Light Sensitization of TiO_2 Surfaces with Alq3 Complexes", Luis G.C. Rego, Robson da Silva, Jose A. Freire, Robert C. Snoeberger III and Victor S. Batista (2010) *J. Phys. Chem. C* **114**, 1317–1325.
9. "Energy Conversion in Natural and Artificial Photosynthesis", Iain McConnell, Gonghu Li and Gary W. Brudvig (2010) *Chemistry & Biology* **17**, 434-447.
10. "Water-Stable, Hydroxamate Anchors for Functionalization of TiO_2 Surfaces with Ultrafast Interfacial Electron Transfer", William R. McNamara, Rebecca L. Milot, Hee-eun Song, Robert C. Snoeberger III, Victor S. Batista, Charles A. Schmuttenmaer, Gary W. Brudvig,

Robert H. Crabtree (2010) *Energy & Environ. Sci.* **3**, 917-923.

11. "Exciton-like Trap States Limit Electron Mobility in TiO_2 Nanotubes", Christiaan Richter and Charles A. Schmuttenmaer (2010) *Nature Nanotechnology* **5**, 769-772.
12. "Reversible Visible-Light Photooxidation of an Oxomanganese Water-Oxidation Catalyst Covalently Anchored to TiO_2 Nanoparticles", Gonghu Li, Eduardo M. Sproviero, William R. McNamara, Robert C. Snoeberger III, Robert H. Crabtree, Gary W. Brudvig, and Victor S. Batista (2010) *J. Phys. Chem. B* **114**, 14214-14222.
13. "Single-Molecule Electron Transfer in Donor-Bridge-Nanoparticle Acceptor Complexes", Shengye Jin, Robert C. Snoeberger III, Abey Issac, David Stockwell, Victor S. Batista and Tianquan Lian (2010) *J. Phys. Chem. B* **114**, 14309-14319.
14. "Study of Redox Species and Oxygen Vacancy Defects at TiO_2-Electrolyte Interfaces", Robson da Silva, Luis G.C. Rego, Jose A. Freire, Javier Rodriguez, Daniel Laria, and Victor S. Batista (2010) *J. Phys. Chem. C* **114**, 19433-19442.
15. "Some Computational Challenges in Energy Research", Victor S. Batista (2010) in *Energy Production and Storage – Inorganic Chemical Aspects*, Crabtree RH (ed), Wiley, Chichester, pp. 191-198.
16. "Electrochemical and Photoelectrochemical Conversion of CO_2 to Alcohols", Robert H. Crabtree (2010) in *Energy Production and Storage – Inorganic Chemical Aspects*, Crabtree RH (ed), Wiley, Chichester, pp. 301-306.
17. "Tunneling Under Control by Sequences of Unitary Pulses", Rajdeep Saha and Victor S. Batista (2011) *J. Phys. Chem. C* **115**, 5234-5242.
18. "Energy Conversion in Photosynthesis: A Paradigm for Solar Fuel Production", Gary F. Moore and Gary W. Brudvig (2011) *Annu. Rev. Condensed Matter Phys.* **2**, 303–327.
19. "Comparing Photosynthetic and Photovoltaic Efficiencies and Recognizing the Potential for Improvement", Robert E. Blankenship, David M. Tiede, James Barber, Gary W. Brudvig, Graham Fleming, Maria Ghirardi, M. R. Gunner, Wolfgang Junge, David M. Kramer, Anastasios Melis, Thomas A. Moore, Christopher C. Moser, Daniel G. Nocera, Arthur J. Nozik, Donald R. Ort, William W. Parson, Roger C. Prince and Richard T. Sayre (2011) *Science* **332**, 805–809.
20. "A Visible Light Water-Splitting Cell with a Photoanode formed by Codeposition of a High-Potential Porphyrin and an Iridium Water-Oxidation Catalyst", Gary F. Moore, James D. Blakemore, Rebecca L. Milot, Jonathan F. Hull, Hee-eun Song, Lawrence Cai, Charles A. Schmuttenmaer, Robert H. Crabtree and Gary W. Brudvig (2011) *Energy Environ. Science* **4**, 2389–2392.
21. "Photocatalytic Water Oxidation Using Manganese Compounds Immobilized in Nafion Polymer Membranes", Karin J. Young, Yunlong Gao and Gary W. Brudvig (2011) *Australian J. Chem.* **64**, 1219–1226.
22. "Fluctuation-Induced Tunneling Conductivity in Nanoporous TiO_2 Films", Steven J. Konezny, Christiaan Richter, Robert C. Snoeberger III, Alexander R. Parent, Gary W. Brudvig, Charles A. Schmuttenmaer and Victor S. Batista (2011) *J. Phys. Chem. Lett.* **2**, 1931–1936.
23. "Wilkinson's Iridium Acetate Trimer as a Water-Oxidation Catalyst", Alexander R. Parent, James D. Blakemore, Gary W. Brudvig and Robert H. Crabtree (2011) *Chem. Comm.* **47**,

11745–11747.

24. “An Organometallic Future in Green and Energy Chemistry?”, Robert H. Crabtree (2011) *Organometallics* **30**, 17-19.
25. “Multifunctional Ligands in Transition Metal Catalysis”, Robert H. Crabtree (2011) *New J. Chem.* **35**, 18-23.
26. “AC Conductivity of Nanoporous Metal-Oxide Photoanodes for Solar Energy Conversion”, Steven J. Konezny, Diyar Talbayev, Ismail El Beggari, Charles A. Schmuttenmaer and Victor S. Batista (2011) Proc. SPIE 8098, 809804.
27. “Covalent Attachment of a Rhenium CO_2-Reduction Catalyst to Rutile TiO_2”, Chantelle L. Anfuso, Robert Snoeberger III, Allen M. Ricks, Weimin Liu, Dequan Xiao, Victor S. Batista and Tianquan Lian (2011) *J. Am. Chem. Soc.* **133**, 6922–6925.
28. “Resolving Heterogeneity Problems and Impurity Artifacts in Operationally Homogeneous Transition Metal Catalyst”, Robert H. Crabtree (2012) *Chem. Rev.* **112**, 1536–1554.
29. “Cp* Iridium Precatalysts for Selective C-H Oxidation via Direct Oxygen Insertion. A Joint Experimental/Computational Study”, Meng Zhou, David Balcells, Alexander R. Parent, Robert H. Crabtree and Odile Eisenstein (2012) *ACS Catalysis* **2**, 208–218.
30. “Tuning Redox Potentials of Bis(imino)pyridine Cobalt Complexes: An Experimental and Theoretical Study Involving Solvent and Ligand Effects”, C. Moyses Araujo, Mark D. Doherty, Steven J. Konezny, Oana R. Luca, Alex Usyatinsky, Hans Grade, Emil Lobkovsky, Grigorii L. Soloveichik, Robert H. Crabtree and Victor S. Batista (2012) *Dalton Trans.* **41**, 3562-3573.
31. “Bioinspired High-Potential Porphyrin Photoanodes”, Gary F. Moore, Steven J. Konezny, Hee-eun Song, Rebecca L. Milot, James D. Blakemore, Minjoo L. Lee, Victor S. Batista, Charles A. Schmuttenmaer, Robert H. Crabtree and Gary W. Brudvig (2012) *J. Phys. Chem. C* **116**, 4892–4902.
32. “Water Oxidation Catalyzed by a Tetranuclear Mn Cluster: $[Mn^{IV}_4O_5(terpy)_4(H_2O)_2](ClO_4)_6$ (terpy = 2,2’:6,2’’-Terpyridine)”, Yunlong Gao, Robert H. Crabtree and Gary W. Brudvig (2012) *Inorg. Chem.* **51**, 4043–4050.
33. "Oxomanganese Complexes for Natural and Artificial Photosynthesis", Ivan Rivalta, Gary W. Brudvig and Victor S. Batista (2012) *Curr. Opin. Chem. Biol.* **16**, 11-18
34. “Synthesis and Computational Studies of Mg Complexes Supported by 2,2':6,2"-Terpyridine Ligands”, Louise M. Guard, Julio L. Palma, William P. Stratton Laura J. Allen, Gary W. Brudvig, Robert H. Crabtree, Victor S. Batista and Nilay Hazari, (2012) *Dalton Trans.* **41**, in press.
35. “Light-driven Water Oxidation for Solar Fuel Production”, Karin J. Young, Lauren A. Martini, Rebecca L. Milot, Robert C. Snoeberger III, Victor S. Batista, Charles A. Schmuttenmaer, Robert H. Crabtree and Gary W. Brudvig (2012) *Coord. Chem. Rev.* **256**, in press.
36. “Interfacial Electron Transfer into Functionalized Crystalline Polyoxotitanate Nanoclusters”, Robert C. Snoeberger III, Karin J. Young, Jiji Tang, Laura J. Allen, Robert H. Crabtree, Gary W. Brudvig, Philip Coppens, Victor S. Batista and Jason B. Benedict (2012) *J. Am. Chem. Soc.* **134**, revision requested.

Posters: Solar Photochemistry

Control of PbSe Quantum Dot Surface Chemistry Using an Alkylselenide Ligand and Size Dependent Multiple Exciton Generation in PbX Quantum Dots

Barbara K. Hughes[1,2], Aaron Midgett[1,2], Daniel A. Ruddy[1], Joseph M. Luther[1], Jeffrey L. Blackburn[1], Arthur J. Nozik[1,2], Justin C. Johnson[1], Matthew C. Beard[1]

[1]National Renewable Energy Laboratory
Golden CO 80401

[2]Department of Chemistry and Biochemistry
University of Colorado
Boulder CO 80309

We synthesized alkylselenide reagents to replace the native oleate ligand on PbSe quantum dots (QDs) in order to investigate the effect of surface modification on their stoichiometry, photophysics, and air stability. The alkylselenide reagent removes all of the oleate on the QD surface and results in Se addition; however, complete Se-enrichment does not occur, achieving a 53% decrease in the amount of excess Pb for 2 nm diameter QDs and a 23% decrease for 10 nm QDs. Our analysis suggests that the Se-ligand preferentially binds to the {111} faces, which are more prevalent in smaller QDs. We find that attachment of the alkylselenide ligand to the QD surface enhances oxidative resistance, likely resulting from a more stable bond between surface Pb atoms and the alkylselenide ligand compared to Pb-oleate. However, binding of the alkylselenide ligand produces a separate non-radiative relaxation route that partially quenches PL suggesting the formation of a dark hole-trap.

We studied multiple exciton generation (MEG) by single photons for quantum dot (QD) consisting of either PbSe, PbS, or a PbS_xSe_{1-x} alloy and for several different QD sizes representing bandgaps in the ranges of 0.6 to 1 eV using ultrafast transient absorption and photoluminescence spectroscopies. In previous reports, we found that the MEG efficiency, η_{MEG}, in PbSe QDs is about 2x higher compared to bulk PbSe, however, little could be said about how η_{MEG} depends on QD size. η_{MEG} can either be defined in terms of how much excess photon energy relative the bandgap energy is needed to produce more than one electron-hole pair or in terms of the competition between hot-exciton cooing and MEG. Here, we find for both PbS and PbS_xSe_{1-x} alloyed QDs that η_{MEG} decreases towards the value of the parent bulk semiconductor for larger sizes. The decrease in η_{MEG} correlates with a decrease in the ratio between the QD radius and the Bohr exciton radius ($\lambda = r/a_B$) as the QD composition changes from PbSe to PbS_xSe_{1-x}. For all PbSe, PbS, and PbS_xSe_{1-x} QD samples η_{MEG} depends linearly on λ by the following, $\eta_{MEG} = 0.7 - \lambda$, for λ between 0.03 and 0.25. Our measurements suggest that quantum confinement enhances MEG.

Influence of Dark States and Environmental Perturbations in Single-walled Carbon Nanotube Luminescence

Jeff Blackburn,[a] Josh Holt,[a] Kevin Mistry,[a] Brian Larsen,[a] Jeff Fagan,[b] Pravas Deria,[c] Ian Stanton,[c] Michael Therien,[c] Garry Rumbles[a]

[a]National Renewable Energy Laboratory, Golden CO
[b]National Institute of Standards, Gaithersburg MD
[c]Duke University, Durham NC

Successful dissociation of photogenerated SWCNT excitons for solar conversion requires electron/hole transfer rates that are competitive with internal exciton recombination rates. However, excitons in SWCNTs tend to have relatively short lifetimes, and the reported photoluminescence quantum yields remain low. These deficiencies may be due in part to strong environmental perturbations of excitons, as well as a number of optically forbidden (dark) exciton states that contribute to losses from the bright singlet exciton population.

The photoluminescence (PL) quantum yield can comment on the competition between radiative and noradiative exciton relaxation pathways. This poster focuses on recent studies aimed at understanding the influence of dark exciton states and environmental perturbations on SWCNT PL. In the first study, we compare ^{12}C and ^{13}C-labeled SWCNTs that are highly enriched in the (6,5) species to identify both absorptive and emissive vibronic transitions.[1] Independent analysis of two sidebands lying near the bright singlet exciton reveals that the sidebands actually arise from coupling to a dark exciton level, which lies at an energy approximately 25 meV above the bright singlet exciton. Our observations support the recent prediction of, and mounting experimental evidence for, the dark K-momentum singlet exciton lying ~25 meV (for the (6,5) SWCNT) above the bright Γ-momentum singlet.

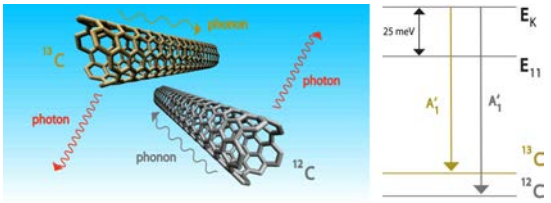

Figure 1. ^{13}C-labeled SWCNTs modify vibrational energies, enabling the unequivocal identification of phonon sidebands arising from a dark exciton level.

In the second study, a collaboration with Michael Therien from Duke, we investigate the impact of solvation environment on SWCNT PL quantum yield using a novel, highly charged aryleneethynylene polymer as a surfactant to produce dispersions into a variety of polar solvents having a wide range of dielectric constants.[2] We find that SWCNT PL quantum yield is strongly dependent on both the polarity and electrophilicity of the solvent. We suggest that highly polar solvents reduce SWCNT quantum yield via dielectric screening of excitons, while electrophilic solvents shift electron-density from the pi electron network, thus creating non-radiative recombination sites. Finally, in the third study, a collaboration with Jeff Fagan from NIST, we demonstrate that SWCNTs with end-caps can be separated from open SWCNTs using density gradient ultracentrifugation.[3] Open SWCNTs are filled with water, and have dramatically reduced PL quantum yields relative to the empty end-capped SWCNTs. Importantly, the spectroscopic signatures of typically produced samples are dominated by the water-filled nanotubes, revealing an important source of the traditionally low reported PL quantum yields.

1. Blackburn, J.L., et al. *Nano Lett.* **2012**, 12, 1398.
2. Larsen, B.A., et al. *J. Amer. Chem. Soc.*, in review.
3. Fagan, J.A., et al. *ACS Nano* **2011**, 5, 3943.

Controlling Charge Dynamics by Interface Engineering in Quantum Dot Heterostructures

Justin C. Johnson, E. Ryan Smith, Joseph Luther, Barbara Hughes, Matt Beard
Chemical and Nanosciences Center
National Renewable Energy Laboratory
Golden CO 80401

Quantum dots (QDs) are dominated by surfaces, which presents a challenge for understanding the complex chemistry but can be an opportunity for manipulating exciton and charge dynamics as well as doping. We have investigated quantum rod heterostructures (QRHs) and surface-modified quantum dots using a variety of spectroscopic methods, including cross-polarized transient grating (CPTG) spectroscopy and temperature dependent photoluminescence (PL) in order to reveal how the interfaces and surfaces influence the photophysics.

CdSe/CdS QRHs are useful platforms for understanding charge separation in nanoscale objects. Although they ostensibly should possess a smooth transition from type-I to quasi type-II behavior, the reality of strain and alloying induced by the imperfect interface results in a more complicated situation. We show by CPTG measurements on a series of QRHs with varying aspect ratios that the exciton produced by band gap excitation spreads mostly radially rather than along the rod's long axis. In addition, for large sizes of CdSe QD seeds (> 4 nm) the exciton becomes oblate rather than spherical due to the low kinetic energy of the electron compared with the strain-induced band bending. The influence of strain on the seed distorts the exciton, leaving the fine structure perturbed such that two CPTG decay pathways are observed (Figure 1, left).

Control of lead chalcogenide QD surface chemistry represents an important but unsolved challenge toward making QDs applicable in photovoltaics and other technologies. We have recently undertaken investigations of PbSe QD surface chemistry using a designed ligand that retains QD solubility. The alkylselenide molecule appears to bind preferentially to the {111} surface of the QD, reducing the native Pb-enrichment by up to 40%. Temperature dependent PL spectroscopy reveals that the rate of surface oxidation is significantly reduced, and that the quenching of surface Pb atoms by the Se group leads to a small concentration of hole traps that modifies the PL temperature dependence and reduces the PL quantum yield (Figure 1, right).

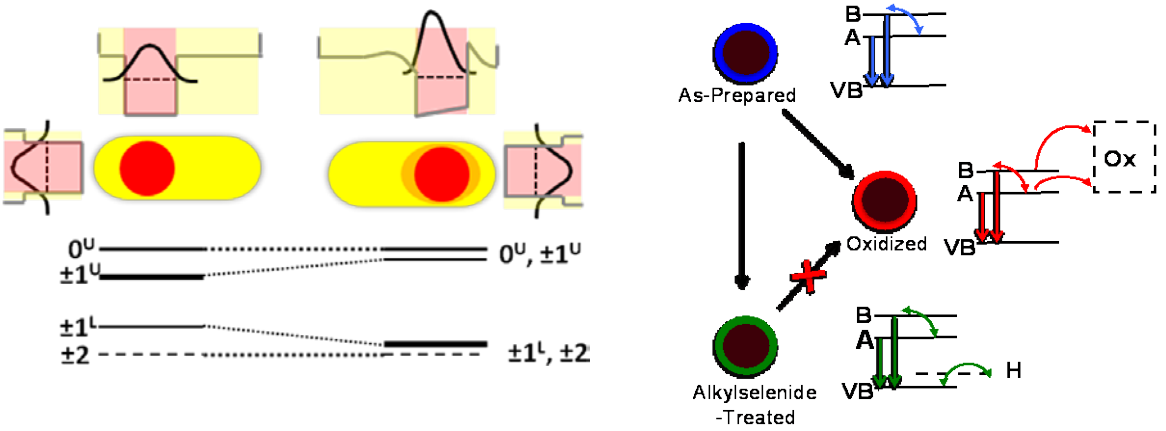

Figure 1. Left, model of exciton fine structure for idealized and strained CdSe/CdS QRH. Right, model of photophysics for as-prepared and alkylselenide treated PbSe QDs.

Theoretical Conversion Efficiency of Solar Photoconversion with Solar Concentration Combined with Multiple Exciton Generation

M. C. Hanna[1], M. C. Beard[1] and A.J. Nozik[1,2]

[1]National Renewable Energy Laboratory
Golden CO 80401
and
[2]Department of Chemistry and Biochemistry
University of Colorado
Boulder CO 80309

Thermodynamic calculations show that all solar cells for the conversion of photons into electricity or fuel will have higher theoretical power conversion efficiencies when concentrated sunlight is used, compared to their use with unconcentrated sunlight (labeled 1X (1 sun intensity)). For conventional (viz, present day) solar cells that produce one electron-hole pair per absorbed solar photon of any energy, the theoretical increase in efficiency is relatively small (40% at 500X vs 33% at 1X). However, when solar concentration is combined with multiple exciton generation (MEG), the increase in theoretical efficiency is greatly enhanced. For the ideal MEG case, where the threshold for exciton multiplications is just twice the HOMO-LUMO transition (bandgap, E_g) and the bandgap of the solar converter is allowed to be an independent variable as the solar concentration varies, the maximum thermodynamic efficiency increases to 75% at 500X (at small bandgaps). If the bandgap is fixed as a function of solar concentration, the maximum theoretical efficiency still increases markedly, becoming 62% at 500X for the staircase MEG characteristic (defined as producing a quantum yield of N when the photon energy is N x E_g after the onset of MEG) and 47% for a linear MEG characteristic. The fixed bandgaps in these two cases are those with maximum conversion efficiency, and are 0.70 eV and 0.93 eV, respectively. The mechanism of these concentration effects are related to the higher MEG quantum yields provided by smaller bandgaps, the contribution of thermal excitation to the electron-hole pair population, the fact that the photocurrent is linear with concentration while the photovoltage is logarithmic, and changes in radiative recombination with photon energy.

Photodetachment and Electron Reactivity in Aliphatic Room Temperature Ionic Liquids

Francesc Molins i Domenech, Benjamin FitzPatrick, Andrew T. Healy and David A. Blank
Department of Chemistry, University of Minnesota
Minneapolis MN 55455

Incorporation of room temperature ionic liquids, RTILs, is rapidly expanding in a vast array of energy technologies, including solar energy conversion. The stability and reactivity under conditions of photolytic and radiolytic exposure are important considerations for these applications. RTILs consisting of aromatic cations, such as imidazolium, and halogen anions are commonly employed. However, both the cation and anion in these liquids react readily with free electrons. By contrast, aliphatic RTILs are more stable under such conditions. This allows for better experimental isolation of electron dynamics and reactivity with electron quenchers. The dynamic range for solvation in RTILs is significantly broadened when compared with most common solvents. The result is a magnification of the influence on reaction dynamics that comes from the solvation-dependent reactivity of the free electrons. In radiolysis studies Wishart and coworkers have demonstrated the higher reactivity that precedes complete solvation, and recently, using 15 ps resolution, they found that there must be significant solvation and reaction on even earlier time scales.[1] Photodetachment provides three orders of magnitude higher time resolution and access to a lower range of initial energies. We present transient absorption, TA, studies following 1-photon photodetachement of two neat pyrrolidinium bis(trifluoromethylsulfonyl)amide RTILs. The results are considered in the context of both the radiolysis results and the recent computational predictions for the dry excess electron in RTILs.[2] TA spectra in the presence of perchloric acid, an electron quencher, demonstrate a bimodal spectrum for the hole in the visible portion of the spectrum. Sub-picosecond quenching reveals previously unobserved reactivity of the pre-solvated electron. Both geminate recombination and reaction with the added quencher indicate that the initial "dry" electron is relatively delocalized, mobile, and has considerable reactive reach.[3]

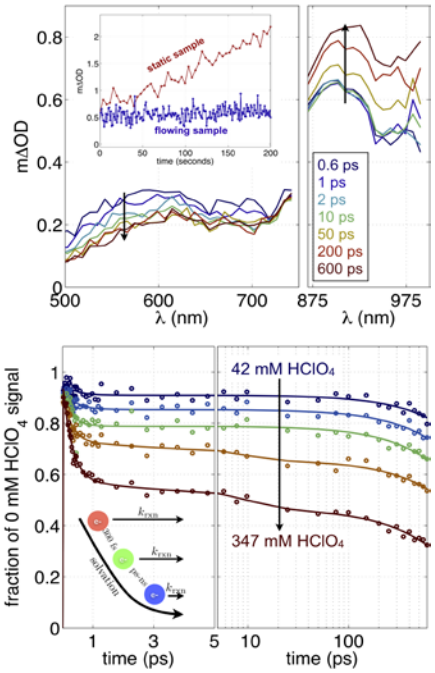

Fig. 1 (top) TA in $[Py_{14}^{+}][NTf_2^{-}]$ after 1-photon photodetachment. (bottom) Time dependent quenching of the free electrons with perchloric acid.

1 J. F. Wishart, A. M. Funston, T. Szreder, A. R. Cook, and M. Gohdo, Electron solvation dynamics and reactivity in ionic liquids observed by picosecond radiolysis techniques, Faraday Discuss. 154, 353-363 (2012).

2 C. J. Margulis, H. V. R. Annapureddy, P. M. De Biase, D. Coker, J. Kohanoff, and M. G. Del Popolo, Dry Excess Electrons in Room-Temperature Ionic Liquids, J. Am. Chem. Soc. 133, 20186-20193 (2011).

3 F. Molins, B. FitzPatrick, A. T. Healy, and D. A. Blank, Photodetachment and electron reactivity in 1-methyl-1-butyl-pyrrolidinium bis(trifluoromethylsulfonyl)amide, J. Chem. Phys., Submitted (2012).

Computational Studies of Pre-Solvated Excess Electron and Hole Localization and the Nature of Polar/Non-Polar and Positive/Negative Structural Fluctuations in Different Room Temperature Ionic Liquids

Claudio J. Margulis[a], Hemant K. Kashyap[a], Harsha V. R. Annapureddy[a], Jeevapani J. Hettige[a], Pablo M. De Biase[a], Edward W. Castner Jr.[b], Cherry Santos[b], N. Sanjeeva Murthy[b], David Coker[c], Jorge Kohanoff[d] and Mario G. Del Pópolo[d]

[a]Department of Chemistry
University of Iowa
Iowa City IA 52242

[b]Department of Chemistry & Chemical Biology
Rutgers, The State University of New Jersey
New Brunswick NJ 08901

[c]Department of Physics
University College of Dublin
Dublin 4, Ireland

[d]Atomistic Simulation Centre
School of Mathematics and Physics
Queen's University Belfast, BT7 1NN, UK

We have recently studied[1] using condensed phase density functional theory the electronic structure of different room-temperature ionic liquids at time zero after the addition of an excess electron or an excess hole. The most interesting finding is that electrons do not necessarily localize close to the positively charge cations. Their pattern of localization is determined by the relative alignment of HOMO/LUMO gaps of anions and cations. In some systems localization is on anions in some others on cations. We have also established the origin of the two energy bands in the excess electron spectrum at time zero. The low energy band is associated with what we call "translational electronic transitions"; these transitions leave the electron in a state of similar character but in a different liquid location. The band at higher energy is due to transitions that often change the character of the electronic state and possibly the species on which electrons localize. These exciting new findings provide a foundation to the novel femtosecond excess electron experiments being carried out in our SISGR team by David Blank and coworkers and are synergistic with ultrafast radiolysis experiments carried out using the LEAF facility at BNL by Wishart and collaborators.

Another aspect of our research has been the elucidation of the very complex organizational patterns and spatial periodicity apparent in SAXS experiments of different room temperature ionic liquids. In collaboration with the Castner group at Rutgers we have been able to quantitatively define the origin of the three main features common to many of these systems. These are the elusive prepeak or first sharp diffraction peak, and what we have identified as the alternation peak and the adjacency peak.[2,3] We find that peaks and negative going peaks at the same frequency correspond to different length scale periodicities, most notably the polar/non-polar long range alternation and the positive/negative charge alternation. These results have possible implications in our understanding of localization of photochemical species, excess electrons and electron transfer.

(1) Margulis, C. J.; Annapureddy, H. V. R.; De Biase, P. M.; Coker, D.; Kohanoff, J.; Del Popolo, M. G. *J Am Chem Soc* **2011**, *133*, 20186.

(2) Kashyap, H. K.; Hettige, J. J.; Annapureddy, H. V. R.; Margulis, C. J. *Chemical Communications* **2012**, in press.

(3) Santos, C. S.; Annapureddy, H. V. R.; Murthy, N. S.; Kashyap, H. K.; Castner, E. W., Jr.; Margulis, C. J. *J. Chem. Phys.* **2011**, *134*, 064501.

Diffusion and Diffusion-Limited Electron Transfer in Ionic Liquids

Anne Kaintz, Min Liang and Mark Maroncelli
Department of Chemistry
The Pennsylvania State University
University Park PA 16802

When modeling fluorescence data on diffusion-limited bimolecular electron transfer in ionic liquids (ILs) we found it necessary to invoke diffusion coefficients of neutral solutes which exceeded Stokes-Einstein predictions, $D_{SE} = k_B T / 6\pi\eta$ (η = viscosity), by significant factors. We therefore performed ^{1}H-NMR pulsed-field gradient measurements to directly determine the diffusion coefficients of the reactant DMA in a range of ionic liquids. These measurements confirmed higher-than-expected diffusion coefficients inferred from the reaction modeling.[1]

We have since extended these NMR measurements to a variety of uncharged solutes in ionic liquids. Figure 1 highlights some of the principal results of this work. On the main panel are plotted the ratios of translational friction coefficients $\zeta_{obs} / \zeta_{SE} = D_{SE} / D_{obs}$ of a series of aromatic solutes relative to Stokes-Einstein (SE) predictions. These data were collected in the series of pyrrolidinium ionic liquids [Pr$_{n1}$][Tf$_2$N] with n=3, 4, 6, 8, 10. For such neutral solutes the friction is smaller than SE predictions by factors of between 2 and 10. The primary determinant of ζ_{obs} / ζ_{SE} is the size of the solute relative to the solvent, V_u/V_v. Literature data on small gaseous solutes confirm this trend over a much wider range of V_u/V_v. Whereas this dependence upon size not been widely appreciated in IL research, comparable, but less dramatic behavior has long been known in conventional solvents. Correlative equations similar to those developed for conventional solvents can be adapted for predicting neutral solute diffusion in ionic liquids. But ions diffusing in ionic liquids behave very differently than do neutral solutes. For example, the open symbols in the top panel of Fig. 1 are data on benzoate diffusion in the [Pr$_{n1}$][Tf$_2$N] series. Comparing the benzoate data to the benzene data on the bottom panel (red circles) one finds a 5- to 10-fold reduction in rate for the ionic versus the comparably sized neutral solute. It is not surprising that friction should increase with the strengthening of intermolecular interactions caused by solute charge. What is surprising is how large the effect is in this case. At present it is not clear whether one can understand the diffusion of charged solutes in ionic liquids with the same approaches used in the case of neutral solutes, and further studies will be undertaken to further explore this question.

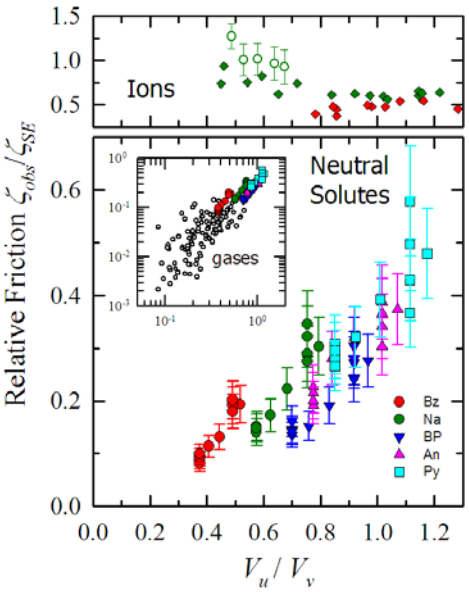

Fig. 1: Relative translational friction coefficients of ions and neutral solutes in ionic liquids plotted versus the solute-to-solvent van der Waals volume ratio. (V_v is the average of cation and anion volumes.)

1. M. Liang, A. Kaintz, G. A. Baker, and M. Maroncelli, Bimolecular Electron Transfer in Ionic Liquids: Are Reaction Rates Anomalously High?, *J. Phys. Chem. B* **116,** 1370-1384 (2012).

Influence of Reactant Charges on Bimolecular Electron Transfer Reactions in an Ionic Liquid

Masao Gohdo and James Wishart
Chemistry Department
Brookhaven National Laboratory
Upton NY 11973

Ionic liquids (ILs) are remarkable media with many potential uses in systems that use charge-transfer reactions to capture, store or utilize solar energy. The molecular-scale polar/non-polar heterogeneity of ionic liquids offers different solvation environments to solutes of different polarities and charge types, owing to the local availability of Coulombic and van der Waals interactions. Work from several laboratories as well as theoretical treatments indicate higher mobilites of neutral solutes in ILs compared to charged ones of the same shape and size (with the difference attenuating as the size of the solute grows larger). Furthermore, depending on the reactant charges the preferred solvation environments may change during the course of a charge-transfer reaction.

To explore the effects of charge type on electron transfer reactions in ILs, we used pulse radiolysis at the BNL LEAF picosecond pulse radiolysis facility to produce solvated electrons in the ionic liquid *N*-methyl-*N*-butylpyrrolidinium bis(trifluoromethylsulfonyl)imide. The electrons were then captured by selected quasi-isostructural biaryl scavengers (biphenyl, *N*-phenylpyridinium cation and methylviologen dication). The resulting biaryl radical electron adducts have charges of -1, 0, and +1 respectively. We measured the rate constants for the reactions of these biaryl radicals with a series of methyl-substituted *p*-benzoquinones, including temperature dependences for selected reactant pairs, and we are presently extending the driving force range using halogenated benzoquinones in order to better estimate activationless electron transfer rate constants (k_{max}) for each biaryl radical species according to Marcus theory. We observe that the rate constants obtained for the reactions of neutral *N*-phenylpyridinyl radical at low driving force are similar to those of biphenyl radical anion at much higher driving force, indicating faster diffusion for the neutral species. Our kinetic results also clearly show that diffusion rates of solvated electrons in the ionic liquid are more like those of molecular anions than of quantum particles.

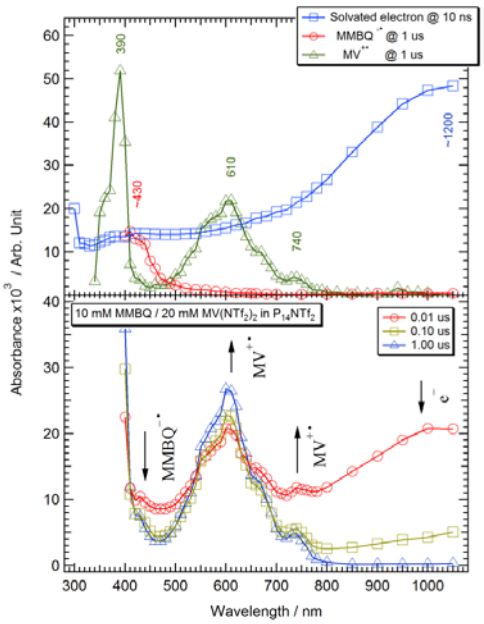

Spectra of radical species e^-_{solv}, $MMBQ^{\bullet-}$ (dimethylbenzoquinone), and $MV^{\bullet+}$ (top); and kinetic spectra at indicated times following electron transfer from $MMBQ^{\bullet-}$ to MV^{2+} (bottom). Data obtained by electron pulse radiolysis at LEAF. (The driving force for this reaction is small enough that it can be followed in both directions by manipulation of reactant concentrations.)

Effects of Linker Torsional Constraints on the Rate of Hole Transfer in Oxidized Porphyrin Dyads

Christopher J. Hondros,[a] Aravindu Kunche,[b] James R. Diers,[a] Dewey Holten,[c] Jonathan S. Lindsey[b] and David F. Bocian[a]

[a]Department of Chemistry University of California, Riverside CA 92521-0403
[b]Department of Chemistry, North Carolina State University, Raleigh NC 27695-8204
[c]Department of Chemistry, Washington University, St. Louis MO 63130-4889

Efficient solar-energy conversion requires that holes generated after excited-state electron-injection can move efficiently away from the anode, thereby preventing charge-recombination. Thus, understanding hole mobility in prototypical light-harvesting and charge-separation systems is of fundamental interest, particularly to the fields of artificial photosynthesis and molecular electronics. One strategy for examining ground-state hole/electron transfer in oxidized tetrapyrrolic arrays entails analysis of the hyperfine interactions observed in the EPR spectrum of the π-cation radical. We have found that ^{203}Tl/^{205}Tl hyperfine "clocks" are greatly superior to those provided by ^{1}H, ^{14}N, or ^{13}C owing to the fact that the ^{203}Tl/^{205}Tl hyperfine couplings are much larger (15-25 G) than those of the ^{1}H, ^{14}N, or ^{13}C nuclei (1-6 G). The large ^{203}Tl/^{205}Tl hyperfine interactions permit accurate simulations of the EPR spectra and the extraction of specific rates of hole/electron transfer. We previously applied the ^{203}Tl/^{205}Tl hyperfine-clock strategy to a variety of porphyrin dyads that are joined at a meso position of the porphyrin macrocycle via linkers of a range of lengths and composition (diphenylethyne, diphenylbutadiyne and (*p*-phenylene)$_n$ where n = 1-4). The hole/electron-transfer time constants were found to be in the hundreds of picosecond to sub-ten nanosecond regime, depending on the specific porphyrin and/or linker. Variable-temperature EPR studies further demonstrated that the hole/electron-transfer process is weakly activated (12-15 kJ mol^{-1}) at room temperature and somewhat below. At lower temperatures, the process is essentially activationless. We proposed that the weak activation is due to restricted torsional motions of the aryl rings of the linker. This proposal has now been investigated using a series of diphenylethyne-linked porphyrin dyads wherein *o*-dimethyl substituents are systematically added to the aryl rings of the linker. These studies demonstrate that torsional mobility in the linker is responsible for activation of the hole-transfer event.

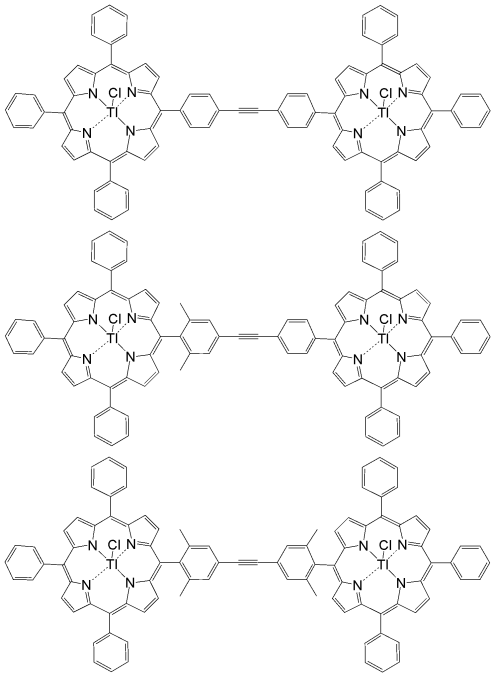

Effects of Substituents on Synthetic Analogs of Chlorophylls: The Distinctive Impact of Auxochromes at the 7- versus 3-Positions

Joseph W. Springer,[a] Kaitlyn M. Faries,[a] James R. Diers,[b]
Chinnasamy Muthiah,[c] Olga Mass,[c] Hooi Ling Kee,[a] Christine Kirmaier,[a]
Jonathan S. Lindsey,[b] David F. Bocian[b] and Dewey Holten[a]

[a]Department of Chemistry, Washington University, St. Louis MO 63130
[b]Department of Chemistry, University of California Riverside, Riverside CA 92521
[c]Department of Chemistry, North Carolina State University, Raleigh NC 27695

Understanding the effects of substituents on the spectra of chlorophylls is essential for gaining a deep understanding of photosynthetic processes. Chlorophyll *a* and *b* differ solely in the nature of the 7-substituent (methyl versus formyl) whereas chlorophyll *a* and *d* differ solely in the 3-substituent (vinyl versus formyl), yet have distinct long-wavelength absorption maxima: 665 (*a)* 646 (*b*), and 692 nm (*d*). Here, the spectra, singlet excited-state decay characteristics, and results from DFT calculations are examined for synthetic chlorins and 13[1]-oxophorbines that contain ethynyl, acetyl, formyl and other groups at the 3-, 7- and/or 13-positions. Substituent effects on the absorption spectra are well accounted for using Gouterman's four-orbital model. Key findings are that (1) the dramatic difference in auxochromic effects of a given substituent at the 7- versus 3- or 13-positions primarily derives from relative effects on the LUMO+1 and LUMO; (2) formyl at the 7- or 8-position effectively "porphyrinizes" the chlorin; and (3) the substituent effect increases in order of vinyl < ethynyl < acetyl < formyl. Thus, the spectral properties are governed by an intricate interplay of electronic effects of substituents at particular sites on the four frontier MOs of the chlorin macrocycle.

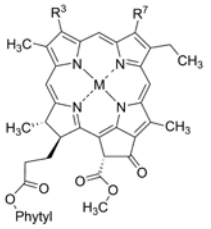

Compound	M	R^3	R^7
Chlorophyll *a*	Mg	vinyl	methyl
Chlorophyll *b*	Mg	vinyl	formyl
Chlorophyll *d*	Mg	formyl	methyl
Pheophytin *a*	H, H	vinyl	methyl
Pheophytin *b*	H, H	vinyl	formyl
Pheophytin *d*	H, H	formyl	methyl

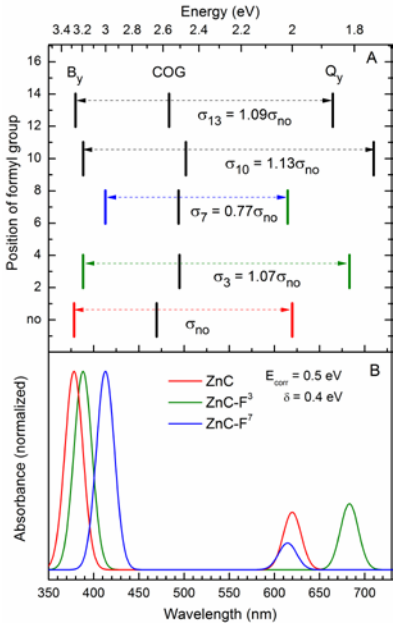

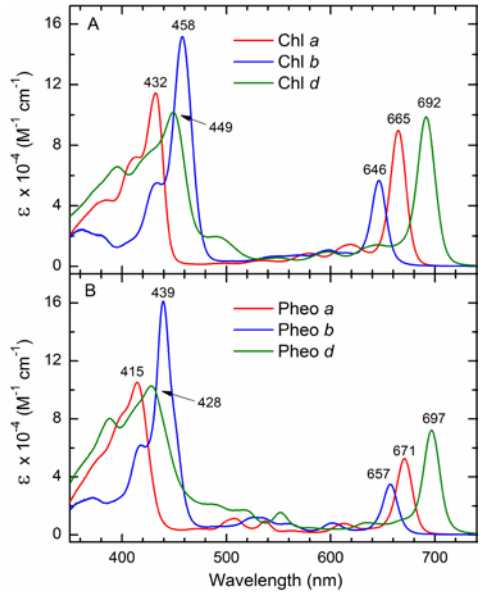

Right. Structure and absorption spectra of (A) chlorophyll a (red), chlorophyll b (blue), and chlorophyll d (green) and (B) pheophytin analogues.

Left. (A) Simulations, based on the four-orbital model, of the $B_y(0,0)$ and $Q_y(0,0)$ band positions and the energy center of gravity (COG) for a zinc chlorin containing no substituents (ZnC) or a single formyl group (F) at the 3-, 7-, 10- and 13- positions. (B) 20-nm wide Gaussian skirts are applied and $B_y(0,0$ intensities are normalized to 1 and $Q_y(0,0)$intensities are referenced to the observed $Q_v(0,0)/B_v(0,0$ ratio for ZnC.

Synthetic Metallobacteriochlorins

Chih-Yuan Chen,[a] Erjun Sun,[a] Dazhong Fan,[a] Masahiko Taniguchi,[a] Eunkyung Yang,[b] Dariusz Niedzwiedzki,[b] Chris Kirmaier,[b] David F. Bocian,[c] Dewey Holten[b] and Jonathan S. Lindsey[a]

[a]Department of Chemistry, North Carolina State University, Raleigh NC 27695

[b]Department of Chemistry, Washington University, St. Louis MO 63130

[c]Department of Chemistry, University of California Riverside, Riverside CA 92521

Bacteriochlorins are attractive candidates for capturing near-infrared light. We have developed a relatively concise, *de novo* synthesis of bacteriochlorins and are employing the bacteriochlorins as constituents in a variety of light-harvesting designs. The bacteriochlorins so obtained are in the free base form. To our surprise, metalation of the synthetic bacteriochlorins, an "ostensibly simple" reaction, proved difficult. An ensuing study, spanning several years, has led to the following insights and methodology for metalation.

- The difficulty of metalation of tetrapyrrole macrocycles increases along the series porphyrin < chlorin << bacteriochlorin.
- The difficulty of metalation of bacteriochlorins decreases with increasing number of electron-withdrawing substituents.
- Metalation of a bacteriochlorin occurs upon treatment with a strong base (e.g., NaH) in THF containing MX_n (method 1): (a) for bacteriochlorins that bear electron-releasing substituents, M = Cu, Zn, Pd, and InCl; (b) for bacteriochlorins that bear two ester (electron-withdrawing) substituents, M = Ni, Cu, Zn, Pd, Cd, InCl, and Sn (but not Al or Au); and (c) a bacteriochlorin with four ester substituents was metalated with Mg.
- Bacteriochlorins that bear ≥2 carbonyl groups can be zincated by typical "porphyrin-type" conditions (ZnX_2 in DMF at 60–80 °C, method 2).
- The average lifetime of the lowest singlet excited state for a set of zinc bacteriochlorins is only slightly shorter than that for the free base analogues (3.4 versus 3.9 ns).
- The long-wavelength absorption (Q_y) band was shifted bathochromically upon metalation from 737 nm (free base, black) to 739 (Pd, blue), 750 (Zn, red), 755 (Cu, green), and 763 nm (ClIn, orange) for the 2,12-di-*p*-tolylbacteriochlorin (structure at left, spectra at right).

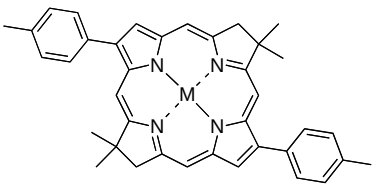

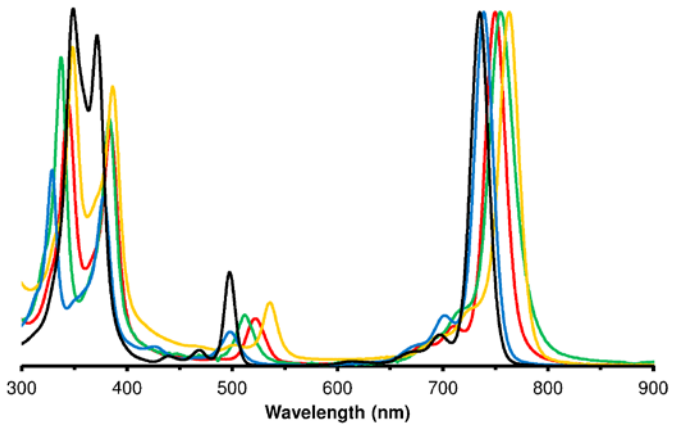

Photoinitiated Electron Collection in Mixed-Metal Supramolecular Complexes: Development of Photocatalysts for Hydrogen Production

Travis White, Dr. Gerald Manbeck, Skye King, Rongwei Zhou, Kevan Quinn, Karen J. Brewer
Department of Chemistry
Virginia Tech
Blacksburg VA 24061-0212

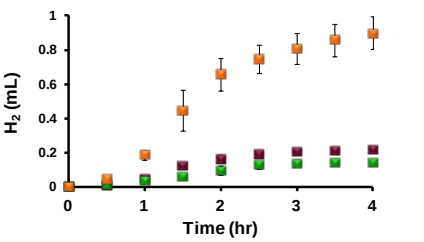

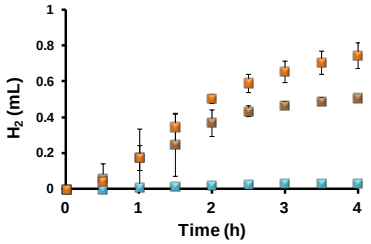

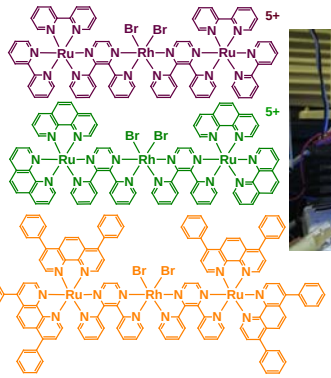

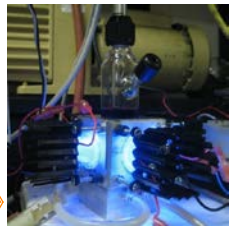

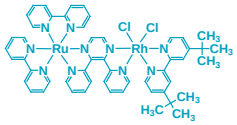

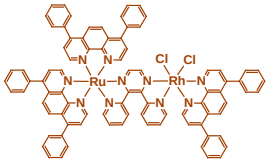

The capture and conversion of the light energy from the Sun is important to energy independence and harvesting this alternative energy source via water splitting provides for hydrogen fuel. H_2 is a high energy fuel containing more energy per gram than any other non-nuclear fuel and provides a clean fuel cycle where H_2 combustion produces the water from which it was produced. This project developed and studied a new class of mixed-metal supramolecular complexes that act as single component water reduction catalysts. The study of series of closely related complexes illustrates the nearly isoenergetic orbitals and excited states where orbital inversion can occur with very minor changes in structure. The nature of the lowest lying orbital and excited state as well as steric protection about the reactive Rh site is critical to functioning providing considerable insight into the critical mechanistic steps in the photocatalysis. These systems couple charge transfer light absorbing metals to reactive metals such as rhodium(III) that will allow these systems to undergo photoinitiated electron collection (PEC) while possessing reactive metal sites capable of delivering collected electrons to a substrate such as H_2O to facilitate the production of H_2. Shown are illustrative examples that illustrate how minor changes can lead to systems that don't undergo PEC, only undergo PEC but dimerize at the Rh(I) site to prevent photocatalysis and finally systems that undergo PEC and act as photocatalysis for water reduction to produce H_2. Preliminary studies of direct synthesis of Rh(I) systems as well as studies showing these complexes are electrocatalysts will be provided.

EPR Analysis of a Transient Species Formed During Water Oxidation Catalyzed by the Complex Ion $[(bpy)_2Ru(OH_2)]_2O^{4+}$

Jamie A. Stull[1], Troy A. Stich[1], James K Hurst[2], R. David Britt[1]

[1] Department of Chemistry
University of California-Davis
Davis CA 95616

[2] Department of Chemistry
Washington State University
Pullman Washington 99164

The ruthenium "blue dimer" $[(bpy)_2Ru(OH_2)]_2O^{4+}$ – the first well-defined molecular complex able to catalyze water oxidation at low potentials – has been the subject of a number of experimental and computational studies. However, the reaction mechanism remains controversial. Of particular interest is the catalytically relevant species of the dimer present prior to oxygen evolution. Herein, we report the first advanced EPR studies of an intermediate that appears under conditions in which the catalyst is actively turning over. This intermediate is observed in solutions known to contain $[(bpy)_2Ru^{V}(O)]_2O^{4+}$, denoted **{5, 5}**. This species has been shown to have a comparable rate constant for the decay of the corresponding g = 2.02 signal and decay of oxygen evolution in photocatalyzed solutions after removal of the illumination source.[1,2] In the present work, CW EPR spectroscopy was used to probe the hyperfine coupling of the Ru ions, while corresponding ligand ^{14}N hyperfine couplings were characterized with ESEEM and HYSCORE methods. Finally, $^{1}H/^{2}H$ ENDOR was performed to monitor any exchangeable protons. Our studies confirm an S = 1/2 species, suggestive of an intermediate with an odd overall electron count (per dimer) and the large metal hyperfine coupling is suggestive of metal centered unpaired spin.

Graphene Charge Transfer and Spectroscopy

Louis E. Brus
Chemistry Department
Columbia University
New York NY 10027

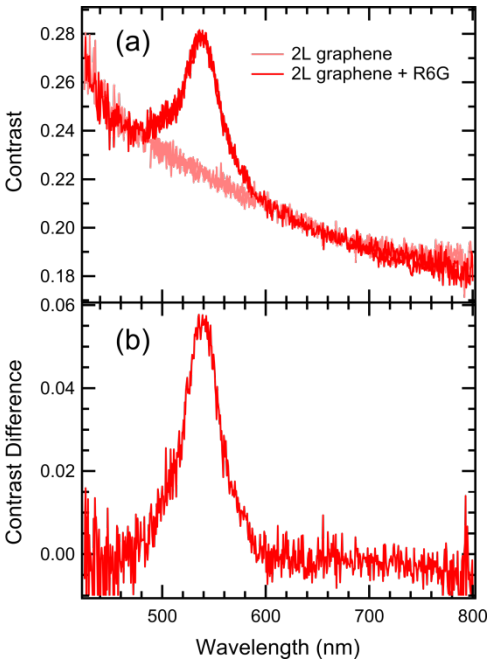

We have explored the question of possible Surface Enhanced Raman spectroscopy from molecules on Graphene substrates. Last year we reported on Fresnel calculations on this thin film system, which did not show any net electromagnetic field enhancement. In order to carefully investigate the question of possible chemical SERS, we studied Rhodamine 6G dye (R6G) on graphene, as R6G is the standard, well characterized molecule for high Raman cross section SERS with Ag particles . By comparing the optical contrast visible spectrum, and the Raman spectrum, we were able to determine the absolute Raman cross section for R6G on the graphene surface. At the left we show the contrast spectrum, with in (a) shows the strong visibleR6G absorption on top of the broad graphene continuum absorption. (b) shows the subtracted R6G spectrum. We find that the R6G section is perhaps a factor of 3 less on the graphene surface, apparently because the R6G absorption is red-shifted away from the laser line. In this system there is no evidence for field enhancement or chemical SERS. Nevertheless, the R6G Raman shows high signal to noise, as interfering dye luminescence, present for example in solution, is strongly quenched by the metallic graphene. In addition, luminescence from the graphene itself is negligible despite 2% optical absorption of the laser. As a net result, graphene makes an excellent substrate for Raman scattering by adsorbed molecular species.

We also studied charge transfer in 1-10 layer (1L – 10L) thick graphene samples on which strongly electronegative NO_2 has been adsorbed. Electrons transfer from the graphene to NO2, leaving the graphene layers doped with mobile delocalized holes. Doping follows a Langmuir-type isotherm as a function of NO_2 pressure. Raman and optical contrast spectra provide independent, self-consistent measures of the hole density and distribution as a function of the number of layers (N). As the doping induced Fermi level shift E_F reaches half the laser photon energy, an intensity resonance in the graphene G mode Raman intensity is observed. We observe a decrease of graphene optical band-to-band absorption in the near-IR that is due to hole doping. Highly doped samples are more transparent, and they are expected to have high metallic conductivity. In thicker samples holes are effectively confined near the surface; the interior graphene layers show an essentially pristine Raman signal.

Structural Control in Photoinduced Electron Transfer Dynamics from Cu^{I}-Diimine Complexes to TiO_2 Nanoparticles

L. X. Chen[1,3], J. Huang[1], M. W. Mara[1,3], A. Coskun[2], N. M. Dimitrijvic[2], O. Kokhan[1], A. B. Stickrath[1], R. Ruppert[5], J. F. Stoddart[3], J.-P. Sauvage[4]

[1]Chemical Sciences and Engineering and [2]Center for Nanoscale Materials
Argonne National Laboratory, Argonne IL 60439

[3]Department of Chemistry, Northwestern University, Evanston IL 60208

[4]Institut de Science et d'Ingénierie Supramoléculaires and [5]Institut de Chimie,
Université de Strasbourg, 67000 Strasbourg (France)

Photoinduced electron transfer (ET) from transition metal complexes into semiconductor nanoparticles (NPs) has been studied extensively on account of their relevance to photocatalysis, and dye-sensitized solar cells (DSSCs). The high cost and low abundance of the most commonly used ruthenium dye inhibit applications of current DSSCs on a large scale. Therefore, equivalent or better dye sensitizers of the first-row metal complexes, such as Cu(I) diimine complexes have long been sought. The MLCT states of Cu(I) diimine complexes undergo the Jahn-Teller distortion, have solvent-dependent lifetimes, and structure-dependent intersystem crossing (ISC). While the excited state structural dynamics of several Cu(I) complexes alone have been studied, our study here intend to establish the dynamics and efficiency of interfacial electron injection from Cu^{I} complexes into TiO_2 NPs in DSSC mimics (Fig. 1). The electron transfer (ET) and charge recombination (CR) dynamics of a DSSC mimic, $[Cu^{I}(dppS)_2]^{+}$ (dppS=2,9-diphenyl-1,10-phenanthroline disulfonic acid disodium salt)–TiO_2 nanoparticle (NP) hybrid have been investigated by combining optical transient absorption (TA), electron paramagnetic resonance (EPR), and X-ray transient absorption (XTA) spectroscopies. We observed an efficient ultrafast ET (τ = 0.4 ps) from the singlet ^{1}MLCT state of $[Cu^{I}(dppS)_2]^{+}$ to TiO_2 NPs and a slow CR (τ ~ 2.5μs) dynamics in $[Cu^{I}(dppS)_2]^{+}/TiO_2$. XTA studies revealed a flattened pseudo-tetrahedral geometry in $[Cu^{I}(dppS)_2]^{+}$, which weakened the spin-orbit coupling and resulted in a relatively slow intersystem crossing rate of $(13.7\ ps)^{-1}$. Consequently, it becomes achievable to have the fast electron injection from the singlet MLCT state of $[Cu^{I}(dppS)_2]^{+}$ to TiO_2 NPs. These results demonstrate structural control of the excited state properties in designing efficient, stable and abundant light-harvesting materials.

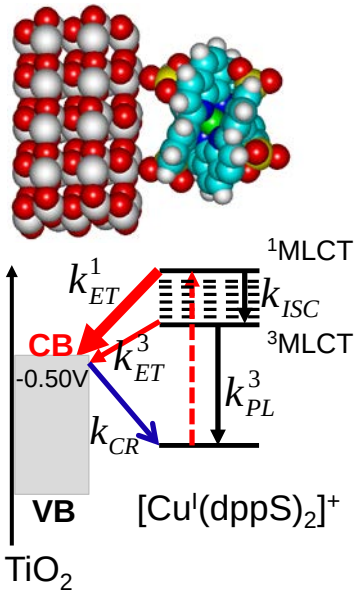

Figure 1. The molecular structure of $[Cu^{I}(dppS)_2]^{+}$ and the diagram of electron injection and recombination model in $[Cu^{I}(dppS)_2]^{+}/TiO_2$ hybrid.

The Crystalline Nanocluster Ti-O Phase as a Fully Structurally Defined Model for Charge Injection in Photovoltaic Cells

Philip Coppens and Jason B. Benedict
Department of Chemistry
University at Buffalo, State University of New York,
Buffalo, New York 14260-3000

Homodisperse polyoxotitanate clusters both with and without attached chromophores can be synthesized and crystallized to allow precise determination of the atomic structure by X-ray diffraction methods. We have synthesized new clusters, including non-functionalized Ti34, previously only available functionalized with dimethylaminobenzoic acid, two different Ti28 clusters, one of which incorporating an Na atom (Fig. 1), the second with a stoichiometry different from Ti28 that was previously synthesized, and Ti29 also with a Na atom. The Na is incorporated with typical six-coordinate binding to oxygen atoms, similar to its binding in 18-membered crown ethers as demonstrated for Ti28 in Fig. 1b. A survey of the structures of 13 functionalized carboxylate and acetylacetonate linked clusters with 17 or more Ti atoms shows the binding to be limited to the chelate-bidentate and the bridging modes (Fig. 2), contrary to the observation of 5 different binding modes in smaller clusters. Chromophores with acetylacetonate anchor groups synthesized so far exclusively bind in the chelate-bidentate mode, whereas carboxylic acid terminated substituents more frequently are observed to have the bridging mode, with the exception of dimethylaminobenzoate and dimethylaminocinnamate in which a strong electron donating substituent is present. The organic dye coumarin 343 is a chelating linker but does not bind completely through its carboxylic group as common for other acids. Instead it binds to the titanium atom through one oxygen of the acid group and the adjacent carbonyl of the ester group. Theoretical calculations for isonicotinic acid (INA) and nitrophenylacetylacetonate (NPA) functionalized Ti17 clusters confirm the experimentally observed binding modes to correspond to a lower energy than the alternative modes. However, they do not predict the observed difference between the cinnamic acid (CA) and dimethylaminocinnamic acid (DMACA) binding to Ti17, which are bridging and chelate respectively. Although kinetic effects may play a role, we have never observed more than one binding mode to occur for a single chromophore/cluster combination. Density of state (DOS) of functionalized clusters with the sensitizers linked in both the chelating and the bridging modes will be presented.

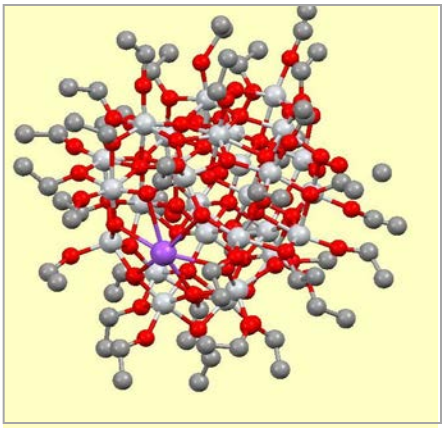

Fig. 1a. (above) Molecular structure of $Ti_{28}Na$ showing the Na atom coordinated by six oxygen atoms. Purple: Na, silver: Ti; red: O, blue: N, grey: C. Fig. 1b (below). Coordination of Na. 5-coordinate Ti pink.

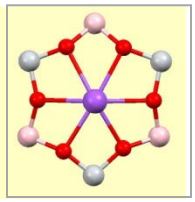

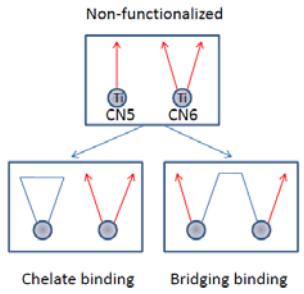

Fig. 2. Schematic representation of the functionalization reaction. Red arrows represent the alkoxide ligands, blue lines the attached chromophores.

Exploration of Thermodynamic Properties in New Singlet Fission Molecular Systems for Controlling Photochemical Transformations

Niels Damrauer, Paul Vallett, Jamie Snyder, Carsten Habenicht, Ryan Michael, Tarek Sammakia
Department of Chemistry and Biochemistry
University of Colorado at Boulder
Boulder CO 80309

Previous efforts in our laboratory (*PRL* **105**, 257403 (2010)) have identified shaped laser fields that are optimal for manipulating singlet fission (SF) yields in polycrystalline tetracene thin films. These studies have pointed towards the importance of low-frequency intermolecular (inter-monomer) motions affecting the interaction of π-systems as a way of modulating SF rate constants. These observations motivated the design of bi-chromophoric bis-tetracene molecules where inter-chromophore coupling can be controlled. The new molecules are inspired by synthetic/photophysical work in Paddon-Row's group (*JACS* **1993**, *115*, 4345-4349) where bis-naphthalene systems exhibited Davydov splitting of electronic absorption (a hallmark of interchromophore coupling) that could be systematically controlled by the alkyl spacer size.

The primary subject matter of our poster is the three dimeric SF molecular platforms shown in Fig. 1. We will describe progress and pitfalls in their synthesis. We will then go on to describe and will present extensive computational explorations of thermodynamic properties in $\mathbf{A_{tet}}$ – $\mathbf{C_{tet}}$ with respect to SF. We focus on both gas-phase and solvated dimers and characterize Davydov splitting using time-dependent DFT with and without analytical gradients. It will be shown that in each of these dimeric systems, and in all of the environments explored, SF is enthalpically favored. It will also be shown that the size of the alkyl spacer and the bridging geometry allows for tuning of electronic coupling and that the principal quantum number of states in the singlet manifold has a very significant influence on the degree of electronic coupling.

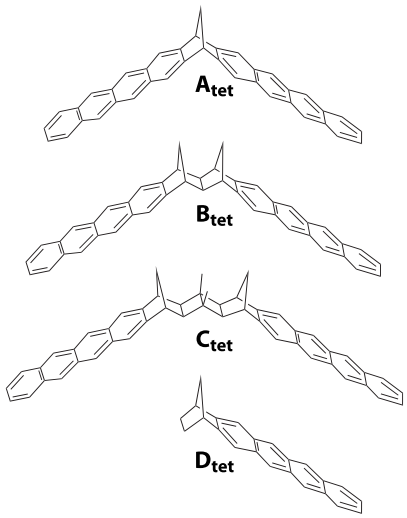

Fig. 1. Systems designed for the systematic study of interchromophore coupling on singlet fission.

This poster will also describe our efforts to control morphology in thin films of tetracene grown via vacuum deposition. These efforts are important for at least two reasons. First, there is currently a lack of consensus in the community about the time-scale and temperature-dependence of SF dynamics in thin-film tetracene. We aim to better understand how dynamics are impacted by film morphology especially the density of crystallite grain size. Second, our working interpretation of our previous laser-pulse-shaping control results suggests the involvement of an excited-state relaxation channel that competes directly with SF. We would like to understand whether grain size and film morphology/quality affects controllability, thereby pointing towards the source of the competing dynamics.

Synthesis, Characterization, and Redox Properties of Cobalt Complexes with a Perfluorinated Ligand for Water Oxidation Catalysis

Laleh Tahsini[1], Arnold L. Rheingold[2] and Linda H. Doerrer[1]
[1]Department of Chemistry
Boston University, Boston MA 02215
[2]Department of Chemistry and Biochemistry
University of California San Diego, La Jolla CA 92093-0358

Current global energy needs resulting from increased human population pressure mandate major scientific efforts toward developing sustainable, low-cost, and environmentally sound energy resources. The catalytic separation of water into its elements using solar energy followed by their recombination provides a way to recover the photochemical energy stored in O-H chemical bond. Heterogeneous water oxidation catalysts (WOC) can efficiently oxidize water[1] but are intractable to many analytical techniques. In contrast, homogenous catalysts can bring molecular-level clarity to our understanding of the water oxidation reaction.

The susceptibility of C-H bonds to strong oxidants used in water oxidation lead us to use highly fluorinated ligands with stronger C-F bonds in this study. The fluorinated alkoxide complexes of a bidentate ligand are soluble in water, and display some promise toward the ultimate goal. . We report herein the synthesis and characterization of mononuclear cobalt(II) complexes, $(NR_4)_2[Co(ddfp)_2]$ [H_2ddfp = perfluoropinacol and R = **1a**,methyl, **1b** *tert*-butyl] as moderately air-stable compounds in contrast to the previously reported[2] K^+ analogues. Their solvent-dependent redox behavior will be discussed, including C-C bond cleavage of the pinacolate ligand and formation of a tetrahedral cobalt(II) complex, $(NR_4)_2[Co(Hhfpd)_4]$ [hfpd = hexafluoropropanediolate and R = methyl **2a**, *tert*-butyl **2b**]. The five-coordinate Co center in $[Co(OH_2)_6][Co(ddfp)_2(OH_2)]$, **3**, suggests that a mononuclear, not dinuclear, step for O-O bond formation will obtain if water oxidation is achieved. This aquo complex is more stable to O_2 than related four-coordinate species.

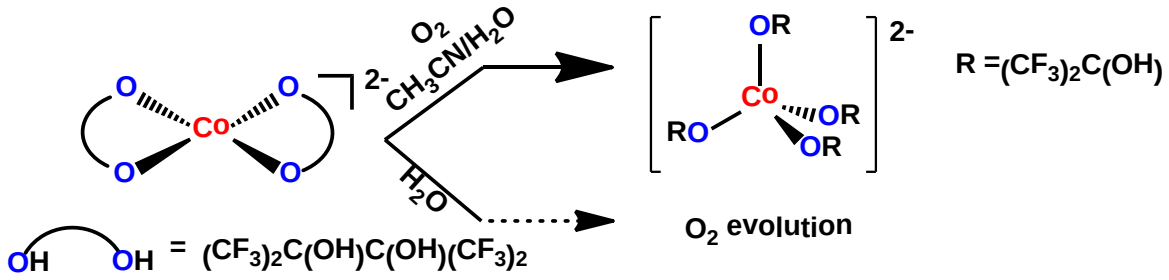

[1] (a) Kudo, A.; Miseki, Y. *Chem. Soc. Rev.* **2009**, *38*,253-278. (b) Youngblood, W. J.; Lee, S.-H. A.; Maeda, K.; Mallouk, T. E. *Acc. Chem. Res.* **2009**, *42*, 1966-1973.

[2] Cantalupo, S. A.; Fiedler, S. R.; Shores, M. P.; Rheingold, A. L., Doerrer, L. H. *Angew. Chem. Int. Ed.* **2011**, *50*, 1-7.

Photo-Induced Charge Separation in a Cu(I) Bis-Phenanthroline Based Systems: Chromophore-Acceptor Diads and DSSC Dyes

Megan Lazorski, Lance Ashbrook and C. Michael Elliott
Department of Chemistry, Colorado State University
Fort Collins CO 80523

Bisphenanthrolinecopper(I) complexes have long been recognized to have similar photophysical properties to $Ru(II)L_3$ but with some notable differences: (1) ligand lability in the ground state, (2) changes in coordination geometry upon photoexcitation and oxidation and (3) different redox potentials (relative to $Ru(II)L_3^{2+}$) in the ground and excited states. These differences present challenges when designing molecular photoinduced charge separation systems. However, with the proper positioning of the electron transfer donor (D) and acceptor (A), molecular D-C-A triad systems based on bisphenanthrolinecopper(I) chromophores undergo photoinduced multi-step charge-separated state (CSS) formation with high quantum efficiency. Moreover, the spin chemistries for the Cu(I) and Ru(II) systems are qualitatively similar, as reflected in magnetic field studies of the CSS recombination to the ground state.

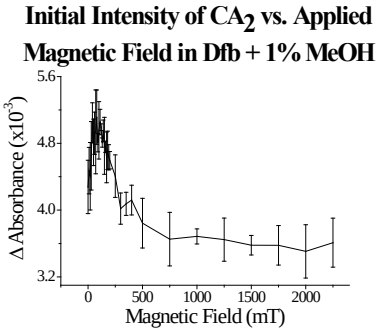

In contrast to analogous Ru(II) based systems, Cu(I) C-A diads also form a relatively long-lived charge-transfer (CT) state in polar solvents (i.e., 40 ns) in which the Cu is oxidized to Cu(II) and one of the viologen acceptors is reduced (a similar observation was made earlier for related $Cu(I)\text{-}MV^{2+}$ diads by Meyer et. al). However, the magnetic field dependence of the recombination kinetics of the C-A diad is dramatically different from the D-C-A triad. For the diad, the CT state lifetime is unaffected by the field but the CT formation quantum efficiency (Φ_{CT}) is field dependent. An increase of ca. 18% in initial intensity occurs between ca. 0 and 100 mT followed by a monotonic decrease at higher applied fields reaching a plateau of about 80% of the initial intensity at about 750 mT. While we have not yet quantitatively modeled the spin chemistry, we speculate that the quantum efficiency for oxidative quenching of the CuL_2^{+*} is large (approaching 1) irrespective of the spin-state of the Cu MLCT; however, only the ^{3}MLCT component of the population results in CT that is long enough lived to be observed on the time scale of our experimental setup. The applied field either changes the equilibrium distribution of the $^{3/1}$MLCT or changes the rate of intersystem crossing.

The efficiency with which the C-A and D-C-A undergo oxidative quenching prompted us to consider related Cu(I) chromophores as dyes in DSSCs. Constable et al. reported that bis(6,6'-dimethyl bipyridine)Cu(I) complexes functioned as reasonable sensitizers in DSSCs; however, the inherent instability in I^- led to degradation. With $Co^{2+/3+}$ based mediators, stability is not an issue. Given several recent examples where incorporating a secondary donor into the dye, resulted in dramatic increases in cell efficiency thus we have embarked on studies with this C-D copper dye.

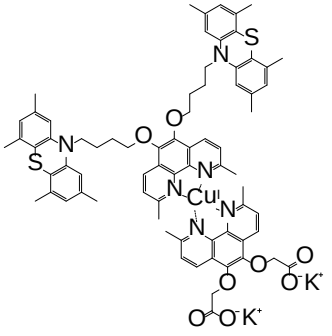

Quantum Dynamics in Light Harvesting

Graham R. Fleming
Physical Biosciences Division
Lawrence Berkeley National Laboratory
Berkeley CA 94720

The technique of two-dimensional Fourier transform electronic spectroscopy has enabled much progress in the understanding of the dynamical structure of energy flow in photosynthetic light harvesting. Using a coherence-specific polarization sequence, we measured the decay of total coherence in light harvesting complex II (LHCII) of plants. The decay consists of a fast component (47 fs) and a much slower component (800 fs). In parallel theoretical work, we show that the fast component arises from superpositions of uncoupled levels while the longer-lived decay results from electronically mixed superpositions. The mixing leads to a correlation in the fluctuation of the levels which effectively decreases the amplitude of the fluctuations felt on the coupled sites. This picture of why coherence is long-lived in light harvesting complexes complements the adiabatic picture we presented earlier

A second extension of 2D spectroscopy is to use 2-color 2D spectroscopy to study interactions between pigments such as carotenoids and chlorophylls that are widely separated in energy. We recorded 2-color 2D spectra on bacterial reaction centers (RCs) where we excited the carotenoid (Car) S_2 band and probe the accessory bacteriochlorophyll Q_y band. We found two parallel pathways from Car S_2 to Q_y of BChl, one via Q_x and the other via the Car S_1 state. Combining 1-color 2D experiments with the 2-color version, we conclude that the S_1 pathway dominates with a 4:1 ratio. Figure 1 shows 1- and 2-color spectra demonstrating the energy transfer.

We also applied 2D spectroscopy to the B- band of the bacterial RC. We found clear resolution of the B_A and B_B bands and resolved energy transfer between B_B and B_A in < 100 fs. This was confirmed by a polarization study comprising all parallel and cross-peak specific polarization sequences which show a clear difference between the diagonal peak and the cross peak and clearly shows that energy transfer between the two states occurs from 70 fs. This is a very surprising result and presumably, given the separation of the two accessory BChl, must involve transfer through P, the special pair.

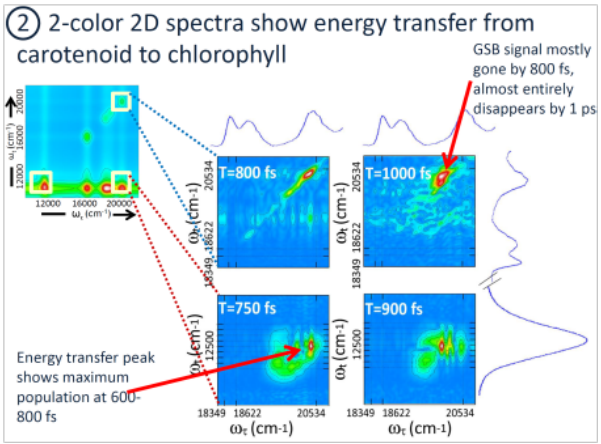

In a major review in Annual Review of Condensed Matter Physics, we explored the connection between entanglement – "spooky action at a distance" – and delocalized excitons. Using the simplest entanglement measure, concurrence, we showed that the two concepts represent different views of the same phenomenon and it is not possible to assign a functional role of one vs the other. Having said this, we also showed that the use of entanglement measures can provide more detailed information on quantum delocalized states than can traditional methods such as the inverse participation ratio.

Perturbation of the Electron Transport Mechanism in TiO_2 Films by Proton Intercalation

Adam F. Halverson, Kai Zhu, Peter T. Erslev, Jin Young Kim,
Nathan R. Neale and Arthur J. Frank

Chemical and Materials Science Center
National Renewable Energy Laboratory
Golden CO 80401

This study addresses a long-standing controversy about the transport mechanism in nanoporous TiO_2 films that are commonly used in dye-sensitized solar cells and related photosystems. Most researchers believed that the slow electron transport in TiO_2 films is due to electrons undergoing multiple trapping in exponential conduction band tail trap (CBT) states. A key prediction of this model is that the activation energy (E_a) of the electron diffusion coefficient should scale with the position of the quasi-Fermi level or, equivalently, scale with the photoelectron density (n). However, many reported studies have failed to validate this model. Using temperature-dependent time-of-flight and random walk simulations, we found that proton intercalation from water/moisture in an organic liquid electrolyte is the cause of the discrepancies between observation and prediction.

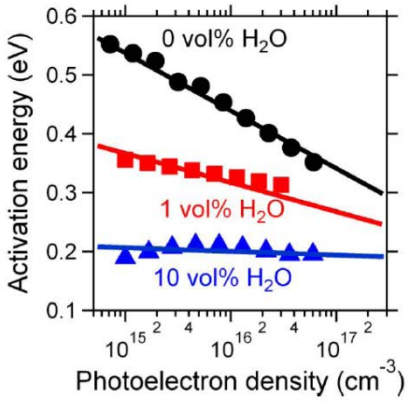

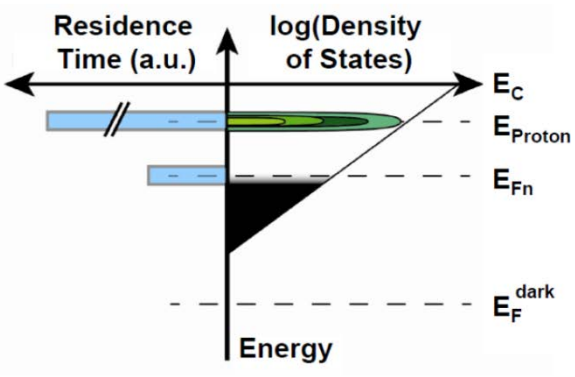

These measurements revealed that increasing the water content in the electrolyte leads to increased proton intercalation into the TiO_2 films, slower transport, and dramatic changes in the dependence of E_a on n in the films. Random-walk simulations based on a microscopic model incorporating exponential CBT trap states combined with a proton-induced shallow trap level with a long electron residence time accounted for the observed effects of proton intercalation on E_a. The mechanistic insight gained from this study on the effect of water/moisture on the transport properties of nanostructured metal oxides should find important usage in controlling the electronic properties of oxide-based electrodes for sensitized solar energy conversion and related processes.

Electronic Structure Calculations of Nanomaterials: Theory and Applications

Tom Hughes, Jing Zhang, Louis Brus, Mike Steigerwald and Richard A. Friesner
Department of Chemistry
Columbia University
New York NY 10027

We have continued to develop our approach to improving the accuracy of DFT calculations, with a particular focus on transition metals. Results demonstrating large improvements in the calculation of spin splittings, redox potentials, and metal-ligand bond energies, will be presented. We have also incorporated dispersion interactions into our model. These results, combined with prior work, will soon enable us to assemble a complete, automated model for carrying out corrected DFT calculations, with near-chemical accuracy for organic systems, and somewhat larger errors for transition metal containing systems (but vastly improved as compared to standard DFT methods, including the most recent currently available functionals).

We have pursued two principal applications over the past several years. The first is modeling of ruthenium based catalysts for water splitting developed by Meyer and coworkers, on which we have reported previously. The second application we have pursued is modeling of TiO_2 nanostructures in an effort to understand the functioning of the Gratzel cell. We have built large models of TiO_2 nanoparticles passivated by water-derived ligands (OH, H_2O, etc.) and investigated the electronic structures of these models. We have also studied what happens when a Li atom or Li+ cation is introduced at various locations into the model. There are various proposals as to how electrons become trapped in the nanoparticle and how transport of these trapped electrons occurs. One important possibility is that the electrons are stabilized by cations (Li+ or H+, e.g.) and that the diffusion of the electrons is really a coupled electron-proton motion in the nanoparticle lattice, referred to in the literature as ambipolar diffusion.

We have initially benchmarked our cluster model by computing a number of important quantities that can be compared with experiment, such as the open circuit voltage and conduction band shifts due to Li^+ cations. Agreement with experiment for a significant number of such key quantities is demonstrated, to within ~0.1eV. Correction terms for the Ti redox potentials, obtained from our previous studies of redox potentials in transition metal complexes, are essential in achieving this agreement. We have then constructed models for electron trapping states in which a Ti^{4+} ion near the surface of the particle is reduced by an electron, and then stabilized by a Li^+ cation. We calculate barrier heights for coupled migration of the electron and cation to a neighboring site and these agree well with data extracted from experimental electron diffusion kinetics. These results support the ambipolar diffusion model and provide a proposed microscopic picture of an electron trapping state in the Gratzel cell.

Finally, we have substantially improved the parallel performance of Jaguar for this problem and are now getting good speedups on as many as 64 processors. This acceleration of time to solution has been essential in treating large (~350 atom) clusters.

Model Dyes for Study of Molecule/Metal Oxide Interfaces and Electron Transfer Processes

Elena Galoppini,[1] Andrew Kopecky,[1] Keyur Chitre,[1] Gerald J. Meyer,[2]
Patrik Johansson,[2] Robert A. Bartynski,[3] Sylvie Rangan[3]

[1]Department of Chemistry, Rutgers University, Newark NJ
[2]Department of Chemistry, Johns Hopkins University, Baltimore MD
[3]Department of Physics and Astronomy, Rutgers University, New Brunswick NJ

The scope of this research is to design and synthesize model dyes to control the molecule/semiconductor contact (binding, orientation, aggregation, distance) and to study how such parameters influence binding and interfacial charge transfer processes. The poster will describe our progress in two areas of research.

1. Electron Transfer Studies of N3-type Dyes (*Galoppini, Meyer*)**.** The photophysical properties of three rigid-rod N3-type Ru(II) complexes of increasing length (D0, D1 and D2) were characterized by spectroscopic and electrochemical methods in solution and on nanocrystalline TiO_2 or ZrO_2 thin films. Vibrational relaxation to the luminescent excited state occurred on a picosecond time scale with rate constants that decreased with the number of phenylenethynylene spacer units in fluid solution. The bridge length dependence for excited state injection and for charge recombination were both consistent with the attenuation factor of $\beta = 0.27 \pm 0.05$, despite the fact that the injection reaction occurred on a 10^6 faster time scale than recombination. Charge recombination took place on two different time scales attributed to electron tunneling, diffusion of the TiO_2 electrons and interfacial electron transfer. In addition, there is also evidence that suggest that the so called *Stark effect* also affects charge recombination. This is evident by the earlier onset of charge recombination of D0 versus D1 and D2, as the Fermi-level of the TiO_2 is raised.

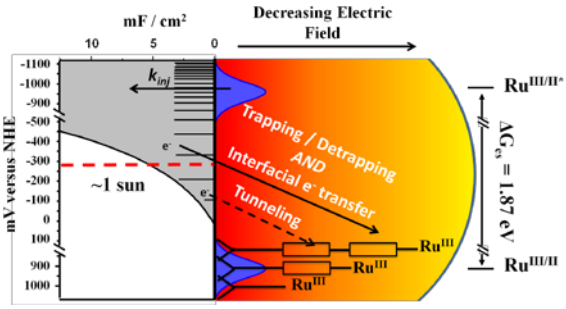

2. Click Synthesis and Study of Homoleptic Star Ru(II) Complexes (*Galoppini, Bartynski, Meyer; with P. Persson*)**.** One strategy to provide enhanced interfacial control is to develop new molecular sensitizers and tailor-made anchor units capable of providing enhanced control of the surface binding and interfacial electronic properties. The development of nano-sized homoleptic complexes of Ruthenium ("star" complexes), aim at shielding the metal center from the heterogeneity of the semiconductor surface, resulting in reduced aggregation and degradation and unprecedented control over the charge transfer processes (slower recombination). Homoleptic ($[Ru(L)_3]^{2+}$) and heteroleptic ($Ru(NCS)_2(bpy)(L)$) complexes carrying rigid anchor-cum-spacer ligands (L), comprised of ethynylene-phenylene spacer groups and a designated anchor group, have been synthesized by click chemistry and studied computationally and experimentally in solution and on metal oxide surfaces. The poster will describe new synthetic approaches, solution properties, first principles DFT and TD-DFT calculations, injection and recombination data, and STM studies.

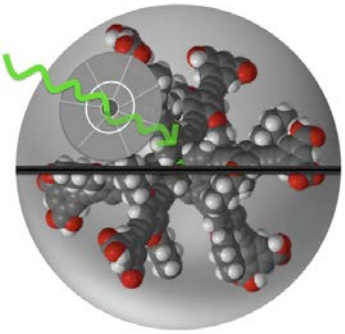

Exciton Quenching by Free Charge Carriers and Other Tales of Intrigue in Organic Semiconductors

Brian A. Gregg, Ziqi Liang and Russell A. Cormier
Chemical and Materials Science Center
National Renewable Energy Laboratory
Golden, Colorado 80401

Normally, the first property measured in any new *inorganic* semiconductor is its doping density. But this has apparently never been measured in an organic semiconductor. We introduce compensation experiments as a means of measuring the doping density and doping-induced exciton quenching in organic semiconductors. By adding increasing quantities of a compensating n-type dopant (cobaltocene) until a sharp minimum in conductivity is observed, we determine the (uncompensated) p-type doping density of poly(3-hexylthiophene), P3HT: p_{unc} = 1.2 x 10^{18} cm^{-3}. There are thus ~24 times more bound holes than free holes (polarons), p_f = 5 x 10^{16} cm^{-3}. Beyond the compensation point, the semiconductor is doped n-type. Concurrent photoluminescence intensity measurements reveal an almost perfect mirror symmetry to the conductivity, showing a sharp maximum coincident with the minimum in conductivity. This suggests that excitons are quenched almost exclusively by free charge carriers, not bound charges. The photoluminescence lifetime at the compensation point is nearly 1 ns, more than double its uncompensated value and apparently the longest lifetime yet observed in solid P3HT. The decay is close to single exponential, showing almost quencher-free behavior at this point despite the the fact that there is ~0.03 mol% $CoCp_2^+$ in the film along with various compensated defects and the usual structural disorder.

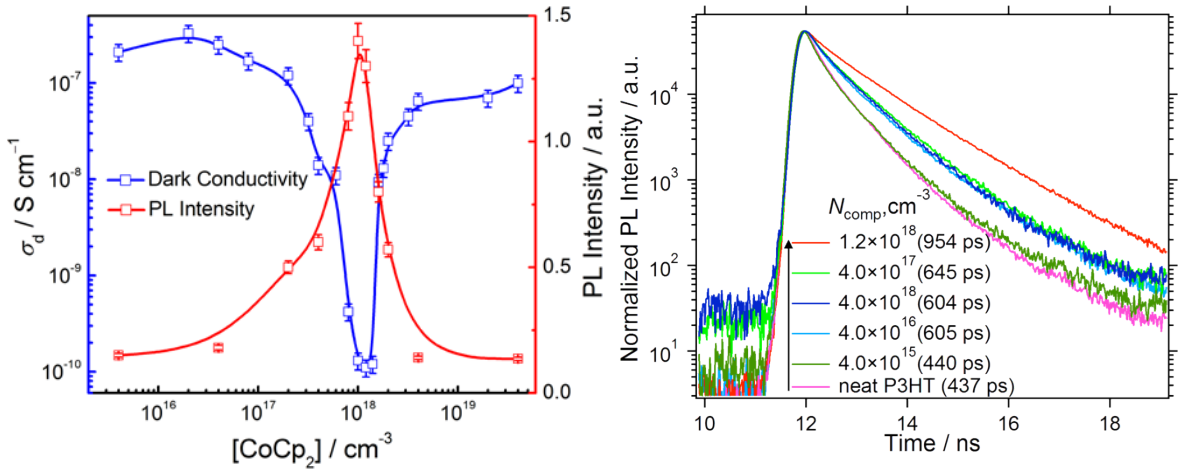

Figure Left. The low-field dark conductivity of P3HT films (left axis) *vs* the concentration of cobaltocene added to the film. The corresponding change in photoluminescence intensity is also shown (right axis). The compensation point occurs at [$CoCp_2$] = 1.2 x 10^{18} cm^{-3} = p_{unc}.
Right. Photoluminescence decays of neat and cobaltocene-compensated P3HT films. The average lifetime is in parentheses. Note that the 4 x 10^{18} cm^{-3} sample is past the compensation point.

Kinetic and Mechanistic Investigations of CO_2 Reduction Catalysts Following One-Electron Reduction

David C. Grills and Etsuko Fujita
Chemistry Department, Brookhaven National Laboratory
Upton NY 11973-5000

The catalytic reduction of CO_2 to useful products (e.g. CO, HCO_2^-, etc.) using transition metal complexes as catalysts, has been the subject of intense investigation for many years. A variety of different catalysts have been employed, including Co and Ni tetraaza-macrocycles, Fe and Co metalloporphyrins, and Re and Ru-based complexes with α-diimine ligands. In all photochemical cases, initiation of the catalytic cycle involves photoexcitation of the catalyst or an added photosensitizer, followed by one-electron reduction of the catalyst to form the one-electron reduced species (OER). The subsequent mechanism for the formation of the two-electron reduction product (i.e. CO or HCO_2^-) depends on the catalyst. For example, the OER of a Co macrocycle will bind CO_2 and transfer two electrons to the bound CO_2 molecule.[1] For Re-based catalysts, it is believed that two OERs combine to form a CO_2-bridged dimer, in which each OER transfers one electron to the CO_2 molecule.[2] However, depending on the reaction conditions (e.g. $[H^+]$, etc.), other pathways may exist that involve different intermediates, e.g. M-COOH species.

Pulse radiolysis, which involves the ionization of solvent molecules by a short pulse of high-energy electrons, is a powerful method for generating the one-electron reduced form of a solute. However, transient detection methods have mainly been limited to the UV-VIS-NIR regions, thus providing little structural information. We have recently developed unique nanosecond time-resolved infrared (ns-TRIR) detection capabilities for pulse radiolysis,[3] which has opened up the possibility of detailed kinetic and mechanistic investigations of the OERs of photochemical CO_2 reduction catalysts by monitoring specific molecular vibrations, such as ν(CO) of metal-bound CO_2 and/or CO spectator ligands, and ν(CN) of macrocyclic ligands. We will highlight our recent efforts in this area, investigating the one-electron reduction of catalysts such as $[Re(bpy)(CO)_3(CH_3CN)]^+$, $[Ru(bpy)_2(CO)(H)]^+$ and $Co^{II}L^{2+}$ in CH_3CN, in the absence and presence of CO_2. The goal is to identify reduced intermediates and monitor their reactivity in order to develop an improved mechanistic understanding of photochemical CO_2 reduction with these and related catalysts.

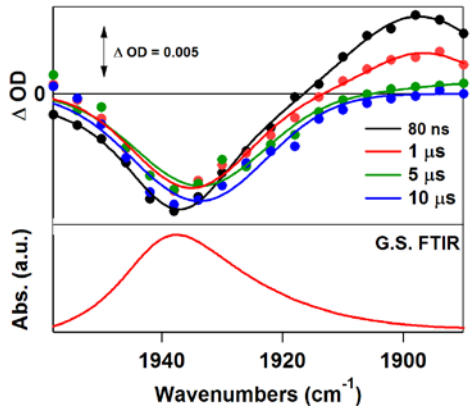

TRIR spectra of $[Ru(bpy)_2(CO)H]^+$ in CH_3CN following pulse radiolysis under Argon.

L =

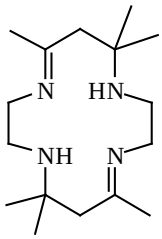

1. Schneider, J; Jia, H; Muckerman, J. T.; Fujita, E. *Chem. Soc. Rev*. **2012**, *41*, 2036-2051.
2. Agarwal, J.; Fujita, E.; Schaefer, H. F. III; Muckerman, J. T. *J. Am. Chem. Soc.* **2012**, *134*, 5180-5186.
3. Grills, D.C.; Cook, A.R.; Fujita, E.; George, M.W.; Preses, J.M.; Wishart, J.F. *Appl. Spectrosc.* **2010**, *64*, 563-570.

Porphyrin Polymers for Solar Energy Harvesting

Paul A. Liddell, Gerdenis Kodis, Michael Kenney, Robert A. Schmitz, Bradley J. Brennan, Devens Gust, Thomas A. Moore, Ana L. Moore

Department of Chemistry and Biochemistry
Arizona State University
Tempe AZ 85287

We have previously reported the preparation of porphyrin and porphyrin-fullerene dyad conducting polymers via electropolymerization on electrodes.[1,2] Studies of the properties of these films were stymied by the insolubility of the films, which could not be removed from the electrodes. We now report the synthesis and spectroscopic investigation of soluble conducting porphyrin polymer **1**. The polymer is made by palladium-catalyzed chemical polymerization of monomer **2** in solution. The multiple hexyl chains on each porphyrin render the polymer soluble in organic solvents. Absorption spectra in 2-methyltetrahydrofuran show that whereas model monomer **3** has a normal porphyrin absorption spectrum with a sharp Soret band at 414 nm and longest-wavelength Q-band at 641 nm, model compound **4**, which features the *meso*-amino group, has a very broad Soret band at 421 nm and broad Q-band absorption that extends out to about 720 nm. The polymeric material has a spectrum similar to that of **4**, but with more broadening. Thus, absorption throughout the visible is excellent. Emission from the polymer features a broad band whose wavelength maximum is strongly solvent dependent, indicating significant charge separation in the excited state to form an intramolecular charge transfer (ICT) state. Time resolved emission studies show local excited state(s) (LE) that relax to the ICT state on a time scale of tens to hundreds of ps. The ICT state itself has a lifetime of about 7 ns in nonpolar solvents and ~5.4 ns in polar solvents. The lifetime decreases slightly with increasing chain length.

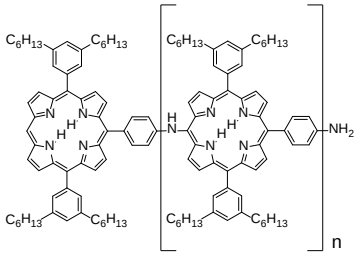

1

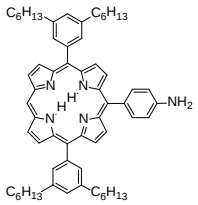

2

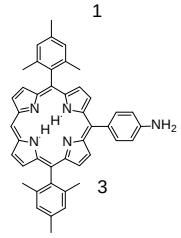

3

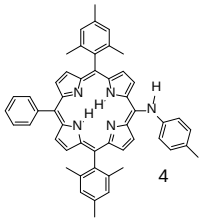

4

Fluorescence anisotropy measurements were carried out in 2-methyltetrahydrofuran on samples of **1** with $n = 3$, and a time constant for excitation transfer between porphyrins of 200 ps was determined. Thermodynamic calculations are consistent with rapid equilibration between the ICT state and an LE state, with excitation transfer occurring from the LE state.

Experiments are in progress to determine the electrochemical properties of the polymer, including the charge mobility in cast polymer films. These will help determine the applicability of such polymers to solar energy conversion systems.

(1) Liddell, P. A.; Gervaldo, M.; Bridgewater, J. W.; Keirstead, A. E.; Lin, S.; Moore, T. A.; Moore, A. L.; Gust, D. *Chem. Mater.* **2008,** *20*, 135-142.
(2) Gervaldo, M.; Liddell, P. A.; Kodis, G.; Brennan, B. J.; Johnson, C. R.; Bridgewater, J. W.; Moore, A. L.; Moore, T. A.; Gust, D. *Photochem. Photobiol. Sci.* **2010,** *9*, 890-900.

Temperature-Dependent Spectroelectrochemical Measurements of Conduction Band Energies

Jesse W. Ondersma and Thomas W. Hamann
Department of Chemistry
Michigan State University
East Lansing MI 48823

The photoanode material plays a critical role in the charge injection and recombination reactions in dye-sensitized solar cells. The conduction band edge, $\mathbf{E}_{cb,}$ is arguably the most important physical property of the photoanode that determines the injection efficiency and electron lifetime (i.e. recombination). In this work we employed temperature-dependent spectroelectrochemical measurements to determine $\mathbf{E}_{cb}$ and the absorptivity, α, of conduction band electrons for mesoporous TiO_2 films. These measurements consist of monitoring the absorption of near-infrared wavelengths by thin film semiconducting electrodes while varying both bias potential and temperature. Additionally, the absorbance measurements presented were performed under steady state conditions which overcomes errors associated with a potential scan rate dependence. Initial results on extending these measurements to other metal oxide materials will also be presented. Our overall objective is to make a controlled systematic investigation of the relationship of material property (e.g. $\mathbf{E}_{cb}$) to the relevant processes in dye-sensitized solar cells.

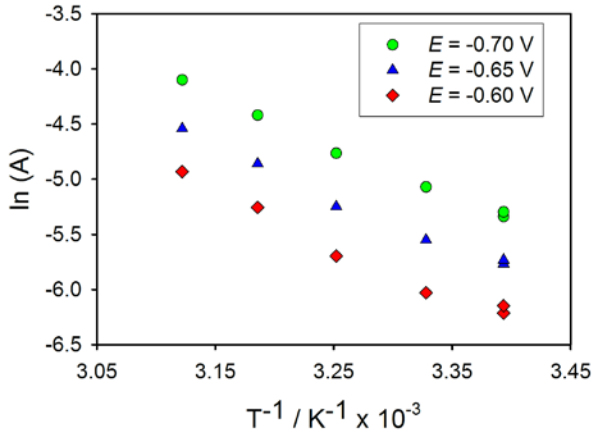

Femtosecond Transient Absorption Imaging of Carrier Dynamics in Single Nanostructures

Bo Gao,[1] Hongyan Shi,[1] Gregory V. Hartland,[2] Huili Xing[3] and Libai Huang[1]
[1]Notre Dame Radiation Laboratory, [2]Department of Chemistry and Biochemistry,
[3]Department of Electrical Engineering, University of Notre Dame, Notre Dame IN 46556-5670

We have demonstrated transient absorption microscopy (TAM) as a novel tool to image carrier and phonon dynamics in single nanostructures with simultaneously high spatial (~ 200 nm) and temporal resolution (~ 200 fs). Until now, the majority of dynamical measurements on single nanostructures are based on photoluminescence (PL). Transient absorption imaging approach offers two key advantages over PL based methods: 1) A time resolution of ~ 200 fs. This fast time resolution is important because many critical events such as electron-phonon coupling occur on such sub-picosecond time scales. 2) The measured signal is based on absorption, which means we can also study samples with low or even zero fluorescence quantum yield.

Here we present two examples of such transient absorption microscopic studies. Femtosecond transient absorption microscopy was employed to study the excited-state dynamics of *individual* semiconducting single wall carbon nanotubes (SWNTs). This unique experimental approach removes sample heterogeneity in ultrafast measurements of these complex materials. Transient absorption spectra of the individual SWNTs were obtained by recording transient absorption images at different probe wavelengths. These measurements provide new information about the origin of the photoinduced absorption features of SWNTs. Transient absorption dynamics traces were also collected for individual SWNTs. The dynamics show a fast ~ 1 ps decay for all the semiconducting nanotubes studied. We attributed this fast relaxation to coupling between the excitons created by the pump laser pulse and the substrate.

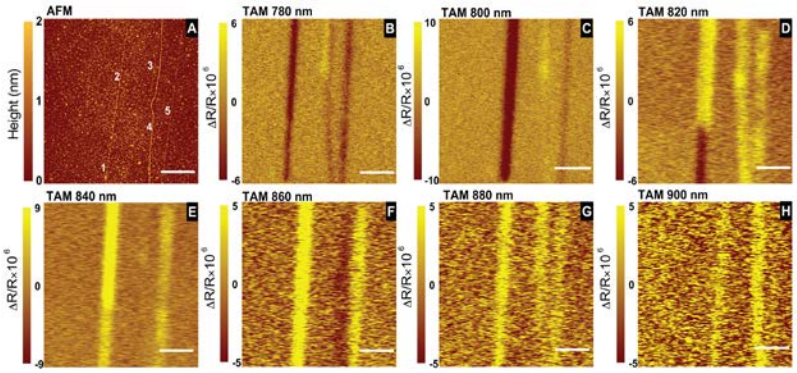

Figure 1. (A) Tapping mode AFM height image of the SWNT-1, -2, -3, -4 and -5. (B) to (H) TAM images with pump/probe wavelength of 390/780 nm, 400/800 nm, 410/820 nm, 420/840 nm, 430/860 nm, 440/880 nm and 450/900 nm respectively. All TAM images were collected at a pump-probe delay of 0 ps. Scale bars are 2 μm in all images.

Recent success in fabricating graphene has inspired researchers to search for semiconducting analogues of graphene in hopes to retain 2D crystallinity while providing a bandgap. In particular, monolayer MoS_2 has recently emerged as a promising candidate. The second study we present here is the investigation of exciton dynamics in atomically thin and semiconducting MoS_2 crystals. By controlling the dielectric environment around monolayers of MoS_2 crystals, our measurements provide a comprehensive understanding on intrinsic exciton dynamics, quantum confinement effect, exciton-phonon coupling, as well as on how the dielectric environment alters optical properties and energy relaxation processes in these novel 2D crystals.

New Redox Shuttles for Dye-Sensitized Solar Cells

Joseph T. Hupp
Department of Chemistry
Northwestern University
Evanston IL 60208

The single greatest point of loss in champion and near-champion cells is associated with the large driving force required for dye regeneration by the redox shuttle after electron injection. For cells based on iodide/tri-iodide shuttles, the energy required is typically 500 to 600 mV; if less driving force is employed, back electron transfer from the photo-electrode to the attached dye becomes significant and photocurrents suffer. We have shown elsewhere that losses of this magnitude limit energy conversion efficiencies to a (not yet achieved) maximum of about 13%. For cells featuring *tris*-bipyridyl or phenanthroline complexes of cobalt(II) and cobalt(III), the minimum driving force required is ca. 400 mV, in principle allowing for cells of 15 to 16% efficiency. Nevertheless, the best single-chromophore cells with this type of shuttle have attained efficiencies of only about 10%. Among the limitations of cobalt shuttles in their present form are slow diffusion (resulting in transport-limited photocurrents) and, depending on the chromophore, comparatively large dark currents (resulting in diminished photovoltages, due to displacement of the photo-electrode's quasi-Fermi level to energies well below the conduction band-edge, the nominal maximum steady-state energy level).

This poster will describe fundamental electron transfer and photochemical energy conversion studies with new families of shuttles based on Ni(IV/III) dicarbollides, Co(III/II) dicarbollides, and Cu(II/I) macrocyclic complexes. For the dicarbollides, electron transfer (ET) is coupled to rotation of dicarbollides, thereby creating a significant inner-sphere barrier that suppresses dark current generation and inhibits back ET. For the macrocylic systems, dark-current-suppression/ back-ET-inhibition is achieved via oxidation-state dependent coordination and release of a solvent molecule or intentionally added auxiliary ligand. These systems lack the high-driving-force requirements of the iodide/tri-iodide system, as well as its corrosiveness and its undesirable propensity to associate with highly polarizable organic light-harvesters. Furthermore, they are more stable than the archetypal fast redox shuttle, ferroecene/ferrocenium, and diffuse faster than *tris*-bipyridyl or phenanthroline complexes of cobalt. Pairing of these systems with appropriate light harvesters so as to achieve high photo-voltages will be discussed, as will emerging design rules for shuttles.

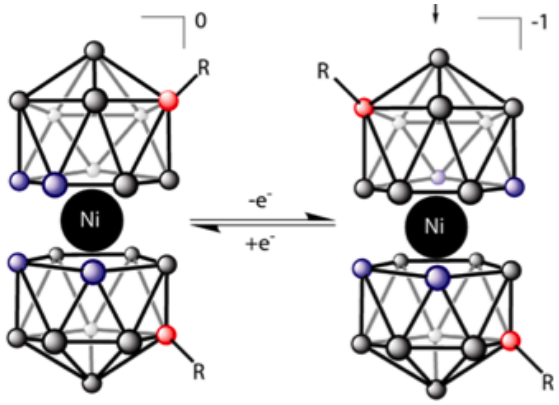

Three Easy Studies in Redox Photochemistry

James K. Hurst
Department of Chemistry
Washington State University
Pullman WA 99164-4630

Our current level of understanding of three projects relating to solar photocatalysis and use of membrane-organized assemblies, as outlined below, will be presented.

***Anomalous reactivity of ceric ammonium nitrate (CAN)*:** Very long ago, we published observations of unusual EPR and resonance Raman (RR) bands appearing in solutions of the ruthenium "blue dimer" ($[(bpy)_2Ru(OH_2)]_2O^{4+}$, **{3,3}**) when oxidized with CAN. Our provisional assignments, that the EPR signal was due to **{4,5}** and a prominent concentration-dependent RR band at ~680 cm^{-1} band was due to ion-pairing between Ce^{4+} and **{5,5}**, are now known to be incorrect. Very recently, these data have been reinterpreted by others in terms of formation of a peroxo-containing intermediate as part of a catalytic cycle of water oxidation. This assignment is also incorrect, as can be easily shown by examining the O-isotope dependent properties of the RR band. Ongoing advanced EPR and RR studies (in collaboration with R.D. Britt/Jamie Stull, UC Davis and Jeanne McHale/Fritz Knorr, WSU, respectively) are expected to provide insights into the structure of this species. Recent results from our laboratories indicate that it accumulates only in nitric acid solutions. Given the widespread use of CAN as a chemical oxidant for studies in water oxidation catalysis by polyimine transition metal ions, it is perhaps imperative that this nitrate-dependent chemistry be understood.

***Proton photoreduction reactions mediated by pyrylium ions*:** We have recently determined that the one-electron reduction potentials for a series of low-potential pyrylium ions ($Py^{+/o}$) are sufficient to drive H_2 photoproduction from neutral aqueous solutions. We have now also demonstrated pyrylium-dependent photosensitized H_2 formation from solutions that contain water-soluble Zn porphyrins, sacrificial electron donors, and colloidal Pt as additional reaction components. In ongoing studies, we are evaluating performance parameters (Py^o quenching rates, H_2 quantum yields, pH dependence, microphase environment) upon reactivity with the intention of incorporating these reactions into membrane-organized integrated chemical systems for generation of H_2.

***Polymerosomes as organizing matrices for transmembrane photoredox reactions*:** Biomimetic approaches to solar photoconversion often utilize bilayer membranes as organizational components; however, their fragile nature introduces considerable instability into these assemblies. As an alternative, we have been investigating more robust vesicles formed from block copolymers whose greater thickness presents a different challenge, namely, that they are best suited for systems that can transversely separate charge by diffusional processes. We have found that $Py^{+/o}$ works well as a redox relay in these vesicles, allowing very efficient cyclic transmembrane reduction of an occluded electron acceptor. Ongoing studies are directed at characterizing this system using a variety of potential redox mediators.

Carrier Interactions in Quantum Dots

Byungmoon Cho, William K. Peters, Austin P. Spencer, Trevor L. Courtney and David M. Jonas
Department of Chemistry and Biochemistry
University of Colorado
Boulder CO 80309

Carrier multiplication is a potential route to 3rd generation photovoltaics. The coupling between carriers can be studied through Auger recombination (the inverse of carrier multiplication) and two-dimensional spectroscopy (which is sensitive to coupling through the bi-exciton binding energy). Avoiding repetitive excitation of incompletely relaxed quantum dots is a crucial problem for Auger recombination studies. Recently, Bawendi has reported evidence that the bi-exciton Auger ionization model of charging may not account for quantum dot blinking, and Klimov has suggested a new charging process. Measurements of Auger recombination out to 1 ns delay for absolutely calibrated excitation probabilities of up to 10 (Fig. 1) suggest charging. For <Neh> below 1, the data are consistent with accumulated charging models with a product of charged state quantum yield and lifetime in the range $\phi\tau$ ~ 10-50 ms. However, for <Neh> above 2, the data are quantitatively inconsistent with accumulated charging models.

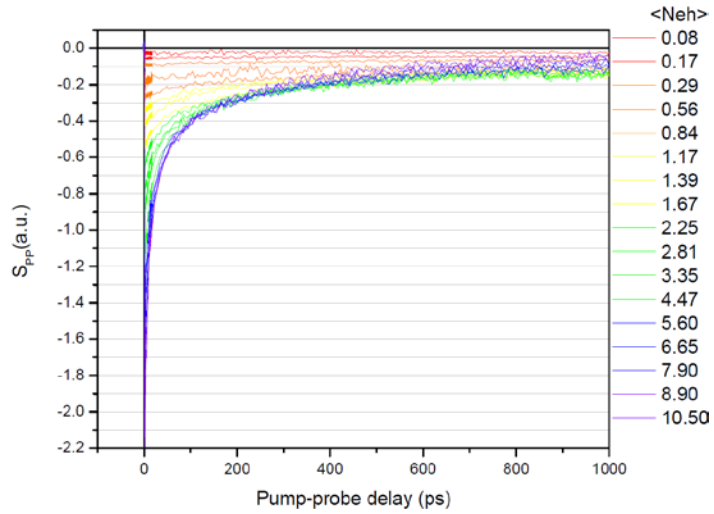

Figure 1. Degenerate pump-probe transients for 8 nm diameter PbS quantum dots in a sample cell spinning at 3000 rpm. Average excitation probabilities range from <Neh> = 0.08 to 10.5. The signal at 1 ns delay is largest for <Neh> ~ 4, which is inconsistent with the saturated monotonic increase expected for Auger recombination. It might be explained by charging at high excitation probabilities.

To enable studies of Auger recombination without accumulated charging, we have built a new beam scanning apparatus with a 1.3 s interval between excitations of the same sample volume. Tests of the apparatus for pump-probe spectroscopy on a dye are shown in Fig. 2 (right), which shows that beam scanning does not reduce signal to noise.

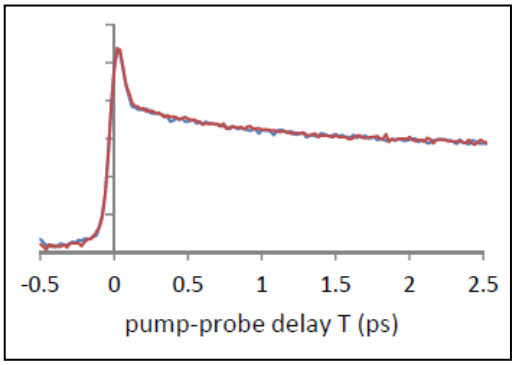

We are also working to record femtosecond 2D spectra covering the bandgap region for quantum dots with the short-wave infrared (1-2 μm) bandgaps required for third generation photovoltaics.

Tracking Excited State Interactions in Graphene Oxide-Semiconductor Mesoscale Architectures

Ian Lightcap and Prashant V. Kamat
Radiation Laboratory and Department of Chemistry and Biochemistry
University of Notre Dame
Notre Dame IN 46556

Graphene's atomic thinness and large sheet surface area combined with excellent electron transport properties make it an ideal material for optimizing electron transport within quantum dot (QD) films while minimizing incident light absorption. Careful control of graphene loading is required to extend QD films into mesoscopic scale, where an essential balance must exist between maximizing contact with QDs while minimizing incident light absorption by graphene. Examination of excited state interactions between QDs and graphene with different levels of oxidation enables us to manipulate energy and electron transfer processes in a controlled fashion. The kinetics of excited state interactions between colloidal CdSe QDs and graphene, and the performance-enhancing qualities of their composites toward the realization of 3-D sensitization in Quantum Dot Sensitized Solar Cells (QDSC) will be discussed.

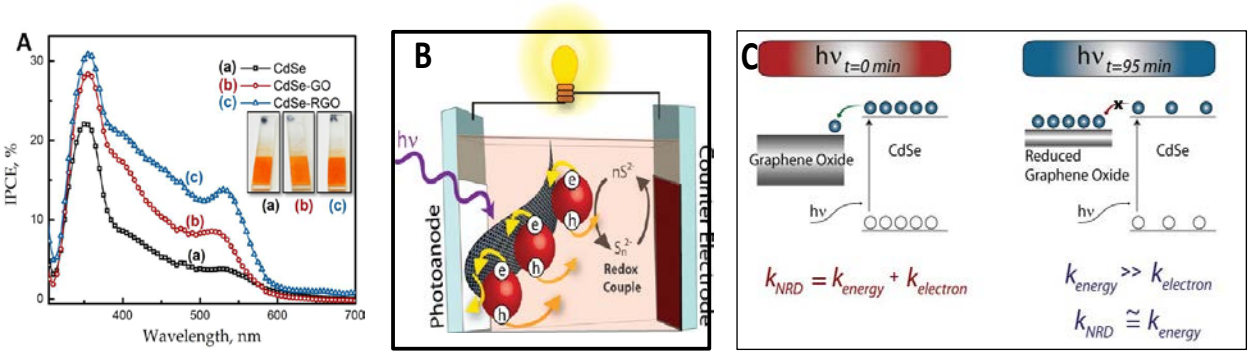

Figure 1. (A) Photocurrent action spectra of CdSe films with and without GO and RGO. (B) RGO aided electron transport in QDSC and (C) Determination of energy and electron transfer components of CdSe quenching by RGO.

Upon photoexcitation, CdSe QDs undergo electron transfer to graphene oxide (GO) forming first reduced graphene oxide (RGO), followed by electron storage. Both electron transfer and energy transfer to GO/RGO contributes to the deactivation of excited CdSe QDs. Electron and energy transfer rates from photoexcited CdSe colloidal quantum dots (QDs) to graphene oxide (GO) and reduced graphene oxide (RGO) were isolated by the analysis of excited state deactivation lifetimes as a function of degree of oxidation and charging of GO. Apparent rate constants for energy and electron transfer determined for CdSe-graphene oxide composites were 5.5×10^8 s^{-1} and 6.7×10^8 s^{-1}, respectively. The enhanced photoresponse of highly dispersed graphene-CdSe QD composites demonstrates the beneficial nature of electron transfer through graphene sheets in QD films. Incorporation of graphene oxide in QD films represents a significant step towards overcoming conductivity problems inherent to QD films, and as such, opens a new avenue towards improved sensitizer loading and performance in QDSCs.

Interfacial Charge Transfer Dynamics in Core/Shell Nanocrystals: The Role of Island Growth and Inhomogeneous Shell Thickness

Zhong-Jie Jiang and David F. Kelley
University of California, Merced
Merced, California 95343

Island formation is well known in two-dimensional epitaxial semiconductors. The analogy in core/shell semiconductor nanocrystals is shell thickness inhomogeneity. Both correspond to nanoscale surface roughness and are caused by lattice mismatch. The rate of interfacial charge transfer reactions in which the charge tunnels through the shell to an adsorbed acceptor depends critically on the shell thickness and hence on the extent of shell thickness inhomogeneity. This phenomena has been studied in type-II ZnTe/CdSe core/shell with an adsorbed hole acceptor (phenothiazine). A model has been developed to understand the results in which considers each particle to have a Poisson distribution of shell local thickness. The experimental results and decay curves calculated using this model are depicted in the figure below and are compared to a model in which surface roughness is not considered.

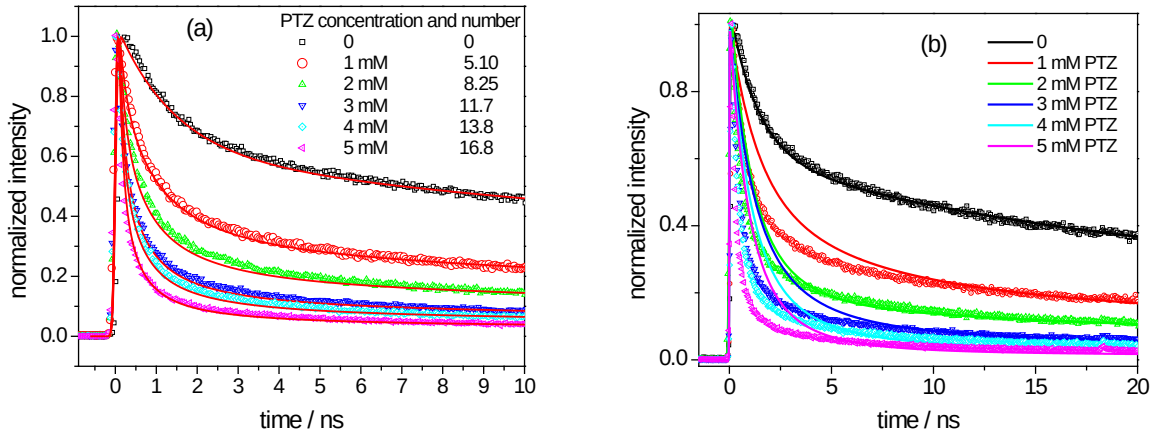

Experimental luminescence decays as a function of PTZ concentration as indicated. Also shown are decay curves calculated assuming (a) each particle has a Poisson distribution of shell thicknesses and (b) the particles have a uniform shell.

The hole transfer rates are taken to be proportional to the hole density at the particle surface and determined by an effective mass approximation wavefunction calculation. This calculation gives a β value of 6.0 nm^{-1}. The number of adsorbed phenothiazine acceptors and hence the overall luminescence quenching rate is determined from a Monte-Carlo calculation that samples this distribution and a distribution of PTZ numbers. The only adjustable parameters in the model are the phenothiazine adsorption constant and the phenothiazine-hole coupling. The figure shows that much better agreement is obtained when surface roughness is considered. We suggest the surface roughness is a results of core/shell lattice mismatch, much as occurs in epitaxial systems. The extent of lattice mismatch is related to interdiffusion of the core and shell materials.

The Possible Role of Radicals of the Carotenoid Astaxanthin and its Esters in Photoprotection

Lowell D. Kispert,[a] A. Ligia Focsan,[a] Adam Magyar,[a] Nikolay E. Polyakov[b] and Péter Molnár[c]
[a]Department of Chemistry, The University of Alabama, Tuscaloosa AL 35487-0336 USA
[b]Inst. of Chemical Kinetics & Combustion, Institutskaya Str. 3, 630090, Novosibirsk, Russia
[c]Department of Pharmacognosy, University of Pécs, Rókus u. 2, Pécs, Hungary

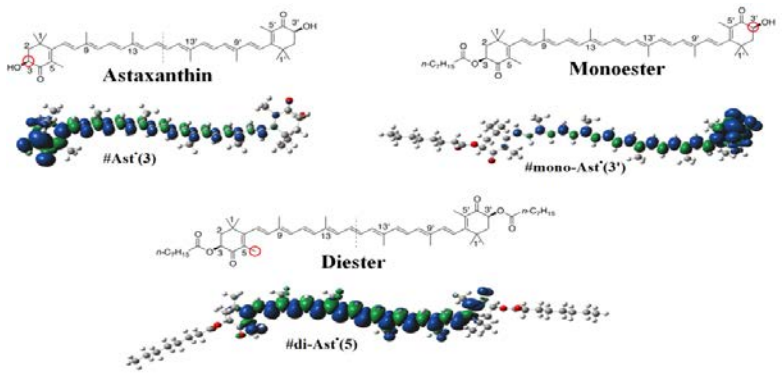

Carotenoids are a class of pigments wide spread in nature, which also serve as antennas, photo- protective devices and intermediate electron carriers in photosynthetic reaction centers. At high light intensities, photo-synthetic organisms gather more light than they need and quench what is not needed to avoid unwanted photochemical reactions. It was found [Holt, Fleming, et al., *Science* **2005**, *307*, 433-436] that a charge transfer state forms between zeaxanthin (Zea) and chlorophyll, (Chl) transiently producing $Zea^{\bullet+}$ and $Chl^{\bullet-}$ in LHC II, with the excess energy dissipated through the C-C vibrational modes of $Zea^{\bullet+}$. Recently an additional step has been proposed [Focsan, et al., *J. Phys. Chem. B* **2008**, *112*, 1806-1819] where proton loss from $Zea^{\bullet+}$ forms the neutral radical # $Zea^{\bullet}$, which would be a very efficient quencher of the excited states. In some unicellular green algae such as *Haematococcus pluvialis* (HP), astaxanthin accumulates in a huge amount (up to 30 mg/g) under high light conditions and in the presence of excess metal ions. Under stress, HP accumulates 1% of cell mass as carotenoids consisting of 70% monoesters of astaxanthin, 10% diesters of astaxanthin, 5% astaxanthin and 5% each of lutein, canthaxanthin and β-carotene. DFT calculations and pulsed EPR measurements have been carried out on the UV produced radicals of astaxanthin and its mono- and diesters. This is an attempt to learn the most likely neutral radicals formed from the radical cation and possibly a reason for the excess monoester. DFT calculations showed and were confirmed by EPR that the deprotonation of the astaxanthin radical cation at the carbon C3 methine position resulted in the lowest energy neutral radical due to resonance stabilization upon the OH proton migration to the carbonyl oxygen. This preferred proton loss occurs at either end of the symmetrical radical. However this is not the case for the diester where proton loss occurs preferentially at the C5- methyl group, then C-9, C-13 and least favorable at C3 – in other words, proton loss occurs in the center of the carotenoid and not at the ends. For the monoester, proton loss is preferred from the C-3′ methine end where the ester group is not attached followed by proton loss from the C5′-methyl group. Proton loss from the ester end is more difficult by 9 to 17 Kcal for C-5 < C-9 < C-13 << C3. These results suggest that the presence of 70% monoester may indicate a unicellar membrane that requires a carotenoid with one hydrophobic tail and one hydrophilic end.

Energy Transfer in Conjugated Polyelectrolyte Dendrimers

S. Kömürlü, J. Szmytkowski, F. Feng, S-H Lee, S. Ellinger,
J. R. Reynolds, K. S. Schanze, V. D. Kleiman
Department of Chemistry, University of Florida
Gainesville FL 32611-7200

We present new data investigating the excited state dynamics of ionic conjugated-dendrimers in polar solvents. The mono-dispersity of dendrimers (typical sizes of 1-10 nm) is provided by well-defined iterative synthesis and their properties (i.e solubility, aggregation, quenching) can be tailored by modification of the end-groups. Light-harvesting properties can be incorporated into dendritic structures by using π-conjugated chromophores with different chemical compositions (thienylene groups, phenylene-ethynylene (PE) with different number of ring units) allowing for modulations of spectra and energy-gaps between energy-donor and acceptor units.

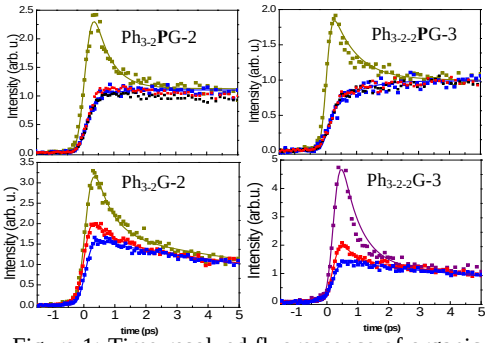

Figure 1: Time-resolved fluorescence of organic dendrimers (top) and ionic (bottom) detected at different emission energies.

The use of different (ionic) end-groups engineered to increase solubility in polar solvents is explored here. Energy-transfer rates for the ionic forms of the extended phenylene-ethynylene dendrimers (Fig1, bottom) are not too different from their ester analogs (Fig1, top). For ionic CPE-Ds the interaction energies are larger and the Förster radii are smaller. The presence of ionic groups leads to intra-molecular interactions and decreases energy-transfer efficiency. The outer PE units of the $Ph_{3\text{-}2\text{-}2}G\text{-}3$ are more affected by the intra-molecular interactions due to the globular structure and the excitation localized in the periphery is not transferred to the core, leading to decreased efficiency and faster kinetics. In contrast, for thienylene-containing dendrimers, energy transfer in the ionic dendrimers is faster than in their ester analogs, due to the collapse of the dendrimer structure and stronger interaction between periphery and core.

Recently we begun investigating a new family of π-conjugated molecules: Donor–Acceptor-Donor oligomers, where electron – rich and electron-deficient moieties are combined to yield HOMO-LUMO gaps of comparatively low energy. Transient Absorption spectroscopy (Figure 2) is used to investigate the charge-transfer character of the excited states of di-functionalized thiophene oligomers with an EDOT-benzothiadiazole core. Preliminary results show two "bleach" transitions and a new photo-induced absorption band at energies near those expected for stimulated emission. We will present results from further exploration of the excited state dynamics of this D-A-D oligomer and a comparison with other oligomers where the donor and acceptor strength is systematically varied.

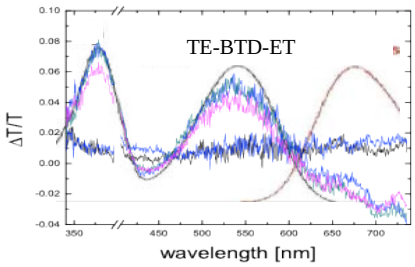

Figure 2: Transient Absorption. A small decrease on the signals is observed between 20 ps (blue) and 100 ps (magenta). (Δt=0 plotted in dark blue). Absorption (black) and emission (red) are also shown.

"Energy Transfer in Extended Thienylene-Phenylene-Ethynylene Dendrimers" Sevnur Kömürlü, Seoung Ho Lee, Tracy McCarley, Kirk S. Schanze, and Valeria D. Kleiman *J. Phys. Chem. B* 2011**, 115**, 15214–15220.

"Compact Phenylene-Ethynylene π-Conjugated Dendrimers in Polar and Non-Polar Solutions" S. Kömürlü, F. Feng, S-H Lee, K. S. Schanze, and V. D. Kleiman. *Submitted*.

π-Conjugated Donor-Acceptor-Donor Ions for Solar Energy Conversion

Coralie A. Richard,[1] Leandro A. Estrada,[1] Dinesh G.(Dan) Patel,[2] Fude Feng,[2] Yu-ya Ohnishi,[2] Khalil A. Abboud,[2] So Hirata[2], Kirk S. Schanze,[2] John R. Reynolds[1]

[1] Schools of Chemistry and Biochemistry/Materials Science and Engineering
Center for Organic Photonics and Electronics
Georgia Institute of Technology, Atlanta, Georgia, 30332

[2] Department of Chemistry, University of Florida, Gainesville, Florida 32611

Organic dyes for dye sensitized solar cells (DSSCs) are commonly based on linear push-pull structures employing covalently linked electron donors and electron acceptors. To develop a better understanding of the fundamental electron injection and subsequent processes in the operation of DSSCs, we report on symmetric and tunable π-conjugated donor-acceptor-donor (D-A-D) oligomers that incorporate a carboxylate group for binding onto metal oxide interfaces.

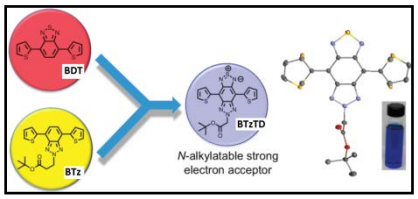

Figure 1: Chemicals structures of BDT, BTz and BTzTD based D-A-D compounds.

We initially focused on the D-A-D molecules shown in Figure 1 where the acceptor is based on benzotriazole (BTz), benzothiadiazole (BTD) and the recently reported hybrid acceptor benzo(triazole-thiadiazole) (BTzTD). [1] We computationally and experimentally compared the strength of the acceptors, and demonstrated that the central atoms (N or S) play an important role in determining the accepting ability of the acceptor core. The greater polarizability of the central sulfur atom leads to enhanced electron accepting ability in BTzTD and BTD, whereas the central nitrogen in BTz has smaller molecular orbitals that are less polarizable. The dominant non-radiative decay rates added to the lack of triplet-triplet absorption in molecules containing BTD and BTzTD point to efficient charge transfer in THF. This is more evident after elongation of the π donor system.

In addition, we synthesized a set of compounds where the core is based on dibenz[a,c]phenazine (DBP -**1**,**2**) and dithieno[a,c]-phenazine (DTP-**3**,**4**) as shown in Figure 2. We used different positional isomers to compare the effect of the conjugation pathways on optical, electrochemical, and photophysical properties. Extinction coefficients of these compounds exceed 40 000 M^{-1} cm^{-1}. The Stokes shifts are ~ 144 nm for compounds **1** and **3**, 28nm for **2** and 68nm for **4** in toluene, indicating a significant structural reorganization of **1** and **3** upon photoexcitation. DTP **3** has a higher HOMO level (-5.68 eV) due to it enhanced electron richness. In addition, the LUMO energies of all dyes vary from -3.45 to -3.72 eV and are all well above the TiO_2 conduction band (- 4.0 eV), as needed for facile electron injection.

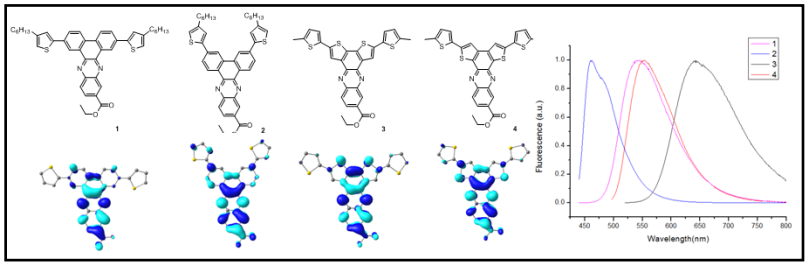

Figure 2: *left.* Chemical structures of positional isomers of BDT and BTD. *Right*. Fluorescence spectra of dyes 1-4.

[1]: "It Takes More Than an Imine: The Role of the Central Atom on the Electron-Accepting Ability of Benzotriazole and Benzothiadiazole Oligomers" Patel,D. G.; Feng, F.; Ohnishi,Y-y.; Abboud, K.; Hirata, S.; Schanze, K. S.; Reynolds, J. R., *J. Am. Chem. Soc.*, **2012**, *13*, 2599-2612.

Conjugated Polyelectrolyte Oligomers, Dendrimers and Polymers: Aggregation, Energy Transport and Amplified Quenching

Fude Feng, Seoung-Ho Lee, Sevnur Kömürlü, Danlu Wu, Jie Yang, Sung Won Cho, Adrian Roitberg, Valeria D. Kleiman and Kirk S. Schanze
Department of Chemistry, University of Florida, Gainesville FL 32611-7200

Conjugated polyelectrolytes (CPEs) feature a π-conjugated backbone functionalized with ionic solubilizing groups such as $-SO_3^-$, CO_2^- and $-NR_3^+$. CPEs exhibit "amplified quenching" wherein a very small concentration of an oppositely charged electron or energy transfer quencher gives efficient fluorescence quenching. We have been investigating amplified quenching in CPEs, with the objective of understanding the underlying mechanism(s) for the process. Another important aspect for study involves the relationship between macromolecule aggregation, interchain energy transfer and amplified quenching.

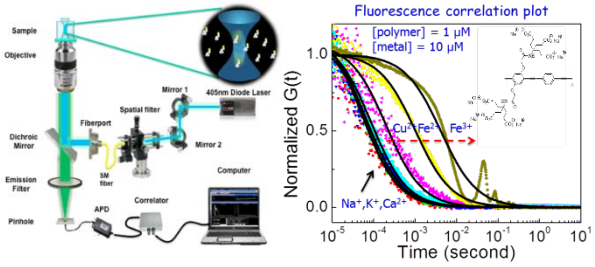

LEFT: Schematic of fluorescence correlation spectroscopy set-up. RIGHT: Fluorescence correlation plots for the polymer shown (inset) in the presence of mono- and di-valent cations.

Fluorescence correlation spectroscopy (FCS) is used to study aggregation of CPEs and structurally-related conjugated polyelectrolyte dendrimers (CPE-D) and oligomers (CPE-O) in solution. FCS measures the diffusion time of single fluorescent macromolecules or aggregates, enabling determination of their molecular weight (size). FCS of anionic CPEs in aqueous solution shows that monovalent cations (Na^+, K^+) do not induce aggregation of the polyelectrolyte chains; however, polyvalent cations (Ca^{2+}, Cu^{2+}, Fe^{2+}, Fe^{3+}) induce formation of high molecular weight aggregates. Correlation of FCS and Stern-Volmer quenching results reveals a direct relationship between the ability of the cation to induce polyelectrolyte aggregation with its ability to quench the fluorescence.

Three families of π-conjugated polyelectrolyte dendrimers (CPE-Ds) have been studied by using optical spectroscopy and Stern-Volmer quenching. In water the CPE-Ds exhibit considerable inter-chromophore interaction, yet FCS indicates that these macromolecular structures are not strongly aggregated. These inter-chromophore interactions occur within single CPE-D structures, which undergo partial "collapse" in aqueous solution. CPE-Ds exhibit the amplified quenching effect, and a third generation dendrimer is quenched effectively by a single electron- or energy-acceptor quencher ion.

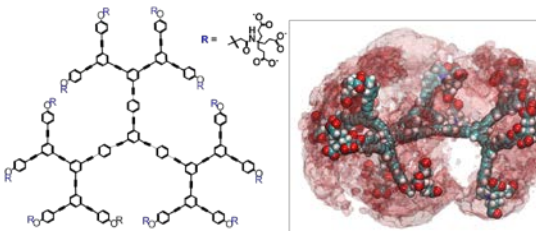

LEFT: Chemical structure of third generation conjugated polyelectrolyte dendrimer. RIGHT: Oxygen occupancy contours computed from molecular dynamics simulation of the third generation CPE-D.

Parallel studies have examined conjugated polyelectrolyte oligomers (CPE-O), monodisperse molecules containing two $-CH_2-COO^-Na^+$ units on every repeat. The CPE-Os are highly soluble in water, and FCS reveals that they exhibit little tendency to aggregate in solution. Addition of Ca^{2+} to solutions of the CPE-Os induces strong changes in the optical spectra, suggesting the formation of a J-aggregate multimer. Remarkably, all of the oligomers exhibit amplified quenching, and quenching of the nine-mer with a monocation cyanine dye gives $K_{SV} \sim 10^7\ M^{-1}$.

1. "Photophysics and Amplified Quenching in Conjugated Polyelectrolyte Dendrimers", Feng, F.; Lee, S.-H.; Cho, S. W.; Kömürlü, S.; McCarley, T. D.; Roitberg, A.; Kleiman, V. D.; Schanze, K. S., submitted.

2. "Light Switch Effect Upon Binding of Rudppz to Water Soluble Conjugated Polyelectrolyte Dendrimers", Feng, F.; Lee, S.-H.; Schanze, K. S., submitted.

Photophysics of Single to Multiple Excitons in Single Walled Carbon Nanotubes

Nicole Briglio, Bradford Leosch, Michael Odoi, Julie A. Smyder and Todd D. Krauss
Department of Chemistry
University of Rochester
Rochester NY 14627

Semiconducting single-walled carbon nanotubes (SWNTs) display remarkably stable and size-tunable photoluminescence at near-infrared (NIR) wavelengths, making them fundamentally interesting and technologically relevant materials. However, while the brightest individual SWNTs typically have a photoluminescence (PL) efficiency or quantum yield (QY) of about a few percent, the QY of the ensemble is over an order of magnitude lower. It is currently not understood whether the poor QY of SWNTs is an intrinsic property or the result of extrinsic quenching mechanisms indicative of non-optimal sample quality.

Correlated measurements of PL and topography were performed for individual SWNTs on quartz using epifluorescence confocal microscopy and atomic force microscopy (AFM). Surprisingly, only ~11% of all SWNTs were found to be highly emissive, suggesting that the ensemble QY is low because only a small population of SWNTs fluoresces strongly. Individual SWNTs also displayed notable differences in PL intensities, line widths, and photostability, which demonstrates the important influence of the local environment on the optical characteristics of individual SWNTs.

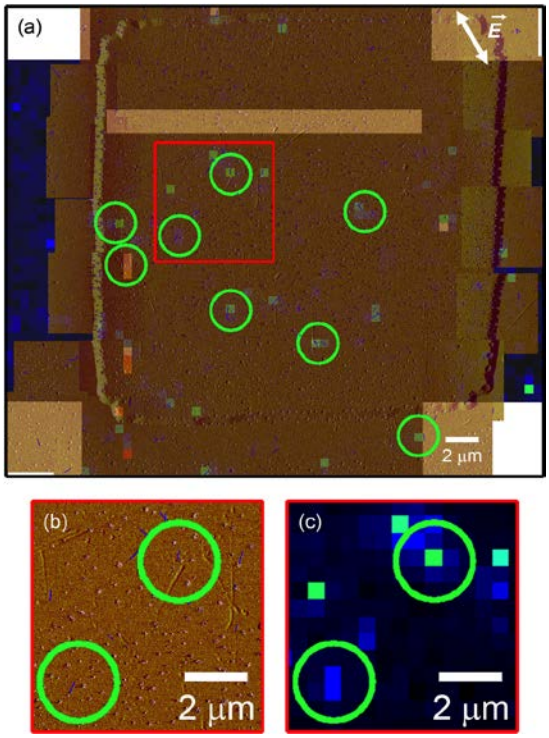

Figure 1. (a) Overlaid topography (tan) and PL (blue) images for individual SWNTs. Blue lines highlight the location of SWNTs and green circles indicate areas for which PL spectra were observed. Zoom-in of (b) topography and (c) PL images for the boxed area in (a).

We will also present studies of exciton-exciton annihilation (Auger recombination) and multiple electron-hole pair generation (MEG) in isolated SWNTs of a single chirality using ultrafast transient absorption spectroscopy. Our studies are motivated by the idea that Auger recombination and MEG are inverse quantum mechanical processes, and so it is expected that materials with fast Auger recombination rates will exhibit a high efficiency of MEG. For (6,5) SWNTs Auger annihilation lifetimes are about 1 ps, with larger diameter SWNTs ((8,6) and (8,7) SWNTs) having slightly longer Auger lifetimes. The origin of the diameter dependence on the Auger lifetime and the resulting structural dependence on MEG efficiency will also be discussed.

Photoinduced Charge Separation and Charge Transport in DNA

Frederick D. Lewis
Department of Chemistry
Northwestern University
Evanston IL 60208

The π-stacked base pairs of DNA provide a unique medium for the experimental investigation of the distance and pathway-dependence of photoinduced charge separation. We have studied the dynamics and efficiency of photoinduced charge separation in capped hairpins in which a stilbene hole acceptor and hole donor are separated by polypurine sequences consisting exclusively of adenine or guanine, diblock purines consisting of adenine and guanine or deazaadenines blocks, and triblock sequences consisting of adenine, deazaadenine, and guanine blocks Figure 1.[1] More efficient charge separation in di- and tri-block systems can be attributed to the creation of energy gradients for hole transport which favors charge separation vs. charge recombination (Scheme 1). Our current work is directed at two major objectives: (a) development of detailed experimental evidence in support of conceptual models for the charge separation and charge migration process in DNA and (b) development of a donor-acceptor labeled DNA conjugate which permits direct measurement of the dynamics and efficiency of electron (negative charge) transport in DNA.

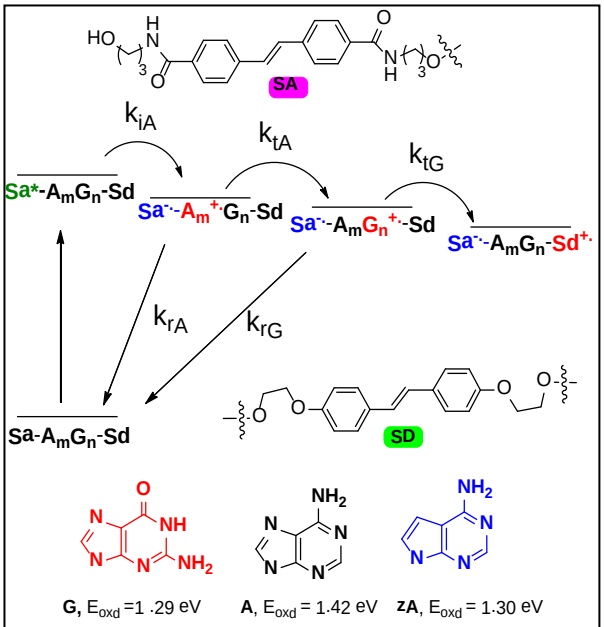

Figure 1. Structures of stilbene chromophores and purine nucleobases and mechanism for charge separation in a diblock capped hairpin.

Photoinduced charge separation in DNA was initially assumed to occur via a tunneling mechanism, which was later amended to allow for charge separation followed by incoherent hole hopping. Both mechanisms assume that the initial state is a locally excited acceptor, in our case the stilbenedicarboxamide singlet state, and ignore the possible involvement of exciplex and exterplex (triplex) intermediates in the charge separation processes. Hole transport has been proposed to occur via either holes localized on a single base or highly delocalized polarons. Solvation plays a crucial role in determining the extent of hole localization.

An impediment to the study of electron transport in DNA is the highly negative reduction potential of the naturally occurring pyrimidines, thymine and cytosine. We are investigating the use of pyrimidine analogs with less negative reduction potentials including fluorouracil and pyrrolocytosine as well as the appropriate selection of chromophores for electron injection and electron trapping.

(1). Thazhathveetil, A. K.; Trifonov, A.; Wasielewski, M. R.; Lewis, F. D. *J. Am. Chem. Soc.* **2011**, *133*, 11485.

Bio-Inspired Electro-Photonic Structure for Dye Sensitized Solar Cells

Rudresh Ghosh, Yukihiro Hara, Leila Alibabaei, Rene Lopez
Department of Physics and Astronomy
University of North Carolina at Chapel Hill
Chapel Hill NC 27713

Efficient absorption of photons and effective carrier extraction are usually antithetical goals in traditional photovoltaic device configurations. Typical solar cell designs try to maximize photon capture by increasing the thickness of the absorbing layer, but this is detrimental to charge harvesting since increased transport path lengths lead to increased carrier recombination. We believe that it is important to integrate materials and all-scale cell structures, going beyond the flat cell paradigm, to enable solar cells overcome this dilemma and reach their full potential. The objective of our program is to comprehensively redesign the full opto-electronic properties of Dye Sensitized Solar Cells (DSSCs) to develop the ultimate cell structure at all length scales that will enable perfect light capturing and electron harvesting.

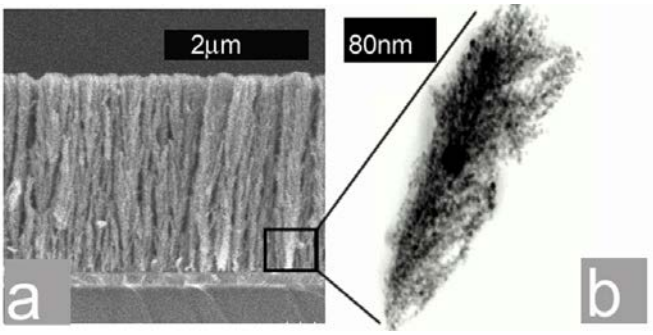

Figure 1. (a) Laser ablated Ta:TiO_2 shows vertically aligned hierarchical nanostructure, STEM image of (b) Ta:TiO_2 base of the structure.

We have developed a high surface area oxide fabrication technique by pulsed laser deposition that offers a tree-like hierarchical arrangement of nanoparticles that preserves a high surface area for dye loading while building direct highways to transport the charges toward the bottom contacts (fig 1). The technique is amenable for doping and by adding 1.0 atomic-% Ta in TiO_2 photoanodes, we have achieved 8.1% energy conversion efficiencies with N719 dye in standard conditions.

As it is the case with most green-crops, to let the trees grow randomly probably will limit their energy-harvesting efficiency. We have established a method to control the growth of our tree-like structures by "seeding" them in precise locations via nano-patterning to build ordered structures that can improve transport and light absorption via photonic effects. Fig. 2 shows how pre-pattern substrates can govern the tree development. The trees grow well out of any surface, but to incorporate this seeding technique in working devices we have also worked in large area fabrication of such nano-patterns made of transparent conductors such as fluorinated tin oxide (FTO) and indium tin oxide (ITO).

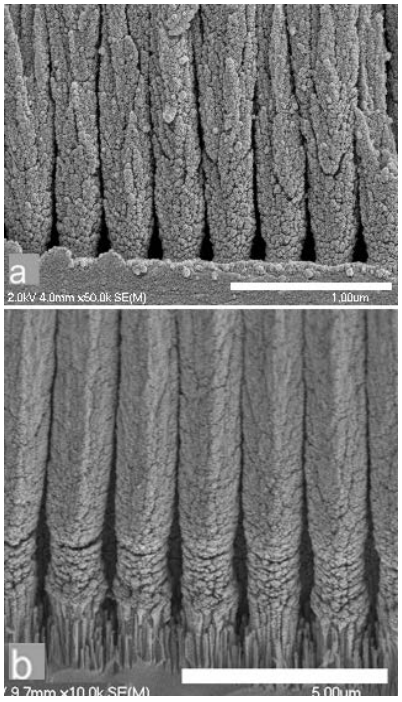

Figure 2. Laser ablated Ta:TiO_2 nano-trees growing out from defined locations a) 300 nm seed-spaced pattern and b) 1.5 µm seed-spaced pattern.

Dye-Sensitized Photocathodes under Depletion Conditions: Light-Stimulated Hole Injection into p-GaP

Michelle J. Price, Zhijie Wang, Anisha Shakira, Junsi Gu and Stephen Maldonado
Department of Chemistry
University of Michigan
Ann Arbor MI 48109-1055

This poster presentation describes our latest results in the analysis/design of sensitized photoelectrode systems that feature light-stimulated hole injection between a discrete, adsorbed, and photoexcited sensitizer and a p-type semiconductor photoelectrode (Figure 1). We present empirical and modeling data that demonstrate the process of dye-sensitized hole injection at p-type phosphides. In total, the data indicate that internal quantum yields for dye-sensitized hole injection can be intrinsically high at p-type semiconductor electrodes operating under depletion conditions (Figure 2). The major implications from these results are that (1) a wide variety of sensitizer types may be used for effecting sensitized hole injection including quantum dots and (2) dye-sensitized photocathodes can be envisioned that function with high external quantum yields in aqueous electrolytes. Data along these two fronts will be shown.

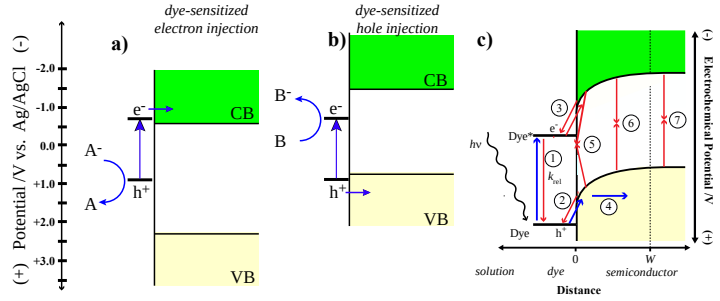

Figure 1. Depiction of dye-sensitization at semiconductor photoelectrodes. (a) Dye-sensitized electron injection from a photoexcited chromophore at the surface of a metal oxide semiconductor. (b) Dye-sensitized hole injection from a photoexcited chromophore at the surface of a phosphide semiconductor. (c) Dye-sensitized hole injection from a photoexcited chromophore at the surface of a phosphide semiconductor under depletion conditions. The constituent processes that (blue) favor and (red) limit the magnitude of the net collection sensitized photocurrent are indicated. These processes are (1) optical excitation/relaxation of the dye, (2) hole transfer between the dye and semiconductor, (3) electron transfer between the dye and semiconductor, (4) electric-field-induced transport within the semiconductor, (5) charge recombination at surface states at the semiconductor interface, (6) charge recombination in the depletion region, and (7) charge recombination in the bulk of the semiconductor.

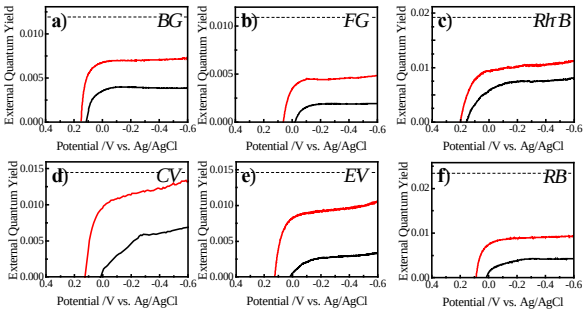

Figure 2. Measured potential dependence for net photocurrent generation of p-GaP(100) electrodes poised at -0.6 V vs. Ag/AgCl while illuminated with monochromatic light and immersed in (black) deaerated 1 M KCl(aq) or aerated 1 M KCl(aq) containing 50 μM dissolved dye; *BG* = brilliant green, *FG* = fast green fcf, *Rh B* = rhodamine B, *CV* = crystal violet, *EV* = ethyl violet, *RB* = rose bengal. The dashed line near the top indicates the projected response for an ideal monolayer coverage of each dye operating with an internal quantum yield of 1 (i.e. every absorbed photon yields a collectable charge).

Electron Transfer Dynamics in Efficient Molecular Solar Cells: Iodide Oxidation Mechanisms

Byron H. Farnum, Atefeh Taheri, Patrik Johansson and Gerald J. Meyer
Departments of Chemistry and Materials Science & Engineering
Johns Hopkins University, Baltimore MD 21218

The oxidation of iodide results in the formation of diiodide ($I_2^{\bullet-}$) and triiodide (I_3^-) in fluid solution. Photo-initiation of iodide oxidation with visible light thus provides a fundamental means by which solar photons can be converted to chemical energy in the form of I-I bonds. This bond formation chemistry is also of major importance in dye-sensitized solar cells where I^-/I_3^- is the most widely used redox mediation. We have previously reported the oxidation of iodide using the metal-to-ligand charge transfer (MLCT) excited states of Ru-tris(diimine) compounds in fluid solution.[1] Visible light generation of the MLCT excited-states in the presence of I^- resulted in electron transfer reactions that generated I-I bonds. In acetonitrile solutions, iodide oxidation proceeded through an iodine atom intermediate and $I_2^{\bullet-}$ appeared as a secondary reaction product. In dichloromethane solutions, iodide oxidation rates were greatly enhanced due to strong ion-pair interactions between the Ru-tris(diimine) compounds and iodide. Recent mechanistic studies of iodide oxidation will be the focus of this poster presentation.

A series of Ru-tris(diimine) compounds have been prepared to further characterize excited state electron transfer in acetonitrile. The compounds prepared allowed the free-energy change for electron transfer (ΔG^o) to be systematically varied over a 400 meV range. A strong driving force dependence was apparent with diffusion limited rate constants for exergonic reactions and values on the order of 10^9 M^{-1} s^{-1} for $\Delta G^o \geq 0$ eV. The temperature dependence was also quantified. After corrections were made for diffusion, analysis of the activated rate constants with Marcus theory provided insights into the factors that underlie the rapid electron transfer measured for endergonic reactions as shown in the accompanying figure.

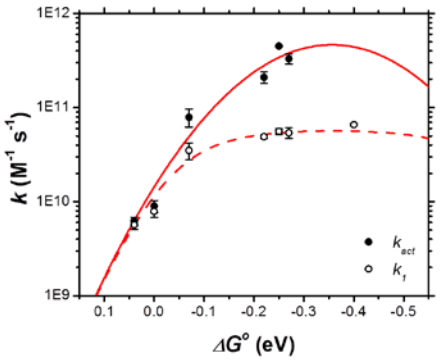

Marcus plot showing observed (k_1) and activation (k_{act}) rate constants for the reaction $Ru^{2+}* + I^- \rightarrow Ru^+ + I^{\bullet}$.

In unpublished work, we have continued studies of iodide oxidation in low dielectric constant solvents where ion-pairing is expected and is clearly evident. One particularly rewarding study still in preliminary stages involves the photo-oxidation of iodide by $Ru(deebq)(bpy)_2^{2+}$, where deebq is 4,4'-$(CO_2Et)_2$-2,2'-biquinoline, in tetrahydrofuran solution. Pulsed laser excitation resulted in the immediate appearance of $I_2^{\bullet-}$ and $Ru(deebq^-)(bpy)_2^+$ under conditions where control experiments showed that the $I^- + I^{\bullet} \rightarrow I_2^{\bullet-}$ reaction was much slower. Taken together, the data provide compelling evidence for the concerted formation of I-I bonds from an excited state. Electrochemical studies designed to identify conditions where concerted I-I bond formation might be initiated by an oxidized compound anchored to a metal oxide surface will also be presented.

[1]For a recent review, see: **Iodide Chemistry in Dye-Sensitized Solar Cells: Making and Breaking I-I Bonds for Solar Energy Conversion.** Rowley, J.G.; Farnum, B.H.; Ardo, S.; Meyer, G.J. *J. Phys. Chem. Lett.* **2010**, *1*, 3132.

Search for a Small Chromophore with Efficient Singlet Fission

Akin Akdag, Zdeněk Havlas and Josef Michl
Department of Chemistry and Biochemistry
University of Colorado, Boulder CO 80309 USA
Institute of Organic Chemistry and Biochemistry
Academy of Sciences of the Czech Republic, Prague, Czech Republic

Singlet fission (SF), in which an S_1 chromophore and its S_0 neighbor share energy to produce a pair of triplet excited species, offers a route beyond the Shockley-Qeisser limit, but has only been observed in very few compounds. Design rules are needed if it is to become widely exploitable. Two desirable features of a prospective SF sensitizer are: (i) A suitable arrangement of S_0, S_1, T_1, and T_2 energy levels in the chromophore that makes SF slightly exoergic and the reverse process, T_1-T_1 annihilation, endoergic, and (ii) strong coupling between two or more chromophores (excitation sites) in the sensitizer. Presently, we address the first condition, $E(T_2)$, $E(S_1) > 2E(T_1)$. It is likely to be met in two classes of parent structures, alternant hydrocarbons and biradicaloids.

The chromophores that are known to undergo SF efficiently (tetracenes, pentacenes, 1,3-diphenylisobenzofurans, carotenoids) contain about 20 atoms from the first full row in the monomer, making highly accurate detailed calculations of the SF process difficult if not impossible. In order to perform such calculations, it is important to find chromophores that contain no more than 10 such atoms in the molecule and yet meet the energy criterion. We were inspired by indigo, a large biradicaloid that does. It can be thought of as a pair of captodatively stabilized radicals.

We combined a pair of -NR-CH$^{\cdot}$-CO- radicals into a planar biradicaloid in ways leading to structures **1** - **5** containing no more than 10 atoms from the first full row. Large-active-space CASPT2 calculations with a large basis set revealed than one of them had its energy levels perfectly lined up for SF and another two were very close (Figure 1). These parent structures are not known but certain simple derivatives are. It remains to be seen whether the parent systems can be prepared and exhibit SF. If they do, they will be excellent candidates for detailed theoretical studies.

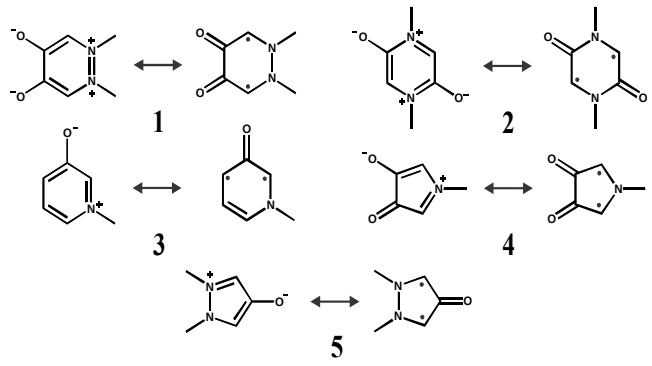

Chemical structures of biradicaloids **1** - **5**.

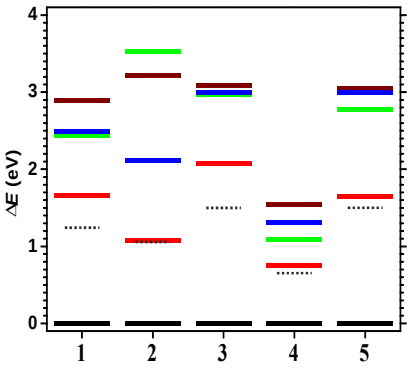

Figure 1. Relative adiabatic state energies: ■ S_0, ■ T_1, ■ S_1, ■ T_2, ■ S_2. Dotted line: $E(S_1) / 2$.

Triplet Transport and Prospects for Fast Triplet Creation in Conjugated Polymers

Paiboon Sreearunothai[1], Sadayuki Asaoka[1], Andrew R. Cook[1], Xiang Li[1], Matthew Bird[1], Garry Rumbles[2], Natalie Stingelin[3] and John R. Miller[1]

[1]Chemistry Department, Brookhaven National Laboratory, Upton NY 11973

[2]National Renewable Laboratory, Golden CO

[3]Department of Materials, Imperial College London, London SW7 2AZ

Triplet excited states created in polyfluorene (pF) molecules having average lengths up to 170 repeat units, were transported to and captured by trap groups at the ends. Almost all of the triplets attached to the chains reached the trap groups ruling out the presence of substantial numbers of defects that prevent transport. The transport yields a diffusion coefficient D at least 3 x 10^{-4} cm^2s^{-1}, which is 30 times that typical molecular diffusion, and close to a value for triplet transport reported by Keller (J. Am. Chem. Soc. 2011, 133, 11289-11298). The remarkable observation is that nearly all triplets created in the pF chains reached the end trap groups in less than 40 ns. The results point to the conclusion that few, if any, triplet excitons are trapped in the chains, despite the exquisite sensitivity of triplet excitons to their environment, which arises because the Förster dipole mechanism is not available for triplets, which must depend on steeply distance-dependent two-electron exchange matrix elements of the Dexter mechanism.

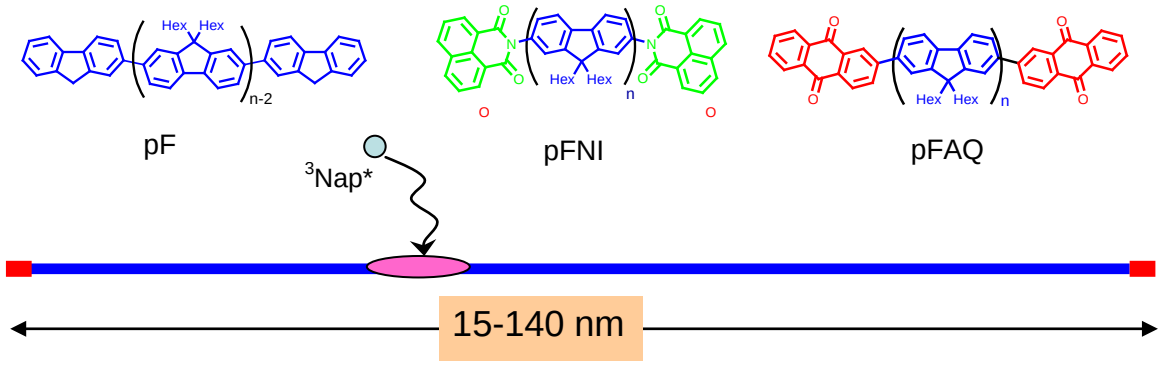

The triplet states were created in solution by pulse radiolysis; time resolution was limited by the rate of attachment of triplets to the pF chains. Naphthylimide (NI) or anthraquinone (AQ) groups attached to the ends of the chains acted as traps for the triplets, although AQ would not have been expected to serve as a trap on the basis of triplet energies of the separate molecules.

Direct photoexcitation is useful for study of singlet, but not triplet transport because intersystem crossing is slow and the kinetics of any triplets produced are hopelessly entangled with the behavior or their singlet precursors. We are therefore seeking faster methods to create triplets and inject them into molecules. Early results suggest that pulse radiolysis might supply such a method. The experiments use ~ 7 ps electron pulses from Brookhaven's LEAF accelerator and an optical fiber single-shot detection system that measure transient absorption with a time resolution < 20 ps. Future work will seek to verify and elucidate triplet formation on this time scale. Future work will also seek rapid creation of triplets and ions in solid films, where preliminary experiments suggest efficient triplet formation.

Strategies for Two-Electron CO_2 Reduction Catalysis

James T. Muckerman and Etsuko Fujita
Chemistry Department, Brookhaven National Laboratory
Upton NY 11973-5000

Tabulated standard reduction potentials at pH 7 in water clearly indicate that multi-electron reduction of CO_2 is necessary to avoid having to produce aqueous $CO_2^{\bullet-}$. This can be seen graphically in the form of a Latimer-Frost (free energy vs. oxidation state) diagram taken from the older pulse radiolysis literature[1] (Fig. 1) that shows the three additional odd-electron intermediates in CO_2 reduction beyond CO or formic acid that have very high energy. Such a diagram underscores the need for carrying out at least two-electron reductions to convert CO_2 to fuels. We are exploring several successful strategies for carrying out two-electron reductions in this context with a combined experimental and theoretical approach, and have identified at least three distinct routes. One is to bind CO_2 to certain transition-metal complexes that have three available adjacent oxidation states, e.g., Co(III), Co(II) and Co(I). If such a catalyst is designed with the middle state as the resting state, it can be reduced once, bind CO_2 through a two-electron oxidative addition reaction, then reduced again to return to its resting state. The reduction chemistry can occur after the first or second reduction. An example of such a catalyst is the $Co(HMD)^{2+}$ (HMD = a 1,4,8,11-tetraaza macrocycle) complex[2] shown in Fig. 2.

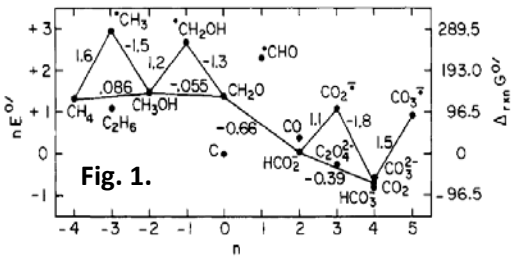

Fig. 1.

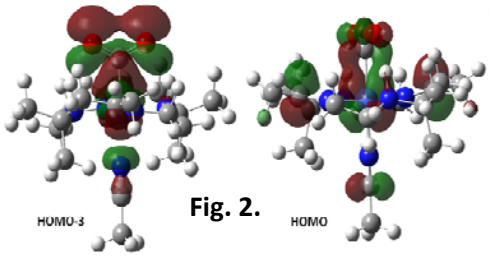

Fig. 2.

Another approach is to exploit a disproportionation reaction involving two one-electron-reduced (OER) species. This strategy is exemplified by our recent work on the $Ru(bpy)_2(pbn)^{2+}$ (pbn = 2-(2-pyridyl)benzo[*b*]-1,5-naphthyridine) photocatalyst that produces the NADPH-like $Ru(bpy)_2(pbnHH)^{2+}$ hydride donor via the disproportionation of two OER $Ru(bpy)_2(pbnH^{\bullet-})^{2+}$ intermediates,[3] and also by the $Re(bpy)(CO)_3(Cl)^0$ catalyst that forms a carboxylate-bridged dimer between two catalyst species through the reaction of CO_2 with two OER $Re(bpy)(CO)_3^0$ species. This dimer can react with another CO_2 molecule resulting in the net disproportionation of two $CO_2^{\bullet-}$ species.[4]

A third approach is the sequential ionic hydrogenation reaction on CO_2 or on CO ligands of a TM complex. Both protonation followed by hydride transfer and hydride transfer followed by protonation pathways are possible. The choice of TM complexes and hydride donors can be guided by consideration of thermodynamic hydricities. A variant of the hydride ion as the carrier of the two electrons involved in a reduction step is the insertion of CO_2 into a metal-hydride bond, as has been demonstrated for the case of CO_2 insertion into $Ru(H)(bpy)(tpy)^+$.[5]

1. Koppenol, W. H.; Rush, J. D. *J. Phys. Chem.* **1987**, *91*, 4429-4430. Reprinted with permission from ref. 1. Copyright (1987) American Chemical Society
2. Schneider, J; Jia, H; Muckerman, J. T.; Fujita, E. *Chem. Soc. Rev*. **2012**, *41*, 2036-2051.
3. Polyansky, D. E.; Cabelli, D.; Muckerman, J. T.; *et al.*, *Inorg. Chem.* **2008**, *47*, 3958-3968.
4. Agarwal, J.; Fujita, E.; Schaefer, H. F. III; Muckerman, J. T. *J. Am. Chem. Soc.* **2012**, *134*, 5180-5186.
5. Creutz, C.; Chou, M. H.; Hou H.; Muckerman, J. T. *Inorg. Chem.* **2010**, *49*, 9809-9822.

Metal-Templated Self-Assembly of Cobaloxime-Based Photocatalysts

Karen L. Mulfort, Anusree Mukherjee, Oleksandr Kokhan, David M. Tiede
Division of Chemical Sciences and Engineering
Argonne National Laboratory
Argonne IL 60439

Natural photosynthetic systems precisely position molecular light-harvesting and catalytic modules into complex, hierarchical protein host frameworks which create directional electron transfer pathways and stabilize long-lived charge separated states. Remarkably, these complex structures are composed wholly of earth-abundant elements and structurally bound by generally weak but specific supramolecular interactions. Supramolecular assembly techniques offer mechanisms to 1) stabilize traditional small molecule electrocatalysts, 2) promote efficient photoinduced electron transfer (PET) and stabilization of charge-separated states, and 3) enable dynamic self-healing pathways. This poster will describe our recent efforts to implement biological design principles to develop and discover new abiotic photocatalysts towards the goal of artificial photosynthesis.

In the interest of exploring viable connection motifs for supramolecular H_2 photocatalysts, we have synthesized new $Ru(bpy)_3^{2+}$-based photosensitizers bearing glyoxime functionality (Figure). Self-assembly to form the equatorially-linked cobaloxime-based photocatalyst of these compounds with Co(II) in acetone solution was achieved simply by adding a stoichiometric amount of $CoCl_2$. Despite the nearly identical redox and optical parameters of $Ru(bpy)_2$(**L1**)$\cdot 2PF_6$ and $Ru(bpy)_2$(**L2**)$\cdot 2PF_6$, we find that the subtle differences in the linkage between photosensitizer and catalyst sites have dramatic implications for the kinetics following visible excitation. Notably, the transient spectra of the $Co[Ru(bpy)_2$(**L2**)$\cdot 2PF_6]_2Cl_2$ assembly displays striking spectral features between 485-650nm which correlate with spectrum of the Co(I) reduced state of the cobaloxime macrocycle. A tentative hypothesis to describe the multi-exponential kinetics following MLCT excitation is presented in Figure B. Additional transient optical spectroscopy measurements will be coupled with high-resolution structural characterization techniques such as X-ray scattering and X-ray absorption spectroscopy to fully map the structure-function landscape of the supramolecular assemblies under real conditions relevant to photocatalysis. These fundamental studies will be discussed in the context of actual measures of H_2 catalysis efficiency.

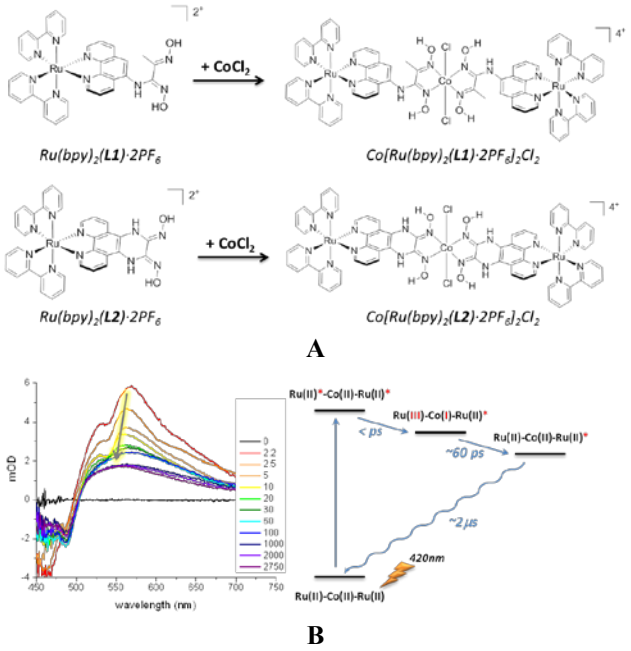

Figure. A) Chemical structures of two new glyoxime-functionalized $Ru(bpy)_3^{2+}$ analogs and equatorially-linked cobaloxime assemblies. B) Transient spectra of $Co[Ru(bpy)_2$(**L2**)$\cdot 2PF_6]_2Cl_2$ in CH_3CN following 420nm excitation and proposed energy level diagram.

Doping Main Group Elements into Germanium Nanocrystals Using the Mixed-Valence Reduction Method

Nathan R. Neale and Daniel A. Ruddy
Chemical and Materials Science Center
National Renewable Energy Laboratory
Golden, CO 80401

Group IV nanocrystals (NCs) composed of single phase, alloyed, or doped Si, Ge, or Sn could potentially be used to form printable inks for depositing low-cost solar cells, infrared detectors and related devices that would interface well with the existing PV and microelectronics infrastructure. However, only recently have studies been carried out to characterize their optoelectronic properties primarily due to the lack of synthetic protocols for preparing well-defined samples of these quantum-confined materials.

We will present an expansion of the mixed-valence iodide reduction method for the synthesis of Ge NCs to incorporate low levels (~1 mol%) of Groups III, IV, and V elements to yield main-group element-doped Ge NCs (Ge:E NCs). Nearly all main group elements (E) that surround Ge on the periodic table may be incorporated into Ge:E NCs via co-reduction of main group element iodide precursors (EI_n) in the synthesis (Figure 1a), which results in minor changes to the photoluminescence (Figure 1b). This synthetic methodology yields doped/alloyed NCs that exhibit a remarkably high E incorporation into the product (>45% of E added to the reaction) that surmounts the difficulties in achieving high doping efficiency typically encountered in NC syntheses. It is proposed that the reduction potential and the Lewis acidity of iodide precursors are the key determinants in the incorporation of E into Ge:E NCs. The significant reduction potential differences between Group III EI_3 and GeI_n precursors combined with the inherent Group III Lewis acidity changes the typical Ge NC growth kinetics such that only a moderate amount of E is incorporated for Al and Ga (ca. 50%). In contrast, the more similar reduction potentials of Group IV and V precursors to those of GeI_n precursors combined with the inherent Group IV and V Lewis basicity results in little effect on the NC growth profiles and near 100% incorporation.

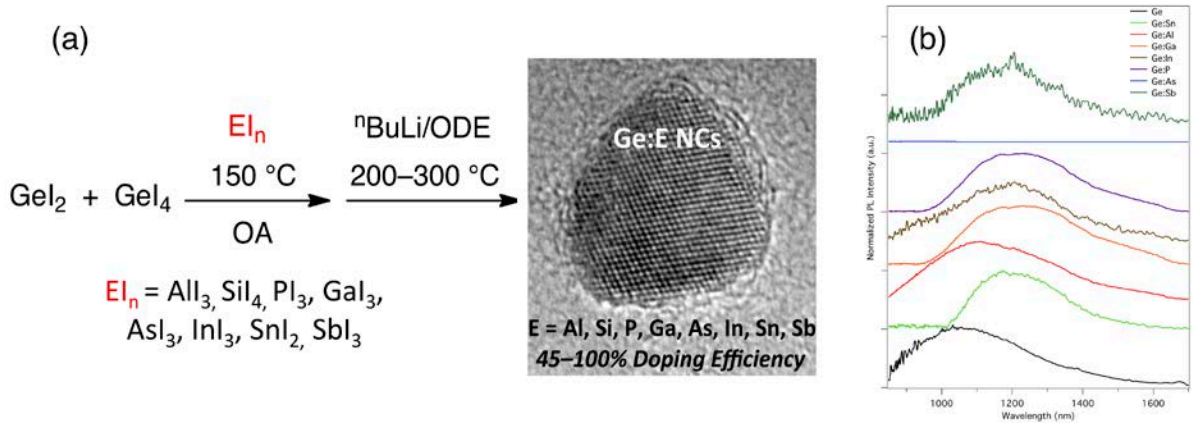

Figure 1. (a) Doping of Ge nanocrystals via the mixed-valence reduction method (b) photoluminescence doped Ge:E nanocrystals.

Proton-Coupled Electron Transfer Kinetics for the Hydrogen Evolution Reaction of Hangman Porphyrins

Manolis M. Roubelakis, D. Kwabena Bediako, Dilek K. Dogutan and Daniel G. Nocera
Department of Chemistry
Massachusetts Institute of Technology
Cambridge MA 02139-4307 USA

Hangman porphyrins catalyze the hydrogen evolution reaction. The hangman group is observed to facilitate HER by mediating a proton-coupled electron transfer (PCET) reaction. The details of the PCET pathway have been determined by comparing rate constants associated with the ET and PT processes of the hangman system to those of the corresponding values measured for porphyrins that lack an internal proton relay. The proton tunneling rate for rapid intramolecular proton transfer from the carboxylic acid hanging group to the reduced metal center has been measured for the cobalt and nickel systems. This PCET pathway provides a facile pathway for the formation of M(II)H (M = Co, Ni), which leads directly to H_2 generation.

Single-Molecule Interfacial Charge Transfer in Hybrid Organic Solar Cell

Caleb M. Hill[1], Daniel A. Clayton[1], HongWei Geng[1], Dehong Hu[2], Shanlin Pan[1]
[1]Department of Chemistry, The University of Alabama, Tuscaloosa AL 35487
[2]Pacific Northwest National Laboratory, Richland WA 99352

Hybrid organic photovoltaic devices (HOPVs) have been extensively studied over the past decade due to their distinct advantages (solution processibility, low material cost) over their traditional Si-based counterparts. Despite these efforts, however, HOPV technology has yet to exceed efficiencies for practical use. Improving these efficiencies demands a thorough understanding of the physical processes involved in their operation: light absorption, exciton diffusion, charge separation, and charge collection. Due to the complicated interplay between them, making meaningful conclusions about any of these factors is challenging for improving device efficiency.

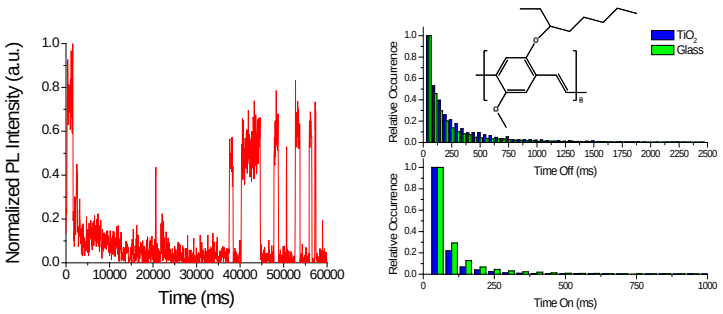

(A) (B)

Figure 1. A: Normalized fluorescence trajectory for a single MEH-PPV molecule and its corresponding molecular structure. B: "On" and "Off" state distributions for MEH-PPV molecules on glass and TiO_2 substrates.

The central goal of this project is to investigate the interfacial charge transfer dynamics of single fluorescent polymer molecules at a TiO_2 electrode with ordered nanostructure by using combined methods of electrochemistry and single molecule spectroscopy. A typical fluorescence trajectory for a single poly[2- methoxy-5-(2'-ethylhexyloxy)-p-phenylene vinylene] (MEH-PPV) molecule on glass can be seen in Figure 1. The blinking in this case is due to the reversible formation of polymer/O_2 complexes which quench the fluorescence of the fluorophores on the polymer chain due to intrachain energy transfer. The distributions of the two states follow a power law. Shorter "On" times and longer "Off times" were observed on TiO_2 surface, attributable to charge transfer between the MEH-PPV molecules and the TiO_2 substrate. This is consistent with dynamic fluorescence measurement results as shown in Figure 2. Much low population of emissive MEH-PPV molecules and short lifetime are obtained on TiO_2 surface.

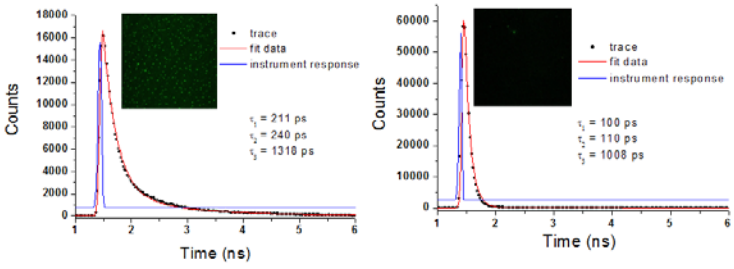

(A) (B)

Figure2. A: Lifetime trace and fitted curve of pristine MEH-PPV on cover glass substrate, and single molecule MEH-PPV fluorescence. B: Lifetime trace and fitted curve of pristine MEH-PPV on TiO_2 substrate, and single molecule MEH-PPV molecule fluorescence image.

Exciton Relaxation and Carrier Recombination in Nanometer Size Polyoxotitanate Clusters

Jianhua Bao,[1] Zhihao Yu,[1] Lars Gundlach,[1] Jason B. Benedict,[2] Philip Coppens,[2] Hung Cheng Chen,[3] John R. Miller[3] and Piotr Piotrowiak[1]

[1]Department of Chemistry, Rutgers University, Newark NJ 07102

[2]Department of Chemistry, University at Buffalo, SUNY, Buffalo NY 14260

[3]Chemistry Department, Brookhaven National Laboratory, Upton NY 11973

Exciton relaxation and recombination in polyoxotitanate clusters, Ti17cat4 and Ti17 was investigated by ultrafast optical spectroscopy and pulse radiolysis at the LEAF facility (BNL). The monodisperse clusters offer a unique, well defined bridge between small molecules and dye-sensitized anatase nanoparticles. Depolarization experiments on the Ti17cat4 cluster show that the initial exciton rapidly evolves into the fully charge separated state. The spectral component belonging to the injected e^- depolarizes within 100 fs. The component associated with the hole localized on the catechol ligand undergoes slower depolarization (~2 ps), consistent with hopping between the four degenerate catechol sites. The observed hole dynamics agrees very well with the results of modeling. The recombination of the charge-separated state exhibits three rates indicating the presence of geminate and bulk processes, as well as the involvement of "dark" states, possibly triplet polaron-excitons.

Combined pump-probe and pulse radiolysis experiments help in the spectral assignment of the transient species and provide additional insights into the electron-hole correlation. In the case of the unsubstituted or "bare" TiO_2 clusters, optical excitation generates e-h pairs, which because of the small size of the cluster remain strongly coupled to one another (the maximum spatial separation of the charges is 1 nm). As a result, the absorption of spectra of the quasi-conduction band electron are perturbed by the nearby positive charge. Preliminary results on Ti17 show that the spectra of the directly excited cluster (Figure 1 a) differ markedly from the spectrum of the excess electron in the $Ti17^{\bullet-}$ species generated by pulse radiolysis (Figure 1b). The broad maximum of the former is at ~650 nm while the latter shows a better defined peak at 1000 nm. The difference is caused by the Coulomb and exchange interaction in the directly excited cluster.

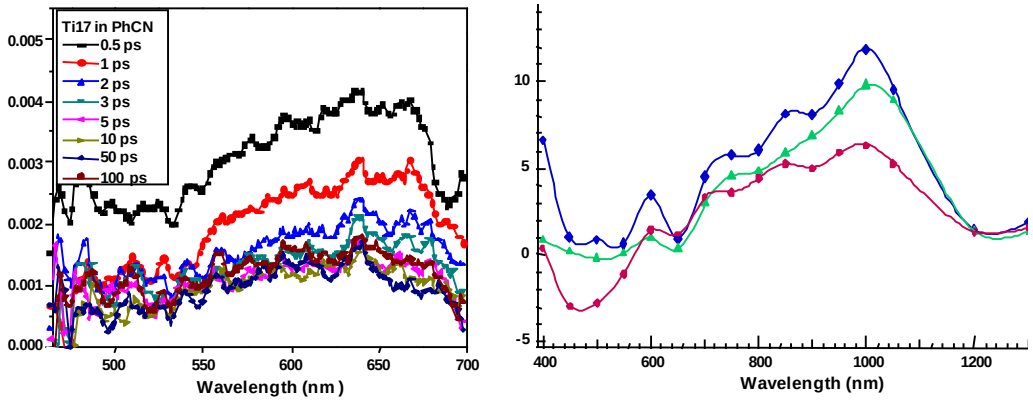

Figure 1. (a) Pump-probe spectra of Ti17 in BzCN obtained with direct excitation of the bandgap of the cluster; (b) spectra of the $Ti17^{\bullet-}$ species obtained via pulse radiolysis in the sam solvent.

Directionality of Electron Transfer in Type I Reaction Center Proteins

Oleg G. Poluektov, Lisa M. Utschig and David M. Tiede
Chemical Sciences and Engineering Division
Argonne National Laboratory
Argonne IL 60439

Our natural photosynthetic research focuses on resolving fundamental mechanisms of photochemical energy conversion in photosynthetic proteins and using this information in the design of bio-inspired materials for solar fuels production. The efficient charge separation that occurs within reaction center (RC) proteins is the most important step of photosynthetic solar energy conversion. Both Type I and Type II RCs contain two branches of potential electron transfer chains, labeled A and B (see Figure 1). From the primary electron donor, P, which is a dimer of chlorophyll molecules, these two nearly symmetrical chains of cofactors extend across the membrane. In Type II RCs, e.g., Photosystem II (PSII), light-driven primary electron transfer (ET) reactions take place exclusively through the A-branch of redox-active components (unidirectional ET). Unlike Type II RC, the directionality of ET in the Type I RC, Photosystem I (PSI), has been a long debated question. Recently, using advanced high-frequency time-resolved EPR methods, we were the first to definitively prove that ET in PS I proceeds down both nearly symmetrical cofactor branches (bidirectional ET) (Figure 1). In our experiment, ET along the B-branch in PSI was observed at low temperature (100 K) and under strongly reducing conditions. These results recently have been confirmed by a number of mutagenesis studies of Type I RCs. In the mutagenesis experiments, either A- or B-branch is shutting down, thus ET is redirected from one branch to the other. Therefore, the asymmetry of ET along the A- and B-branches in native PSI cannot be determined with a mutagenesis approach. The same argument is valid for PSI samples prepared under strongly reducing conditions.

To prove that the reduction condition of the PSI preparation does not influence our conclusion on directionality of ET in PSI and to clarify the degree of the ET asymmetry, we have spectroscopically characterized biochemically modified PSI RCs wherein the terminal acceptor iron-sulfur centers, F_A/F_B, and F_X, have been sequentially removed to prevent secondary ET from phylloquinones (A1) to F_x (Figure 1). For these modified RCs, we find that ET occurs along both A- and B- branches and the ratio of ET through the A- and B- branches is close to 1. Together with previously reported data, the concomitant structural and kinetic information obtained with HF EPR shed light on the mechanism of regulation bidirectional ET in PSI.

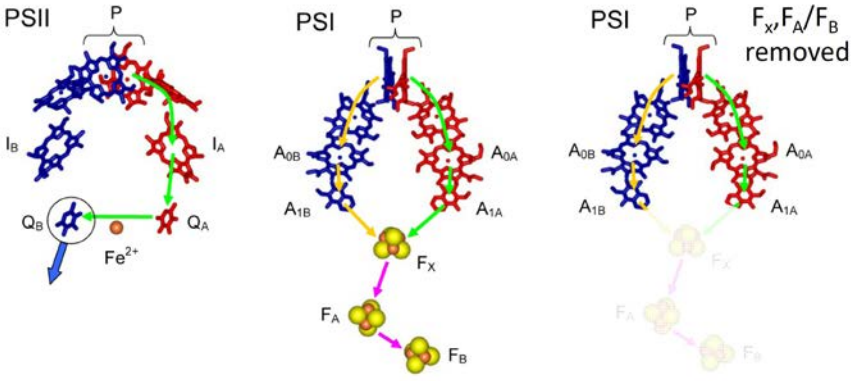

Figure 1 Schematic structure and ET pathways in Type II (left), Type I (center), Type I with iron sulfur complexes removed (right) RCs. Red – A-branch, Blue – B-branch.

Photosynthetic Reaction Center – Molecular Catalyst Hybrid Complexes for Solar Hydrogen Production

Lisa M. Utschig, Sunshine C. Silver, Karen L. Mulfort, Pingwu Du,
Oleg G. Poluektov and David M. Tiede

Chemical Sciences and Engineering Division
Argonne National Laboratory
Argonne IL 60439

Solar energy conversion of water into the environmentally clean fuel hydrogen offers one of the best long-term solutions for meeting future global energy demands. Nature provides highly evolved, finely tuned molecular machinery for solar energy conversion. Recently, we have created a hybrid complex that utilizes one of Nature's specialized energy converters, the Photosystem I (PSI) reaction center (RC) protein, to drive H_2 production from a *molecular* catalyst. The new hybrid architecture was realized by simple self-assembly of PSI with a well-known molecular H_2 electrocatalyst, $Co(dmgH)_2pyCl$. The resultant complex uses light to rapidly produce H_2 directly from water. The maximum rate for the photoreduction of water by this hybrid was measured to be 170 mol H_2 (mol PSI)$^{-1}$ min^{-1}, with a total turnover number of 5200 mol H_2 (mol PSI)$^{-1}$, which compares favorably to related synthetic photosensitizers and nears that of our PSI/Pt nanoparticle hybrid, which reports the best turnovers for a PSI-Pt system with 350 mol H_2 (mol PSI^{-1}) min^{-1} (or 21,034 mol H_2 (mol PSI^{-1}) h^{-1}). Importantly, the PSI-cobaloxime biohybrid accomplishes solar photocatalysis using inexpensive, earth abundant elements to make a clean fuel and creates new opportunities for solar fuel production that merges synthetic inorganic and biochemical capabilities.

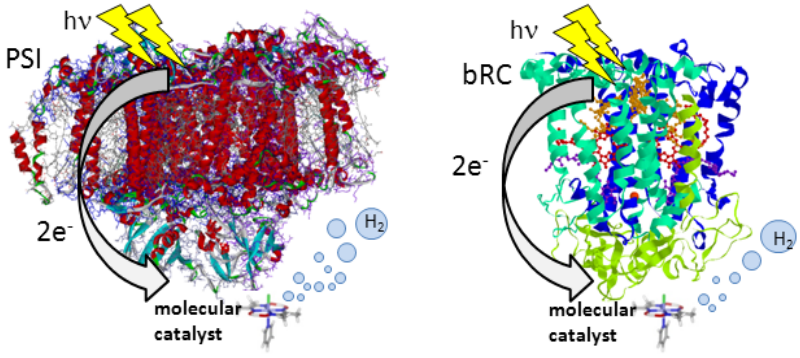

Figure 1 Photocatalytic scheme of new PSI-catalyst and bRC-catalyst hybrid systems for hydrogen production.

We are expanding upon this work by developing new bioinorganic and acceptor protein-based strategies to form PSI biohybrid complexes. Our current research efforts explore the interaction and catalytic activity of PSI with (1) different cobalt and nickel catalysts and (2) catalyst-bound flavodoxin/ferredoxin acceptor proteins. In an alternative design strategy, we are creating novel hybrids that use the light-induced chemistry of the *bacterial RC* (bRC) to drive H_2 production from molecular catalysts. Optical and EPR spectroscopic studies of both PSI- and bRC-catalyst hybrid systems will help elucidate important structure-function interactions between the protein and catalyst as well as define fundamental dynamic electron transfer mechanisms involved in the coupling of RC photochemistry with multiproton-coupled electron transfer at the catalyst sites.

Proton-Coupled Electron Transfer Reactions with NADH-Model Ruthenium Complexes

Dmitry E. Polyansky, Diane Cabelli, Etsuko Fujita and James T. Muckerman
Chemistry Department
Brookhaven National Laboratory
Upton NY 11973-5000

Proton-coupled electron transfer (PCET) is an essential part of efficient catalytic transformations, light-induced charge separation and charge transfer. Charge leveling and low energy pathways avoiding highly energetic intermediates contribute to the efficiency of PCET reactions. We are studying the reactivity of transition metal complexes containing bio-inspired nicotinamide adenine dinucleotide phosphate (NADPH) model ligands to examine mechanistic details of PCET reactions such as hydrogen atom transfer (HAT) or hydride ion transfer.

The photoexcitation of **$[Ru(bpy)_2(pbn)]^{2+}$** results in HAT from a hydroquinone (H_2Q) donor and produces **$[Ru(bpy)_2(pbnH^{\bullet})]^{+}$**. On the other hand, despite a similar driving force for HAT, the excited state of the geometric isomer **$*[Ru(bpy)_2(ipbn)]^{2+}$**, is not quenched owing to steric hindrance around the basic nitrogen atom. Based on the large H/D KIE (6.2) and the dependence on the steric factors, we proposed that the quenching of **$*[Ru(bpy)_2(pbn)]^{2+}$** takes place through a one-step HAT mechanism. The analysis of the quenching data, similar to one proposed by Meyer et. al. (J. *Am. Chem. Soc.*, 2007, **129**, 6968), reveals that the equilibrium is mainly shifted towards the precursor complex ($K_A \approx 30$ M^{-1}) and becomes more favorable as the driving force for HAT increases. However, the interaction between para-substituted phenols and **$*[Ru(bpy)_2(ipbn)]^{2+}$** is more complex than that of H_2Q. In the sequence MeO–, Ph– and NO_2–, the quenching rates decrease as expected, but the quenching does not conform to the Stern-Volmer relation due to a strong ground-state interaction between phenols and **$[Ru(bpy)_2(pbn)]^{2+}$**.

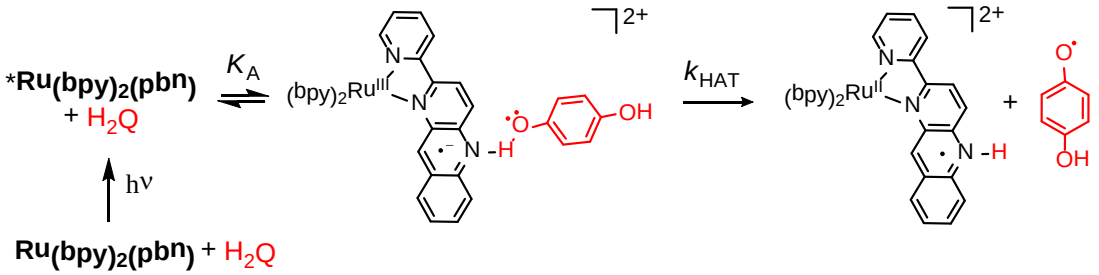

Acknowledgements: We thank our coworkers P. Achord, B. W. Cohen and J. Schneider for their assistance; C. Creutz, D. C. Grills and N. Sutin for helpful discussions; and our collaborators R. P. Thummel, and K. Tanaka.

Polyansky, D.; Cabelli, D.; Muckerman, J. T.; Fujita, E.; Koizumi, T.; Fukushima, T.; Wada, T.; Tanaka, K., *Angew. Chem. Int. Ed.* **2007**, *46*, 4169-4172.
Polyansky, D. E.; Cabelli, D.; Muckerman, J. T.; Koizumi, T.; Fukushima, T.; Tanaka, K.; Fujita, E. *Inorg. Chem.* **2008**, *47*, 3958-3968.
Fukushima, T.; Fujita, E.; Muckerman, J. T.; Polyansky, D. E.; Wada, T.; Tanaka, K. *Inorg. Chem.* **2009**, *48*, 11510–11512.
Cohen, B. W.; Polyansky, D. E.; Zong, R.; Zhou, H.; Ouk, T.; Cabelli, D. E.; Thummel, R. P.; Fujita, E. *Inorg. Chem.* **2010**, *49*, 8034–8044.
Cohen, B. W.; Achord, P.; Cabelli, D.; Fujita, E.; Muckerman, J. T.; Polyansky, D. E.; Tanaka, K.; Thummel, R. P.; Zong, R. *Faraday Discuss.* **2012**, *155*, 129.

An Optimal Driving Force for Converting Excitons into Free Carriers in Excitonic Solar Cells

David Coffey and Garry Rumbles
Chemical and Materials Sciences Center
National Renewable Energy Laboratory
Golden, Colorado 80401

A general but limiting characteristic in excitonic photovoltaics is that a portion of the incident photon energy appears necessary for dissociating excitons into separated charges, resulting in an energy loss of conversion. Currently, the mechanism underlying this process is unclear. Here we describe the development of an experimental approach for measuring charge-creation yields in systems related to polymer-based solar cells. We use the method to examine three conjugated polymer films containing a low concentration of twelve fullerene acceptors chosen to control the driving force for photo-induced electron transfer and observe two unexpected features: the existence of an optimal driving force and a loss in carrier yield if this force is exceeded[1]. These observations have implications for improving the design of excitonic photovoltaic devices and suggest an underlying electron-transfer mechanism that is consistent with a Marcus Formulation.

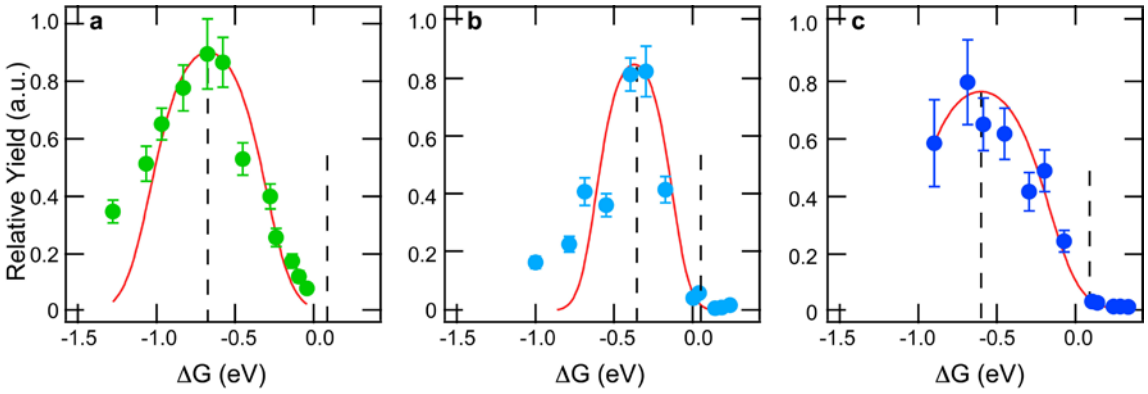

Figure 1. Relative carrier yield versus driving force, ΔG, for three fluorene-containing polymers of different ionization potenial: a) F8T2, b) F8, and c) F8BT. The driving force for electron transfer is controlled by a series of 12 substituted fullerenes of differing electron affinity and exciton energy.

DOE Sponsored Solar Photochemistry Publications 2011-2012

1. D.C. Coffey, B.W. Larson, A.W. Hains, J.B. Whitaker, N. Kopidakis, O.V. Boltalina, S.H. Strauss, and G. Rumbles. *J. Phys. Chem. C*, Accepted Manuscript (doi: 10.1021/jp302275z)

2. Dayal, S., N. Kopidakis and G. Rumbles (2012). *Faraday Discussions* 155: 323-337. (doi:10.1039/c1fd00081k)

3. A.J. Ferguson, N. Kopidakis, S.E. Shaheen, G. Rumbles. The *Journal of Physical Chemistry C* 2011, 115, 23134–23148. (doi: 10.1021/jp208014v)

4. Rance, W. L., A. J. Ferguson, T. McCarthy-Ward, M. Heeney, D. S. Ginley, D. C. Olson, G. Rumbles and N. Kopidakis (2011). *Acs Nano* 5(7): 5635-5646. (doi:10.1021/nn201251v)

pH Control of Intramolecular Energy Transfer and Oxygen Quenching in Ru(II) Complexes Having Coupled Electronic Excited States

Tod Grusenmeyer, Jin Chen, Yuhuan Jin*, Jeff Rack*, Russell Schmehl
Department of Chemistry
Tulane University
New Orleans LA 70118

This work illustrates the control of excited state energy transfer processes via variation of pH in transition metal complexes having ligands with acidic substituents.[1] In these systems a Ru(II) complex having two carboxylated bipyridyl ligands is covalently linked to pyrene via one of two different pyrene derivitized bipyridyl ligands (fig. 1). The energy of the Ru to carboxy-bipyridine ^{3}MLCT state is pH dependent while the pyrene triplet energy remains unchanged with solution acidity (fig. 2). At pH 0 the ^{3}MLCT state is the lowest energy state and, as the pH is raised and the carboxy-bipyridyl ligands are successively deprotonated, the energy of the ^{3}MLCT state rises above that of the pyrene triplet, resulting in a significant increase in the lifetime of the observed emission. Detailed analysis of ultrafast and micro-second time resolved excited state decays result in a description of excited state decay that involves initial equilibration of the ^{3}MLCT and pyrene triplet states followed by relaxation to the ground state (fig. 3). The lifetime of excited state decay is defined by the position of the equilibrium, going from 2μs at pH 0 to >10 μs at higher pH as the equilibrium favors the pyrene triplet. In addition, quenching of the excited state by dissolved oxygen *exhibits a pH dependence that parallels that of the* excited state lifetime. At high pH the pyrene containing complexes are very sensitive to oxygen and are readily quenched.

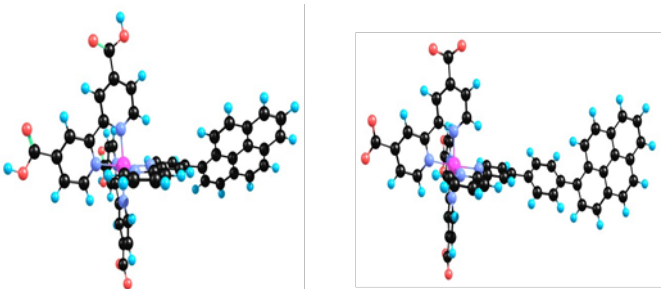

Fig. 1.: $[Ru(dcbH_2)_2(pyr\text{-}bpy)]^{2+}$ and $[Ru(dcbH_2)_2(pyr\text{-}ph\text{-}bpy)]^{2+}$

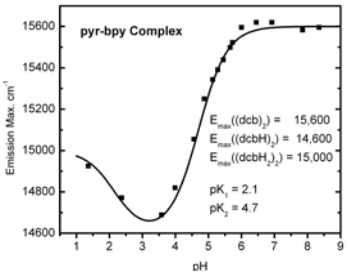

Fig. 2: Emission maximum vs. pH and fit.

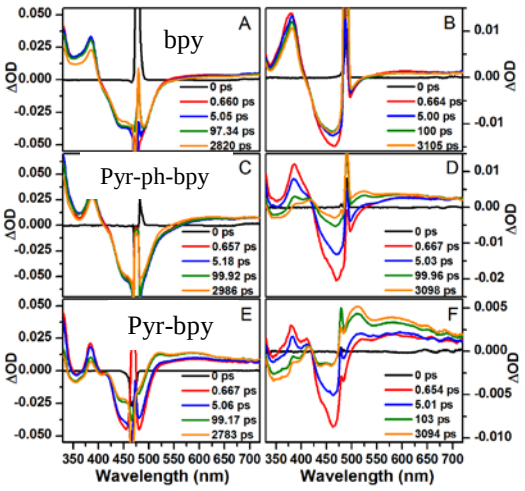

Fig. 3: TA spectra of complexes on ps time scale showing MLCT to IL energy transfer in D, E and F.

*Department of Chemistry, Ohio University, Athens, OH.

1. Tod A. Grusenmeyer, Jin Chen, Yuhuan Jin, Jonathan Nguyen, Jeffrey J. Rack, Russell H. Schmehl, *J. Am. Chem. Soc.*, **2012**.

Dynamics and Transient Absorption Spectral Signatures of the Single-Wall Carbon Nanotube Electronically Excited Triplet State

Jaehong Park, Pravas Deria and Michael J. Therien
Department of Chemistry
Duke University
Durham NC 27708

We utilize fs-μs time domain pump-probe transient absorption spectroscopy to interrogate for the first time the electronically excited triplet state of individualized single-wall carbon nanotubes (SWNTs). These studies exploit (6,5) chirality-enriched SWNT samples and poly[2,6-{1,5-bis(3-propoxysulfonicacidsodiumsalt)}-naphthylene]ethynylene (PNES), which helically wraps the nanotube surface with periodic and constant morphology (pitch length = 10 ± 2 nm), providing a self-assembled superstructure that maintains structural homogeneity in multiple solvents. Spectroscopic interrogation of such PNES-SWNT samples in aqueous and DMSO solvents using E_{22} excitation and a white-light continuum probe, enables E_{11} and E_{22} spectral evolution to be monitored concomitantly. Such experiments not only reveal classic SWNT singlet exciton relaxation dynamics and transient absorption signatures, but demonstrate spectral evolution consistent with formation of a triplet exciton state. Transient dynamical studies evince that (6,5) SWNTs exhibit rapid $S_1 \rightarrow T_1$ intersystem crossing (ISC) (τ_{ISC} ~20 ps), a sharp $T_1 \rightarrow T_n$ transient absorption signal ($\lambda_{max}(T_1 \rightarrow T_n)$ = 1150 nm; full-width-at-half-maximum, FWHM, ~350 cm^{-1}), and a substantial T_1 excited-state lifetime (τ_{es} ~15 μs). Consistent with expectations for a triplet exciton state, T_1-state spectral signatures and T_1-state formation and decay dynamics for PNES-SWNTs in aqueous and DMSO solvents, as well as those determined for benchmark sodium cholate suspensions of (6,5) SWNTs, are similar; likewise, studies that probe the ^{3}[(6,5) SWNT]* state in air-saturated solutions demonstrate $^3O_2$ quenching dynamics reminiscent of those determined for conjugated aromatic hydrocarbon excited triplet states.

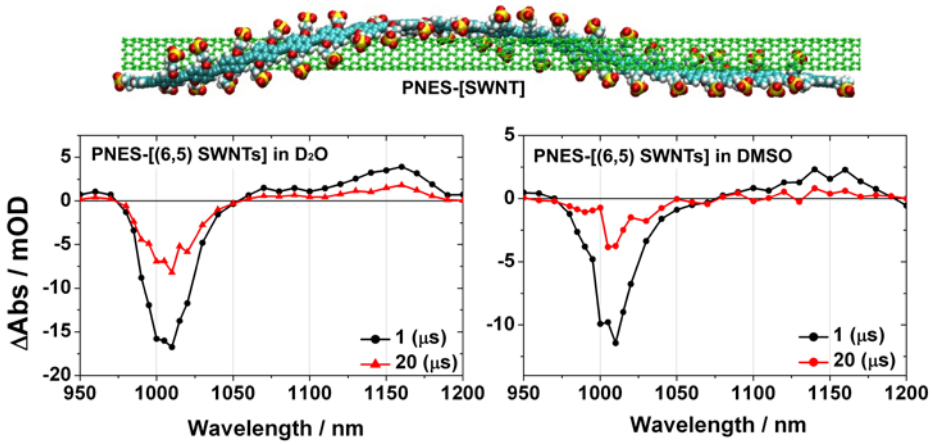

A Molecular Light-driven Water Oxidation Catalyst

Nattawut Kaveevivitchai, Raghu Chitta, Ruifa Zong,
Maya El Ojaimi and Randolph P. Thummel

Department of Chemistry
University of Houston
Houston TX 77204-5003

We have found that certain Ru(II)-terpyridine (tpy) complexes effectively catalyze the decomposition of water to form dioxygen. These complexes possess a halogen or water molecule either axial (type 1) or equatorial (type 2) with respect to the bound tpy. Activation of these catalysts requires a stoichiometric sacrificial oxidant. Ceric ammonium nitrate works well in this regard. This oxidant can be replaced by a Ru(II) polypyridine complex whose excited state looses an electron to sodium persulfate to provide a Ru(III) species that can, in turn, activate the catalyst. Furthermore, this same photosensitizer-catalyst combination has been incorporated into a ligand-bridged dyad **3** so that we now have a *single molecule* that is capable of oxidizing water using light and sodium persulfate as a sacrificial electron acceptor. The appropriate choice of catalyst, photosensitizer, and light source is critical to the optimal functioning of the system and the influence of these factors will be discussed.

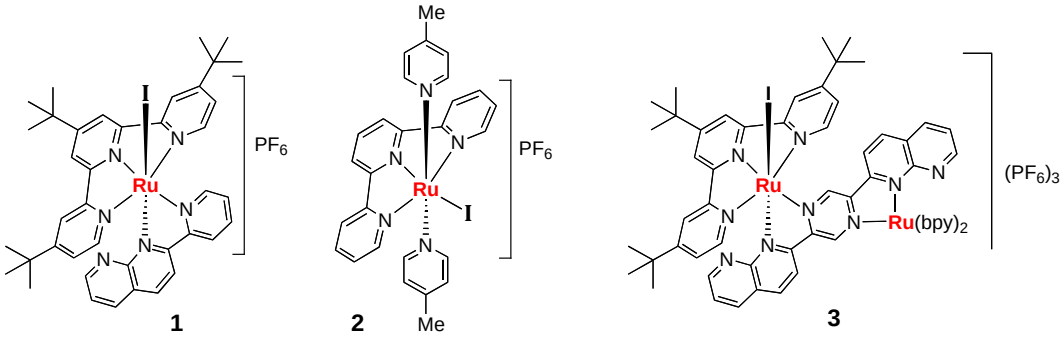

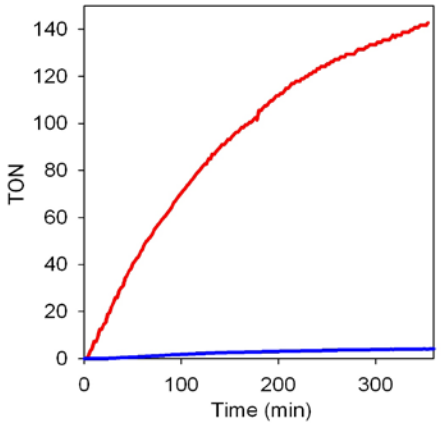

Figure 1. TON for oxygen production using dyad **3** (.0063 μmol, red) and catalyst **1** (0.2 μmol) + $[Ru(bpy)_3]Cl_2$ (0.8 μmol, blue); $Na_2S_2O_8$ (8 mmol).

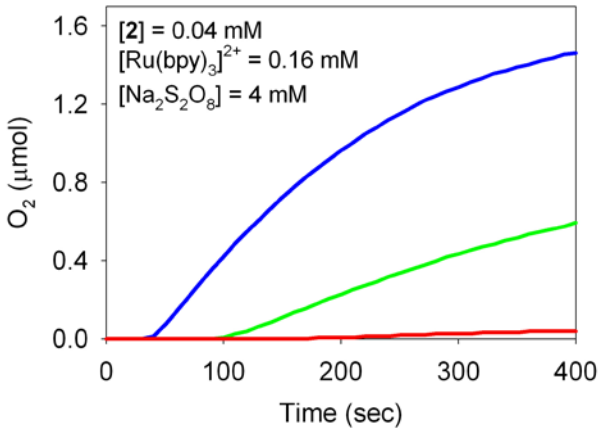

Figure 2. Rate of O2 production for catalyst **2** and $[Ru(bpy)_3]^{2+}$ as a function of the color of the exciting light (blue, green, red)

Energy and Electron Transfer within Self-Assembling Chlorophyll-Based Cyclic Donor-Acceptor Arrays

Victoria L. Gunderson, Amanda L. Smeigh, Chul Hoon Kim, Dick T. Co
and Michael R. Wasielewski
Department of Chemistry
Northwestern University
Evanston IL 60208-3113

To understand the fundamental structural relationships that drive both self-assembly and light-driven functionality in supramolecular antenna systems for artificial photosynthesis, we synthesized a zinc methyl pyrochlorophyllide a (Chl) derivative with a meta-pyridyl ligand at the Chl 20-position (**1**). In non-coordinating solvents, such as toluene, the pyridyl ligand nitrogen atom facilitates self-assembly by coordinating to the zinc metal center of another Chl. Small- and wide-angle X-ray scattering (SAXS/WAXS) experiments reveal the formation of discrete cyclic trimers with a radius of gyration of 8.3 Å. Femtosecond transient absorption spectroscopy shows that singlet-singlet annihilation occurs within the cyclic trimer as a result of energy transfer between the Chls that occurs with an (11 ± 1 ps)$^{-1}$ rate constant.

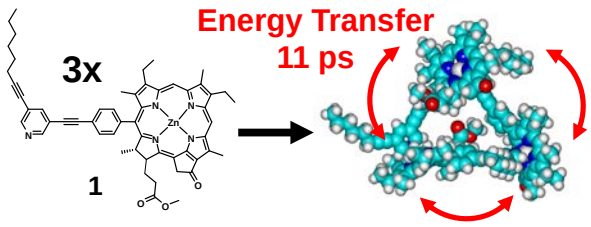

To apply this idea to photodriven charge separation, we have also prepared a series of Chl-based donor-acceptor triad building blocks that self-assemble into cyclic tetramers. Chlorophyll *a* was converted into zinc methyl 3-ethylpyrochlorophyllide *a* (Chl) and then further modified at its 20-position to covalently attach a pyromellitimide (PI) acceptor bearing a pyridine ligand and one or two naphthalene-1,8:4,5-bis(dicarboximide) (NDI) secondary electron acceptors to give Chl-PI-NDI and Chl-PI-NDI$_2$ (**2**). The pyridine ligand within each ambident triad enables intermolecular Chl metal-ligand coordination in dry toluene, which results in the formation of cyclic tetramers in solution, as determined using SAX/WAXS. Femtosecond and nanosecond transient absorption spectroscopy of the monomers in toluene-1% pyridine and the cyclic tetramers in toluene shows that the selective photoexcitation of Chl results in intramolecular electron transfer from ^{1*}Chl to PI to form Chl$^{+\bullet}$-PI$^{-\bullet}$-NDI and Chl$^{+\bullet}$-PI$^{-\bullet}$-NDI$_2$. This initial charge separation is followed by a rapid charge shift from PI$^{-\bullet}$ to NDI. Charge recombination in the Chl-PI-NDI$_2$ cyclic tetramer (τ_{CR} = 30 ± 1 ns in toluene) is slower by a factor of three relative to the monomeric building blocks (τ_{CR} = 10 ± 1 ns in toluene-1% pyridine). This indicates that the self-assembly of these building blocks into the cyclic tetramers alters their structures in a way that lengthens their charge separation lifetimes, which is an advantageous strategy for artificial photosynthetic systems.

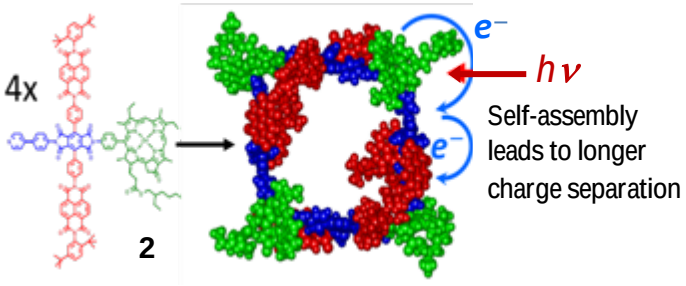

Exciton Delocalization and Dissociation in Quantum Dot-Organic Complexes

Adam Morris-Cohen, Matthew Frederick, Victor Amin, Mark Peterson and Emily Weiss
Department of Chemistry
Northwestern University
Evanston IL 60208-3113

This poster describes two categories of useful interactions between colloidal semiconductor nanocrystals (quantum dots, QDs) and organic ligands:

(i) a strong electronic coupling between the orbitals of a set of ligands – phenyldithiocarbamates – with the orbitals of the QD excitonic state. This mixing dramatically lowers the energy of the QD exciton. The bathochromic shift is due, specifically, to delocalization of the excitonic hole into the ligand shell (this conclusion is based on the dependence of the magnitude of the delocalization on the size and material of the QD), Figure 1. The physics of this effect is relatively simple (it follows the rules of a particle-in-a-sphere), but the chemistry of the QD-dithiocarbamate interaction is complicated and interesting. The current topics of exploration are the dependence of the delocalization on the energy of the orbitals of the dithiocarbamate (tuned by para-substitution of the ligand), and the effect of the delocalization on the fluorescence of the QD.

(ii) photoinduced charge transfer from the QD to a redox-active viologen ligand adsorbed to its surface. This poster focuses particularly on quantifying the contribution of the QD-viologen binding equilibrium and the intermolecular structure of the QD's native ligand shell in dictating the observed interfacial charge transfer rate, and on using the energy of charge transfer emission to determine the geometry of the donor-acceptor pair, Figure 2.

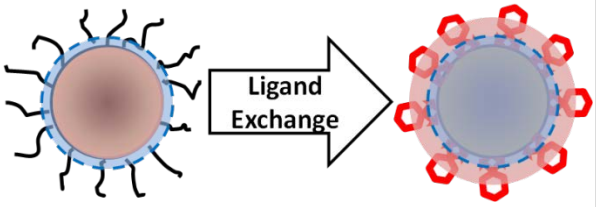

Figure 1. Ligand exchange from native insulating ligands to dithiocarbamates delocalizes the excitonic wavefunction of a quantum dot into the ligand shell.

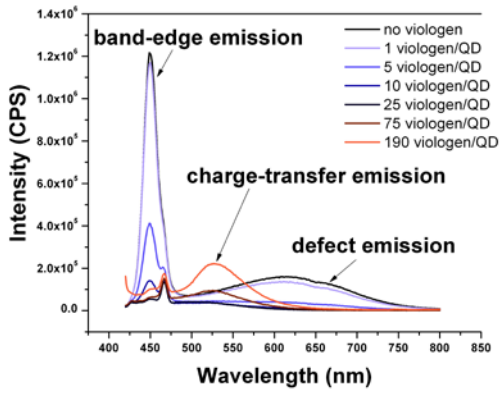

Figure 2. Charge transfer emission from recombination of an ion pair within a QD-viologen donor-acceptor system.

Tuning Photochemical Function of Multimetallic Assemblies Linked by Artificial Oligopeptide Scaffolds

Joy A. Gallagher, Meng Zhang, Sha Sun, Carl Myers and Mary Beth Williams
Department of Chemistry
The Pennsylvania State University
University Park PA 16802

Artificial oligopeptides with pendant ligands serve as scaffolds to tether together multiple metal complexes in relative arrangements that are determined by the peptide. When the artificial peptides are presented with transition metal ions, multimetallic structures self-assemble. Changing the ligands, metal ions, and peptide structure tune the photochemical properties to ultimately enable long-distance electron transfer and long-lived charge separated states. In this poster we describe recent results and the first demonstration of these structures for photocatalysis.

We have recently incorporated hydroxyquinoline (hq) ligands on the peptide backbone; reaction with zinc acetate led to a fluorescent multimetallic duplex with three Zn^{II} coordinative crosslinks. Binding was monitored using spectrophotometric absorbance and emission titrations; NMR spectroscopy and mass spectrometry confirmed the identity and stoichiometry of the product structure. Zn-oligopeptide duplex formation had a sigmoidal titration curve, an equilibrium constant larger than the monomeric analog, and Hill coefficient > 1, all of which indicate positive binding cooperativity, A higher than expected quantum yield for the trimetallic complex suggested a structure in which the central chromophore is shielded from solvent by π-stacking with neighboring Zn complexes. Building on this work, we have synthesized heterofunctional oligopeptides containing hq and bipyridine (bpy) ligands to investigate the effect of the local environment on the excited state lifetime of the $[Zn(hq)_2]$ complex within the structure. We find that the number of proximal $[Zn(bpy)_2]^{2+}$ to the hq complex dictates the stability of the excited state, and can be used to tune the radiative relaxation rate and wavelength of the emitted photon.

In separate experiments, $[Zn(bpy)_2]^{2+}$ has been shown to modestly quench the $[Ru(bpy)_3]^{2+}$ excited state when these are linked by an artificial oligopeptide scaffold. To investigate the causes of this behavior, ^1H NMR spectroscopy was used to quantitatively monitor changes in the structure and environment of the Ru oligopeptide complex during a titration as Zn^{2+} is added. Using spectral assignments from 1 and 2D NMR spectra, the spectrophotometric titrations reveal that Zn^{2+} binding causes significant shifts that are a direct result of changes in the local environment and are the combination of electrostatic interactions between the two dication metal complexes and strain induced by the metal ion crosslinking the strands.

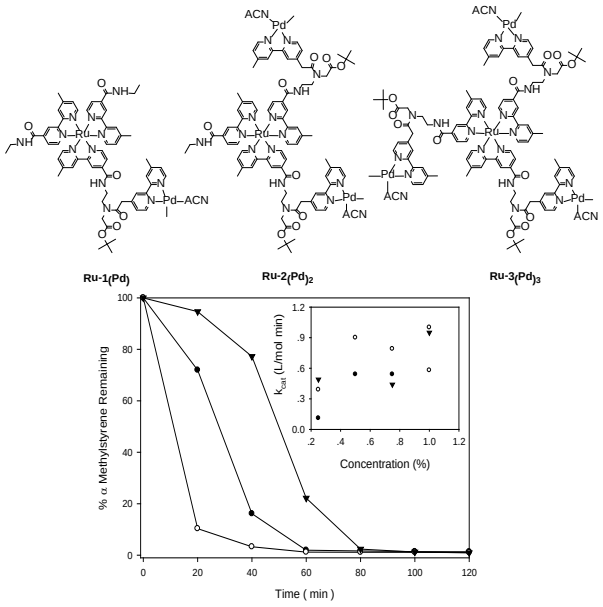

Plots of the amount of α-methylstyrene remaining in the reaction mixture following irradiation with light > 455 nm in CD_3NO_3 solutions containing 1.8 M α-methylstyrene and (●) 0.02 M **Ru-1**(Pd); (○) 0.02 M **Ru-2**$(Pd)_2$; and (▼) 0.02 M **Ru-3**$(Pd)_3$ Inset: Plot of k_{cat} versus RuPd catalyst concentration.

The $[Ru(bpy)_3]^{2+}$ oligopeptide complex was also used to create heterometallic structures with 1 - 3 bound Pd^{2+} to form photocatalysts for the dimerization of α-methylstyrene. Unlike previously reported Ru-Pd compounds, these aeg-linked structures do not contain conjugated bridges, sensitization proceeds by electron transfer, and the catalysts have faster reaction rates. This is the initial evidence for the ability to use this artificial oligopeptide scaffold to create functional catalytic assemblies.

Posters: Catalysis at Surfaces

High-Potential Photoanodes for Visible Light-Induced Water Oxidation

Gary F. Moore, Steven J. Konezny, Hee-eun Song, Rebecca L. Milot, James D. Blakemore, Julianne Thomsen, Lauren Martini, Lawrence Cai, Victor S. Batista, Charles A. Schmuttenmaer, Robert H. Crabtree and Gary W. Brudvig

Department of Chemistry
Yale University
New Haven CT 06520-8107

We have studied a series of high-potential porphyrin photoanodes (HPPPs) for use in photoelectrochemical cells.[1,2] The anodes consist of pentafluorophenyl-substituted free-base and metalloporphyrin photosensitizers bearing anchoring groups for attachment to TiO_2 or SnO_2 nanoparticles. Photoelectrochemical measurements demonstrate that the photosensitizers extend the absorption of the bare anode well into the visible region. Terahertz spectroscopic studies show the photoexcited dyes are capable of injecting electrons into the conduction band of an underlying metal-oxide with appropriate energetics. The reduction potentials of the resulting photogenerated porphyrin radical cations range from ~1.35 - 1.65 V vs NHE. This is demonstrated by the ability of dye-sensitized solar cells, containing our HPPPs, to use the Br_3^-/Br^- redox couple as a regenerative electron mediator with superior performance compared to results obtained using the lower-potential I_3^-/I^- relay.[2] Computational modelling of the structures and equivalent circuits assists in a molecular-based understanding of these systems. Recent efforts have focused on modification of the anchoring groups used for surface attachment and variation of the electronic properties of the photosensitizer. These modifications enable a photoelectrochemical cell containing a HPPP and an Ir-based water-oxidation catalyst to perform visible light water splitting with zero bias voltage and no UV-light requirement. In future work, we aim to provide quantitative efficiency data on the basis of a better understanding of the loading of the components and the oxygen output of the cell.

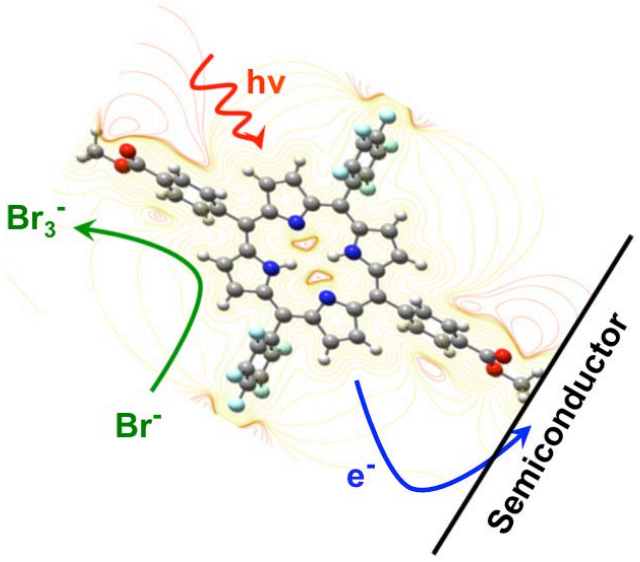

References

1. G. F. Moore, J. D. Blakemore, R. L. Milot, J. F. Hull, H. Song, L. Cai, C. A. Schmuttenmaer, R. H. Crabtree, and G. W. Brudvig (2011) *Energy Environ. Science* **4**, 2389–2392.

2. G. F. Moore, S. J. Konezny, H.-e. Song, R. L. Milot, J. D. Blakemore, M. L. Lee, V. S. Batista, C. A. Schmuttenmaer, R. H. Crabtree and G. W. Brudvig (2012) *J. Phys. Chem. C* **116**, 4892–4902.

Diode Linkers, Self Assembly and Anchor Strategies for Solar Applications

Lauren Martini, Laura Allen, Gary F. Moore, Steven J. Konezny, Rebecca L. Milot, James D. Blakemore, Lawrence Cai, Victor S. Batista, Charles A. Schmuttenmaer, Robert H. Crabtree and Gary W. Brudvig

Chemistry Department
Yale University
New Haven, CT, 06520-8107

Multielectron oxidations, such as water splitting, need the redox states of the catalyst to be successively advanced. These reactions may be enhanced by using linkers that encourage one-way transit of photoinjected electrons so that back transfer does not undo the work of the initial photoinjection. We have designed linkers that have this diode or rectifier property. Thus, for **1** we see a strong rectification both *in vitro* and *in silico* (NEGT/DFT) with preferred electron flow in the direction shown by the arrow, but on reversal of the peptide bond (**2)** that property is lost.

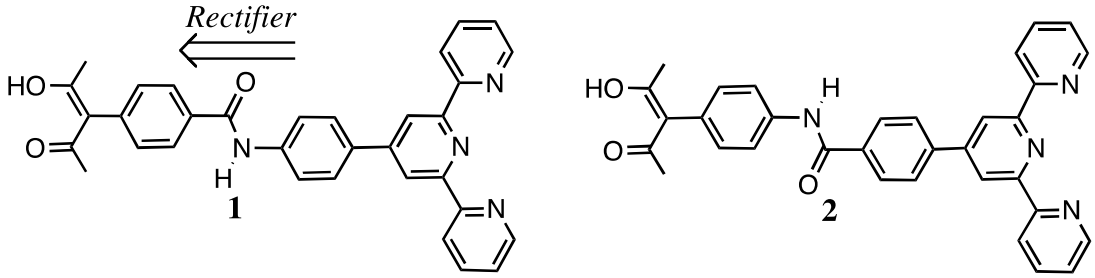

Isonicotinamide pattern linkers (**3**) with Q = COOH (**a**), PO_3H_2 (**b**), $C(COMe)_2$ (**c**) and CONHOH (**d**) for binding to P25 TiO_2 NPs were compared in terms of water stability and electron photoinjection efficiency. **3a** was an efficient injector but was detached on prolonged (17 h) water treatment. **3b-c** were stably attached but gave somewhat less efficient injection (by ultrafast THz spectroscopy). Only **3d** combined efficient injection with stable attachment.

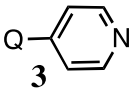

We were able to self-assemble a T-shaped construct on TiO_2 NPs consisting of a type 3 linker with a high-potential Zn porphyrin attached via the pyridine group. Complexation was verified by UV-visible spectroscopy.

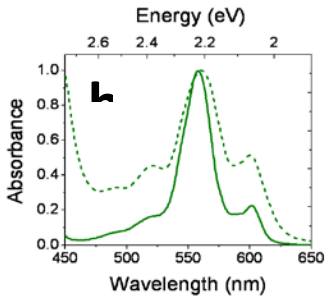

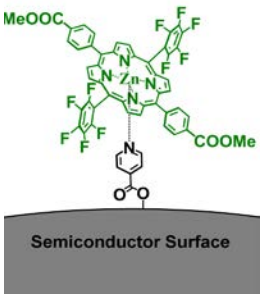

Effect of Molybdenum Doping on the Photoelectrochemical Properties of Electrochemically Prepared n-Type $BiVO_4$ Electrodes

Yiseul Park, Jason A. Seabold and Kyoung-Shin Choi
Department of Chemistry
Purdue University
West Lafayette IN 47907

N-type $BiVO_4$ electrodes were prepared by a new simple electrodeposition method and studied as photoanodes for sulfite and water oxidation under illumination (AM 1.5G, 100 mW/cm^2). The $BiVO_4$ electrodes maintained considerable photocurrent for photo-oxidation of sulfite, but generated significantly reduced photocurrent for photo-oxidation of water to oxygen, also decaying over time, suggesting that the photoelectrochemical performance of $BiVO_4$ for water oxidation is mainly limited by its poor catalytic ability to oxidize water. In order to improve the water oxidation kinetics of the $BiVO_4$ electrode, a layer of FeOOH was placed on the $BiVO_4$ surface as an oxygen evolution catalyst using a new photodeposition route. The resulting $BiVO_4$/FeOOH photoanode exhibited significantly improved photocurrent and stability for photo-oxidation of water, which is one of the best among all oxide-based phoatoanode systems reported to date. In particular, the $BiVO_4$/FeOOH photoanode showed an outstanding performance in the low bias region (i.e., E < 0.8 V vs. RHE) reaching 1.0 mA/cm^2 at only *ca.* 0.5 V vs. RHE, which is critical in determining the overall operating current density when assembling a complete p-n photoelectrochemical diode cell. The performances of $BiVO_4$ electrodes for photoelectrochemical oxidation of both sulfite and water were also significantly enhanced by Mo-doping (Figure 1). Two different Mo-doping methods (e.g. co-deposition and post-deposition surface treatment) were developed, which resulted in different Mo distributions in the $BiVO_4$ layer and, therefore, different effects. In this study, various electrochemical and photoelectrochemical characterizations were performed and discussed to better understand the role of the FeOOH layer and Mo-doping in charge transport, electron-hole recombination, and interfacial hole transfer processes.

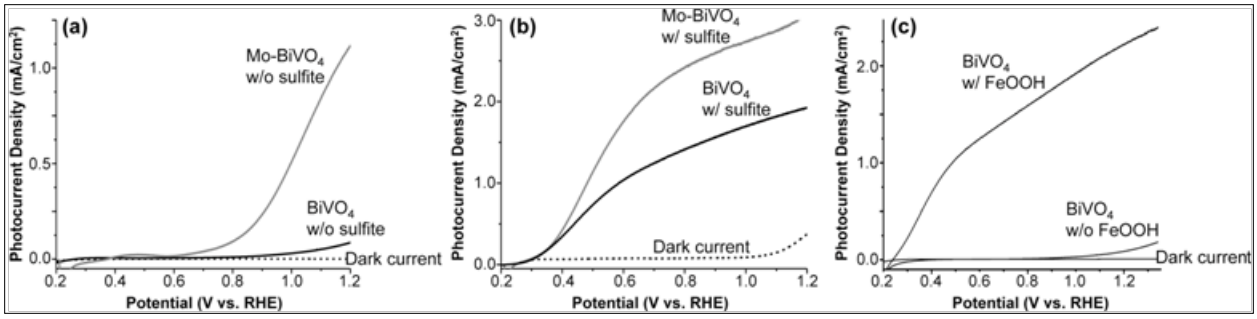

Figure 1. Photocurrent-potential plots of $BiVO_4$ photoanodes showing the effect of Mo-doping (a) on water oxidation and (b) on sulfite oxidation and (b) the effect of adding FeOOH oxygen evolution catalyst on water oxidation obtained in 0.1 M KH_2PO_4 (pH 7) under AM 1.5G illumination (100 mW/cm^2) (scan rate = 10 mV/s). 0.1 M Na_2SO_3 was added for sulfite oxidation.

CO_2 Hydrogenation and Formic Acid Decomposition with Ir Complexes with Pendent Bases

Jonathan F. Hull,[a] Wan-Hui Wang,[b] Yuichiro Himeda,[b] James T. Muckerman[a] and Etsuko Fujita[a]

[a]Chemistry Department, Brookhaven National Laboratory, Upton NY 11973-5000 USA

[b]National Institute of Advanced Industrial Science and Technology, Tsukuba Central 5-2, 1-1-1 Higashi, Tsukuba, Ibaraki 305-8565, Japan

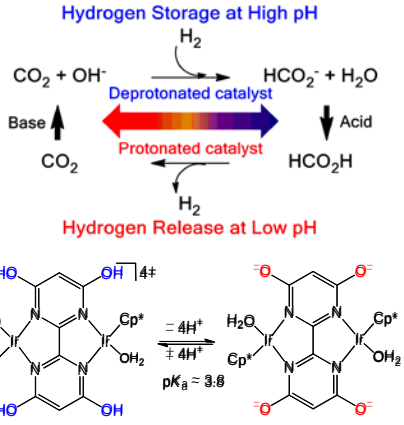

Advanced catalysts for electro- and photocatalytic water splitting and CO_2 reduction are central for solar fuel generation. Exceptionally high catalytic activities for CO_2 hydrogenation to formate were observed for $[(H_2O)Cp^*Ir(4,4',6,6'\text{-}(OH)_4\text{-bpm})IrCp^*(OH_2)]^{4+}$, **1**, and $[Cp^*Ir(6,6'\text{-}(OH)_2\text{-bpy})(OH_2)]^{2+}$, **2a**, (bpm = 2,2'-bipyrimidine, bpy = 2,2'-bipyridine) at ambient temperature and pressure in water, and under only slightly harsher conditions initial rates were up to 53,800 h^{-1} and 46,600 h^{-1}, respectively.[1,2] These complexes also act as catalysts for formic acid decomposition to produce H_2 and CO_2 without any detectable CO upon changing the pH of the aqueous solution. We observe a TOF of 228,000 h^{-1} at 90 °C and TON of 308,000 at 80 °C with catalyst **1**, the highest TOF and TON yet reported. The –OH moieties on the bpm or bpy ligand are pH responsive, allowing H_2 storage to be turned on or off by adjusting the pH of the solution. CO_2 hydrogenation is facilitated because, in addition to electronically activating the catalyst, the $-O^-$ on the ligand facilitates H_2 heterolysis by acting as a pendent base. We are currently carrying out detailed experimental and theoretical investigations of the mechanism and kinetics of these catalysts. Recent progress with related species shown below will be also discussed.

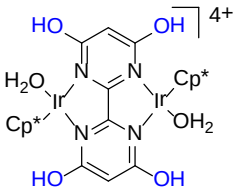

1

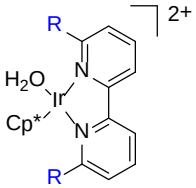

2a R = OH
2b R = OMe
2c R = Me
2d R = H

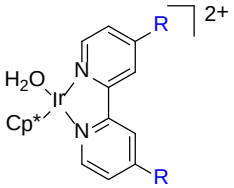

3a R = OH
3b R = OMe
3c R = Me

1. Hull, J. F.; Himeda, Y.; Wang, W.-H.; Hashiguchi, B.; Periana, R.; Szalda, D. J.; Muckerman, J. T.; Fujita, E. "Reversible Hydrogen Storage using CO_2 and a Proton-Switchable Iridium Catalyst in Aqueous Media under Mild Temperatures and Pressures," *Nature Chemistry*, **2012**, DOI: 10.1038/NCHEM.1295.

2. Wang, W.-H.; Hull, J. F.; Muckerman, J. T.; Fujita, E.; Himeda, Y. "Combined Ligand Effects Enhance Iridium(III)-Catalyzed Homogeneous Hydrogenation of Carbon Dioxide in Water near Ambient Temperature and Pressure," submitted.

Electron Transfer Induced Excitation of Vibrational Modes: Implications for Solar Energy Conversion

Lars Gundlach
Department of Chemistry & Biochemistry
University of Delaware
Newark DE 19716

Electron transfer (ET) induced excitation of vibrational modes is a process that has received little attention in experimental and theoretical investigations of ET in system that are relevant for solar energy conversion. Recently, we found that a large amount of energy (~400 meV) is transferred from the electronic excited donor state of an organic dye molecule to vibrational excitation of the cation molecular product state during ET to a TiO_2 electrode.[1] The electron was thus injected well below the energy level of the molecular excited state (Fig.1). This process is of practical importance, e.g. for utilizing the excess energy of hot electrons in photovoltaic devices. It constitutes an additional loss channel that is poorly understood so far and has to be considered in all devices employing a light absorber that give rise to sufficient coupling between the excited electronic state and vibrational modes or phonons in the absorber material. In addition to DSSCs discussed above, this type of scattering can occur, e.g. at the electrode/polymer interface in organic solar cells,[2] at the quantum-dot/semiconductor interface in q-dot solar cells,[3] and in metal organic complexes relevant for artificial photosynthesis.[4] Energy transfer from the excited electronic state to vibrational excitation of the electron donor can be studied by either measuring the spectrum of the injected electrons in the electron accepting material (Fig.1), or by measuring the vibrational excitation of the oxidized donor after ET. The later approach is a promising way to gain insight into energetics and dynamics of ET induced vibrational excitation. It has not been exploited in comparable systems so far. Measurements in this direction are underway in our lab. Understanding ET coupled vibrational excitation is a prerequisite for controlling the transformation of energy in material systems that are relevant for PV applications. It allows for designing donor/acceptor combinations where ET coupled vibrational excitation is either reduced for efficient utilization of hot carriers, or to find schemes that utilize the energy stored in the vibrational excitation for charge separation, e.g. in molecular dyads, or in coupled dye quantum dot light harvesting assemblies.

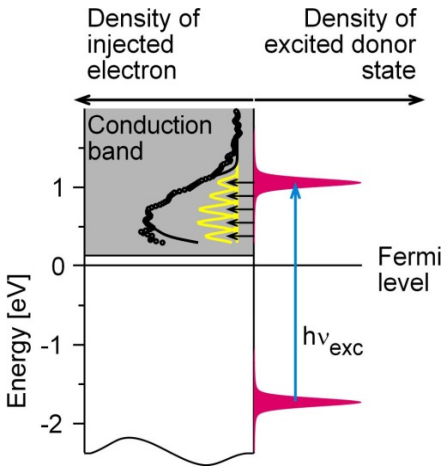

Fig. 1: Spectrum of injected electrons and scheme illustrating ultrafast non-adiabatic electron transfer. The energy distribution of the excited molecular donor state (upper red curve) is much narrower than the energy distribution of the injected electron. The latter spreads from the donor state to lower energies in the electronic acceptor states and shows vibrational structure.

[1] L. Gundlach, F. Willig, ChemPhysChem (2012) in print; L. Gundlach, T. Letzig, F. Willig, J. Chem. Sci. **121** (2009) 561.
[2] K. Kanemoto, M. Yasui, T. Higuchi, D. Kosumi, I. Akai, T. Karasawa, H. Hashimoto, Phys. Rev. B **83** (2011) 205203.
[3] W. A. Tisdale, K. J. Williams, B. A. Timp, D. J. Norris, E. S. Aydil, X.-Y. Zhu, Science **328** (2010) 1543.
[4] M. S. Lynch, B. E. Van Kuiken, S. L. Daifuku, M. Khalil, J. Phys. Chem. Lett. **2** (2011) 2252.

Photoemission Studies on a Model Visible Light Photocatalyst: $LaFeO_3$

Michael A. Henderson, Sara E. Chamberlin and Mark H. Engelhard
Chemical and Materials Sciences Division and Environmental Molecular Sciences Laboratory
Pacific Northwest National Laboratory
Richland WA 99352

The limitations of TiO_2, and many other wide bandgap semiconducting materials, to function adequately as visible light photocatalysts has motivated researchers to explore the properties of more complex semiconductors. Several iron-based ternary oxides show promise as potential visible light photocatalysts. In particular, metal ferrites ($MFeO_3$) have been shown to catalyze a variety of visible light photoreactions. An example of this class of oxides is $LaFeO_3$, which is a charge transfer insulator with an optical band gap of ~2.2 eV and demonstrated visible light activity for degradation of various organic dyes.

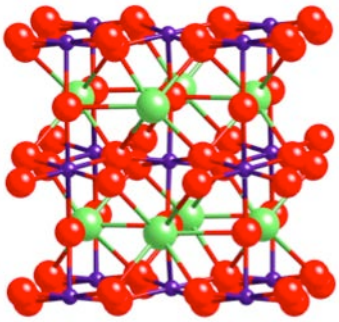

$LaFeO_3$: La (yellow), Fe (blue) and O (red).

We have examined the chemical and photochemical properties of $LaFeO_3$ starting with photoemission studies of a commercially available powder that possesses an average 10 nm particle size. X-ray diffraction confirmed that the powder was highly crystalline with the expected diffraction features for $LaFeO_3$ in the perovskite structure. However, weak diffraction features were also detected for hematite (α-Fe_2O_3) in this powder. Calibrations of the diffraction intensities led to an estimated hematite concentration of ~7%. The $LaFeO_3$ powder was pressed in a metal mesh for XPS analysis. The binding energies for Fe, O and La in the powder were consistent with those expected for $LaFeO_3$. The as-received powder was contaminated with sulfate and carbonaceous species, most likely from airborne exposure. Heating the powder in vacuum at 400°C resulted in loss of most of the sulfate, suggesting this impurity was present as surface species. However, appearance of a very weak Fe^{2+} feature on the high binding energy side of the prominent Fe 2p Fe^{3+} feature indicated that vacuum annealing initiated some surface reduction, perhaps in connection with removal of the sulfate. Further annealing at 500 °C depleted both remaining sulfate and surface C, but also resulted in additional Fe^{2+}. Work will be presented on the reoxidation of the surface and adsorption of various probe molecules such as water and CO_2, as well as initial assessments of the photoactivity of $LaFeO_3$.

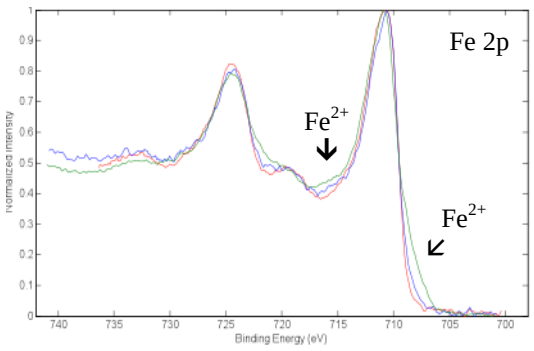

Fe 2p XPS spectra from $LaFeO_3$: as-received (red), heated at 400°C (blue) and 500°C (green) in vacuum for 1 hour.

This work was supported by the US Department of Energy, Office of Basic Energy Sciences, Division of Chemical Sciences, Geosciences & Biosciences. Pacific Northwest National Laboratory (PNNL) is a multiprogram national laboratory operated for DOE by Battelle. The research was performed using EMSL, a national scientific user facility sponsored by the Department of Energy's Office of Biological and Environmental Research and located at PNNL.

Solar Energy-Driven Multi-Electron-Transfer Catalysts for Water Splitting: Robust and Carbon-Free Nano-Triads

Elliot N. Glass, Chongchao Zhao, Zhuangqun Huang, John Fielden, Alex L. Kaledin, Yurii Geletii, William Rodríguez-Córdoba, Djamaladdin G. Musaev, Tianquan Lian, Craig L. Hill

Department of Chemistry
Emory University
Atlanta GA 30322

One of the specific technical objectives of our integrated experimental-computational project is to prepare and characterize tunable and POM-based molecular metal-to-metal charge transfer (MMCT) chromophores, which will be used as the light-harvesting component of our all-inorganic photo-driven water oxidation triads to overcome the well-known hydrolytic instability of organic dyes. To date our team has made considerable progress toward all program goals.

1. Recently [JACS, **2011**, *133*, 20134], we reported, $[P_4W_{35}O_{124}\{Re(CO)_3\}_2]^{16-}$ (**1**), a complex comprising the $[Re(CO)_3]^+$ unit supported on a POM, the defect Wells-Dawson-type $[\alpha_2\text{-}P_2W_{17}O_{61}]^{10-}$, that exhibits an intense Re-to-POM charge transfer transition. The UV-vis spectrum of **1** in CH_2Cl_2 and in H_2O shows an intense broad absorption (up to 700 nm) covering the entire UV and visible regions. It has high visible absorptivity (ε_{400nm} ~ 6,200 and 4,500 $M^{-1}\cdot cm^{-1}$ in water and CH_2Cl_2, respectively). Importantly, **1** is free of the oxidatively and hydrolytically unstable polypyridyl ligands. The origin of high visible absorptivity of **1** was investigated by computational methods. Based on these studies, the visible absorption of **1**, is attributed to the Re-to-POM ligand charge transfer transition.

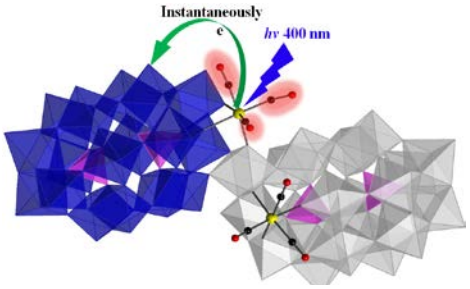

2. The second approach is based on incorporation of a redox active transition metal into a POM-framework. At first, we are focused on the cobalt-centered Keggin anions, $[Co^{II}_2(H_2O)W_{11}O_{39}]^{8-}$ (**2**), $[Co^{III}Co^{II}(H_2O)W_{11}O_{39}]^{7-}$ (**3**), $[Co^{II}W_{12}O_{40}]^{6-}$ (**4**) and $[Co^{III}W_{12}O_{40}]^{5-}$ (**5**). Extensive studies show that **2** and **3** have strong absorptions that tail into the visible, with extinction coefficients of around 1000 $M^{-1}cm^{-1}$ at 400 nm. Photo-excitation of **2** at 400 nm produces a ground state bleach at 620 nm, and an intense absorption band appears at 475 nm. Decay kinetics indicate an excited state lifetime of ca. 100 ps, and the excited state absorption spectrum shows similar features to its one-electron-oxidized ($Co^{III}Co^{II}$) counterpart **3**; suggesting photo-induced injection of the electron into the polytungstate ligand resulting in a $Co^{II}Co^{III}$ inter-valence-charge transfer chromophoric unit. This conclusion was also confirmed by our DFT calculations. Both DFT and EPR indicate that the central Co atom in **3** is Co(III).

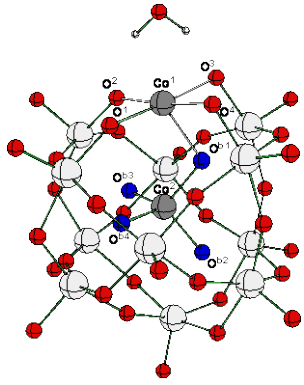

Charge Transfer Dynamics in Semiconductor–Chromophore–Polyoxometalate Interfaces: Towards Water-Oxidizing Photoelectrodes

J. Fielden, X. Xiang, Z. Huang, W. Rodríguez-Córdoba, N. Zhang, Z. Luo, Y.Geletii,
D. G. Musaev, T. Lian and C. L. Hill
Department of Chemistry
Emory University
Atlanta GA 30322

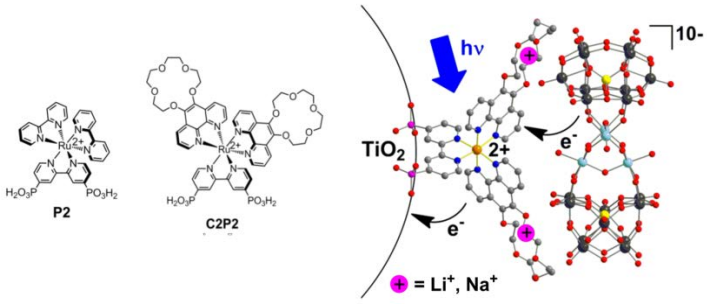

Triadic photoelectrodes have been assembled from semiconducting metal oxides (TiO_2 and SnO_2), Ru-polypyridyl photosensitizers (P2 and C2P2, see Figure) and the water oxidation catalyst $[\{Ru_4O_4(OH)_2(H_2O)_4\}(\gamma\text{-}SiW_{10}O_{36})_2]^{10-}$ (Ru_4POM). Electron transfer processes in these triads and their parent metal oxide–sensitizer dyads have been studied by visible and mid-IR transient absorption spectroscopy (TAS), and preliminary investigations made of the photoelectrochemical (PEC) performance of the systems. Upon excitation at 515 nm, TiO_2–P2 shows femtosecond and picosecond timescale electron injection processes from the sensitizer to the TiO_2 conduction band (monitored at 5000 nm), respectively corresponding to injection from the unrelaxed ^{1}MLCT and relaxed ^{3}MLCT excited states. For theTiO_2–P2–Ru_4POM triad, the slower injection is suppressed, possibly due to competing electron transfer from the ^{3}MLCT excited states of P2 to Ru4POM. On SnO_2, however, electron injection is independent of the presence of Ru_4POM, as the lower conduction band edge increases the driving force for electron transfer to the metal oxide. Visible TAS of both TiO_2 and SnO_2 based systems indicates substantially faster (*ca*. 1 ns) decay of the P2 ground state bleach (GSB) in the presence of Ru_4POM, suggesting electron transfer from the catalyst to the oxidized dye. Furthermore, in the SnO_2–P2–Ru_4POM system a long-lived positive absorption band is observed after the GSB decay is completed, which by spectroelectrochemistry is tentatively assigned to oxidized Ru_4POM. Triads based on the crown–ether derivatized sensitizer C2P2 have similar overall behavior to the P2-based systems, but show improved electron injection when the crown ether is metallated with Li^+/Na^+. PEC measurements indicate substantial (up to 100%) photocurrent enhancements in the presence of Ru_4POM, with metallated C2P2 based electrodes showing higher photocurrents and greater stability than those based on P2.

Charge Separation Dynamics in Covalently Linked Sensitizer and POM Complexes

Alexey Kaledin,[1] Xu Xiang,[1] Benjamin Matt,[2] Guillaume Izzet,[2] Anna Proust,[2]
Jamal Moussa,[2] Hani Amouri,[2] William Rodríguez-Córdoba,[1] Zhuangqun Huang,[1]
Djamaladdin G. Musaev,[1] Tianquan Lian,[1] Craig L. Hill[1]

[1]Department of Chemistry, Emory University
Atlanta, Georgia 30322

[2] Institut Parisien de Chimie Moléculaire, Université Pierre et Marie Curie Paris 06
75252 Paris France

The development of efficient and robust electrode-sensitizer-catalyst triads remains one of the major challenges in the field of solar-fuel conversion. Our team is investigating three approaches for constructing triadic/dyadic photoelectrode systems containing polyoxometalate (POM)-based water oxidation catalysts (WOCs). These include a) direct attachment of WOCs to narrow band gap oxide semiconductor electrodes (such as Fe_2O_3), b) Development of all inorganic POM based light harvesting complexes with metal-POM charge transfer transitions, and 3) TiO_2-sensitizer-POM triads. We have made excellent progress in all three approaches, which are covered in our other posters and the talk. In this poster, we focus a recent study of a series of covalently linked POM-sensitizer complexes (Figure 1) in collaboration with Anna Proust's group at the University of Paris 6, France.

The heteroleptic cyclometalated iridium(III)-polyoxometalate dyads were synthesized by coupling a new neutral Ir(III) complex bearing two 2-phenylpyridyl (ppy) and a pyridylcarboxylate (pic) ancillary ligands with a unique pendant terminal alkynyl tether to an organo-silyl or organo-tin derivatized POM electron acceptor moiety. Using transient absorption (TA) spectroscopy and computation, we show that upon excitation of the MLCT transition in the Ir complex, the electron is transferred to the POM. This assignment is confirmed by spectroelectrochemistry and computation. The TA spectra of the charge separated state consist of reduced POM and oxidized Ir complexes. The charge separation and recombination rates depend sensitively on the structure of the POM and the chemical linkage between the sensitizer and the POM. The charge separation rate is faster with the –Si-O- linkage compared to the Sn-O bond, and the ET rate to the Keggin POM is much faster than that to the Dawson POM. The molecular origins of the linker and POM dependence are being investigated in an ongoing computational study.

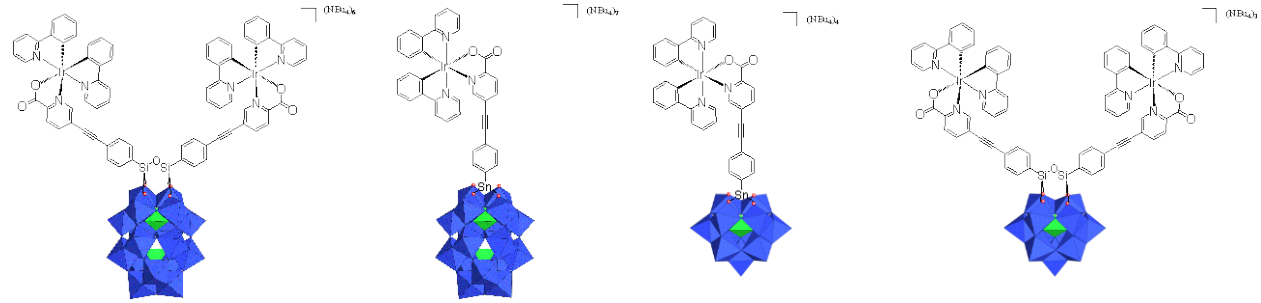

Figure 1. Structures of four covalently linked sensitizer-POM complexes.

Thin Film and Single Crystal Studies of $LaTiO_2N$ and $La_2Ti_2O_7$

Limin Wang, Andrew Malingowski, Peter Khalifah
Department of Chemistry
Stony Brook University
Stony Brook NY 11794-3400

Prior measurements on $LaTiO_2N$ have showed that this semiconductor has a band gap (~2.2 eV) which absorbs most of the visible light spectrum and also has band edge energies appropriate for driving both half reactions for overall water splitting. This system has not yet been shown to be capable of overall water splitting, but merits further investigation due to the tunable nature of its perovskite structure. It was previously demonstrated that epitaxial $LaTiO_2N$ thin films could be generated by treating the surface of $La_2Ti_2O_7$ single crystals with ammonia gas at high temperatures. $La_2Ti_2O_7$ has a perovskite-related structure, a wide band gap (~3.7 eV), and is known to be capable of driving overall water splitting with a high quantum yield using high-energy uv photons.

The full optical constants of both $LaTiO_2N$ and $La_2Ti_2O_7$ were for the first time investigated using spectral ellipsometry. Both semiconductors were found to have very large absorption coefficients ($\alpha > 10^5$ cm^{-1}) at energies slightly above their band gap. The optical response of $LaTiO_2N$ appeared to feature separate oscillators representing excitations from oxygen and nitrogen *2p* states, with the nitrogen oscillators located about 1 eV lower in energy than those of oxygen. The optical properties of $LaTiO_2N$ were found to be in good agreement with the results of first principles calculations carried out by our collaborators (Wei Kang, Mark Hybersten, BNL CFN), and have demonstrated the appropriateness of the theoretical methods chosen to study the partially ordered anion lattice of this semiconductor.

It is also demonstrated that thin films of $LaTiO_2N$ can be prepared on top of single crystals of $La_5Ti_5O_{17}$, a reduced titanate which is sufficiently conductive to serve as a back electrical contact for $LaTiO_2N$ films. This enabled the first photoelectrochemical measurements of highly crystalline $LaTiO_2N$, done with our collaborators (Qixi Mi, Nathan Lewis, Caltech) Under a high applied bias, water oxidation quantum yields of 20% were obtained at uv energies and 5% in the visible range with the photoresponse extending out to the band gap energy of the film (2.2 eV). The photoresponse of this system was only slightly reduced when high energy photons were removed, demonstrating the appropriateness of this system for harvesting visible light photons. Short term stability studies showed no noticeable decay over the investigation period (~200 turnovers).

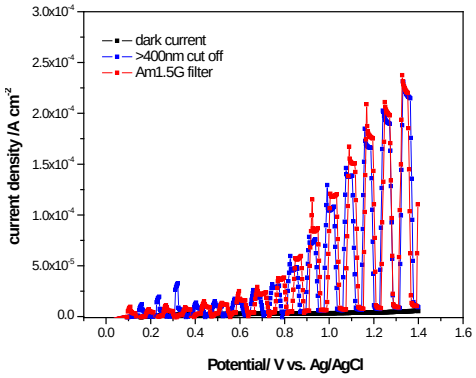

Collaborative surface science studies (John Lofaro, Michael White, SBU/BNL) have been initiated to explore the surface structure of $La_2Ti_2O_7$ and its interactions with water. Preliminary results suggest that the surface is La-rich, and that the binding of water to the (001) cleavage plane occurs by moderate strength chemisorption (250 – 325K) at low surface coverage through a mechanism which does not depend on defects.

The Ongoing Transformation of Atomic Resolution Transmission Electron Microscopy

C. Kisielowski [1,2], B. Barton[3], P. Specht[3]
Joint Center for Artificial Photosynthesis[1], National Center for Electron Microscopy[2]
Materials Sciences Division[3]
Lawrence Berkeley National Laboratory
Berkeley CA 94720 USA

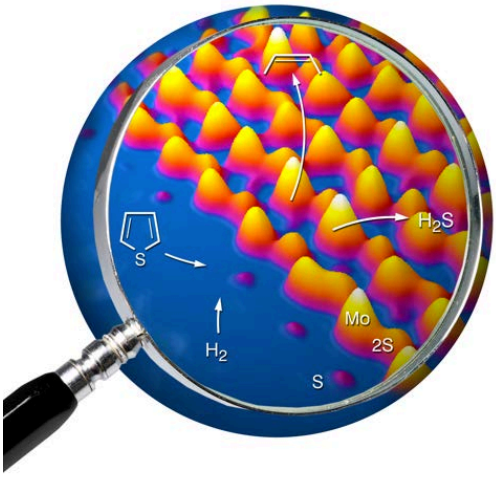

Desulfurisation catalysis: Detection of single sulfur atoms at the edge of industry-style MoS_2 crystals. Angewandte Chemie – Int. Ed. 50 (2011) 10153.

In recent years the TEAM Project delivered next-generation transmission electron microscopes of extraordinary performance. They are operated at the National Center for Electron Microscopy (NCEM) with great success since they allow for dynamic studies (<1 kHz) with single atom sensitivity across the Periodic Table of Elements. Image resolution is now limited at a fundamental level to ~ 0.5 Å by the Coulomb scattering process itself and by beam-sample interactions. As a result, it is not longer attempted to improve on resolution or to maintain structural integrity of beam sensitive materials. Instead, "hit and destroy" concepts are explored where fast exposure techniques outrun or monitor the materials disintegration. Alternatively, one may speculate about a possible reduction of beam-sample interactions by allowing for optimized energy dissipation or even self-healing of the samples during observation.

This investigation suggests that a further development of electron microscopy using variable voltages (20 - 300 kV) and dose rates as small as 1 - 10 electrons/Å^2/s will enable capturing the complex structure of hybrid materials at atomic resolution. The proposed technique improves on the contrast of hard and soft matter components and reduces beam-sample interactions. At this point we have demonstrated that single carbon atoms remain reasonably stable at low voltage even if non-periodic structures are exposed to a high dose. A dose rate reduction allows for the detection of single edge atoms in industry-style catalysts in both scanning (see figure) and broad-beam imaging modes. Preliminary dynamic experiments suggest that even conformational changes of single molecules will become detectable with a minimal loss of a resolution. Further, the developed principle can be applied to study the functionality of hybrid materials at elevated temperature and pressure. Consequently, extension of the concept to environmental microscopy will enable studying the functionality of atom clusters and single molecules in conditions of well-defined chemical potentials. Such capabilities are currently not available but are of general interest to material, chemical, and biological sciences and can help to improve our understanding of artificial photosynthetic systems that will produce transportation fuels from sunlight*.

* NCEM is supported by the Scientific User Facilities Division of the U.S. Department of Energy.

Solar Energy Conversion Properties of Cu_2O and Coupling Earth Abundant Catalyst to Absorbers for Solar-Driven Water-Splitting Cells

Emily Warren, Chengxiang Xiang, Ron Grimm, Nathan S. Lewis
Department of Chemistry and Chemical Engineering
California Institute of Technology
Pasadena, California 91125

Low cost, earth-abundant light absorbers are of great interest for use in terrestrial photovoltaics and in artificial photosynthesis. After early research work in the 1980s, cuprous oxide (Cu_2O) has recently received renewed interest for such applications. The major challenge for this material is the lack of suitable n-type heterojunction partners, due to its extremely low electron affinity (3.2 eV vs. vacuum) and deleterious interface reactions, which motivates the study of preparing interfaces that are electrically passive and chemically inert.

We employed semiconductor/liquid junctions as a noninvasive method to investigate the energy-conversion properties of Cu_2O and demonstrated high open-circuit voltage (V_{oc}=820 mV) and near ideal photoelectrochemical performance of Cu_2O photoelectrodes in contact with decamethylcobaltocene$^{+/0}$ ($Me_{10}CoCp_2^{+/0}$) redox couple. Cu_2O photoelectrodes that were passivated by 0.5 nm of AlO_x using Atomic Layer Deposition (ALD) exhibited similar open-circuit voltage and reduced short-circuit current density due to the series resistance in contact with nonaqueous metallocene redox couples. We also demonstrated successful attachment of organic moieties including perfluoronated silanes to Cu_2O photoelectrodes, which behaved as a buffer between the copper oxide surface and aqueous environment necessary for photoelectrochemical water-splitting reactions. The observed surface passivation of Cu_2O substrates provided a promising route for fabrication of high efficiency cells with suitable emitter materials that form high barrier-height to Cu_2O substrates.

Silicon microwires (SiMW) grown by the VLS process are promising materials to serve as photocathodes to drive the hydrogen evolution reaction (HER) as part of an artificial photosynthesis device. However, a challenge to using these materials to drive a fuel-forming reaction has been coupling these materials to a suitable catalyst. Prior work has focused on the development of pn junction Si microwire arrays as efficient photovoltaic devices, but using these materials for solar-driven chemical reactions presents additional challenges.

We identified that Ni-based metal alloys are promising HER catalysts, and developed techniques to electrodeposit alloys of Ni and Mo onto Si in a way that maintains good electrical contact between the semiconductor and metallic catalyst. We demonstrated that electrodeposition of Ni-Mo onto high surface area SiMW arrays exhibited similar performance as Pt evaporated onto the same structure. We have investigated the effects of different catalyst deposition conditions, different pn junction profiles, and the effect of light trapping features on the performance of these SiMW HER photocathodes. SiMW photocathodes tested at pH 4.6 in a three-electrode electrochemical cell under 1-sun illumination achieved V_{oc}s of 490 mV (relative to the hydrogen evolution potential) and overall photocathode conversion efficiencies >2%. We have demonstrated that these photocathodes can operate under short-circuit conditions for over an hour with less then a 10% loss in current density. Additionally, we have shown that it is possible to peel the pn junction SiMW arrays off of the growth substrate in a flexible polymer, to create a flexible photocathode membrane to drive the HER.

Metal-to-Ligand Charge Transfer Excited States on Surfaces and in Rigid Media. Application to Energy Conversion

Akitaka Ito, Daniel P. Harrison, John M. Papanikolas and Thomas J. Meyer
Department of Chemistry
The University of North Carolina at Chapel Hill
Chapel Hill NC 27599

We are exploring a variety of optical, catalytic, and electron transfer phenomena in thin films containing polypyridyl complexes.

Electropolymerized Films for Optical, Membrane, and Catalytic Applications. Electropolymerization– polymerization at the surface of an electrode induced by an applied potential– is being exploited to produce thin films of electro- and/or photochemically active polypyridyl complexes on electrode and semiconductor surfaces. This well established, and useful, technique was first developed at UNC in a Meyer-Murray collaboration and is based on reductive polymerization of vinyl-derivatized polypyridyl complexes or oxidative polymerization of pyrrole-containing complexes. In contrast to other attachment strategies, which involve direct bonding to the electrode, electropolymerization has the advantage of not requiring surface modification and can be applied to any conducting substrate regardless of surface composition or morphology including functionalization of high surface area carbon electrodes. Film thickness can be controlled by controlling polymerization conditions (time, scan rate, concentration, etc.). These techniques have been used to form thin, multi-layered structures containing single-site ruthenium and other metal complexes including precursors to known catalysts in solutions. The intra-film reactivity of film-bound sites has been investigated and progress made in comparing solution and flm-based reactivity in both substitution and electron transfer reactions.

Long-Range Energy Transfer Dynamics in Optically Transparent Films. Poly(ethyleneglycol) dimethacrylate films and monoliths undergo thermal or photochemical polymerization to give optically transparent materials with features conformable to the nanoscale. We reported previously on the spectroscopic and photophysical properties of a series of polypyridyl ruthenium(II) complexes in a PEG-DMA containing nine ethylene glycol spacers (PEG-DMA550) in both fluid and film environments and have extended those measurements to a series of Os(II) complexes. At the PEG-DMA550 fluid-to-film transition, the Metal-to-Ligand Charge Transfer (MLCT) emission energies and excited-to-ground state 0-0 energy gaps (E_0) increase due to a "rigid medium effect."

We have also demonstrated long-range energy transfer from $Ru(bpy)_3^{2+}$* to two modified anthracene derivatives in rigid PEG-DMA550 films. Two different kinetic timescales for energy transfer quenching were observed, a rapid partial quenching followed by slow diffusional quenching. The kinetics of rapid exchange (Dexter) energy transfer to anthracene in mixed films were analyzed by application of energy transfer theory. The appearance of triplet-triplet annihilation provides evidence for long-range energy transfer and multiple photon effects. In films containing complex, anthracene incorporated into the polymeric network, and added methyl viologen as an electron transfer trap, ultra-long-range energy transfer sensitization of electron transfer has been observed over >90 Å.

Combinatorial Search for Metal Oxide Semiconductors that Photoelectrolyze Water

B. A. Parkinson
Department of Chemistry and School of Energy Resources
University of Wyoming
Laramie WY 82071

We are continuing the search for new oxide semiconductors that have suitable band gaps, band positions and stability to be capable of sustained photoelectrolysis of water. We believe that a tandem photoelectrolysis system, such as that shown in Figure 1, has the most potential to be efficient, inexpensive and stable. We have continued looking into the $Co_{3-x-y}Fe_xAl_yO_4$ spinels, that were identified in an earlier combinatorial study, and showed a promising band gap of ~1.6 eV and showed p-type behavior. We are currently producing combinatorial libraries of a related material series where Ga is substituted for Al in this structure. Semiconducting phases with band gaps in the range of 1.2-1.8 eV are being identified and characterized.

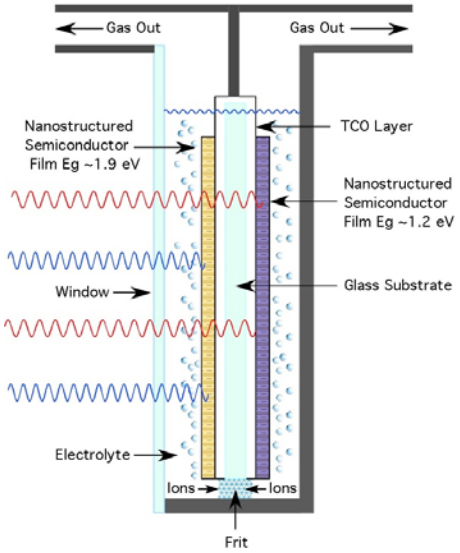

Figure 1 A tandem photoelectrolysis cell configuration with nanostructured thin films of oxide semiconductors on one substrate that is coated with a transparent conducting oxide on both sides. The larger band gap material is on the illuminated side of the cell. A frit of the proper area and porosity to allow ion flow but not add substantial resistance to the cell and prevent convective mass transfer of electrolyte is positioned at the bottom of the cell.

DOE Sponsored Hydrogen Program Publications 2009-2012

1. Michael Woodhouse and B. A. Parkinson, "Combinatorial Approaches for the Identification and Optimization of Oxide Semiconductors for Efficient Solar Photoelectrolysis", Chemical Society Reviews, 38(1), 197-210, (2009)

2. Jianghua He and B. A. Parkinson, "A Combinatorial Investigation of the Effects of the Incorporation of Ti, Si, and Al on the Performance of α-Fe_2O_3 Photoanodes", ACS Combinatorial Science, 13, 399-404, (2011)

3. F. E. Osterloh and B. A. Parkinson, "Recent developments in solar water-splitting photocatalysis", MRS Bulletin, 36(1), 17-22, (2011)

Theoretical Studies of Quantum Dots for Solar Energy Harvesting

Oleg V. Prezhdo
Department of Chemistry
University of Rochester
Rochester NY 14627

Semiconductor quantum dots (QDs) exhibit strong absorption cross sections across a broad energy range, enhancing light harvesting. Multiple exciton generation (MEG) has the potential to increase photovoltaic efficiencies by creating additional charge carriers. Extraction of hot electrons from QDs can increase photocurrent. Solar applications of QDs depend critically on interplay of photoinduced dynamics.

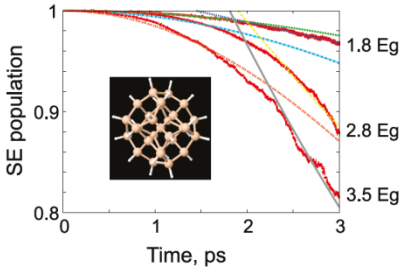

We developed time-domain ab initio simulation of Auger phenomena, including MEG and ME recombination (MER). It is the first theoretical approach describing phonon-assisted processes and early dynamics. MEG starts below electronic threshold, strongly accelerating with energy. Ligands are particularly important to phonon-assisted MEG. Short-time Gaussian component gives 10% of MEG, justifying rate theories that assume exponential dynamics. MER is preceded by electron-phonon relaxation to low energies.

High-level ab initio electronic structure calculations on Si and PbSe QDs indicate that charging, doping, dangling bonds and other defects introduce new intra-band transitions, shift optical absorption spectra and push the normal excitonic and multiexcitonic transitions to higher energies. These defects can dramatically reduce MEG yields. Generally, doping and charging have strong effects, while dangling bonds cause less severe changes, due to surface reconstruction.

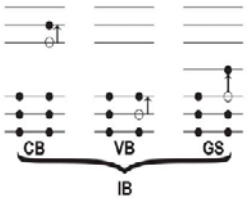

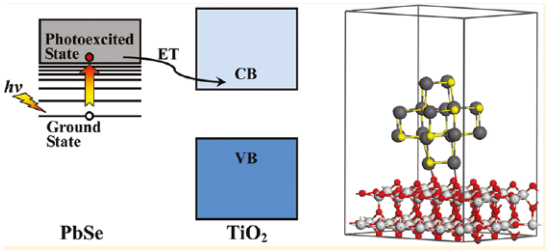

We performed ab initio nonadiabatic molecular dynamics simulations of the ultrafast photoinduced electron transfer (ET) from a PbSe QD into TiO_2, showing that the ET successfully competes with energy losses. Compared to molecule-TiO_2 interfaces, the QD-TiO_2 system exhibits pronounced differences that arise due to the larger size and higher rigidity of QDs relative to molecules.

1. S. A. Fischer, C. M. Isborn, O. V. Prezhdo, "Excited states and optical absorption of small semiconducting clusters: dopants, defects and charging", *Chem. Science*, **2**, 400 (2011).
2. L. L. Chen, et al. "Shape and temperature dependence of hot carrier relaxation dynamics in spherical and elongated CdSe quantum dots", *J. Phys. Chem. C*, **115**, 11400 (2011).
3. S. A. Fischer, O. V. Prezhdo "Dopant effects on single and multiple excitons in small Si clusters: high-level ab initio calculations", *J. Phys. Chem. C*, **115**, 10006 (2011).
4. Kim H.-D., O. V. Prezhdo, "Time-domain ab initio study of Auger and phonon-assisted Auger processes in a semiconductor quantum dot", *Nano Lett.*, **11**, 1845 (2011).
5. S. V. Kilina, et al. "Theoretical study of electron-phonon relaxation in PbSe and CdSe quantum dots: evidence for phonon memory", *J. Phys. Chem. C*, **115**, 21641 (2011).
6. R. Long, O. V. Prezhdo "Ab initio nonadiabatic molecular dynamics of the ultrafast electron injection from a PbSe quantum dot into the TiO_2 surface" , *J. Am. Chem. Soc.*, **133**, 19240 (2011).
7. H. M. Jaeger, S. Fischer, O. V. Prezhdo "The role of surface defects in multi-exciton generation of lead selenide and silicon semiconductor quantum dots", *J. Chem. Phys.*, **136**, 064701 (2012).
8. Kim H.-D., O. V. Prezhdo "Multiple exciton generation and recombination dynamics in small Si and CdSe quantum dots: an ab initio time-domain study", *ACS Nano*, **6**, 1239 (2012).

Catalytic Water Splitting with Ru Complexes: Analysis of Reactive Intermediates

Dooshaye Moonshiram[1], Thomas J. Meyer[2], Yulia Pushkar[1]
[1]Department of Physics
Purdue University
West Lafayette, Indiana 47907 USA
[2]Department of Chemistry
University of North Carolina at Chapel Hill
Chapel Hill, North Carolina 27599 USA

Water is an optimal source of electrons and protons for realization of artificial photosynthesis. However, the lack of efficient and stable catalyst which can assist water splitting impedes the practical use of this reaction in sunlight to energy conversion assemblies. Analysis of catalytic mechanisms of known catalysts should result in identification of the energetic barriers for this reaction and result in guided design of next generation of stable and active catalysts.

Blue Dimer (BD) *cis*-$[(bpy)_2(H_2O)Ru^{III}ORu^{III}(OH_2)(bpy)_2]^{4+}$ (bpy is 2,2-bipyridine) is one of the first molecular defined catalysts capable of catalytic water splitting. In this catalysts formation of the reactive species with Ru^V=O fragments is held responsible for reactivity towards water with the formation of the O-O bond. Using time resolved Uv-vis kinetic analysis combined with freeze quench sample preparation we followed the reaction of BD with oxidant (ceric ammonium nitrate, denoted Ce(IV)) which results in O_2 evolution. We were able to trap short lived (few seconds) BD [4,5] intermediate (numbers in brackets denote oxidation states of Ru centers). For this intermediate we reproduced EPR spectrum reported previously[1], confirmed oxidation states of Ru centers by Ru K-edge XANES and detected short Ru^V=O (1.70Å) bond by Ru K-edge EXAFS. Labeling of the Ru^V=O fragment with O^{17} allowed us to record unusually high (about 60 G) O^{17} hyperfine splitting in the EPR spectrum. These data confirm high spin density on the oxygen in the Ru^V=O fragment proposed previously from DFT calculations[2].

We also demonstrated that short lived BD [4,5] intermediate reacts with water with the formation of peroxo species. From EPR and Ru K-edge XANES we assigned the oxidation state of the Ru centers in this peroxo intermediate to [3,4]. EXAFS demonstrated that this intermediate has modified ligand environment as compared with BD[3,4] stable catalysts. Resonance Raman experiments with $H_2O/H_2O^{18}/D_2O$ exchanges shown the presence of the unique band undergoing 46 cm^{-1} shift with O^{18} labeling. This confirmed the presence of the O-O fragment. Spectra were insensitive to H_2O/D_2O exchange which ruled out presence of the –OOH fragment. Combined EPR, EXAFS, Raman and DFT calculations suggested the structure with the peroxo fragment attached "side on" to Ru center[3]. Obtained data allow for modeling of the reaction mechanism.

References

1. Cape, J. L.; Lymar, S.V.; Lightbody, T.; Hurst, J.K., *Inorg. Chem.* **2009,** *48*, (10), 4400-4410.
2. Yang, X.; Baik, M. H., *J. Am. Chem. Soc.* **2006,** *128*, (23), 7476-7485.
3. Moonshiram, D.; Jurss, J. W.; Concepcion, J. J.; Zakharova, T.; Alperovich, I.; Meyer, T. J.; Pushkar, Y., *J. Am. Chem. Soc.* **2012,** *134*, (10), 4625-36.

Kinetic Evaluation of Reductant Generation Using Sacrificial Reagents for Hydrogen Generation in Homogeneous Photocatalytic Systems

Bing Shan and Russell Schmehl
Department of Chemistry
Tulane University
New Orleans LA 70118

In recent years significant effort has been put forth developing homogeneous and heterogeneous catalysts for hydrogen production via reduction of water in a wide variety of solutions. Many have been examined under photochemical conditions, demonstrating that hydrogen is formed in the presence of a photosensitizer, sacrificial electron donor, catalyst and water. What is lacking in nearly all of these systems, is a measure of the quantum efficiency for hydrogen production. There are several steps in photochemical hydrogen generation and even the most active catalysts examined by electrochemical methods may be relatively ineffective in photochemical systems. The reactions associated with a typical photochemical hydrogen production system include

$$S + h\nu \rightarrow S^* + D \leftrightharpoons \{S^*,D\} \leftrightharpoons \{S^-,D^+\} \rightarrow S^- + D^+ \quad (1)$$

$$D^+ \rightarrow P \quad (2)$$

$$S^- + Cat \rightarrow S + Cat^- \quad (3)$$

$$Cat^- + H^+ \rightarrow Cat + \tfrac{1}{2} H_2 \quad (4)$$

$$S^- + D^+ \rightarrow S + D \quad (5)$$

Of critical importance are the processes associated with eq. 2 involving electron transfer quenching of the excited chromophore, S*, and separation of the ions produced in the photoredox reaction from the geminate ion pair. These processes, especially charge separation, are often assumed to be of high efficiency. In addition, the decomposition of the sacrificial electron donor, eq. 3, must be rapid relative to the back electron transfer reaction, eq. 6. Figure 1 illustrates this for a system in which $[Ru(5Clphen)_3]^{2+}$ is reductively quenched with tri-toluylamine in the presence and absence of triethylamine. If decomposition of the sacrificial donor is faster than reaction with S^-, the rate of reaction of S^- with the catalyst, Cat (eq. 4), serves as the determining reaction for regeneration of the chromophore, S. This rate depends on a variety of factors including the one electron reduction potential of S.

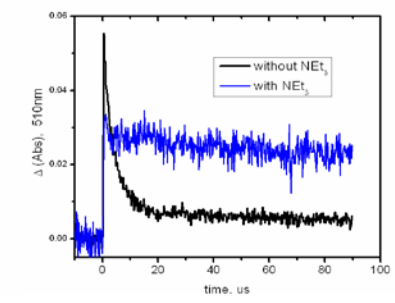

Fig. 1 : Transient absorption decays at 510 nm observed following (black) photolysis of $[Ru(5Cl phen)_3]^{2+}$ and TTA and (blue) the reactants including NEt_3.

This work intends to present an evaluation of some of the photosensitizer, sacrificial donor systems employed in photochemical hydrogen production systems and introduce a new system. We are also developing an experimental method for determination of hydrogen production quantum. Such a system can provide a method for comparing the effectiveness of different catalysts for hydrogen generation in photolytic systems.

Ultrafast and Chemically Specific Microscopy for Atomic Scale Imaging of Nano-Photocatalysis

A. Dolocan,[1] D. Acharya,[2] H. Park,[1] R. Cortes,[2] N. Camillone[1] and P. Sutter[2]
[1]Chemistry Department; [2]Center for Functional Nanomaterials
Brookhaven National Laboratory
Upton NY 11973

Characterizing chemical transformations at the molecular level with combined high temporal and spatial resolution has been a long-standing challenge. Our work aims to break new ground in probing the fundamental mechanisms of photocatalysis by developing new approaches for the nanoscale mapping of the dynamics of nonequilibrium charge populations (photoexcited "hot carriers") and of the chemical reactions they drive.

1.Ultrafast scanning tunneling microscopy (STM): Atomic-scale observations of laser-stimulated phenomena have been attempted since the invention of STM, yet simultaneous sub-ps and sub-nm resolution has so far not been achieved. We are addressing this challenge for the purpose of probing ultrafast hot-carrier dynamics at the atomic scale. By implementing a new approach to ultrafast-laser-excited STM we have successfully overcome issues related to optical interference and thermal expansion effects, thus isolating small photocurrents from much larger dc tunneling currents. On extended Ag(111) surfaces we identified conditions providing a pure tunneling signal by canceling the net photoelectron current between sample and tip. Ag nanoparticles were used to probe the spatial distribution of the STM-detected ultrafast two-pulse correlation signal (fig. 1). Systematic differences in the cross-correlation near single Ag particles demonstrate that simultaneous sub-ps temporal and sub-nm spatial resolution has been achieved, paving the way for probing size-dependent electron dynamics in nanoparticles.

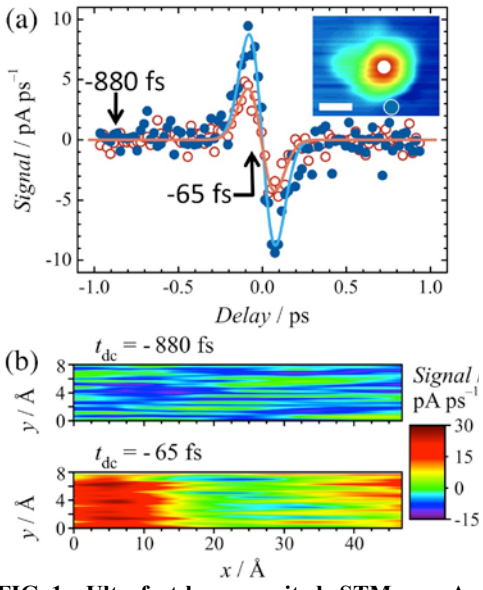

FIG. 1. Ultrafast-laser excited STM on Ag nanoparticles. (a) Sub-ps two-color cross-correlation measurements with STM tip adjacent to and atop a single Ag particle (inset: topography, scale bar: 2 nm). The dependence of the signal on both tip location and optical delay demonstrates simultaneous sub-ps temporal and sub-nm spatial resolution. **(b)** Maps of the STM-detected ultrafast signal across the Ag particle.

2. Site-specific electron-induced surface chemistry: Combining cryogenic STM and fs laser pulses enables us to study the pathways of electron-mediated reactions by comparing thermal and photo-activated processes, and by injecting charge carriers from the STM tip into individual adsorbates. Studies of adsorption, diffusion, thermal desorption and electron-mediated reactions have focused on CO_2 and H_2O, relevant to photocatalytic hydrogenation reactions on TiO_2(110). Atomically precise electron injection has been used to drive reactions as well as the non-thermal diffusion of bridging oxygen vacancies, the prevalent surface defect on TiO_2(110). Ultimately we aim to understand the fundamental relationship linking photocatalyst structure, thermal and non-thermal excitation, and hot carrier dynamics to the reaction activity and selectivity.

List of Participants

Participants List – 34th DOE Solar Photochemistry Research Meeting

Neal Armstrong
University of Arizona
Dept. Chemistry and Biochemistry
Tucson, AZ 85721
520-730-7365
nra@email.arizona.edu

Allen Bard
University of Texas at Austin
105 E. 24th St Stop A5300
Austin, TX 78712-1224
512-471-3761
ajbard@mail.utexas.edu

Robert Bartynski
Rutgers University
136 Frelinghuysen Rd.
Piscataway, NJ 08854
732-445-5500
bart@physics.rutgers.edu

Tunna Baruah
University of Texas al El Paso
500 W. University Avenue
El Paso, TX 79968
915-747-7529
tbaruah@utep.edu

Matt Beard
National Renewable Energy Laboratory
15013 Denver West Parkway
Golden, CO 80401
303-384-6781
matt.beard@nrel.gov

Jason Benedict
University at Buffalo, SUNY
771 Natural Sciences Complex
Buffalo, NY 14260-3000
716-645-4276
jbb6@buffalo.edu

Jeffrey Blackburn
National Renewable Energy Laboratory
16253 Denver West Parkway
Golden, CO 80401
303-384-6649
jeffrey.blackburn@nrel.gov

David Blank
University of Minnesota
207 Pleasant St SE
Minneapolis, MN 55455
612-624-0571
blank@umn.edu

Andrew Bocarsly
Princeton University
Frick Laboratory, Princeton Univ.
Princeton, NJ 08544
609-258-3888
bocarsly@princeton.edu

David Bocian
University of California, Riverside
Department of Chemistry
Riverside, CA 92521
951-827-3660
David.Bocian@ucr.edu

Kara Bren
University of Rochester
120 Trustee Rd.
Rochester, NY 14627-0216
585-275-4335
bren@chem.rochester.edu

Karen Brewer
Virginia Tech
Department of Chemistry
Blacksburg, VA 24061-0212
540-231-6579
kbrewer@vt.edu

Participants List – 34th DOE Solar Photochemistry Research Meeting

David Britt
UC Davis
1 Shields Ave.
Davis, CA 95616
530-752-6377
rdbritt@ucdavis.edu

Gary Brudvig
Yale University
P.O. Box 208107
New Haven, CT 06477
203-432-5202
gary.brudvig@yale.edu

Louis Brus
Columbia University
Chemistry Department
3000 Broadway
New York, NY 10027
212-854-4041
leb26@columbia.edu

Emilio Bunel
Argonne National Laboratory
9700 S. Cass Avenue
Argonne, IL 60439
630-252-4309
ebunel@anl.gov

Ian Carmichael
Notre Dame Radiation Laboratory
University of Notre Dame
Notre Dame, IN 46556
574-631-4502
carmichael.1@nd.edu

Edward Castner
Rutgers, The State University of New Jersey
610 Taylor Road
Piscataway, NJ 08854
732-445-2564
ecastner@rci.rutgers.edu

Lin Chen
Argonne National Lab/Northwestern Univ.
Building 200, 9700 S. Cass Ave.
Argonne, IL 60439
630-252-3533
lchen@anl.gov

Kyoung-Shin Choi
Purdue University
560 Oval Drive
West Lafayette, IN 47907
765-494-0049
kchoi1@purdue.edu

Philip Coppens
University at Buffalo SUNY Buffalo
732 NSc Complex
Buffalo, NY 14260-3000
716-645-4273
coppens@buffalo.edu

Robert Crabtree
Yale University
225 Prospect St.
New Haven, CT 06520
203-432-3925
robert.crabtree@yale.edu

Carol Creutz
BNL Chemistry
P. O. Box 5000
Upton, NY 11973
631-344-4359
ccreutz@bnl.gov

Richard Crooks
University of Texas
1 University Station A5300
Austin, TX 78712-0165
512-475-8674
crooks@cm.utexas.edu

Participants List – 34th DOE Solar Photochemistry Research Meeting

Niels Damrauer
University of Colorado at Boulder
Dept. Chemistry and Biochemistry
Boulder, CO 80309
303-735-1280
niels.damrauer@colorado.edu

Linda Doerrer
Boston University
590 Commonwealth Ave.
Boston, MA 02139
617-358-4335
doerrer@bu.edu

Richard Eisenberg
University of Rochester
Department of Chemistry
Rochester, NY 14627
585-275-5573
eisenberg@chem.rochester.edu

C. Michael Elliott
Colorado State University
Department of Chemistry
Ft. Collins, CO 80523
970-491-5204
elliott@lamar.colostate.edu

John Endicott
Wayne State University
321 Chemistry
Detroit , MI 48202
313-5787-2607
jfe@chem.wayne.edu

Graham Fleming
Lawrence Berkeley National Laboratory
1 Cyclotron Road
Berkeley, CA 94720
510-643-2735
grfleming@lbl.gov

Marye Anne Fox
University of California, San Diego
9500 Gilman Drive
La Jolla, CA 92093
858-534-3135
chancellor@ucsd.edu

Arthur Frank
National Renewable Energy Laboratory
1617 Cole Blvd.
Golden, CO 80401
303-384-6262
Arthur.Frank@nrel.gov

Heinz Frei
Lawrence Berkeley National Laboratory
1 Cyclotron Road
Berkeley, CA 94720
510-486-4325
HMFrei@lbl.gov

Richard A. Friesner
Columbia University
Department of Chemistry
3000 Broadway, MC 3110
New York, NY 10027
212-854-7606
ec31@columbia.edu

Etsuko Fujita
Brookhaven National Laboratory
Chemistry Department
Upton, NY 11973-5000
631-344-4356
fujita@bnl.gov

Elena Galoppini
Rutgers University
73 Warren Street
Newark, NJ 07041
973-353-5317
galoppin@rutgers.edu

Bruce Garrett
Pacific Northwest National Laboratory
P.O. Box 999 (K9-90)
Richland, WA 99352
509-372-6344
bruce.garrett@pnnl.gov

Wayne Gladfelter
University of Minnesota
Department of Chemistry
Minneapolis, MN 55455
612-624-4391
wlg@umn.edu

Brian Gregg
National Renewable Energy Laboratory
15013 Denver West Pkwy.
Golden, CO 80401
303-384-6635
brian.gregg@nrel.gov

David Grills
Brookhaven National Laboratory
Chemistry Department
Upton, NY 11973-5000
631-344-4332
dcgrills@bnl.gov

Lars Gundlach
University of Delaware
109 Lammot DuPont
Newark, DE 19716
302-831-2331
larsg@udel.edu

Devens Gust
Arizona State University
Dept. Chemistry and Biochemistry
Tempe, AZ 85287
480-965-4547
gust@asu.edu

Thomas Hamann
Michigan State University
578 S. Shaw Lane, RM 411
East Lansing, MI 48824
517-355-9715
hamann@chemistry.msu.edu

Robert Hamers
University of Wisconsin-Madison
1101 University Avenue
Madison, WI 53706
608-262-6371
rjhamers@wisc.edu

Alexander Harris
Brookhaven National Laboratory
Building 555, P.O. Box 5000
Upton, NY 11973
631-344-4301
alexh@bnl.gov

Michael Henderson
Pacific Northwest National Laboratory
P.O. Box 999, K8-87
Richland, WA 99352
509-371-6527
ma.henderson@pnnl.gov

Craig Hill
Emory University
1515 Dickey Dr., NE
Atlanta, GA 30322
404-727-6611
chill@emory.edu

Dewey Holten
Washington University
Chemistry Dept., One Brookings Dr.
St. Louis, MO 63130
314-935-6502
holten@wustl.edu

Participants List – 34th DOE Solar Photochemistry Research Meeting

Michael Hopkins
The University of Chicago
Department of Chemistry
Chicago, IL 60637
773-702-6490
mhopkins@uchicago.edu

Libai Huang
University of Notre Dame
223 A Radiation Lab
Notre Dame, IN 46556
573-631-2657
lhuang2@nd.edu

Joseph Hupp
Northwestern University
2145 Sheridan Road
Evanston , IL 60208
847-441-0136
j-hupp@northwestern.edu

James Hurst
Washington State University
Department of Chemistry
Pullman, WA 99164-4630
509-432-3194
hurst@wsu.edu

Justin Johnson
National Renewable Energy Laboratory
15013 Denver West Parkway
Golden, CO 80401
303-384-6190
justin.johnson@nrel.gov

David Jonas
University of Colorado
215 UCB
Boulder, CO 80309-0215
303-492-3818
david.jonas@colorado.edu

Prashant Kamat
University of Notre Dame
223 Radiation Laboratory
Notre Dame, IN 46556
574-631-5411
pkamat@nd.edu

David Kelley
University of California, Merced
5200 N. Lake Road
Merced, CA 95343
209-228-4354
dfkelley@ucmerced.edu

Peter Khalifah
Stony Brook University
100 Nicolls Rd.
Stony Brook, NY 11794-3400
631-632-7796
kpete@bnl.gov

Christine Kirmaier
Washington University
Dept. of Chemistry, Box 1134
St. Louis, MO 63130
314-725-6157
kirmaier@wustl.edu

Christian Kisielowski
Lawrence Berkeley National Laboratory
One Cyclotron Rd.
Berkeley, CA 94720
510-486-4716
CFKisielowski@lbl.gov

Lowell Kispert
The University of Alabama
Box 870336
Tuscaloosa, AL 35487-0336
205-348-7134
lkispert@bama.ua.edu

Participants List – 34th DOE Solar Photochemistry Research Meeting

Valeria Kleiman
University of Florida
P.O. Box 117200
Gainesville, FL 32611-7200
352-392-4656
kleiman@ufl.edu

Carl Koval
University of Colorado
Dept. of Chemistry - 215 UCB
Boulder, CO 80309-0215
303-506-7042
koval@colorado.edu

Todd Krauss
University of Rochester
120 Trustee Road
Rochester, NY 14627-0216
585-275-5093
krauss@chem.rochester.edu

Nathan Lewis
California Technical University
1200 E. California Blvd.
Pasadena, CA 91125
626-395-6335
nslewis@caltech.edu

Frederick Lewis
Northwestern University
2145 Sheridan Road
Evanston, IL 60208
847-491-3441
fdl@northwestern.edu

Tianquan Lian
Emory University
1515 Dickey Drive NE
Atlanta, GA 30322
404-727-6649
tlian@emory.edu

Jonathan Lindsey
North Carolina State University
CB8204, 2620 Yarbrough Drive
Raleigh, NC 27695-8204
919-515-6406
jlindsey@ncsu.edu

Mark Lonergan
University of Oregon
1253 Department of Chemistry
Eugene, OR 97403
541-346-4748
lonergan@uoregon.edu

Rene Lopez
University of North Carolina at Chapel Hill
343 Chapman Hall, Physics Dept.
Chapel Hill, NC 27713
919-962-7216
rln@physics.unc.edu

Stephen Maldonado
University of Michigan
930 N. University
Ann Arbor, MI 48109-1055
734-647-4750
smald@umich.edu

Thomas Mallouk
Pennsylvania State University
Department of Chemistry
University Park, PA 16801
814-863-9637
tem5@psu.edu

Kent Mann
University of Minnesota
Chemistry Department
Minneapolis, MN 55455
612-625-3563
krmann@umn.edu

Participants List – 34th DOE Solar Photochemistry Research Meeting

Claudio Margulis
University of Iowa
118 IATL
Iowa City, IA 52242
319-335-0615
claudio-margulis@uiowa.edu

Mark Maroncelli
Penn State
104 Chemistry Building
University Park, PA 16802
814-865-0898
maroncelli@psu.edu

James McCusker
Michigan State University
578 South Shaw Lane
East Lansing, MI 48824-1322
517-355-9715
jkm@chemistry.msu.edu

Thomas Meyer
University of North Carolina
Department of Chemistry
Chapel Hill, NC 27599-3290
919-843-8313
tjmeyer@unc.edu

Gerald Meyer
Johns Hopkins
3400 N. Charles St.
Baltimore, MD 21218
410-516-7319
meyer@jhu.edu

Josef Michl
University of Colorado
Dept. Chem. and Biochem., 215 UCB
Boulder, CO 80309-0215
303-492-6519
michl@eefus.colorado.edu

John Miller
Brookhaven National Lab
Chemistry 555
Upton, NY 11973
631-344-4354
jrmiller@bnl.gov

Thomas Moore
Arizona State University
Dept. Chemistry and Biochemistry
Tempe, AZ 85287-1604
480-965-3308
tmoore@asu.edu

James Muckerman
Brookhaven National Laboratory
Chemistry Department
Upton, NY 11973-5000
631-344-4368
muckerma@bnl.gov

Karen Mulfort
Argonne National Laboratory
9700 South Cass Avenue
Argonne , IL 60439
630-252-3545
mulfort@anl.gov

Charles Mullins
University of Texas at Austin
Dept. of Chemical Engr. C0400
Austin, TX 78712
512-471-5817
mullins@che.utexas.edu

Djamaladdin Musaev
Emory University
1515 Dickey Dr.
Atlanta, GA 30322
404-727-2382
dmusaev@emory.edu

Participants List – 34th DOE Solar Photochemistry Research Meeting

Nathan Neale
National Renewable Energy Laboratory
15013 Denver West Parkway
Golden, CO 80401
303-384-6165
nathan.neale@nrel.gov

Marshall Newton
Brookhaven National Laboratory
Chemistry Department
Upton, NY 11973
631-344-4366
NEWTON@BNL.GOV

Anders Nilsson
SLAC National Accelerator Laboratory
2575 Sand Hill Road, MS 31
Menlo Park, CA 94025
650-926-2233
nilsson@slac.stanford.edu

Daniel Nocera
Massachusetts Institute of Technology
77 Massachusetts Avenue
Cambridge, MA 02139
617-253-5537
nocera@mit.edu

Arthur Nozik
University of Colorado
215 UCB
Boulder, CO 80309
303-384-6603
anozik@nrel.gov

Shanlin Pan
The University of Alabama
Department of Chemistry
Tuscaloosa , AL 35487-0336
205-348-6381
span1@bama.ua.edu

John Papanikolas
University of North Carolina at Chapel Hill
Department of Chemistry
Chapel Hill, NC 27599
919-962-1619
john_papanikolas@unc.edu

Bruce Parkinson
University of Wyoming
1000 E. University
Laramie, WY 82071
303-766-9891
bparkin1@uwyo.edu

Hrvoje Petek
University of Pittsburgh
3941 O'Hara Street, G01 Allen
Pittsburgh, PA 15260
412-624-3599
petek@pitt.edu

Piotr Piotrowiak
Rutgers University
73 Warren Street
Newark, NJ 07102
973-517-6482
piotr@andromeda.rutgers.edu

Oleg Poluektov
Argonne National Laboratory
9700 South Cass Ave.
Argonne, IL 60439
630-252-3546
Oleg@anl.gov

Dmitry Polyansky
Brookhaven National Laboratory
Chemistry Department
Upton, NY 11973
631-344-4315
dep@bnl.gov

Oleg Prezhdo
University of Rochester
Department of Chemistry
Rochester, NY 14627
585-276-5664
oleg.prezhdo@rochester.edu

Yulia Pushkar
Purdue University
525 Northwestern Avenue
West Lafayette, IN 97407
765-496-3279
ypushkar@purdue.edu

Jeffrey Pyun
University of Arizona
1306 E. University Blvd.
Tucson, AZ 85721
520-626-1834
jpyun@email.arizona.edu

John Reynolds
Georgia Institute of Technology
901 Atlantic Drive
Atlanta, GA 30332
404-388-4390
reynolds@chemistry.gatech.edu

Garry Rumbles
National Renewable Energy Laboratory
15013 Denver West Parkway
Golden, CO 80401
303-384-6502
garry.rumbles@nrel.gov

Amy Ryan
U.S. Department of Energy
19901 Germantown Road
Germantown, MD 20874
301-903-5805
margaret.ryan@science.doe.gov

Scott Saavedra
University of Arizona
1306 E. University
Tucson, AZ 85721-0041
520-621-9761
saavedra@email.arizona.edu

Kirk Schanze
University of Florida
Department of Chemistry
P.O. Box 117200
Gainesville, FL 32611
352-392-9133
kschanze@chem.ufl.edu

Berny Schlegel
Wayne State University
Department of Chemistry
Detroit, MI 48202
313-577-2562
hbs@chem.wayne.edu

Russell Schmehl
Tulane University
Department of Chemistry
New Orleans, LA 70118
504-862-3566
russ.schmehl@gmail.com

Charles Schmuttenmaer
Yale University
225 Prospect St.
New Haven, CT 06520-8107
203-432-5049
charles.schmuttenmaer@yale.edu

Richard Schrock
Massachusetts Institute of Technology
77 Massachusetts Avenue
Cambridge, MA 02139
617-253-1596
rrs@mit.edu

Participants List – 34th DOE Solar Photochemistry Research Meeting

Udo Schwarz
Yale University
P.O. Box 208284
New Haven, CT 06520
203-432-7525
udo.schwarz@yale.edu

Mark Spitler
U.S. Department of Energy
1000 Independence Ave., SW
Washington, DC 20585
301-903-4568
mark.spitler@science.doe.gov

Peter Stair
Northwestern University
2145 Sheridan Rd.
Evanston, IL 60208-3113
847-491-5266
pstair@northwestern.edu

Peter Sutter
Brookhaven National Laboratory
Building 735
Upton, NY 11973
631-344-3109
psutter@bnl.gov

Michael Therien
Duke University
124 Science Dr. 5330 FFSC
Durham, NC 27708-0346
919-660-1670
michael.therien@duke.edu

Randolph Thummel
University of Houston
Chemistry Department
Houston, TX 77204-5003
713-743-2734
thummel@uh.edu

David Tiede
Argonne National Laboratory
Chemical Sciences and Engineering
Argonne, IL 60439
630-252-3539
tiede@anl.gov

John Turner
National Renewable Energy Laboratory
15013 Denver West Parkway
Golden, CO 80401-3393
303-275-4270
jturner@nrel.gov

Lisa Utschig
Argonne National Laboratory
9700 S. Cass Ave.
Argonne, IL 60439
630-252-3544
utschig@anl.gov

Jao van de Lagemaat
National Renewable Energy Laboratory
15013 Denver West Parkway
Golden, CO 80401
303-384-6143
jao.vandelagemaat@nrel.gov

Claudio Verani
Wayne State University
5101 Cass Ave
Detroit, MI 48202
311-577-1076
cnverani@chem.wayne.edu

Michael Wasielewski
Northwestern University
2145 Sheridan Rd.
Evanston, IL 60208
847-467-1423
m-wasielewski@northwestern.edu

Emily Weiss
Northwestern University
2145 Sheridan Rd.
Evanston, IL 60208-3113
847-491-3095
e-weiss@northwestern.edu

Mary Beth Williams
Penn State
104 Chemistry Building
University Park, PA 16802
814-865-8859
mbw@chem.psu.edu

James Wishart
Brookhaven National Laboratory
Chemistry Department
Upton, NY 11973
631-344-4327
wishart@bnl.gov

Author Index